Universidade de Aveiro
2011
Departamento de Electrónica, Telecomunicações e Informática

Sara Helena Marques Teodoro

Codificação Distribuída em Sistemas com Diversidade Cooperativa

Distributed Coding for Systems with Cooperative Diversity

Universidade de Aveiro
2011
Departamento de Electrónica, Telecomunicações e Informática

Sara Helena Marques Teodoro

Codificação Distribuída em Sistemas com Diversidade Cooperativa

Distributed Coding for Systems with Cooperative Diversity

Dissertação apresentada à Universidade de Aveiro para cumprimento dos requisitos necessários à obtenção do grau de Doutor em Engenharia Electrotécnica realizada sob a orientação científica do Doutor Atílio Gameiro, Professor Associado do Departamento de Departamento de Electrónica, Telecomunicações e Informática da Universidade de Aveiro e co-orientações do Doutor Adão Silva, Professor Auxiliar do Departamento de Departamento de Electrónica, Telecomunicações e Informática da Universidade de Aveiro e do Doutor João M. P. Gil, Administrador da Alma Lux Photographia.

Apoio financeiro da FCT e do FSE no âmbito do III Quadro Comunitário de Apoio.

Aos meus pais e ao meu marido Nuno.

"*And what's the good of diversity?*"
"*I don't know. It's certainly more... interesting."*
Daniel Quinn

"*An expert is a man who made all the mistakes, which can be made, in a very narrow field.*"
Niels Bohr

"*It always seems impossible until is done.*"
Nelson Mandela

"*Try and fail, but don't fail to try.*"
Stephen Kaggwa

"*O tempo que gastaste com a tua rosa é que a faz ser tão importante.*"
Antoine de Saint-Exupery

o júri
presidente

Prof. Doutor João Carlos Matias Celestino Gomes da Rocha
Professor Catedrático da Universidade de Aveiro

Prof. Doutor Américo Manuel Carapeto Correia
Professor Catedrático do Instituto Superior de Ciências do Trabalho e da Empresa de Lisboa

Prof. Doutor Atílio Manuel da Silva Gameiro
Professor Associado da Universidade de Aveiro (Orientador)

Prof. Doutor Rui Miguel Henriques Dias Morgado Dinis
Professor Auxiliar com Agregação da Faculdade de Ciências e Tecnologias da Universidade Nova

Prof. Doutor Vítor Manuel Mendes da Silva
Professor Auxiliar da Faculdade de Ciências e Tecnologia da Universidade de Coimbra

Prof. Doutor Adão Paulo Soares da Silva
Professor Auxiliar da Universidade de Aveiro (Co-orientador)

Doutor João Miguel Pissarra Coelho Gil
Administrador da Empresa Alma Lux Photographia (Co-orientador)

agradecimentos

Agradeço aos meus orientadores Prof. Atílio, João e Adão por todo o apoio e disponibilidade prestados, cujo envolvimento foi fundamental para ultrapassar as diversas dificuldades com que me deparei ao longo deste projecto.

Agradeço aos meus colegas de grupo de trabalho Motion pela partilha de ideias e experiências que longo deste período ajudaram a enriquecer este trabalho.

Agradeço à FCT e ao Instituto de Telecomunicações pelo suporte financeiro prestado que tornou este trabalho exequível.

Ao meu marido Nuno, um muito obrigado pelo apoio constante ao longo deste percurso, que com a sua paciência aceitou os sacrifícios a que este trabalho obrigou e me confortou nos momentos mais difíceis.

Aos meus pais agradeço a confiança que em mim sempre depositaram, que por vezes me fazem pensar que realmente nada é impossível, e pelo apoio que sempre me deram não só nestes últimos anos como ao longo de toda a minha vida.

Aos meus irmãos um obrigado, por também eles compreenderem muitas coisas sem serem precisas palavras e por acreditarem em mim.

Agradeço à minha avó pelo orgulho que tem em mim, que me ajuda a ser confiante.

Aos meus familiares que sempre me apoiaram e me suportaram em todos os sentidos ao longo desta tese, com palavras amigas.

Aos meus amigos que me acompanharam nos momentos menos académicos, por estarem ao meu lado sempre que precisei.

Sem todos eles tudo teria sido mais difícil.

A todos o meu obrigado.

"*When eating bamboo sprouts, remember the man who planted them.*"
Chinese proverb

palavras-chave Codificação distribuída, Codificação espaço-temporal, Codificação espaço-frequência, Diversidade cooperativa, Relays.

resumo O presente trabalho propõe-se a divulgar as mais significativas técnicas de esquemas cooperativos, de forma a ultrapassar alguns dos problemas dos sistemas móveis sem fios da próxima geração, estendendo a área de cobertura destes sistemas, assim como a sua capacidade e fiabilidade. O estudo de diversos esquemas cooperativos é efetuado em termos de capacidade e de taxa de erros, fazendo variar o número de *relays* e de antenas em cada elemento do sistema. Diversos algoritmos com aplicação em sistemas cooperativos são desenvolvidos e propostos ao longo desta tese, como códigos espaço-frequência aplicados de forma distribuída nos *relays*, para sistemas baseados na tecnologia OFDM e sob diversos cenários próximos da realidade. Os sistemas cooperativos são particularmente úteis em situações em que o caminho direto entre dois terminais não está acessível ou tem uma fraca qualidade de transmissão. Tendo este aspeto em consideração, e pretendendo ter a máxima eficiência espetral e máxima diversidade, um algoritmo com precodificação é também proposto para múltiplos *relays*, cada um equipado com uma ou duas antenas. A formulação matemática associada aos algoritmos propostos é apresentada, assim como a derivação da probabilidade de erro teórica. O desempenho dos sistemas assistidos por *relays* usando os algoritmos propostos é comparado em relação a outros esquemas cooperativos equivalentes e a esquemas não-cooperativos, considerando cenários com diferentes qualidades de canal, daí advindo importantes conclusões em relação a estes sistemas.

keywords Cooperative Diversity; Distributed Algorithms; Space-Frequency Block Codes; Space-Time Block Codes; Relays.

abstract Cooperative schemes are promising solutions for cellular wireless networks aiming to improve system fairness, extend coverage and increase capacity. Measurements of these system performances are made in terms of BER and capacity for different configurations, by varying the number of relays and of antennas equipping each node. In this work we propose and evaluate distributed space-frequency codes applied to cooperative systems in a distributed way, with application in OFDM systems and considering realistic scenarios. Moreover, the use of relays is of significant interest to allow radio access in situations where a direct path is not available or has poor quality. Thus, a data precoded relay-assisted scheme is also proposed for a system cooperating with multiple relays, each equipped with either a single antenna or two-antenna array. Mathematical formulation of the proposed algorithms is derived as well as the pairwise error probability. We further present the performances of the proposed algorithms apllied in relay-assisted schemes, and compare them with equivalent cooperative and non-cooperative schemes, for several channel quality scenarios, through which important conclusions are achieved.

Table of Contents

List of Figures

List of Tables

List of Acronyms

0G	Generation zero of mobile cellular communications
1G	First generation of mobile cellular communications
2.5G	Generation 2.5 of mobile cellular communications
3G	Third generation of mobile cellular communications
3GPP	Third generation partnership project
4G	Fourth generation of mobile cellular communications
AF	Amplify-and-forward
AoA	Angle of arrival
AoD	Angle of departure
AWGN	Additive white Gaussian noise
BER	Bit error rate
BLAST	Bell-labs layered space time
BPSK	Binary phase shift keying
BS	Base station
CDMA	Code division multiple access
CRC	Cyclic redundancy check
CSI	Channel state information

CTC	Convolutional turbo coding
DARPA	Defense Advanced Research Projects Agency
DCA	Distributed compound Alamouti
DCS1800	Digital Cellular System 1800
DeF	Decision feedback
DF	Decode-and-forward
DL	Downlink
DOSTBC	Distributed orthogonal space-time block codes
DP	Direct path
DRA	Distributed relay-assisted
DSFBC	Distributed space-frequency block code
DSTBC	Distributed space-time block code
EDGE	Enhanced data rates for GSM evolution
EF	Equalize-and-forward
ETSI	European Telecommunications Standards Institute
FDMA	Frequency division multiple access
FEC	Forward error correction
FER	Frame error rate
GC-STBC	Group-coherent STBC
GPC	Gray precoding code
GPRS	General packet radio service
GSM	Global system for mobile communications
IMT-2000	International mobile telecommunications-2000
IP	Internet protocol
IS	Interim standard
ISI	Inter-symbol interference
ITU	International Telecommunications Union
LAN	Local area networks
LoS	Line-of-sight
LPK	Li, Park, and Kim

LTE	Long term evolution
MIMO	Multiple input multiple output
MISO	Multiple input, single output
ML	Maximum likelihood
MRC	Maximum ratio combining
NRA	Non relay-assisted
ODMA	Opportunity driven multiple access
OFDM	Orthogonal frequency division multiplexing
OFDMA	Orthogonal frequency-division multiple access
O-STBC	Orthogonal space-time block coding
PCS	Personal communications system
PDC	Personal digital cellular
pdf	Probability density function
PEP	Pairwise error probability
PHY	Physical layer
PRA	Precoded relay-assisted
PSD	Power spectral density
QoS	Quality of service
QO-STBC	Quasi-orthogonal space-time block coding
RA	Relay-assisted
RN	Relay node
SDF	Selective decode-and-forward
SFBC	Space-frequency block code
SIMO	Single input, multiple output
SISO	Single input, single output
SNR	Signal-to-noise ratio
SSD	Single-symbol decodable
STBC	Space-time block code
STTC	Space-time trellis code
TBH	Tirkkonen, Boariu and Hottinen

TCM	Trellis coded modulation
TDD	Time division duplexing
TDMA	Time division multiple access
TS-CDMA	Time-division synchronous CDMA
UMTS	Universal mobile telecommunications system
UPC	Used precoding code
UT	User terminal
UTRA	Universal mobile communication system terrestrial radio
VAA	Virtual antenna array
V-BLAST	Vertical Bell-lab layered space time
VMIMO	Virtual MIMO
WLAN	Wireless local area network
WPAN	Wireless personal area network
ZF	Zero forcing

List of Symbols

Scalars

a	Interference between channels in STBCs
A	Amplitude of a signal
a_h	Magnitude of complex valued fading channel
$a_i(t,\tau)$	Time variant amplitude of the i^{th} complex channel attenuation
a_R	Variable that follows a Rayleigh distribution
a_χ	Variable that follows a Chi-square distribution
b	Interference between channels in STBCs
B_c	Coherence bandwidth
B_m	Minimum transmission bandwidth at which time dispersion is observable
B_x	Bandwidth of received signals
c	Light speed
C	Capacity of a channel
$C^{(j)}$	Instantaneous capacity of system j

C_{av}	Average capacity of a system
C_{out}	Outage capacity of a system
C_x	Transmit matrix of space time/frequency block codes
d	Distance between source and destination nodes
$d^2_{\min_A}$	Squared minimum distance for the system A
$d^2_{\min_{QPSK}}$	Squared minimum distance for QPSK symbols
d_t	Distance between two nodes
E_b	Energy per bit
$F(x_k, x_{k+1})$	Bijective function between symbols x_k and x_{k+1}
f_c	Carrier frequency
f_m	Magnitude of the maximum Doppler shift experienced by a signal
$f_{v_i}(\overline{v}_i)$	Probability density function of an exponential variable v_i, with mean $\overline{v}_i$
$f_{v_i}(\overline{v}_i, k)$	Probability density function of a Chi-square variable v_i, with mean $\overline{v}_i$ and n degrees of freedom
G	Coding power gain of the PRA scheme in comparison with another cooperative system
g_i	Maximum ratio combining gain corresponding to link i, which is applied in decoding
G_L	Coding power gain of the PRA scheme in comparison with another cooperative system, for the case of having L relay nodes
$g_{l\_q_r,k,p}$	Equalization coefficients used in MRC at the UT, for RN_l, relay antenna q_r, time slot k and subcarrier p
$g_{M-\text{QAM}}$	Gain obtained with M-QAM modulation in comparison with QPSK one
$g_{q_r,k+i,p}$	Equalization coefficients used in MRC at the UT of RA-1RN schemes concerning the direct path contribution when i is 0 and the cooperative path contribution when i is 1, and for the relay antenna q_r, time slot k and subcarrier p or p+1

$g_{RN\_q_b\_q_r,k,p}$	Equalization coefficients used in MRC at the relay of RA-1RN schemes for the relay antenna q_r, base station antenna q_b, time slot *k* and subcarrier *p* or *p*+1
h	Complex valued scalar channel
$h(t)$	Time variant channel impulse response
$h(t,\tau)$	Time variant channel impulse response or delay spread function
$h_b(t)$	Complex baseband representation of $h(t)$
$h_{br\_q_b\_l\_q_r}$	Complex valued scalar channel between the q_b^{th} antenna of the BS and the q_r^{th} antenna of the RN_l, in time slot *k* and subcarrier *p*
$h_{br\_q_b\_q_r,k,p}$	Complex valued scalar channel between the antenna q_b of BS and antenna q_r of RN in time slot *k* and subcarrier *p*
$h_{bu\_q_b,k,p}$	Complex valued scalar channel between the antenna q_b of BS and UT, in time slot *k* and subcarrier *p*, when the UT has a single antenna
$h_{eq\_q_r,k,p}$	Equivalent channel including the contribution of cooperative links for RA-1RN schemes, related with the antenna q_r
$h_{F,ru\_l\_q_r,k}$	Complex valued flat-fading Rayleigh channel realization for time slot *k*, between the q_r^{th} antenna of RN_l and the UT, for instant *k*
h_i	Complex valued scalar channel for link *i*
$h_{Ib}(t)$	Time variant in-phase component of complex baseband channel impulse response
h_k	Complex scalar channel characterization at time slot *k*
$h_{Qb}(t)$	Time variant in-quadrature component of complex baseband channel impulse response
$h_{R,D}$	Channel response corresponding to relay-to-destination link
$h_{ru\_l\_q_r,k,p}$	Complex channel model between the antenna q_r of RN_l and UT, in time slot *k* and subcarrier *p*, when the UT has a single antenna
$h_{ru\_q_r,k,p}$	Complex channel model between the antenna q_r of RN and UT, in time slot *k* and subcarrier *p*, when the UT has a single antenna
$h_{S,D}$	Complex valued scalar channel corresponding to source-to-destination link

$h_{S,R}$	Complex valued scalar channel corresponding to source-to-relay link
k	Sample instant time
K	Parameter of a Rician fading channel, given by the ratio of the energy in the dominant path by the energy in the scattered paths
k_0	Constant of Friis formula
l	Relay node index
L	Number of relay nodes
m	Non-negative integer values representing discrete-time or sample instant
M	Constellation order
M_A	Modulation order for a specific scheme *A*
N	Number of paths that arrive at the receiver
n	Noise introduced in transmitter system
$n(t)$	Time variant noise introduced in receptor
N_0	Noise energy per complex symbol time
N_B	Number of antennas in base station
N_c	Number of subcarriers in OFDM symbols
n_k	Complex noise at the destination receiver at instant *k*
N_l	Length of the symbol blocks used in OFDM based communications
$N_{\min}$	Number of paths with the minimum distance
N_R	Number of antennas in (each) relay node
$n_{Ri,k}$	Noise power introduced in relay *i*, in time slot *k*
$n_{Ri,k,p}$	Zero mean complex AWGN samples in relay *i*, at time slot k, on subcarrier *p*, with variance of $\sigma^2_{n_{ci}}$
$n_{RN\_q_r,k,p}$	Zero mean complex AWGN samples introduced by antenna q_r of relay in RA-1RN schemes, at time slot k, on subcarrier *p*, with variance of $\sigma^2_{n_{c1}}$

N_{Rx}	Number of receiving antennas
N_T	Number of transmit antennas
N_U	Number of antennas in user terminal
$n_{UT,k,p}$	Zero mean complex AWGN samples in UT, at time slot k, on subcarrier p, with variance of $\sigma^2_{n_d}$
p	Subcarrier position
P_b	Bit error probability
P_e	Error probability
P_{out}	Outage probability
P_R	Received power at a node
P_t	Power transmitted by a node
P_T	Total transmitted power
q_b	Index of antennas in base station
q_r	Index of antennas in relay node(s)
q_u	Index of antennas in user terminal
R	Rate of transmission
r_k	Signal received at time slot k
$\hat{s}_{k,p}$	Estimation in destination of the symbol transmitted by source at time slot k, on subcarrier p
$\hat{s}_{Ri,k}$	Estimation in relay i of the symbol transmitted by source at time slot k
$\hat{s}_{RN,k,p}$	Estimation in relay of the symbol transmitted by source at time slot k and on subcarrier p
$\overline{s}_{k,p}$	Hard-decision symbol of the symbol transmitted by source in time slot k and subcarrier p
$\overline{s}_{R_i,k}$	Hard-decision symbol at a relay i of the symbol transmitted by source in time slot k

$\overline{s}_{R,k}$	Hard-decision symbol at a relay of the symbol transmitted by source in time slot k
s_k	Symbol transmitted by source at instant k
$s_{k,p}$	Symbol transmitted by source at instant k and subcarrier p
SNR	Ratio between the received signal energy over noise energy per complex symbol time
SNR_b	SNR of link BS→RN of a RA scheme with one relay
SNR_d	SNR of link BS→UT of a RA scheme with one relay
SNR_r	SNR of link RN→UT of a RA scheme with one relay
SNR_R	Ratio between the mean received power over the noise power
SNR_t	Ratio between the mean transmitted power over the noise power
SNR_T	Ratio between the total transmitted power over the noise power
t	Real value representing the continuous time variable
T_c	Channel coherence time
T_m	Minimum signal duration at which frequency dispersion becomes noticeable
T_s	Time slot duration
T_x	Duration of received signals
U	Set of possible QPSK symbols
$u^{(i)}$	State of a trellis diagram of order i
u_k	State of a trellis diagram, for transition k
$u_k(i)$	i^{th} bit of a state of a trellis diagram, for transition k
w_c	Carrier angular frequency
$w_{i,k}$	Intermediate signals at instant k, with $i \in \mathbb{N}$
x	Transmitted signal on a BPSK transmission
$x(t)$	Time variant transmitted signal

$\hat{x}$	Estimation of transmitted signal x
$\hat{x}_{k,p}$	Estimation of the signal transmitted by source at instant k and subcarrier p, $x_{k,p}$
$x_b(t)$	Time variant baseband equivalent signal
$\underset{\smile}{x}_k$	Hard-value of the symbol x_k
x_k	Transmitted signal in instant sample k
$x_{k,p}$	Signal transmitted by source at instant k and subcarrier p
y	Received signal on a BPSK transmission
$y(t)$	Time variant received signal
$\hat{y}_k$	Estimation of the signal received at destination at instant k
y_k	Received signal for instant sample m
y_k	Received signal at destination, in time slot k
$y_{Ri,k}$	Received signal at relay i, in time slot k
$y_{Ri,k,p}$	Received signal at relay i, in time slot k and on subcarrier p
$z_{R,k}$	Signal after processing within a relay of the signal previously transmitted by the source at time slot k
z_{R_i}	Signal after the processing done at the relay i
z_{Ri}	Signal after processing within relay i of the signal previously transmitted by the source
$z_{Ri,k}$	Signal transmitted by relay i, in time slot k
α	Path loss exponent
β_{eq}	Total attenuation of a system
γ	Signal-to-noise ratio
Δf	Frequency separation between signals
Δt	Time interval between signals

η_{R_i}	Normalization factor at relay *i*
θ	Angle between source-to-destination and source-to-relay directions
λ	Carrier wavelength
$\lambda_k\left(u_k, u_{k+1}\right)$	Weight associated with the state transition from u_k and u_{k+1}
μ	Normalization factor in precoded symbols in precoded algorithm
μ_{R_i}	Total normalization factor at relay *i*, which includes normalization and equalization
v	Vehicular velocity
v_i	Variables that follow an exponential distribution
ξ_{R_i}	Equalization factor at relay *i*
$\rho(\Delta f, \Delta t)$	Envelope correlation coefficient separated by Δf Hz and Δt seconds
ρ_h	Module of equivalent channel matrix
ρ_m	Ratio between the minimum and maximum of channel power gains
σ^2	Variance of Gaussian distributed variables
$\sigma^2_{n_{c1}}$	Noise variance introduced by RN during the first phase of transmission in RA-1RN schemes
$\sigma^2_{n_{c2}}$	Noise variance introduced by RN during the second phase of transmission in RA-1RN schemes
$\sigma^2_{n_d}$	Noise variance introduced by UT during the first phase of transmission in RA-1RN schemes
σ_{DS}	Delay spread of a channel
σ_n	Standard deviation of real additive noise or of each of the components, real and imaginary, of the complex noise
$\sigma^2_{n_A}$	Noise variance in terminal *A*
$\sigma^2_{n_c,k+1,p}$	Equivalent noise power obtained through cooperation path in RA-1RN schemes, during time slots *k* and *k*+1, on subcarrier *p* or *p*+1
τ	Delay in seconds

τ_0	Delay of the first arrival path
τ_i	Delay of i^{th} arrival path
τ_m	Maximum excess delay of a channel
ν_χ	Degrees of freedom of a random Chi-square variable
Φ	Communication link index
φ	Loss attenuation of a transmitted signal
ϕ	Argument of complex channel attenuation
$\phi_i(t,\tau)$	Time variant argument of the i^{th} complex channel attenuation
φ_{l,q_r}	Long-term channel power of the link between q_r^{th} antenna of RN_l and UT
φ_{PL}	Path loss factor of a channel
φ_{SF}	Slow fading or large-scale-fading attenuation of a channel
ψ	Noise term contribution in RA-1RN schemes

Vectors and matrices

$\mathbf{h}$	Channel vector
$\mathbf{H}$	Equivalent channel matrix
$\mathbf{I}_n$	Identity matrix of dimension n
$\hat{\mathbf{s}}$	Vector with symbols estimated at the destination
$\hat{\mathbf{s}}_{Ri}$	Vector with symbols estimated at the relay i
$\overline{\mathbf{s}}_R$	Vector with the hard-decision symbols obtained at the a relayafter estimation
$\mathbf{u}$	Information sequence vector
$\mathbf{x}$	Transmitted signal from the source vector
$\mathbf{x}_a$	Vector formed by two transmitted symbols over two time instants, when the second one is null

$\mathbf{x}_b$	Vector formed by two transmitted symbols over two time instants, when the first one is null
$\mathbf{y}$	Vector formed by the received signals at the destination

Operators

$(\bullet)^*$	Complex conjugate-transpose operator
$(\bullet)^H$	Hermitian transpose operator
$(\bullet)^T$	Complex transpose operator
$\binom{n}{k}$	*k*-combination of a set of *n* elements
$\hat{\bullet}$	Estimation of $\bullet$
$\underset{\sim}{\bullet}$	Hard-decision value associated with $\bullet$
$\tilde{\bullet}$	Soft-decision value associated with $\bullet$
$\lvert\bullet\rvert$	Magnitude of $\bullet$
$d(\bullet,\bullet)$	Euclidean distance between two symbols
$E\{\bullet\}$	Expectation operator
$J_0(\bullet)$	Zero order Bessel function of the first kind of $\bullet$
$\Pr[\bullet]$	Probability operator
$\mathrm{P}_R(\bullet)$	pdf of a Rayleigh distribution variable of $\bullet$
$\Pr[\bullet\lvert\bullet]$	Conditioned probability operator
$\mathrm{P}_{\chi^2}(\bullet)$	pdf of a Chi-square distribution variable of $\bullet$
$Q(\bullet)$	Complementary cumulative distribution function of an Gaussian random variable with $\bullet$ following a Gaussian distribution $N(0,1)$
$\mathrm{Re}\{\bullet\}$	Real value of a complex number $\bullet$

$Var\{\bullet\}$	Variance of random variable $\bullet$
$\Gamma(\bullet)$	Gamma function of $\bullet$

1 Introduction

1.1 Perspective and Motivation

Cellular wireless systems have been undeniably successful with over 1.4 billion subscribers [GSMA]. The initial systems were designed for a single application: voice. However, a profitable cellular business can no longer rest on voice usage alone. Data services have a different set of characteristics, requiring more bandwidth than traditional voice service. Moreover, users expect to receive the same quality of service on the move as on a wired Internet protocol (IP) connection. In order to enhance the signal processing capabilities several options can be chosen. The application of smart antennas, multiple-input, multiple-output (MIMO) technologies and the usage of higher order modulations are some consensual solutions.

MIMO wireless communications are effective in mitigating channel fading, thus improving the cellular system capacity. However, there is significant correlation between channels of MIMO systems in some environments, and using an antenna array at the user terminal (UT) may not be feasible due to size, cost and hardware limitations. Thus, the very high data rates envisioned for fourth-generation cellular communication systems in reasonably large areas do not appear feasible with the conventional cellular architecture.

Cooperative based systems are promising solutions for wireless systems so that such limitations can be overcome. This can be achieved through cooperation of relay nodes (RNs), either dedicated or user terminals acting as relays, which share their antennas and thereby create a virtual

antenna array. These allow single antenna devices to combine the usual power saving with the spatial diversity without the need for additional co-located physical antenna arrays. Relaying communications present several advantages compared with conventional ones: they reduce the infrastructure development costs, provide additional flexibility in the upgrade of the network, and warrant high transmission rates, avoiding the increase in the density of base stations (BSs). Moreover, they improve the fairness in the access to the network and lead to a more uniform pattern of radiation density. In addition, cooperative systems exploring spatial diversity through RNs result in a capacity enhancement and high reliability communications [PWSH04].

This thesis presents the results of research on relay-assisted (RA) schemes, and development of new algorithms to be implemented in these cooperative schemes. Capacity analysis and bit error performances of the proposed algorithms are evaluated in realistic scenarios and over the most recent technologies.

This introductory chapter provides a survey of wireless communications and cooperative systems, and includes the motivation and objectives of this thesis, as well as the original contributions of this research work. In the next sub-section a very brief overview of the evolution of wireless systems is given. Then, in Section 1.3, we provide the classification of the most important wireless network architectures to allow for a better understanding on where the research work presented in this thesis is applied. The next sections identify and briefly review the most important technologies that are specified in order to meet some of the requirements of current and future communications such as the higher data rates and capacities, spectral efficiency, or higher reliable transmissions. In Section 1.4 we focus on the ones that are directly relevant to our work, namely orthogonal frequency-division multiplexing (OFDM) technology, multiple-antenna schemes and space-time codes whose main principles and motivation are outlined in Section 1.5. The main reference studies related with these technologies are pointed out and their evolution summarily described in these two sections. Then, Section 1.6 continues with the technology overview, concerning the recent advances and the most significant results about cooperative systems, listing the main area contributions. Following this system and technology overview, we then identify the objectives defined for this thesis work in Section 1.7. We explain how the document is organized to present the results of the research work in Section 1.8 and outline the most important contributions of this research work for the advance in the area state of the art in Section 1.9.

1.2 Evolution of Mobile Communications

Wireless communications have undergone a dramatic change in recent years. More and more people are using modern communication services, thus increasing the need for more capacity in transmissions. It all started over a century ago, when radio communications arose, discovered by Maxwell in 1867 and for the first time generated by Hertz two decades later [Maho03]. Wireless communication systems were then developed by Marconi, who showed the great potential of these communications. These first systems were used regularly in the 1920s, giving origin to the mobile communication systems. They were formed by a single transmitter, which was transmitting through all the existent channels for the total coverage area [CEUC97].

A new concept was proposed aiming to achieve higher spectral efficiency. This was the cellular concept, proposed by Ring from Bell Laboratories in 1947. The total geographical area to be covered was divided in adjacent non-overlapping hexagonal-shaped cells, each one served by a BS with a lower-power, which had just part of the total frequency channels of the system available. Thus, the BSs in non-adjacent cells could reuse the frequency channels with negligible interference and increase the number of available channels per user. The cellular network concept is considered to have given rise to the first generation (1G) of mobile communication systems.

In mobile communication systems the term ‘generation’ is used to demark the leaps in technology. Some authors considered that the generation zero (0G) is formed by the pre-cellular systems. The 1G systems were incompatible among each other and their capacity was quickly exhausted with the rapid increase in the number of users. The demand on higher quality of service (QoS) with the above mentioned reasons led to the development of the first fully digital mobile communication systems, named second generation (2G) systems. Specifications of these systems started to be defined in 1982, and led to improvements in the QoS, increased spectral efficiency and lower power BSs. The smaller and cheaper provider structure of the 2G networks was in the market in the 1990s, developed mainly for transmission of voice. Contrarily to the 1G systems, which used frequency division multiple access (FDMA) allocation, the replacing systems used time division multiple access (TDMA) to separate the channels for the different users. One of the most successful systems of this generation was the ubiquitous global system for mobile communications (GSM), which started in Europe and spread to most of the continents all over one hundred countries. Other examples were the digital cellular system 1800 (DCS1800) present in Europe, the Interim standard (IS) in the USA or the personal digital cellular (PDC) in Japan [CEUC97], [Rapp96].

In the 1990s the number of Internet users increased extraordinarily. This led to the research and development of cellular systems, so that they could provide Internet access. However, the 2G systems were limited in handling the packet oriented services required for Internet access, mainly due to the limited bandwidth and its circuit switched nature. Aiming to partially overcome these

limitations, some higher data rate evolutions were introduced, forming the 2.5G systems. Two of these technologies to transmit data packets were the general packet radio service (GPRS) and the enhanced data rates for GSM evolution (EDGE).

Answering to the demand on high speeds in packet transmission, which were not satisfied by the 2.5G, the 3G system arose. The third generation of mobile communication systems, also known as international mobile telecommunications 2000 (IMT-2000), brought new services available in indoor and outdoor scenarios, with high mobility, with different demands on the QoS and bit rates. Advertised with the slogan "Anywhere, anything, anytime", the provided services went beyond the traditional voice calls, offering multimedia applications that could use different services simultaneously, such as video calls and other video applications, high speed Internet, online games, among others. It also allowed for a soft transition to the already existent heterogeneous mobile systems. One of the main 3G systems was the European universal mobile communications system (UMTS), which was based on the wideband code division multiple access (W-CDMA) technology and specified by the European Telecommunication Standard Institute (ETSI). Other systems were the American CDMA2000 and the Chinese time-division synchronous CDMA (TS-CDMA). The International Telecommunication Union (ITU) defined some of the main standards with the intention of facilitating the growth of 3G worldwide [3GPP].

Simultaneously, for small coverage areas, wireless local area network (WLAN) systems were developed with high data rate transmissions, up to 54 Mbps, such as IEEE802.11, IEEE802.16 and HIPERLAN/2. For wireless personal area networks (WPANs), some services were also developed, as for example the Bluetooth [Chts01], [802.16], [ETSI99].

All the architectures until this generation were still cellular, since all users should access a common centralized base transceiver station. Some of the disadvantages included a singular point of failure, load balancing and spectral inefficiency. Furthermore, the output power would have to increase or the size of the cells would have to decrease in these systems, to support the increasingly demanding data rates. There were not viable options for 3G business architecture to overcome those points.

Systems beyond IMT-2000 are commonly referred to as 4G in short, and were originally conceived by the Defense Advanced Research Projects Agency (DARPA). Innumerous attempts to define 4G, from both academia and industry, were tried. However, a well-established and widely accepted definition has not emerged yet. Some characteristics are already considered certain in this architecture. One is the end-to-end IP adoption in networks, so that the users use the same data applications they were using in the wired networks. Another is the peer-to-peer characteristic, where every device is both a transceiver and a repeater for other devices in the network. Contrarily to cellular infrastructures, where users do not contribute to the network, in future communications

users will cooperate, rather than compete, for network resources. Moreover, 4G networks are seen as systems where heterogeneous networks, including technologies from the posterior generations, will interoperate in a seamless manner. Some of the recent studies aiming to achieve that goal can be found in [FFFK06], [BGQS01], [KuBr04] and [FiKa06]. ITU-R Framework Recommendation M.1645 is considered the main official guideline about 4G definition and development [ITUR03].

A strong candidate to the technology underlying 4G is the OFDM-based long term evolution (LTE). Specifications for this technology were introduced by the third generation partnership project (3GPP) Release 8 standard [3GPP07]. It promises the widest range of services from voice transmissions to real-time high-definition video, mobile TV or high speed Internet access. It is also characterized by simplification of user applications and business models with different QoS for different applications and scenarios, and with variable and on-demand bit rates. Furthermore, it allows for flexible spectrum utilization, and the achievement of a high spectral efficiency [ETSI09a]. A backward compatible enhancement of LTE is currently in development as LTE-advanced standard [ETSI09b].

1.3 Wireless Networks

The large number of different applications and services to be used through the existing infrastructures led to the appearance of several wireless network architectures. Architecture is described, by Laneman, as a set of restrictions on the structure of the network [Lane02]. There are two main classes, called infrastructure and ad-hoc networks.

In the first one low-power nodes, e.g., mobile radio terminals, connect locally to high-power points, usually stationary radios (also called access points). These access points are themselves connected via a backbone network. Typically, the backbone network is an existing wire-line arrangement, such as the public switch telephone network or the Internet. In this kind of networks, radio terminals and access points are characterized by asymmetric power and processing. Moreover, all communications occur through at least one access point. Some examples of infrastructure networks are cellular networks, satellite networks and certain wireless LANs.

The second class of wireless networks corresponds to the ad-hoc ones. They were introduced by Kahn under the name of packet radio network [Kahn77]. Numerous authors have examined issues such as scheduling, routing and organizational problems associated with these networks, such as Gupta, Kumar, Grossglauser and Tse [GuKu00], [GrTs02]. In this network, also known as peer-to-peer, radio terminals generally have more symmetric power and processing capabilities and have no need of access points or of a network backbone. Terminals communicate primarily with nearby terminals, and exchange neighbor information to enable routing throughout the network. Network tasks are conceived to be distributed rather than centralized, topology is

dynamic and routing is adaptive. In the cases of dense ad-hoc networks, a clustering algorithm divides the network into a set of clusters, each centered on a clusterhead [KaKu03]. Communication between the source and destination terminals can be made through several intermediate terminals, which is called cascade transmission or multi-hop routing. Cascade transmission potentially conserves energy by combating path loss and limiting interference in the network. However, in spite of being power efficient, multiple-hop routing with too many hops is not desirable for throughput performance [GuKu00]. Other problems in multi-hopping are delay constraints, impact of bottle neck links and error propagation. Multiple antenna systems can help to achieve the vital trade-off between the number of hops and range in a wireless network. Amateur radio, the emerging wireless local area networks and the wireless sensor networks are some examples of ad-hoc networks in operation today [Lane02].

1.4 OFDM Systems

OFDM technology was proposed for digital cellular systems in the mid-1980s and it has also been proved to be effective for digital audio and digital video broadcasting in Europe. Moreover, it has been incorporated into standards by the ETSI [Cimi85]. The IEEE 802.11 standards group recently adopted OFDM modulation for WLANs operating at bit rates up to 30 Mbit/s at 5 GHz. OFDM can largely eliminate the effects of inter-symbol interference (ISI) for high-speed transmission rates in very dispersive environments, and it readily supports interference suppression and space-time coding to enhance efficiency. Dynamic packet assignment can support excellent spectrum efficiency and high peak-rate data access.

The basic idea of OFDM is that the total bandwidth is divided into a number of orthogonal tones, over which multiple data symbols are transmitted in parallel. Let us consider the construction of an OFDM signal using N_c tones, where each of the N_c tone signals is a modulated sinusoid at a certain frequency and the frequencies of those tone signals are equally spaced. In this case, all the tone signals are orthogonal to each other in a time duration T_s, which is the reciprocal of the tone-frequency spacing. An OFDM symbol is the sum of the tone signals for time duration T_s, preceded by a cyclic prefix, which is a cyclic extension of the tone signals. The introduction of the cyclic prefix ensures that, in a multipath channel, and as long as the delay spread does not exceed that of the cyclic prefix, the multipath replicas of the OFDM symbol at the receiver always have an integer number of sinusoid cycles within the time duration T_s, thereby maintaining the orthogonality at the receiver [LaUL04], [LiLi05].

1.5 Multiple Antenna Systems

1.5.1 Diversity Concept

Diversity is a technique that can dramatically improve system performance, mitigating the effect of fading in a channel. This technique consists in ensuring that the information symbols pass through multiple independent signal paths. Several types of diversity can be identified, such as time, frequency, space or cooperative diversity, depending on the resource through each repetition of information is transmitted, as can be seen in more detail in Section 2.3. It is possible to achieve space diversity, or antenna diversity, using multiple antennas in the transmitter and/or receptor. The history of systems that explores this technique is summarized in this section. On the other hand, cooperative diversity is obtained through the use of additional nodes, known as relays, and it is explained in more detail in Section 1.6. Although applicable to any wireless setting, cooperative diversity is most beneficial when other forms of diversity, such as temporal coding, spread-spectrum, and multi-antenna systems cannot be exploited [Lane02].

Wireless MIMO channels can be accomplished through systems where several antenna elements are available at the transmitter and receiver side. Seshadri and Winters [SeWi93] had proposed two signaling schemes that exploit the availability of multiple antennas at the transmitter to provide diversity benefits in the receiver. The landmark contributions by Telatar [Tela99] and Foschini and Gans [FoGa98] have demonstrated that the capacity of a MIMO system exceeds the capacity of a single input, single output (SISO) system. They proved that when the number of transmit antennas, N_T, and receive antennas, N_R, increases, the link capacity grows in theory as $\min(N_T, N_R)$. The extra capacity of MIMO systems in comparison with SISO capacity is provided through spatially uncorrelated sub-channels.

Due to the limited inter-antenna space in mobile terminals, caused by limitations in handset designs, the use of multiple transmitting antennas at the BS attracted attentions. Moreover, the use of multiple antennas can provide significant improvements in a system in terms of capacity or diversity, thus the research in this area has evolved in both directions. Diversity techniques, in both transmitter and receiver, can be combined in MIMO systems to improve reliability in communications, though the capacity gain is sacrificed. This leads to the classical spatial multiplexing-diversity tradeoff for multiple antennas, where the amount of diversity and multiplexing gains that can be simultaneously obtained for a richly scattered Rayleigh fading channel are analyzed [ZhTs03].

1.5.2 Space-Time Codes for MIMO Systems

The benefits of MIMO systems led several authors to investigate and examine suitable coding and decoding methods for multi-antenna systems exploring antenna diversity. The association of MIMO concept with space-time coding is commonly used, aiming to increase robustness and flexibility in multimedia transmissions. Foschini [Fosc96], Alamouti [Alam98] and Tarokh [TaSC98], [TaJC99] contributed to the pioneering work on the construction of suitable space-time block codes (STBCs) to apply in multi-antenna systems, so that MIMO systems could be used to achieve diversity and combat fading using the richness of channels. In a multipath-rich wireless channel, involving multiple antennas at both the transmitter and receiver sides, it is possible to achieve high data rates without increasing the total transmission power or bandwidth.

Among the first developments to design codes that exploit the diversity provided by the use of multiple antennas, lies the work of Foschini and Gans on the Bell-lab layered space-time (BLAST) system, known as vertical BLAST (V-BLAST) architecture [Fosc96], [FoGa98]. The purpose of V-BLAST architecture was to increase capacity while exploring multipath fading. Multiple transmit antennas were used to simultaneously transmit independent data, each one using the same frequency spectrum for every transmission, which leads to high spectral efficiency [Fosc96].

The issue of decoding complexity was addressed by Alamouti [Alam98]. The concept of orthogonal STBC (O-STBC) emerged from this work. The code suggested by Alamouti is optimal for transmitting signals in a complex modulation alphabet over two independent fading channels. Decoding complexity is the strong point of this code. A linear decoding scheme is applied to both symbols, which estimates them by combining the two channels with maximal ratio combining (MRC). This code has rate one, as it transmits two symbols in two time phases, reaching the maximum diversity order, which is of two, for the two-antenna case. STBCs are generally used when the channel is quasi-static and the diversity achieved with transmission yields the same diversity advantage as MRC.

Generally, as we increase the number of antennas, more diversity gain can be obtained on the condition that there is a suitable encoding scheme. However, we cannot design rate one orthogonal encoding schemes for more than two transmitting antennas considering complex constellations. For this reason, previous studies presented O-STBCs for more than two antenna systems with rates less than one [TaJC99]. The properties of these matrices ensure full diversity equal to the number of transmit antennas, and linear maximal likelihood detection. Full spatial multiplexing rate is obtained for real codes. However, proposed complex codes have one half of the rate. Another option for the design of complex modulation STBCs for more than two antennas is by

relaxing the requirement of orthogonality. These codes are referred to as quasi-orthogonal STBCs (QO-STBCs) and their evolution is explained in the next point.

The concept of space-time trellis code (STTC) arose as an approach that combines ideas of trellis-coded modulation (TCM) with a space-time diversity approach, in order to provide additional coding gain to STBCs. They are concatenated with a TCM outer code, which provides coding gain with a reasonable complexity [Unge82]. STTCs were introduced by Tarokh, Seshadri and Calderbank [TaSC98] for open-loop transmit diversity, where no side of the channel state information (CSI) is provided by the receiver to the transmitter. They perform very well in slow fading environments, but have the drawback that decoding complexity grows exponentially with the number of antennas. Contrarily to STBCs that provide diversity gain with very low decoding complexity, STTCs provide both diversity and coding gain in detriment of a higher decoding complexity. Improvements on non-coherent and differential space-time coding and modulation methods were made by Hochwald, Marzetta and others [HoMa00], [HMRS00], [HoSW00].

1.5.3 Quasi-orthogonal STBC

In order to achieve a full rate encoding technique for more than two transmit antennas, the QO-STBC technique has been developed [Jafa01], [ShPa93], [TiBH00]. These codes have been shown to provide half of the maximum diversity possible compared to the orthogonal coding scheme. In addition, the quasi-orthogonal coding schemes are generally more complex, especially for decoding, which can be done with maximum likelihood (ML) decoding by searching pairs of symbols. The performance of these codes is the same than that of the codes from orthogonal designs at low signal-to-noise ratio (SNR), but worse at high SNR, due to the fact that the slope of the performance curve depends on the diversity order.

For open-loop communication systems, the constellation rotation was proposed for the QO-STBC with different modulation schemes [SuXi04]. Although the QO-STBC with the constellation rotation achieves full diversity, this method increases the system complexity because of constellation expansions.

For closed-loop communication systems, the CSI can be used to further improve system performance. Particularly, the CSI can be made available to all transmit antennas through a separate feedback channel. The group-coherent STBC (GC-STBC) with one-bit feedback was proposed in [YuKY06], [BaRW04]. It was pointed out that channel-adaptive QO-STBCs, using two feedback bits per code block, match the ideal 4-path diversity based on the ML decoder and zero forcing (ZF) decoder. Although a lot of partial feedback methods can be adopted to improve the closed-loop system performance, the major problems of such systems are high cost and high complexity due to the need of having more than one radio frequency chain at both link ends.

1.5.4 Drawbacks of MIMO Channels

If we increase the number of transmitters, the diversity gain can be increased, but at the same time the interference from the neighboring signals is also increased. High interference from the neighboring signals not only results in decoding complexity but may also reduce the performance. In order to solve this problem, schemes with selective receive antenna or feedback schemes were proposed, where the maximum diversity is only reached if the scheme is combined with the best antenna receiver selection [LiKL07], [LiPK08], [YuKY06].

MIMO channels promise to meet the required spectral efficiency of future wireless communications. However, as immediate consequences the increased transceiver complexity and the correlation between the transmit and receive antennas are obtained. A high correlation between the antenna elements reduces the MIMO wireless channel towards that of a single link channel. Therefore, the main challenge that a MIMO communication engineer faces in practice is to design an antenna array with mutually decorrelated antenna elements. Correlation between the antenna elements is not only influenced by the surrounding environment but also by the transceiver hardware design. A dominant plane wave, when arriving at the receiving array, is seen to be highly correlated between array elements, whereas a field resulting from impinging waves from all directions tends to be uncorrelated at a distance approximated to one half of the wavelength of antenna elements [VuYu03]. Besides, for line-of-sight communication, the field tends to be highly correlated, thus counteracting the capacity improvement promised by MIMO channels. As for the hardware design, correlation among the antenna elements is observed if their mutual spacing is too small causing electromagnetic coupling [Bala97]. MIMO channels hence promise an increase in capacity only if decorrelated signals are present at the antenna elements. Naturally, physical limitations within the mobile terminal will lead to mutual correlation between the elements thus jeopardizing MIMO capacity bounds [FiKa06].

A solution to overcome these problems is to use cooperative diversity, which is the scope of this thesis. Cooperation by sharing users' antennas can be used to achieve better end-to-end link performance, in both single hop and multi-hop scenarios.

1.6 Cooperative Communications

1.6.1 Relay Channel

The fundamental characteristic of the cooperative systems is the existence of certain network elements, called relays, which receive, process and retransmit some information in order to improve the system performance. The use of relays is considered an important technology for

future wireless systems, because of its potential to increase capacity, extend coverage, and improve access fairness, as well as to provide additional flexibility in the upgrading of the networks.

In classical relay architectures, these additional network elements are located in the network with the specific function of retransmitting information from other users, with no information of their own, with the objective of obtaining spatial diversity, getting better performance, lower rates or lower required power. In a cooperative architecture, with more than one source, terminals can cooperate with one another by serving as relay, leading to a new concept of multi-user cooperation. Results showed that, even though the inter-user channel is noisy, cooperation leads not only to an increase in capacity for both users but also to a more robust system, where users' achievable rates are less susceptible to channel variations [SeEA03a].

The basic ideas behind cooperative communications started with the relay channel definition by Meulen et al. and Cover and Gamal [Meul71], [CoGa79]. In the landmark work [Meul71], the capacity of a three node system was analyzed, for Gaussian channels, in which all nodes cooperate in the same band. The nodes are a source (S), a relay (R) and a destination (D), accordingly to Figure 1-1. The system can be viewed as a broadcast channel from the viewpoint of the source and as a multiple access channel from the destination. However, the main purpose of this groundbreaking work was to support the main channel, by passively enhancing the existent direct path, by using a relay node.

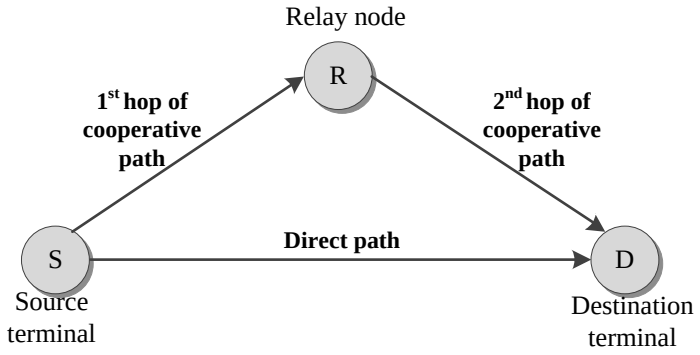

Figure 1-1: Basic three-node cooperative scheme assisted by one relay node.

Cover and Gamal made further progress by developing upper- and lower-bounds on capacity, by analyzing certain non-faded and degraded relay channels [CoGa79]. The capacity of such a relaying configuration was shown to exceed the capacity of a simple direct link. Only later the diversity gain was introduced to relaying cooperation, considering fading channels. The current research work on cooperative communication explores fading channels rather than passively enhancing a specific path of the channel.

1.6.2 Further Benefits of Cooperative Systems

Cooperative communication is one of the recent areas of research with fast growth and it is likely to be used in future systems with the aim of extending coverage or increasing capacity, while having an efficient spectrum use. Cooperation is extensively applied by human beings and animals, and can be seen as the action of obtaining some advantage by sharing, giving or allowing something. Examples of cooperation in nature are numerous such as population of ants, bees, vampire bats, hunting lions and human beings [FiKa06].

Several cooperative algorithms have been proposed and analyzed to demonstrate the potential benefits of cooperation. These algorithms describe the operations and processing modes of each node belonging to a cooperative system, including the sequence of transmitted and received signals in all communication. In some studies cooperative diversity was used as a method for increasing network capacity, as Sendonaris et al., who introduced that concept for uplink, by using a single relay applied on cellular networks [SeEA03a], [SeEA03b].

Harrold and Nix studied the relaying of SISO communications, with the aim of extending the coverage area of the cell [HaNi00]. This relaying consisted of mobile terminals, located in the edge of coverage, being used to cooperate with others, so that the BS is able to communicate with terminals out of range. In spite of the additional power consumed by the relaying process, it was showed that on average all nodes gain. This is justified by the non-linear path loss equation, since the aggregate path loss is reduced when the long distance is broken into several smaller ones.

Laneman et al. proposed several methods, which can lead to a significant reduction of the required power in the destination, through the diversity gain obtained with cooperation, for a specific error rate, while yielding full spatial diversity [Lane02]. Multiple-access protocols were suggested with an efficient energy allocation, based on the regenerative decode-and-forward (DF) and on the non-regenerative amplify-and-forward (AF) relay protocols [LaWo00], [Lane02], [LaWo03]. They extended the proposal to include multiple relays and found the outage limits for repetition-based cooperative diversity and cooperative diversity achieved by space-time codes applied in a distributed way [LaTW04]. The applicability of the suggested protocols to cellular and ad-hoc networks were discussed. Moreover, the power constraint placed on the system is an important factor to be considered for any practical deployment of a cooperative diversity network, both due to interference concerns and to ensure prolongation of battery life of the relay terminal [Haen04].

Other research work in distributed wireless network area was developed by Bletsas et al., who studied the diversity-multiplexing tradeoff in virtual MIMO systems involving multiple relays. This research study had a special focus on low complexity architectures that do not require simultaneous transmissions on the same frequency band. Therefore, they are amenable to practical

implementation with low-cost radios [BlKW06]. In [YuEr06], a theoretical diversity-multiplexing tradeoff study is presented regarding a cooperative system with one and two antennas in a single-relay scheme. Furthermore, in [MuUy08], the Rayleigh performance of a single-relay cooperative scenario with multiple-antenna nodes is investigated, deriving pairwise error probability (PEP) expressions.

In order to get higher diversity orders, one can also consider the use of multiple-relay nodes [LiSa09], [LSSK09]. However, on increasing the number of relays it reduces the bandwidth efficiency of the system, as the source only uses a fraction of the total available degrees of freedom to transmit the information.

1.6.3 Basic Cooperative Communication Protocols

Flexibility of cooperative diversity was highlighted by Nabar et al., who developed three basic cooperative communication protocols for the system in Figure 1-1 [NaBK04]. The three cooperative TDMA-based protocols are summarized in Table 1.1. In these protocols, as in [NoHH04], the RA schemes was formed by the cooperation of available UTs, acting as half-duplex relays, splitting the available time slot into two phases. The source transmits during the first phase and the relays transmit during the second phase, sending a version of the received signal to the intended destination.

TABLE 1.1: TDMA-BASED PROTOCOLS DEFINED IN [NABK04] FOR THREE NODE COOPERATIVE SYSTEM.

	Protocol I	**Protocol II**	**Protocol III**
Phase 1	S→R S→D	S→R S→D	S→R
Phase 2	S→D R→D	R→D	S→D R→D

They implement varying degrees of broadcasting (which are given by the number of nodes simultaneously listening to the source node) and receive collision (which is maximum when the D receives simultaneously from both S and R) in the network. In protocol I, the source communicates with the relay and destination terminals during the first time slot. In the second time slot, both the relay and source terminals communicate with the destination terminal. In protocol II, the source communicates with the relay and destination terminals over the first time slot. In the second time slot, only the relay communicates with the destination. Protocol III is identical to protocol I, apart from the fact that the destination terminal chooses not to receive the direct signal during the first

time slot [NaBK04]. Research on these protocols has proved to be fruitful, since it was found out that the capacity of the network will increase if the source transmits a different symbol in the second phase of transmission [WiRa03], [AzGS05].

1.6.4 MIMO and Relay-Assisted Schemes

Other works resulted from the association of the two high-performance techniques: the use of relaying channels and multiple antennas at the transmitting and receiving sides. The idea of relays mimicking a local antenna array at a user has been termed virtual antenna array (VAA). The concept stems from the contributions [3GPP99] and [HaNi00] on relaying and by [Tela99] and [Alam98] on MIMO communication aspects. This VAA concept, applied to cellular networks, was discussed by Dohler. Generalization of distributed-MIMO multi-stage communication networks, with application in distributed space-time codes, was patented [DSGA01], [DoLA02], [Dohl03]. Ganesan and Sayeed also used the term VAA or Virtual MIMO. However, they considered single transmitter, single receiver multipath channels. It was proposed a simple algorithm that transformed the multipath channel into a VAA system, where space-time codes could be directly applied [GaSa00].

Most of the extensive literature on cooperative relaying diversity considers that relay nodes are equipped with a single antenna, although some works have explored the benefits of multiple antennas in the cooperating nodes. It is fairly easy to deploy multiple antennas arrays in infrastructure-based fixed relay networks, which increases the interest in MIMO relaying [AmAT10].

In [JiHa06], the idea of space-time coding devised for a point-to-point co-located multiple antenna system is applied to a wireless relay network with single antenna nodes. The authors show that in a relay network with a single source, a single destination with L single antenna relays, distributed space-time block codes (DSTBCs) asymptotically approaches the diversity of a co-located multiple antenna system with L transmit antennas and one receive antenna. More recently, in [YiKi07], distributed orthogonal space-time block codes (DOSTBCs) achieving single-symbol decodability were introduced to cooperative networks. The authors considered a special class of these codes (row monomial DOSTBCs), deriving upper-bounds on the maximum symbol-rate. In [SrCR08], single-symbol decodable (SSD) DSTBCs were studied when the relay nodes were assumed to know the corresponding CSI. An upper bound on the symbol rate for such a set up is shown to be one half of the rate of the direct link transmission when this link is available, which is independent of the number of relays. In [HaRa09], a semi-orthogonal precoded DSTBC was proposed, wherein the source performs precoding on the information symbols before transmitting it to all the relays. Several single-antenna relays were considered. A systematic construction of these

codes was presented for more than three relays and higher rates were achieved with the constructed codes than with DOSTBCs. Despite achieving full diversity, these distributed orthogonal algorithms could not achieve full spectral efficiency, since they use two phases for transmission. For this reason, these cooperative systems achieve half of the bandwidth efficiency of the equivalent non-cooperative systems.

1.6.5 Other Techniques Used in Cooperative Systems

Some works were developed with the objective of increasing capacity or diversity order of cooperative systems, using non-orthogonal protocols for cooperative systems with two or more relays, but having no full spectral efficiency, as in [RaRa06] and [KrGB07]. In [RaRa06], a generalized non-orthogonal AF protocol was proposed with a low decoder complexity, achieving better error performances than the orthogonal protocol in [JiHa06], depending on the coding. In [KrGB07], coding strategies were studied for non-orthogonal cooperative channels, using one or more designed space-time precoders, in a protocol where inter-relay communication was allowed. In these non-orthogonal algorithms, transmission via an existing direct path is required. Thus, in situations with poor direct link conditions, performance is significantly degraded and in case of outage of one relay some information can be lost.

Further along the development of cooperative systems, some relay precoder designs were proposed, in order to improve system performance [TaHu07], [ChVa09]. In [TaHu07], the precoder maximizes the capacity between the source and destination nodes in a non-regenerative relay system, with a single RN, considering all the nodes with multiple antennas. In [ChVa09], MIMO relay provides robustness considering imperfect CSI for a multipoint-to-multipoint communication through the use of a relay precoder design.

Specific distributed space-time coding schemes were also suggested. For example in [StEr05], two spatially adjacent mobile terminals cooperate to achieve a lower frame error rate (FER) to one or more destinations, through a quasi-static fading channel. A distributed STTC was designed to maximize the performance for the direct link from either of the terminals to the destination and the relaying link. Furthermore, Hunter and Nosratnia, motivated by the advances on the relay channel and cooperative diversity, introduced coded cooperation, where cooperation is achieved through channel coding methods instead of simple repetitions [NoHH04].

Moreover, a distributed forward error correction (FEC) coding algorithm was proposed, combined with incremental relaying, where a FEC code was implemented at the source and relays, introducing additional redundancy in [BPST10]. Incremental relaying consists in the RN just transmitting when the destination is not able to receive the message from the source correctly. This distributed FEC algorithm has the advantage of having a lower spectral efficiency than distributed

space-frequency block codes (DSFBCs). However, the DSFBCs should be used in applications which require smaller bit error rate (BER) values.

Some works use more complex channel models for cooperative systems, considering the channel links modeled by Rician or Nagakami models. For example, in [AlPB10], the performance of a dual-hop DF cooperative system, with relay selection, was analyzed over Nakagami–*m* fading channels. Numerically evaluated results in that research work show that, although relaying is always beneficial in terms of average symbol error probability, in terms of outage probability it should be disabled whenever the direct link is strong. In [AdYa06] and [SuKS09], performance analysis was made when a dual hop fixed gain relaying system experiences asymmetric fading models in source-relay and relay-destination links. In [SuKS09], the results for the single nodes system under analysis confirmed that the system exhibited an improved performance in a Rician/Rayleigh (source-relay/ relay-destination links) environment compared to a Rayleigh/Rician environment. Analytical expressions for the cumulative distribution function of the end-to-end SNR were derived and used to evaluate the outage probability and the average bit error probability of *M*-QAM modulations [HaAl04]. Moreover, in [ViTH10], the PEP analysis of a DSTBC for two-hop AF relay networks is provided to investigate the achievable diversity gain of the proposed DSTBC for a general channel model in which one hop is modeled by Rayleigh fading and the other by Rician fading. This mixed Rayleigh-Rician channel model allows the analysis of two typical scenarios, where each relay is the neighbor of either the source or the destination.

Adaptive transmission is also a technique to improve the system bit rate by adjusting the transmission mode according to the channel condition. Thus, when a channel is in a good condition, the transmitter can use higher modulation modes. By integrating adaptive transmission and cooperative diversity, a system would be able to benefit from both techniques, improving system performance. However, this performance gain comes at the cost of increased system complexity that is incurred due to the additional complexity of transmitter and receiver design [NeKT09].

1.6.6 Applications of Cooperative Systems

Cooperative techniques have been object of research for different applications in wireless networks, such as cellular networks, sensor networks and wireless ad-hoc networks. For cellular systems, these techniques have been applied to multicarrier communications, such as in OFDM systems. OFDM is widely used for high-speed data transmission in wireless standard technologies, such as IEEE 802.16 and LTE, because of the advantages mentioned previously, such as its ability to eliminate ISI. In fact, relay networks combined with OFDM technology can make a strong platform for future wireless communications [ZhWL10].

A novel selective relaying scheme proposed for OFDM relay networks, called selective orthogonal frequency-division multiple access (OFDMA) relaying, was issued in [DaGC07]. In this relaying scheme, relay selection is done independently for each subcarrier, and thus different subcarriers may be sent by different paths, achieving full diversity gain at the destination.

Furthermore, advances in sensor technology, low-power electronics and radio frequency design enable the development of small sensor networks. These inexpensive sensors can be connected to develop large scale wireless sensor networks for intelligent information collection and surveillance. However, the bandwidth and energy limitations of the sensor appeared as a major challenge on the design of communication schemes for wireless sensor networks [ChYX05]. Virtual MIMO systems also arise as a desired scheme for these sensor networks, in order to extend coverage and increase capacity.

Cooperative diversity has also been a well-researched topic in the cognitive radio area. Spectrum sensing is a crucial issue in cognitive radio networks. Aiming to improve the sensing performance, cooperation among secondary users can be used to collect space diversity. For example in [DuYP10], the diversity order was quantified for various cooperative spectrum sensing strategies.

1.6.7 Standardization

The research in [3GPP99], undertaken from 1996 until 2000 within the scope of the universal mobile communication system terrestrial radio access (UTRA), proposed a relay transmission protocol called opportunity drive multiple access (ODMA), to be applied to UMTS time-division duplexing (TDD). The main purpose of the system was to increase the high data rate coverage cell as well as the capacity of TDD. It also had the goal of providing a distributed network for spot coverage and traffic hotspots. It was rejected as a candidate for UTRA because it was a relaying protocol and not a stand-alone PHY layer technology. However, due to its capacity benefits, it is now an optional protocol for UTRA TDD code division multiple access (CDMA) system.

The new wireless communication standards, LTE-Advanced and IEEE 802.16j -2009, have both adopted relaying as the solution to enhance cell edge performance. The IEEE 802.16 working group has devoted a task group to incorporating relay capabilities in the foundation of mobile Wimax-IEEE 802.16e-2005, in the amendment “Multihop Relay Specification for 802.16” (IEEE 802.16j) [PeHe09]. This was the first commercial wireless network incorporating multi-hop communication. In this case the relays are constrained to communicate in only one direction and are served by a single BS. LTE-advanced is considering more sophisticated relay strategies, as for

example designing relays with the aim of mitigating interference. Therefore, larger performance gains can be expected from the inclusion of relaying [PDFJ08], [PPTH09].

1.7 Objectives

The objective of this thesis is to study the introduction of cooperative methods in wireless communication systems, which has demonstrated its strength in offering increased performances with less complex terminals.

This thesis aims to design communication protocols which yield optimum or near optimum end-to-end data throughput for an information source communicating with an information sink via a given number of relay channels. One of the specific objectives of this research work is to analyze and evaluate several algorithms for different cooperative system configurations in terms of capacity, and compare them with the reference non-cooperative ones, focusing on the relay channel discussion.

The work conveyed by this thesis also aims at proposing and evaluating the combination of SFBCs with RA schemes. We intend to apply space-time codes in a distributed manner, directed towards OFDM-based multiple access technology, often used in recent cellular systems. We focus on the analysis of the impact that the relay channels can have in these cooperative systems for different propagation scenarios, asserting the advantages and disadvantages of these schemes.

The final objective of the thesis is to propose and evaluate the design of an algorithm that allows the spectral efficiency to be maximal, and achieves a similar or better performance than the distributed algorithms referred to in the literature. It is our intention to mathematically formulate the PEP of that algorithm and further extend it to a generic scheme with a multiple number of relays. Evaluation should be performed considering different scenarios and configurations, under requirements of the recent and near future wireless cellular standards.

1.8 Organization of the Thesis

The main research work developed to reach the previously pointed objectives is presented in the following chapters of this thesis. Its structure is described in this section. In Chapter 2, “Fundamentals of Cooperative Communications”, we present the fundamentals of cooperative systems, channel models, as well as assumptions considered throughout the thesis work. An overview of relay protocols and comparisons between them is presented. Furthermore, we introduce a detailed explanation of cooperative algorithms used to diminish some of the drawbacks of future OFDM wireless communications.

In Chapter 3, "Theoretical Capacity of Relay-Assisted Schemes", a theoretical capacity analysis of Virtual MIMO systems is presented, for different cooperative schemes, by varying the number of antennas per terminal and the number of relay nodes. We add the description of the protocols used in the different configurations, deriving the mathematical formulation that leads to the capacity expressions. Based on the instantaneous capacity expressions, outage and average capacities are obtained through Monte Carlo simulations and they are compared to each other and to some reference non-cooperative systems. We then draw conclusions about the benefits that the proposed schemes bring in terms of lower path loss effect and achieved diversity gains.

In Chapter 4, "Distributed SFBC RA Scheme for OFDM Systems", we consider the classical relaying scheme and propose a relay-assisted algorithm for downlink (DL) SFBC OFDM schemes. The performance of these cooperative systems assisted by one relay is assessed and compared against the non-cooperative SFBC OFDM based systems for different configurations, namely evaluating the impact of having different numbers of antennas at the RN. These results are presented under realistic conditions and considering different sets of propagation scenarios.

In Chapter 5, "Data-Precoded Algorithm for Relay-Assisted Schemes", we propose an algorithm that aims at an efficient improvement of the performance of cooperative systems, maintaining the same spectral efficiency as in the non-cooperative end-to-end communication. For the analyzed scheme two relays assist the communication, each equipped with one or two antennas. This new algorithm allows single-antenna mobiles to obtain some of the benefits of MIMO systems. It is presented and compared for different configurations with a different number of relays and antennas in each node, as well as against the equivalent non-cooperative systems with co-located antennas. The precoded algorithm consists in using a simple precoding at source and alternate transmission through relays. By exploiting its trellis structure, this method minimizes the power penalty caused by the higher order modulation of conventional cooperative schemes, while reaching full diversity.

Finally, in Chapter 6, "Conclusions and Future Work", we point out the overall conclusions of this research work and provide the foundations for future work.

1.9 Contributions of the Thesis

The scientific research work developed in this thesis can be synthesized as follows:

- Theoretical analysis of the capacity of relay-assisted schemes for different configurations and comparison of their performances in terms of outage and average capacities with equivalent non-cooperative systems.
- Proposal of a distributed SFBC algorithm for two relay-assisted schemes with a single relay, equipped with one and two antennas for OFDM based systems.

Analytical derivation and assessment of the main signal expressions for those schemes and considering several relay protocols.

- Proposal of a algorithm for two RNs, with almost full spectral efficiency based on the precoding of symbols at source and alternate transmission through both relay. Analytical derivation and assessment of the main signal expressions for those schemes, considering several relay protocols. Analytical derivation of the error probability and the gains obtained with the proposed algorithm against other cooperative algorithms.
- Extension of the data precoded algorithm for a multiple number of RNs equipped with multiple antennas. Analytical derivation of the main signal expressions and gains of the proposed algorithm with other cooperative schemes for the generic configuration case.
- Evaluation of performances of distributed SFBC and precoded algorithms for different configurations of RA schemes, in terms of bit error rates and frame error rates, considering realistic scenarios based on LTE specifications and for several propagation scenarios. Comparison of the RA schemes with these proposed algorithms against non-cooperative reference systems.

The original publications in International Scientific Journals are listed below, from the earliest to the most recent:

- A. Moço, S. Teodoro, A. Silva, H. Lima, and A. Gameiro, "Single and multiple antenna, relay-assisted techniques for uplink and downlink OFDM systems", *IARIA International Journal on Advances in Systems and Measurements*, vol. 3, no. 1 and 2, pp. 22-34, Sep. 2010.

- V. Bota, Zs. A. Polgar, A. Silva, S. Teodoro, M. P. Stef, A. Moço, A. Botos, and A. Gameiro, "Combined distributed turbo coding and space frequency block coding techniques", *EURASIP Journal on Wireless Communications and Networking*, vol. 2010, Article ID 327041, 14 pages, 2010.

- S. Teodoro, A. Silva, J. M. Gil, and A. Gameiro, "Novel precoded relay-assisted algorithm for cellular systems", *EURASIP Journal on Wireless Communications and Networking*, vol. 2010, Article ID 414657, 10 pages, 2010.

- S. Teodoro, A. Silva, J. M. Gil, and A. Gameiro, "Data-Precoded Algorithm for Multiple Relay-Assisted Systems", submitted to *EURASIP Journal on Advances in Signal Processing*, Aug. 2011.

The contributions to International Conferences were the following, also listed from the earliest to the most recent:

- S. Teodoro, A. Silva, J. M. Gil, and A. Gameiro, "Capacity comparison between Alamouti and cooperative VAA with EF and AF relays", in *Proc. of the* 17th

International Conference on Telecommunications (ICT-Mobile Summit '08), Stockholm, Sweden, pp. 1-10, June 2008.

- A. Moço, S. Teodoro, A. Silva, and A. Gameiro, "Relay-assisted cooperative schemes for the UL OFDMA based systems", in *Proc. of the 4th International Conference on Wireless and Mobile Communications (ICWMC'08)*, Athens, Greece, pp. 71-76, Aug. 2008.

- S. Teodoro, A. Silva, J. M. Gil, and A. Gameiro, "Capacity comparison of relay-assisted schemes with and without direct path ", in *Proc. of the 18th International Conference on Telecommunications (ICT-Mobile Summit'09)*, Santander, Spain, pp. 1-10, June 2009.

- S. Teodoro, A. Silva, J. M. Gil, and A. Gameiro, "Virtual MIMO schemes for downlink space-frequency coding OFDM systems", in *Proc. of the 20th IEEE Personal, Indoor and Mobile Radio Communications (PIMRC'09)*, Tokyo, Japan, pp. 1322-1326, Sep. 2009.

- S. Teodoro, A. Silva, J. M. Gil, and A. Gameiro, "Distributed space-frequency block coding for a 2-antenna relay in downlink OFDM systems", in *Proc. of the 9th IEEE International Symposium on Communication and Information Technology (ISCIT'09)*, Incheon, Korea, pp. 853-858, Sep. 2009.

- S. Teodoro, A. Moço, A. Silva, and A. Gameiro, "Performance evaluation of a distributed SFBC relay-assisted scheme for OFDM systems", in *Proc. of the Future Network and Mobile Summit 2010*, Florence, Italy, pp. 1-10, June 2010.

- S. Teodoro, A. Silva, J. M. Gil, and A. Gameiro, "Distributed space-time code using precoding for cellular systems", in *Proc. of the 72nd IEEE Vehicular Technology Conference (VTC'10)*, Ottawa, Canada, pp. 1-5, Sep. 2010.

- S. Teodoro, A. Silva, J. M. Gil, and A. Gameiro, "Data precoded relay-assisted scheme for cellular systems", in *Proc. of the 21st IEEE Personal, Indoor and Mobile Radio Communications (PIMRC'10)*, Istanbul, Turkey, pp. 2413-2418, Sep. 2010.

- S. Teodoro, A. Silva, J. M. Gil, and A. Gameiro, "Precoded multiple relay-assisted scheme for cellular systems", in *Proc. of the 13th International Symposium on Wireless Personal Multimedia Communications (WPMC'10)*, Recife, Brazil, pp. 1-5, Oct. 2010.

2 Fundamentals of Cooperative Communications

2.1 Introduction

In this chapter we introduce some of the basic literature concepts of wireless communications, particularly of cooperative ones, which are needed to understand the proposed work. The chapter reviews the relevant models for channel characterization and provides the main background required for the understanding of cooperative communications, extending the basic overview provided in Chapter 1.

Radio channel modeling is of extreme importance to the performance evaluation of wireless communications, thus the classification of channels in terms of time and frequency is presented in Section 2.1. Some of the main channel models that can be used in communication analysis are also described.

In Section 2.3, we review the main types of diversity. As pointed out in Chapter 1, cooperative diversity is one of the existing forms of diversity. Cooperative communications make use of this type of diversity by relaying information through available distributed channels. Wireless terminals can benefit from the cooperative diversity through the relayed information over multiple paths, resulting in redundancy at the destination. This redundancy allows the destination to essentially average channel variations resulting from fading, shadowing, and other forms of interference. Through cooperative diversity, the reliability of communications can be improved by decreasing error or outage probabilities for a given transmission rate. Cooperative communications

can also be used to increase the transmission rate. In both cases, cooperation allows for tradeoffs between target performance and required transmitted rates. In the following section, the main elements that form the cooperative communications as well as basic cooperative schemes are introduced. Some of them are object of study in the next chapters. Jointly with relays characterization, the main existent relay protocols are defined, where the main processing operations and the flowing of signals in this type of communications are explained.

Then, in Section 2.5, the fundamentals about signals detection are mentioned for point-to-point communications, comparing coherent with non-coherent detection methods. Detection for cooperative communications is also referred to, with focus on the availability of the CSI among the existent nodes.

2.2 Channels Characterization

Modeling the radio channel is fundamental to evaluate the performance of wireless communications. There have been many studies about channel models of different types. Some of them are briefly described in this section.

2.2.1 Classification of Channels Concerning Time and Frequency

Time dispersion and frequency-selective fading are both manifestations of multipath propagation with delay spread and each one implies the presence of the other. Time dispersion extends such a signal in time that the duration of the received signal is greater than that of the transmitted signal. The minimum transmission bandwidth at which time dispersion is observable, B_m, is inversely proportional to the maximum excess delay of the channel, τ_m. Relation between both variables depends on the system. The constant of proportionality usually used is 1/4, resulting in the relation

$$B_m = \frac{1}{4\tau_m}, \tag{2.1}$$

where the maximum excess delay is obtained by

$$\tau_m = \max_i \left(\tau_i - \tau_0 \right), \tag{2.2}$$

τ_i is the delay of i^{th} path and τ_0 is the delay of the first arrival path.

Frequency-selective fading filters attenuate certain frequencies of the transmitted signal more than others. If the bandwidth of the transmitted signal is sufficiently narrow, then all the transmitted frequency components will receive about the same amount of attenuation, having no frequency selective fading.

A measure of the transmission bandwidth at which distortion becomes appreciable is often based on the channel coherence bandwidth. The coherence bandwidth, B_c, indicates the minimum frequency separation needed so that the attenuation of the amplitudes of two frequency components becomes decorrelated. The coherence bandwidth can also be regarded as the maximum frequency separation for which propagation conditions are strongly correlated. Formally, the coherence bandwidth is the bandwidth for which the auto co-variance of the signal amplitudes at two extreme frequencies reduces 3 dB. A measurement of decorrelation is the value of envelope correlation coefficient, $\rho(\Delta f, \Delta t)$. The frequency components become decorrelated when this coefficient takes the target value of 0.5, that is $\rho(B_c, 0) = 0.5$ [Stee92].

The envelope correlation coefficient for two signals for separated by Δf Hz and Δt seconds, for a Rayleigh-model and assuming that the delay profile has an exponential shape and the incident power is isotropically distributed, is equal to

$$\rho(\Delta f, \Delta t) = \frac{J_0^2(2\pi\Delta t)}{1+(2\pi\Delta f)^2 \sigma_{DS}^2}, \tag{2.3}$$

where $J_0(\cdot)$ is the zero order Bessel function of the first kind, and σ_{DS}^2 is the delay spread of the channel. To observe the decorrelation of two signals as their frequency separation is increased, Δt is set equal to zero in (2.3), which gives the frequency correlation function in the expression that follows

$$\rho(\Delta f, 0) = \frac{1}{1+(2\pi\Delta f)^2 \sigma_{DS}^2}. \tag{2.4}$$

The correlation bandwidth is thus obtained from (2.4) for the target of 0.5 resulting in the following expression

$$B_c = \frac{1}{2\pi\sigma_{DS}}. \tag{2.5}$$

Frequency dispersion and time-selective fading appear in time variant channels, due to Doppler spreading. Frequency dispersion results in the signal bandwidth being stretched, so that the received bandwidth of the signal is different from that of the transmitted signal. The minimum signal duration at which frequency dispersion becomes noticeable, T_m, is given by

$$T_m = \frac{1}{4 f_m}, \tag{2.6}$$

where f_m is the magnitude of the maximum Doppler shift experienced by the signal. The maximum Doppler shift for a vehicular velocity of v is represented by $f_m = v/c$, with c

representing the velocity of light. Time selective fading can cause signal distortion, because the signal may change its characteristics while the signal is being transmitted.

A signal is said to have a short duration when it is passed through the channel before any significant change in the channel characteristics can take place. As the signal duration is increased, the channel is able to change while the signal is still in transmission, thereby causing distortion. We can estimate the duration of the transmitted signal at which distortion becomes noticeable, by referring to it as the channel coherence time, T_c. Analogously to the channel coherence bandwidth, the coherence time is defined by $\rho(0,T_c)=0.5$. To observe the decorrelation of two signals as their time separation is increased, Δf is set equal to zero in (2.3), resulting in the expression

$$\rho(0,\Delta t)=J_0^2(2\pi\Delta t). \tag{2.7}$$

Setting (2.7) to 0.5 we obtain an approximation for coherence time presented as

$$T_c=\frac{J_0^2(2\pi\Delta t)}{2}\approx\sqrt{\frac{9}{16\pi f_m^2}}, \tag{2.8}$$

which indicates the maximum time duration for which propagation conditions are strongly correlated.

The coherence time and coherence bandwidth are properties of a channel and may be used to know how a transmitted signal will be affected according to its bandwidth and time duration. These classifications, related to the bandwidth and the duration of the transmission signal are summarized in Figure 2-1. They emphasize the differences between distorting and dispersive channels. The shaded area of the figure indicates the physical restriction that limits the time-bandwidth product of a signal to be less than ½. T_x is the duration of the received signal, obtained by the transmitted signal duration added to channel delay spread. Similarly, B_x is the bandwidth of the received signal. Therefore, through Figure 2-1 and according to the above explanation we easily obtain the classification of the channel in terms of time and frequency. This is made by comparing the bandwidth of transmission with B_c and B_m and the signal duration with T_c, and T_m. If the bandwidth of a transmission is less than the coherence bandwidth of the channel, the channel does not have a frequency selective fading and distortion time. The channel is viewed as having a flat response across the transmission band and is therefore referred to as being frequency-flat. Similarly, if the duration of the received signal is less than the coherence time, the channel is constant for the duration of the signal transmission. For this reason the channel is referred to as time-flat.

When a channel is flat in both frequency and time, it is called a flat-flat channel. On the other hand, if a channel is not flat either in frequency or in time, it is often referred to as non-flat

channel. In another example, if the signal duration is lower than T_c and the bandwidth of transmission is between B_m and B_c bandwidths, then the channel is characterized as frequency distorting and time flat.

More generally, the channels are often classified as narrowband or wideband. A *narrowband* channel is flat in frequency and has no dispersion in time. In the *wideband* channel models, the symbol rate is sufficiently high so that each symbol is spread over adjacent symbols causing inter-symbol interference. This happens when the bandwidth of the transmitted signal oversteps the coherence bandwidth, as well as when the signal time duration exceeds coherence time. The channel is said to be frequency selective and time dispersive.

In addition, *wideband directional* channel models deal with both temporal and angular domains. In these models, additional parameters are considered such as angle-spread, which corresponds to the maximum angle deviation between the arrival angles of the signals with which signals are correlated. The channel is considered as directional for transmissions with angles of arrival that exceed the angle-spread [Stee92], [Jake74].

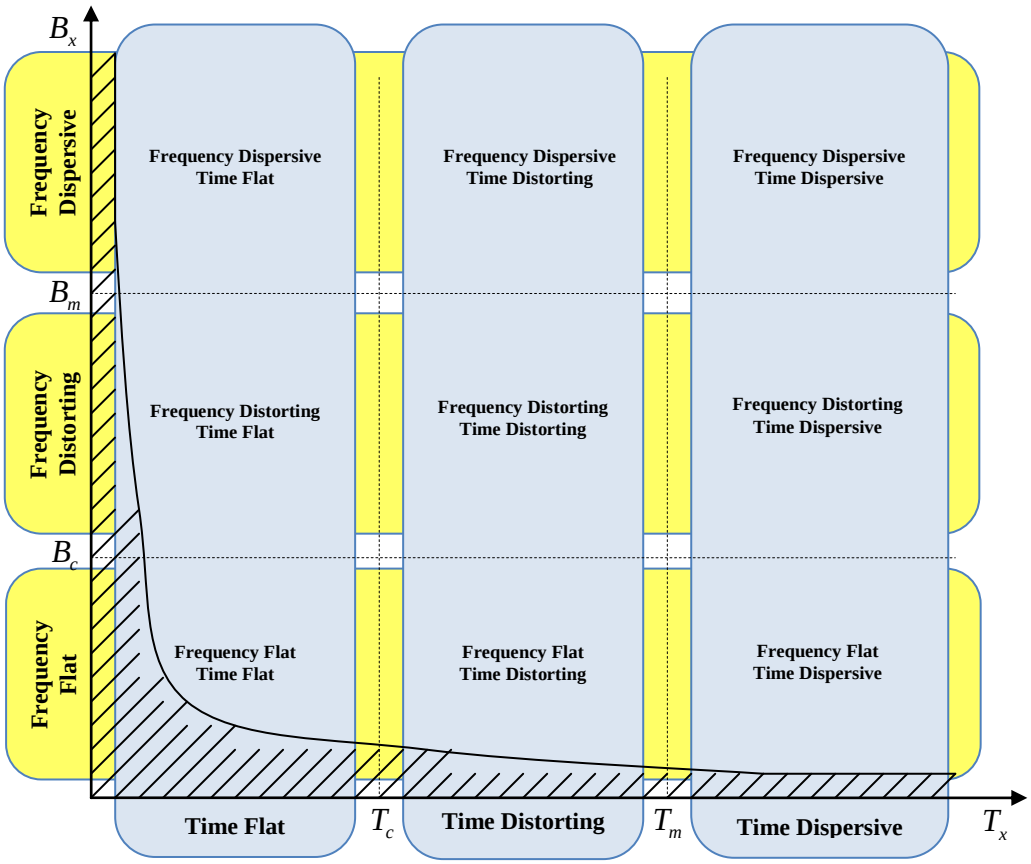

Figure 2-1: Channel classification in relation to frequency and time (based on [Jake74]).

2.2.2 Statistics for Channel Modeling

Through several channel measures, channel characterizations were constructed into models that are valid over a range of conditions, setting how quickly channels change and how much they vary. These models have the knowledge of their inaccuracy and dependence on external factors. They are important and are used as approaches in experiences and theoretical comparisons.

The transmitted signals can be affected by large-scale and small-scale propagation effects, which can be characterized by models. Let us consider the relation between the output signal $y(t)$ and the input $x(t)$ given by the following expression

$$y(t) = x(t)\varphi + n(t), \tag{2.9}$$

where $|\varphi|^2$ is the loss in power of the transmitted signal:

$$|\varphi|^2 = |\varphi_{PL}|^2 |\varphi_{SF}|^2. \tag{2.10}$$

The effects that contribute to these losses are noticeable over relatively long distances and are referred to as large-scale propagation effects. Path loss is one of these effects that contribute to signal impairment by reducing its power, as represented in (2.10) by $|\varphi_{PL}|^2$. The path loss is the attenuation suffered by a signal as it propagates from the source to the destination. Another effect that contributes for the loss in the transmitted power is shadow fading or slow fading. This one results from the transmitted signal being obstructed by different objects as it travels to the receive antennas and is represented in (2.10) by $|\varphi_{SF}|^2$.

The path loss factor, generally characterized by

$$|\varphi_{PL}|^2 = \frac{k_0}{(d_t)^{\alpha}} \tag{2.11}$$

is dependent on the transmission distance, d_t, and on a constant , k_0, taken from the Friis expression. This constant includes parameters that are related to the physical setup of the transmission, such as signal wavelength and antennas height. The path loss factor also depends on the path loss exponent, α, which is itself dependent on the environment. The path loss exponent characterizes the rate of decay of the signal power with the distance, taking values in the range of 2 (which corresponds to free space propagation) to 6. Typical values for the path loss exponent are 4, for an urban macro cell environment, and 3, for urban micro cell [LiSa09].

The slow fading or large-scale-fading factor is caused by reflections in large objects as it travels to the receiving antennas, which we call shadow effect. Since the nature and location of the obstructions that cause this effect cannot be known in advance, the loss introduced by this effect is a random variable. More specifically, it follows a log-normal distribution, according to

$$10\log_{10}\left(\left|\varphi_{SF}\right|^2\right) \sim N\left(0,\sigma_{SF}^2\right). \tag{2.12}$$

As a result of the random reflectors, scatterers and attenuators that a transmitted signal encounters in a wireless communication, multiple copies of the transmitted signal arrive at the destination, through different paths. The channel that characterizes such a communication is referred to as *multipath channel*. Besides the mentioned random objects, other factors influence a multipath channel. The speed of the mobile terminal or of the surrounding objects and the transmission bandwidth of the signal are some of them. The multiple copies of the transmitted signal that arrive at the destination are added, creating either constructive or destructive interference with each other.

The corresponding channel characterization, $h(t,\tau)$, for frequency and time selective channels is given by the expression

$$h(t,\tau)=\sum_{i=0}^{N-1} a_i(t,\tau)e^{j\phi_i(t,\tau)}\delta\left(\tau-\tau_i(t,\tau)\right), \tag{2.13}$$

with $a_i(t,\tau)$ and $\phi_i(t,\tau)$ as the amplitude and argument of complex channel attenuation values and *N* as the number of resolvable paths at the receiver.

The term *fading* describes the variation of the local channel due to the varying phases and amplitudes of the scatterers. *Fast fading*, also called small-scale-fading, derives from reflections in small objects and is noticeable at distances in the order of the signal wavelength.

There are an extended number of different models that characterize a fast fading channel, with different complexity degrees and specific parameters that the user can choose, as observed in the channel characteristics and classifications in the previous section. Several statistical distributions use fast fading models in the characterization of the behavior of channel envelope. They are Rayleigh, Rice, Nagakami, Weibull distributions, among others.

The additive white Gaussian noise (AWGN) channel is the simplest channel model. It is equivalent to having the noise generated in the receiver when the transmission path is ideal, where the noise is assumed to have a constant power spectral density (PSD) over the channel bandwidth, and a Gaussian amplitude probability density function (pdf).

It is possible to have a Gaussian channel in digital mobile radio, like in microcells having a line-of-sight (LoS) with essentially no multipath. Even when there is multipath fading, but the mobile is stationary and there are no other moving objects, the mobile channel can be considered to be Gaussian, with the effects of fading represented by a local path loss.

The Gaussian channel is often used to provide an upper bound on system performance. The multipath fading effect increases BER performance of a given SNR channel. By using techniques

to combat multipath fading, such as diversity, equalization, channel coding, data interleaving, and so forth, we can observe how close the BER performance approaches that of the Gaussian channel.

If each multipath component in the received signal is independent, then the pdf of its envelope is characterized as being of Rayleigh. This is the simplest probabilistic model for the channel filter taps and it is based on the assumption that there are a large number of statistically independent reflected and scattered paths with random amplitudes in the delay window corresponding to a simple tap. The phase of the i^{th} path is $2\pi f_c \tau_i$ or $2\pi d_i/\lambda$, where d_i is the distance travelled by the i^{th} path, f_c and λ are carrier frequency and wavelength respectively. As the reflectors and scatterers are far away from the carrier wavelength ($d_i \gg \lambda$), it is reasonable to assume that the phase for each path is uniformly distributed between 0 and 2π and that the phases of different paths are independent.

A path is the sum of a large number of small independent circular symmetric complex random variables. According to Central Limit Theorem, each path is in fact circular symmetric, i.e., follows $CN\left(0,\sigma^2\right)$ [TsVi05]. Its magnitude is that of a Rayleigh random variable, with a pdf given by

$$p\left(a_R\right) = \frac{a_R}{\sigma^2} e^{-\frac{a_R^2}{2\sigma^2}}, a_R \geq 0, \tag{2.14}$$

and with mean and variance given respectively by

$$E\left\{a_R\right\} = \sqrt{\frac{\pi}{2}}\sigma \tag{2.15}$$

and

$$Var\left\{a_R\right\} = \frac{4-\pi}{2}\sigma^2 . \tag{2.16}$$

To simplify we refer to the channel envelope as $a_R = \left|h(t)\right|$, and σ^2 represents the variance of Gaussian distributed variables. In order to have a unitary power for channels the variance should be given by $\sigma^2 = 1/2$.

A Rayleigh fading profile channel can be modeled using the arrangement shown in Figure 2-2. Basically it is formed by two quadrature channels, starting with the two Gaussian noise sources. The outputs from these blocks are applied to filters that represent the effects of Doppler frequency shifts. These filters do not change the Rayleigh envelope statistics of the channel model, but introduce the necessary correlation between frequency components in the channel. The channel is characterized by the sum of the quadrature components $h_{I_b}(t)$ and $h_{Q_b}(t)$, and can be represented as

$$h(t) = \mathrm{Re}\left\{h_b(t)e^{j\omega_c t}\right\}, \tag{2.17}$$

where $h_b(t)$ is the complex baseband representation of $h(t)$. This model is quite reasonable for scattering mechanisms where there are few reflectors. It is adopted primarily due to its simplicity in typical cellular situations, with a relatively small number of reflectors.

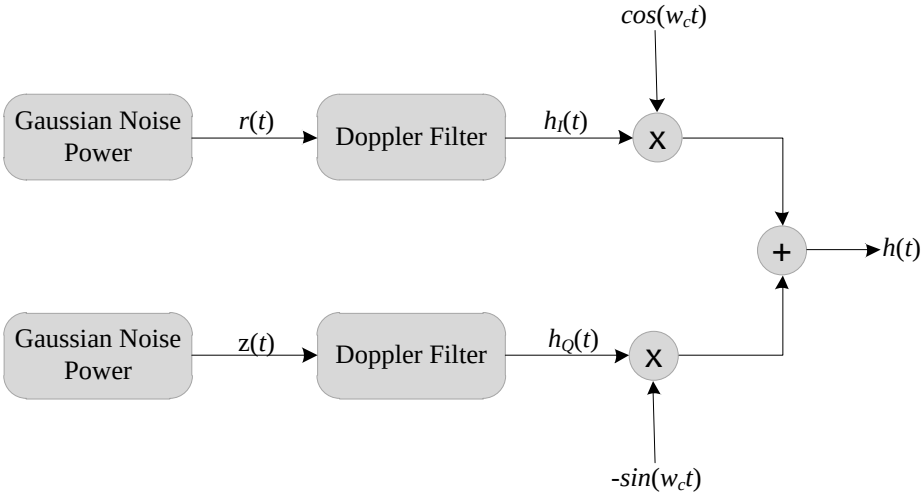

Figure 2-2: Model to generate a Rayleigh fading profile.

In the cases where there are fixed scatterers or signal reflectors in the medium, besides the randomly moving scatterers, the channel cannot be modeled as having a zero-mean. In this case the envelope can be characterized by a Rice distribution, and the channel is said to be Rician. This model has a dominant path (in general the line-of-sight path or specular path) and a large number of independent paths. This dominant path may significantly decrease the depth of fading.

The parameter *K*, which characterizes this model, is the ratio of the energy in the dominant path to the energy in the scattered paths. The larger the *K*, the more deterministic the channel is. Notice that when *K* is zero the channel is Rayleigh, whereas if *K* is infinite the channel is Gaussian. The magnitude of such a random variable is said to have a Rician distribution and its density has a quite complex form [Stee92], [TsVi05].

Nagakami-*m* distribution is also an alternative statistical model for the envelope of the channel model. This model can be used in conditions that are either more or less severe than Rayleigh distribution, and it includes the Rayleigh distribution as a special case. This model was shown to be the best option for data signals received in urban radio multipath channels [Proa01].

2.3 Basic Diversity Forms

Diversity is a technique that can dramatically improve system performance, reducing the effect of fading in a channel. This technique consists in ensuring that the information symbols pass through multiple independent signal paths.

Diversity techniques that mitigate the effects of shadowing from buildings and objects are called macrodiversity, while the techniques that reduce the multipath fading effect are named microdiversity. *Macrodiversity* is generally implemented by combining received signals by several BSs or access points. The coordination required among these points is implemented as part of the networking protocol in infrastructure-based wireless networks.

Microdiversity techniques are usually applied by realization of independent fading paths, which can have receiver diversity, transmitter diversity or both. The mainly known types of microdiversity are time, frequency and space diversity, briefly referred to in Section 1.5.1. However, there are other types as well, such as polarization and directional diversity.

Due to multipath fading the communication channel changes its characteristics over time. Therefore, transmitting at different time leads to diversity, called *time diversity*. In this case we transmit the overall signal over different time slots, with longer duration than the coherence time. Time diversity does not require an increased transmitted power. However, it does lower the data rate, since data is repeated for different time slots rather than new data being sent in those time slots. Time diversity can also be achieved through other techniques, as coding and interleaving: information is coded and the coded symbols are dispersed over time in different coherence periods, so that different parts of the codewords may experience independent fades.

Another type of diversity is achieved by transmitting the same narrowband signal at different carrier frequencies, where the carriers are separated at least by the coherence bandwidth. This results in *frequency diversity*, since the different characteristics of the channels change at different frequency carriers, caused by frequency selective fading.

Furthermore, channels used from different points in space have their own unique fading characteristics, leading to diversity if transmission occurs from several different points, which is called *space diversity*. This type of diversity can be achieved using multiple antennas in the transmitter and/or receptor, and it is referred to as *antenna diversity*. With the development of multiple antenna systems, space-time coding techniques arise, using space and temporal diversity techniques simultaneously [TsVi05].

The use of MIMO systems leads to optimum results in terms of spectral efficiency and to lower probability of incorrectly decoding data. Although the equipment at the BS in a cell can be readily equipped with a multi-element antenna array, physical size limitations of cellular mobile terminals preclude the fitting of more than two antenna elements. The challenge now to wireless

network designers is how to achieve the high capacities offered by MIMO in a cellular or ad-hoc environment.

Space diversity can be reached when additional nodes, named relays as referred to in Section 1.6, cooperate in a point-to-point communication. These nodes can be other users or dedicated terminals with the objective of helping other users' communications. Through this form of diversity, called *cooperative diversity*, it is possible to increase the capacity or the reliability of a system, with a low infrastructure cost. Cooperative diversity appears as a promising application for the demanding future networks [TsVi05], [KlSS96], [Gold05]. This is the focus of this thesis.

2.4 Elements of Cooperative Systems

In this section, we summarize some of the main elements of cooperative systems and illustrate some of their advantages.

2.4.1 Characterization of Relay Nodes

Relays appeared as one of the main ways of achieving cooperative diversity. They bring some benefits to the system such as path loss savings and macrodiversity gains, which allow to combat shadowing. Moreover, diversity gain can be achieved due to the presence of independent paths from the relay to the destination as well as coverage extension, among other benefits.

Two types of relays can be found: dedicated or cooperative-user. They can be *dedicated* and fixed nodes, with the only objective of helping other users through cooperation. In this case, these fixed nodes are usually wirelessly connected to the source, and they are called infrastructure relays. They can also be *cooperative-user*, which can act as terminal nodes, transmitting their own information, or as RNs, transmitting information of other users. Exemplification of a downlink transmission from a BS to a UT is in Figure 2-3, in a cellular application. In this figure Relay 1 is a cooperative-user and Relay 2 is a dedicated relay. In this example relays are helping other users within the cell range coverage. However, as mentioned before, relays can be strategically located so that coverage can be extended as in Figure 2-4.

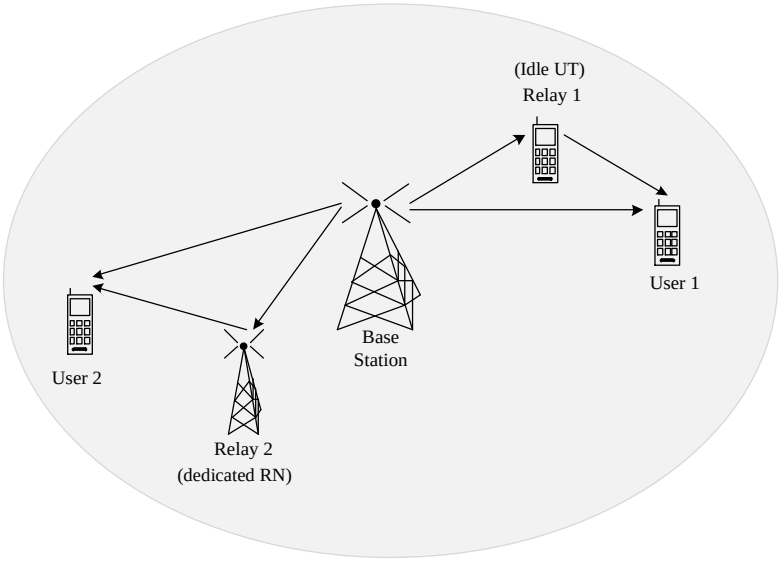

Figure 2-3 : Cooperative transmission scheme illustrating dedicated and cooperative-user relays.

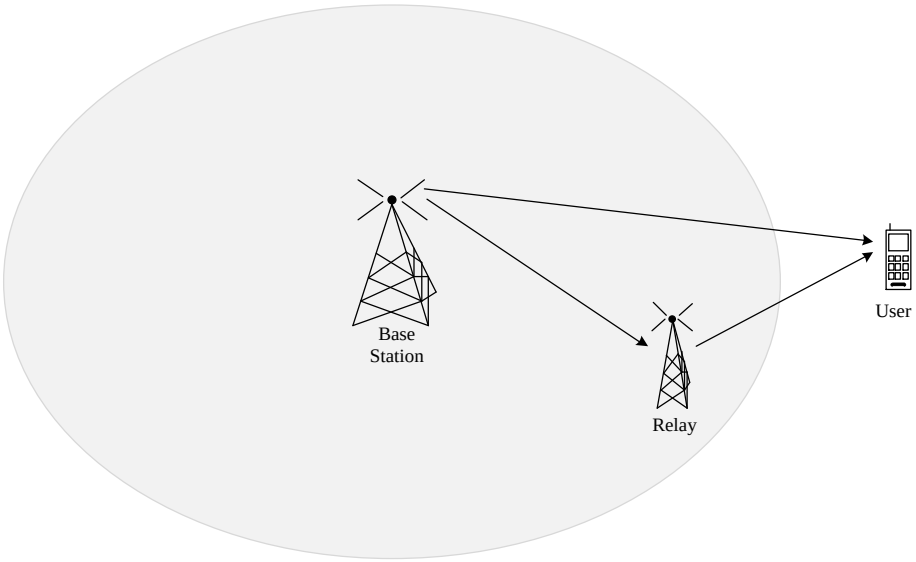

Figure 2-4 : Cooperative transmission scheme illustrating cell coverage extension.

Relays can have two modes of allocation resources (time or frequency) for reception and transmission: *half-duplex* or *full-duplex*. In the first case relays cannot transmit and receive at the same time or frequency, while full-duplex relays transmit and receive simultaneously. The relay type usually used is the half-duplex, due to practical constraints in hardware to transmit and receive in the same time or frequency block, since in most wireless systems transmission and reception are coupled at the same antenna. As a result, relays require at least two orthogonal time or frequency blocks to receive and transmit.

Concerning the direction, relays can be *one-way* or *two-way*, when they cooperate just in one direction or in both directions (uplink and downlink), respectively. In the case of two-way

relays, both cooperative links must have good quality of transmission. Despite the higher complexity in relay selection for this case, the total overhead needed will be reduced, since when the relays are selected we can transmit in both directions.

2.4.2 Basic Cooperative Systems

Let us consider the basic point-to point communication system, formed by a source sending a signal to a destination through a continuous direct link, as represented in Figure A-1, in Annex A. Other reference non-cooperative schemes that are used for comparison purposes in our research study are also described in that annex. Both nodes are equipped with single antennas and the scheme is referred to as SISO system. The channel link that allows the communication between these two terminal nodes is represented by $h_{S,D}$. If a RN, also equipped with a single antenna, is used to help in this point-to-point communication, the simplest cooperative scheme is obtained, as shown in Figure 2-5. This scheme is generally referred to as the classical three-node cooperative system. In this case the maximum diversity that can be achieved is of 2. Two types of links are identified in this scheme: cooperative and non-cooperative links. The *cooperative channel links* are identified by $h_{S,R}$ and $h_{R,D}$, which correspond to the source-to-relay and relay–to-destination channel links, respectively. The non-cooperative link corresponds to the direct path. In this scheme, the existence of communication through the direct link is essential if it is intended to achieve space diversity.

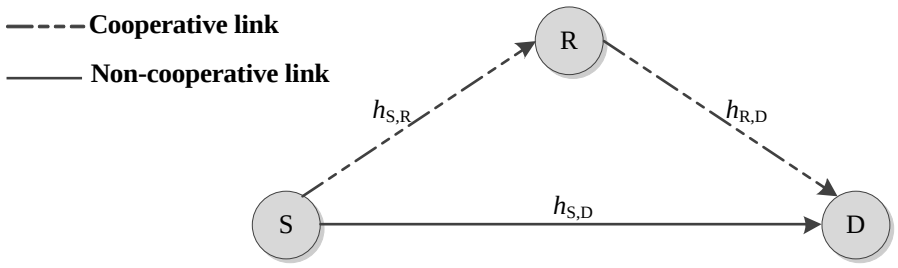

Figure 2-5 : RA scheme with one relay and all nodes equipped with a single antenna.

The RA system with two relays is shown in Figure 2-6. The maximum diversity achieved through this cooperative scheme is of 2 or 3, depending on whether we consider or not the existence of communication through the direct link. Such a system is considered a virtual multiple input, single output (MISO) system when viewed from the destination, or a virtual single input, multiple output (SIMO) when viewed from the source. Viewing the two relays as part of a MISO system, we further implement Alamouti coding in a distributed manner. The communication is divided into two phases, since the relays are considered to be half-duplex. During the first phase, two information symbols are broadcast from S to R_1 and R_2, while during the second phase they are

retransmitted using Alamouti coding. This code and other space-time codes useful for this study are defined in Annex A, with applicability in both cooperative and non-cooperative schemes.

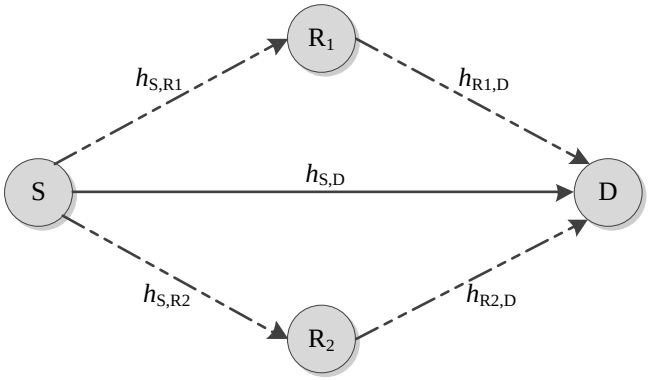

Figure 2-6: RA scheme with two relays and all nodes equipped with a single antenna.

A general scheme with L relays cooperating in the source-to-destination communication is represented in Figure 2-7. The channel link between nodes A and B is represented by $h_{A,B}$, with $A \in \{S, R_1, R_2, ..., R_L\}$ and $B \in \{R_1, R_2, ..., R_L, D\}$. The maximum diversity order achieved is of $L+1$. For each of these mentioned schemes various procedures and actions can be performed in relays, which depend on the relay protocol adopted.

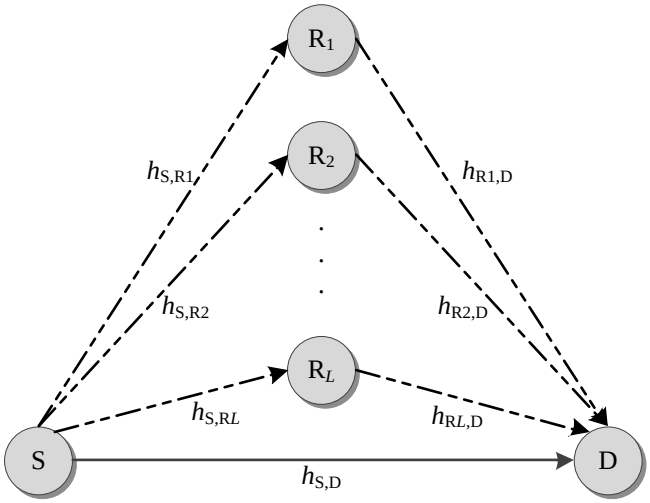

Figure 2-7: RA scheme with L relays and all nodes equipped with a single antenna.

The two most common performance measure used for evaluation of a cooperative system are the symbol or bit error rate and the capacity of the system, which corresponds to the maximum achievable data rate that can be transmitted over the link with an arbitrary low probability of error. Moreover, the throughput performance measure describes the actual achievable data rate over the communications. This performance measure differs from the capacity due to practical limitations, such as finite allowable modulation size for the data transmission or higher layer overhead

requirements. At last, radio link quality is a performance measure that is evaluated based on the success rate of decoding of a specified signaling channel, control or synchronization. This parameter can be directly used as a reliability measure of the radio link that we intend to analyze.

2.4.3 Types of Relay Selection

The relay selection is an important issue, mainly when the relays are cooperative-users. Relay selection schemes are categorized in two main approaches: opportunistic relaying or partial relay selection. In *opportunistic relaying* the relay is selected according to the best global CSI of both channels source-to-relay and relay-to-destination. One of the ways to select the relays starts by expressing the equivalent SNR of each relay as the minimum of source-to-relay and relay-to-destination channels. Then, the relay selected is the one with the highest equivalent SNR, i.e., this method uses a max-min strategy to select the relay with the best-worst channel. This selection process is done in the destination terminal, assuming that the CSI of all the relay links is known in that terminal. After the selection, the identification of the chosen relay is sent to the source using the feedback channel. From a broader perspective, opportunistic relaying can be viewed as a form of "smart routing" in a local area with frequent routing table updates. Opportunistic relaying performs better than partial relay selection, although it needs more feedback.

In *partial relay selection* the RN is selected to cooperate according to the CSI of only one of the two hops of cooperative path: either the link from the source to the relay or the link from the relay to the destination. In the first option, all the relays should send back their CSI to the source, and the source selects the relay with the highest SNR to forward the information toward the destination terminal. In the other option, also called *selection cooperation*, it is the destination that knows the CSI of the relay links and selects the relay with the highest SNR. Through a feedback channel, the destination informs the selected relay to retransmit the information it has received [ToHA10], [BKRL06].

A lot of research on relay selection has been developed, using different strategies, mainly using the current observed channel conditions, somewhat with some complexity due to implementation and on-line computation, with the objective of choosing relays that provide high quality cooperative links and ensure very low BERs. This complexity can be reduced, for example with a relay-selection policy that considers finite-state Markov channels in the relay selection. It has several advantages: a centralized control point in the network is not needed, and relays can freely join and leave from the set of potency relays as it is presented in [WeRS10].

2.4.4 Relay Protocols

Based on the forwarding strategy and processing made at the relays, several commonly used relay protocols were defined. Relay protocols can be divided into fixed and non-fixed relaying groups. In *fixed relaying* protocols, relays are always used for cooperation, while in *non-fixed relaying* protocols, relays can transmit in different processing modes or even remain idle, depending on channel conditions. Fixed relaying strategies have lower bandwidth efficiency than the non-fixed ones, because half of the channel resources are always allocated to the relays.

A typical cooperation strategy for these fixed relaying protocols is modeled with two orthogonal phases, either in TDMA or FDMA, to avoid interference between the two phases. In the first phase, a source broadcasts its information to the destination and the relays. In the second phase, the relays help the source by forwarding the received information to the destination, after some processing or not, depending on the protocols used, which are presented below.

One of the simplest protocols is the *amplify-and-forward*, where relays and destination receive a noisy version of the signal transmitted by the source. Then, relays amplify and retransmit the received signal. The destination combines properly the information sent by the source and the relays and makes a final decision on the transmitted information. Since the destination receives multiple copies of the intended signal through multiple independent channels, spatial diversity can always be achieved. Obviously the major drawback of this protocol is the noise amplification at the relays. The block diagram of the transmission through the cooperative links of the scheme in Figure 2-5 is shown in Figure 2-8. This transmission is formed by two hops. The first hop is from the source to the relay and the second from the relay to the destination.

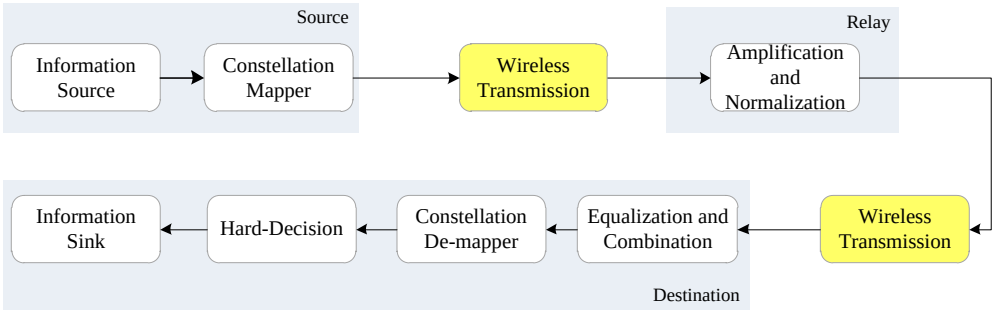

Figure 2-8: Block diagram of the cooperative links transmission with AF protocol.

In the *decode-and-forward* protocol, the relays decode the symbol information, in order to eliminate the noise effect, and re-encode them before retransmitting information to the destination. When the channel quality in the link between source and relay is good, this protocol brings higher performances to cooperative systems than AF, due to its powerful error correction capability. This happens for example when relays are closer to the source than to the destination. However, in

situations of deep fading, decoding errors may occur at the relays. In these situations, relays re-encode the incorrect bits, which lead to propagation errors. Thus, worse results will be obtained with this one than with AF protocol [LaTW04]. The corresponding block diagram is exemplified in Figure 2-9.

The *demodulation-and-forward* protocol has a lower complexity on relay implementation. The corresponding block diagram for each cooperative link is in Figure 2-10. It is a simple forwarding method that eliminates the effect of noise amplifications simply by demodulating the signal in relays, without decoding. Then, it remodulates and reconstructs the signal, forwarding it to the destination. Despite being simpler, it does not have as good performances as DF protocol, when the first cooperative-hop link has good transmission quality.

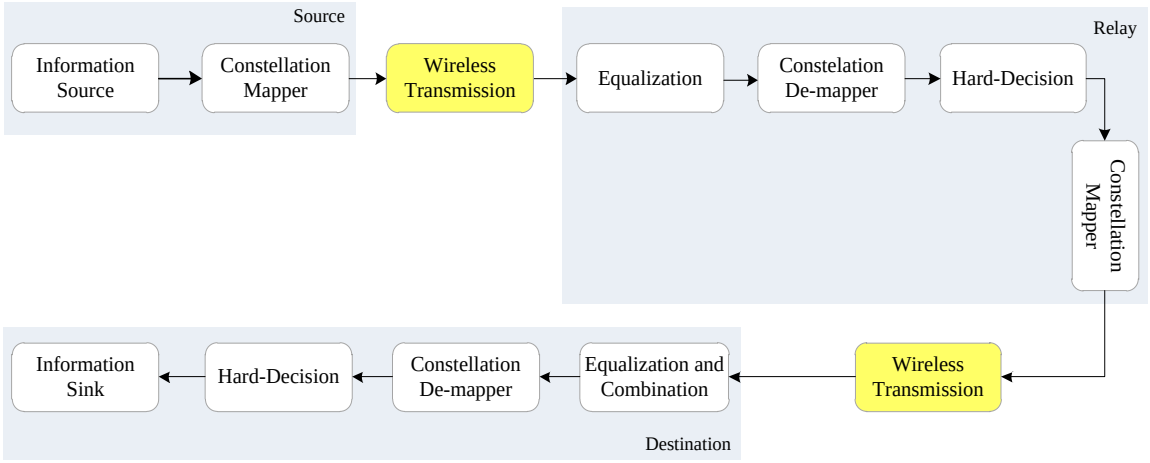

Figure 2-9: Block diagram of the cooperative links transmission with DF protocol.

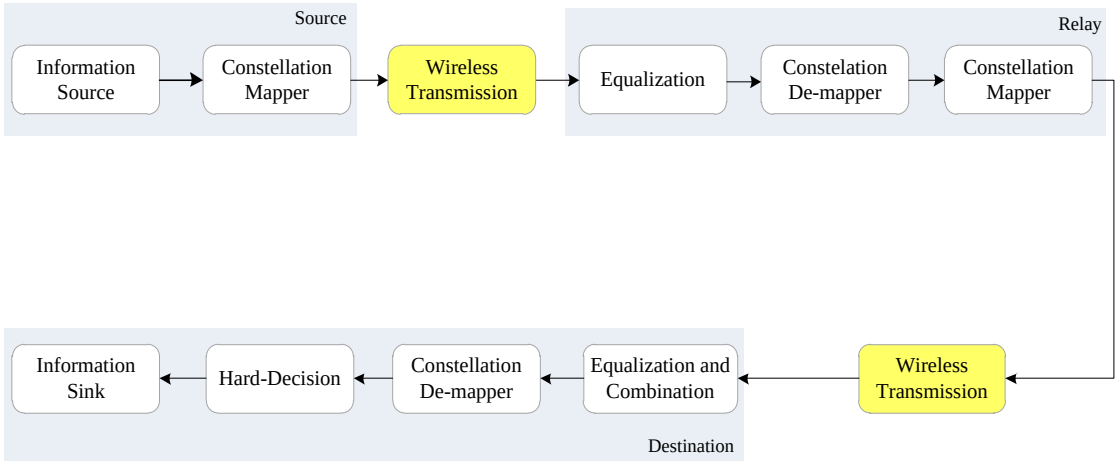

Figure 2-10: Block diagram of the cooperative link transmission with the demodulation-and-forward protocol.

In *Equalize and Forward* (EF) relay protocol, the relays should know the channel between the source and themselves, so that they can equalize the signals before retransmitting them. However, they do not demodulate or decode the signal without a decision being made in relays. It avoids premature decisions in the relay and leads to better results than with DF when the first cooperative link has a lower SNR. Despite having a slightly higher complexity than AF, it has better results, since there is less interference in the channel contribution of the first cooperative link. It also avoids the need for the destination knowing the CSI of the first cooperative link. Block diagram of cooperative transmission is shown in Figure 2-11.

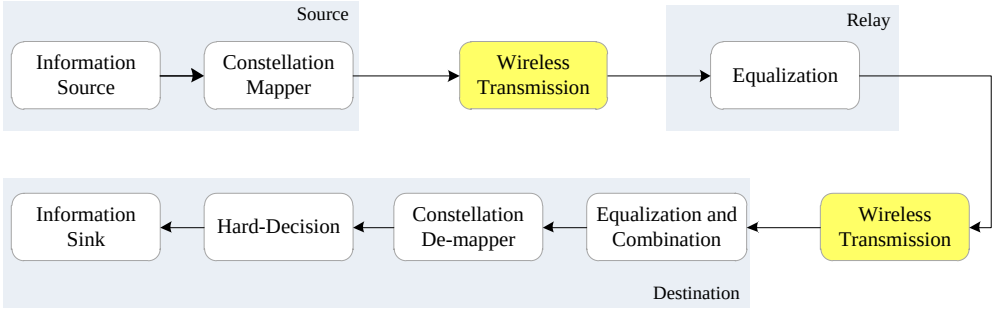

Figure 2-11: Block diagram of the cooperative link transmission with EF protocol.

Coded cooperation is another protocol, where the cooperation results in incremental redundancy in the codeword when compared with the original one. In this case, the relays segment their source data into blocks, which are encoded with an error detection code, e.g., a cyclic redundancy check (CRC) code. These codes have exceptional error coverage and minimal loss of rate. Each block is then encoded with a FEC code, so that, for an overall rate, we could have total coded symbols allocated to each source block. These algorithms can overcome the drawbacks of a simple cooperation based on repetition coding [HuSN06].

In the previous relay protocols the relay only receives half of the total resources (time or frequency), which severely limits the achievable rate. Aiming to avoid that, one can use the *compress-and forward* relay protocol. In this case, instead of sending a replica of the received signal, we can think of quantizing it and sending the resulting finite sequence of bits. The destination can then reconstruct the relay observation, and the duration of the second phase can be made arbitrarily short, depending on the quantization accuracy provided by the high quality of the second cooperative hop. It provides higher capacity rates than DF protocol, as shown in [SiMV10].

Concerning the non-fixed relaying protocols, there are also some methods proposed in the literature. *Selective decode-and-forward* is an alternative protocol, where the relay chooses to cooperate or not, based on its decoding result. If the received information in a relay is perfectly decoded, DF protocol is used, otherwise it remains idle. The analysis of the decoding results as

correct or not can be achieved through the use of CRC codes. Moreover, in order to select whether the relay cooperates or not, one can set an SNR threshold at relays, and they will only forward the source data if the received SNR is larger than that threshold [JiHa06], [LiSa09].

An even more complete protocol, based on selective DF, is the *adaptative relay protocol*. In this case, according to whether the received bits in each relay have been perfectly decoded or not, relays adaptively select DF or AF relay protocols, respectively. Therefore, this protocol combines the benefits from both AF and DF, effectively mitigating the noise amplification and avoiding propagation errors, according to the channel characteristics [LiVu08].

For the *incremental relaying protocol*, it is assumed that there are feedback channels from the destination to the relays. In this method, the destination informs the relays through those channels when the message from the source is not correctly received, so that the relays do not need to retransmit it. The relay just retransmits information when the destination is not able to receive the message from the source correctly. If the BS transmission is not successful in the first phase, relays can use any of the fixed relaying protocols to transmit.

Comparisons between the performances of some of the presented protocols are made in several works, particularly in [TSGG09a] and [LSSK09].

2.5 Coherent and Non-Coherent Detection over Wireless Channels

2.5.1 Point-to-Point Detection

We analyze a simple detection case in a flat fading channel, for simplicity, when the channel can be represented by a single discrete-time complex filter tap h_k, for each different time *k*. The output signal of the general system is given by

$$y_k = x_k h_k + n_k, \tag{2.18}$$

where $n_k \sim \mathrm{CN}(0, N_0)$. It is assumed that the channel is distributed as Rayleigh fading distribution, i.e., $h_k \sim \mathrm{CN}(0,1)$. For binary phase shift keying (BPSK) signaling the input signal is given by $x_k = \pm A$, where *A* is the amplitude and the symbols x_k are independent over time. This signaling scheme fails, even in absence of noise, as the phase of the received signal y_k is uniformly distributed between 0 and 2π regardless of whether $x_k = \pm A$ is transmitted.

Let us analyze the performance of the same scheme with the detection in an AWGN channel without fading. A sufficient statistic for BPSK signaling is $\mathrm{Re}\{y_k\}$ and the error probability is

$$P_e = Q\left(\frac{A}{\sqrt{N_0/2}}\right) = Q\left(\sqrt{2\gamma}\right), \tag{2.19}$$

where $\gamma = \frac{A^2}{N_0}$ is the signal to noise ratio per symbol time for this system and Q(.) is the complementary cumulative distribution function of a random variable.

For the same modulation, BPSK, we can also obtain a coherent detection over a Rayleigh fading, supposing that the channel gains are known at the receiver, although still being random. In practice this is done either by sending a known sequence (called a pilot or training sequence) or by a direct decision, estimating the channel earlier using symbols detector.

Knowing the channel gains, *coherent detection* of BPSK can be performed on a symbol by symbol basis. We can focus on one s*y*mbol transmission for a specific time slot and drop the time index, i.e.,

$$y = xh + n\,. \tag{2.20}$$

Detection of symbol *x* through *y* is done in a similar way to that of the AWGN case, based on the sign of the real sufficient statistic

$$\mathrm{Re}\left\{\frac{h^*}{|h|}y\right\} = |h|x + \mathrm{Re}\left\{\frac{h^*}{|h|}n\right\}, \tag{2.21}$$

where $\mathrm{Re}\left\{\frac{h^*}{|h|}n\right\} \sim N\left(0, N_0/2\right)$.

The error probability of detecting *x* as function of the received signal to noise ratio is

$$P_e(\gamma) = Q\left(\frac{A|h|}{\sqrt{N_0/2}}\right) = Q\left(\sqrt{2\gamma}\right), \tag{2.22}$$

where $\gamma = \frac{E_b a_h^2}{N_0}$, with a_h being the magnitude of h and E_b the bit energy, i.e., A^2. To obtain the error probability when a_h is random with distribution $N(0,1)$, we must average $P_e(\gamma)$ over the pdf of γ. That is, we must evaluate the integral

$$P_e = \int_0^\infty P_e(\gamma)\, p(\gamma)\, d\gamma \tag{2.23}$$

where the $p(\gamma)$ is the probability function of γ when a_h is random. When a_h is Rayleigh-distributed, a_h^2 has a Chi-square probability distribution with two degrees of freedom. Consequently, has a exponential given by

$$p(\gamma) = \frac{1}{\bar{\gamma}} e^{-\gamma/\bar{\gamma}}, \gamma \geq 0, \tag{2.24}$$

where $\bar{\gamma}$ is the average signal-to-noise ratio and is defined as the ratio between the average received signal energy per complex symbol time over noise energy per complex symbol time. The noise energy per complex symbol time is named N_0.

Replacing (2.22) and (2.24) in (2.23), we obtain the error probability for BPSK transmission in a Rayleigh fading channel [Proa01]:

$$P_e = \frac{1}{2}\left(1 - \sqrt{\frac{\gamma}{1+\gamma}}\right). \tag{2.25}$$

In order to provide carrier frequency signal to the receiver, avoiding the *M*-PSK phase ambiguity, *differential coding* can be employed. The information phase to be communicated is modulated on the carrier as the difference between two adjacent transmitted phases and the receiver takes the difference of two adjacent phase decisions to arrive at the decision on the information phase [SiAl05].

In *non-coherent detection* the receiver does not make any attempt at estimating the carrier phase. For BPSK modulation, non-coherent detection solutions establish different magnitudes for different symbols or use a special type of coding between symbols. One example of coding of those symbols is a simple orthogonal modulation scheme, a form of binary pulse-position modulation, in which for a pair of time samples $\mathbf{x}_a = (A, 0)$ is transmitted for one symbol and $\mathbf{x}_b = (0, A)$ is transmitted for another. The detection is performed based on the correspondent pair of time samples received (y_0, y_1). The optimal rule is simply to decide that $\mathbf{x}_a$ is transmitted if $|y_0|^2 > |y_1|^2$ and decide for x_b otherwise [Tse05].

For the orthogonal scheme the average received energy per symbol time is $A^2/2$, resulting in the expression for SNR

$$\gamma = \frac{A^2}{2N_0}. \tag{2.26}$$

We can express the error probability of the orthogonal scheme in terms of SNR energy ratio, through the direct integration of the probability $P\left(|y_1|^2 > |y_0|^2 \mid x_a\right)$ [TsVi05]:

$$P_e = \frac{1}{2(1+SNR)}. \tag{2.27}$$

In Figure 2-12, the error probabilities of coherent and non-coherent BPSK over a Rayleigh fading channel and for BPSK over an AWGN channel are compared. The performance of the coherent detection mode scheme is, as expected, better than the non-coherent one for BPSK

modulation. It is evident that in the first case the CSI is known at the receiver, which helps in signal estimation. The difference between the two modes is approximately constant for the whole SNR range and equal to about 3 dB. However, this difference is negligible when compared to the detection of BPSK over an AWGN channel. This error probability decays very fast with the SNR, compared to BPSK over a Rayleigh fading channel. This is justified by the fact that Rayleigh fading channels are random, contrarily to Gaussian channels, which results in a larger amount of errors. For example, a gain of 17 dB is obtained in the Gaussian channel model comparatively to the non-coherent BPSK for an error probability target of 10^{-3}. For lower error rates even higher differences are obtained.

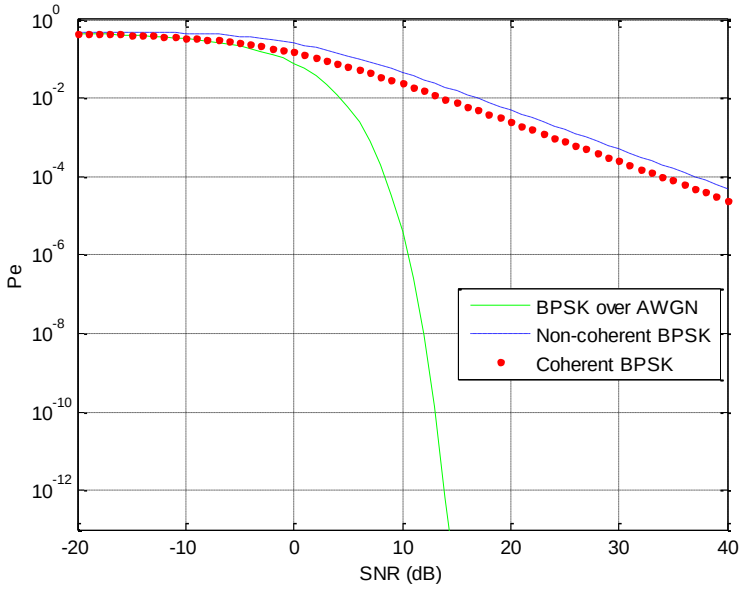

Figure 2-12: Performance of BPSK over a Rayleigh fading channel with coherent and non-coherent detection and BPSK over an AWGN channel.

2.5.2 Detection for Cooperative Systems

In some situations a point-to-point system performance under fading channels is unsatisfactory from a practical point of view. Regardless of their spectral efficiency, error probability decays very slowly for uncoded communications, as shown in Figure 2-12, where it decreases as $1/SNR$, when the channel exhibits Rayleigh fading. This poor performance arises because we have a single signal path and therefore, with fading, there is a probability of being in a deep fade so limiting the average performance. One solution to improve fading channel performance is to make use of cooperative diversity, by passing through multiple independent signal paths. This improves the system performance, making the communication reliable, as long as one of the paths is strong.

For cooperative communications different detection modes can be applied. Not only do they differ in the node where detection can be made, but also in the type of detection. Consequently different detection strategies can be identified depending on the CSI available in cooperative communications, as well as on the different relay protocols. Some strategies are summarized in Table 2.1.The first strategy presented is motivated by the scenarios where the network topology and/or the channels conditions fluctuate rapidly. In this case a differentially-encoded algorithm can be designed for cooperative systems, dispensing CSI estimation at all nodes of the system, unlike other schemes, such as maximum ratio combining and equal gain combining [IkAh08]. However, some degradation is obtained, similarly to the point-to-point detection, due to being a non-coherent detection [HiSL05], [ZhLi05], [SCHG11]. In this strategy, selection combining, which is a simple technique for non-coherent detection, can be used at the receiver, thus resulting in performances close to the coherent detection systems [IkAh08].

In some cases coherent detection is used assuming that the CSI is knowledge at the receiver and/or transmitter. Channel estimation techniques were explored for these systems, through prior transmissions to allow channel knowledge or transmission of pilots simultaneously to data transmissions, e.g., in [NRSG09]. Thus, the second strategy class that we consider does not involve any transmission of CSI links to the source or relay terminals from outgoing channels. However, nodes can receive CSI, for example, by their incoming channels, through the use of pilots or training sequences. Extending CSI at the receivers, it is possible to code information and coherently detect information in the destination, improving both the spectral efficiency and the BER performance of these systems. This scenario is considered, for example, in the cooperative models in [LaWo03], [LaTW04]. The transmission strategies can be viewed as *dumb* cooperation since they spend little overhead to get the CSI.

A more informed class of strategies (strategy 3 in Table 2.1) involves some CSI knowing at the BS in terms of amplitude. Knowing CSI at the transmitter is possible through the use of feedback channels and small overheads, which requires a small fraction of the channel coherence time [BKRL06]. These strategies are usually used with the objective of selecting relays. Relay selection methodologies are explained in Section 2.4.3, and are used for example in [BlKW06], [SeEA03a]. With this method we have more power and bandwidth efficiency than with dumb cooperation, since we can choose the best relay for the communication.

The most informed class of strategies has the knowledge of CSI in all the nodes (strategy 4 in Table 2.1), including both amplitude and phase information. This allows the use of *distributed beamforming* [SeEA03a]. Beamforming exploits coherent combination of signals at the receiver, and it can be very efficient in power and bandwidth. However, effective distributed beamforming

requires accurate carrier synchronization between the source and relays, but much simpler codes than those designed for dumb cooperation can be employed [FiKa06].

In the following chapters we will describe, in detail, some algorithms for cooperative schemes by using distributed codes or a data precoding method. For these algorithms, we consider strategies 2 or 3 of Table 2.1, using coherent detection in the UT and/or RNs. If the relays use regenerative relay protocols, coherent detection can be used by knowing just the prior channels to the relays and the destination. Otherwise the UT needs to know CSI of all the channels that participate in the communication so that coherent detection can be possible. BS is considered to have the CSI until the relays in the algorithms in which relay selection is needed.

TABLE 2.1: EXAMPLES OF DETECTION STRATEGIES USED IN COOPERATIVE COMMUNICATIONS.

	Availability of CSI			**Detection Methods**
	BS	**RN**	**UT**	
Strategy 1	No	No	No	Non-coherent detection
Strategy 2	No	S→R channels	R→D channels	Coherent detection
Strategy 3	S→R channels (amplitude)	S→R channels	R→D channels	Coherent detection
Strategy 4	S→R channels	S→R channels R→D channels	R→D channels	Beamforming and coherent detection

3 Theoretical Capacity of Relay-Assisted Schemes

3.1 Introduction

The main objectives of this chapter are to present algorithms for relay-assisted schemes and evaluate them in terms of capacity, for different configurations. We consider different algorithms for cooperative systems with one or two single-antenna RNs and considering the cases with and without the communication through the direct link. The main signal expressions of such systems are derived when considering AF, EF and DF relay protocols. Reference non-cooperative systems are also referred to for comparison purpose. These relay-assisted schemes are analyzed in terms of capacity performance, thus providing a fundamental limit on the data throughput of cooperative systems. System definition is made in Section 3.2, while the main expressions for the signals transmitted and received during the communication process are derived in Section 3.3. Then, in Section 3.4, the theoretical capacity expression for each scheme is deduced for various protocols. Finally, several propagation scenarios are defined by varying the path loss factor and relative position of the relays, for which the curves of average and outage capacities are evaluated through Monte Carlo simulations. The obtained results for the relay-assisted schemes and the equivalent non-cooperative systems are compared in Section 3.5 and some general conclusions for relay-assisted schemes are extrapolated in Section 3.6.

3.2 System Definition

Let us define the nomenclature used in this thesis. Scalar variables are indiscriminately designated by non-bold capital or lower case letters. When using bold, we are referring to vectors in the case of using lower case letters and to matrices if we are using capital letters. Some of the operations used are complex conjugate-transpose, Hermitian transpose and complex transpose operators, respectively designated by $(\bullet)^*$, $(\bullet)^H$ and $(\bullet)^T$. When referring to complex variables, where each component follows a Gaussian distribution, the variable is said to be characterized by a complex normal distribution $CN(\mu,\sigma^2)$, where μ and σ are the mean and the standard deviation of the variable.

Furthermore, the characteristics of a RA system, with one and two cooperating relays, are presented in this chapter. The relay protocols applied to them are AF, EF and DF and the cooperative schemes are:

- RA scheme with one relay and without space-time coding;
- RA scheme with one relay and with distributed SFBC;
- RA scheme with two relays and with direct path (DP);
- RA scheme with two relays and without DP.

For comparison purposes, non-cooperative MISO and SISO systems are also considered. The MISO system makes use of spatial diversity, and it is formed by two transmitter and one receiver antennas at source and destination, respectively, as shown Figure A-2 (in Annex A). It employs Alamouti coding in the co-located antennas, according to Table A.1, in Annex A [Alam98]. The reference SISO system is a simpler communication between two single antenna nodes (Figure A-1). In both cases, the distance between transmit and receive antennas is the same and designated by d.

In the RA schemes the distance between the source and destination is maintained the same. The scheme with two cooperative relays is shown in Figure 3-1, where the position of the relays in relation to source and destination is highlighted. The two relays are placed half way between source and destination at an angle θ, i.e., the distance S-R_i or R_i-D is $d/(2\cos(\theta))$, with $i=1,2$. The derivations could be easily extended for other cases.

Transmission from source to destination involves four cooperative channels, h_1 and h_2 between S-R_1 and S-R_2, and h_3 and h_4 between R_1-D and R_2-D, respectively. In our analysis we consider the existence or the non-existence of a DP between the source and the destination, represented by h_d. The scheme with a single relay can be seen in Figure 3-1 if the relay R_2 is not

taken into account. In these situations the DP must be considered so that some diversity is achieved.

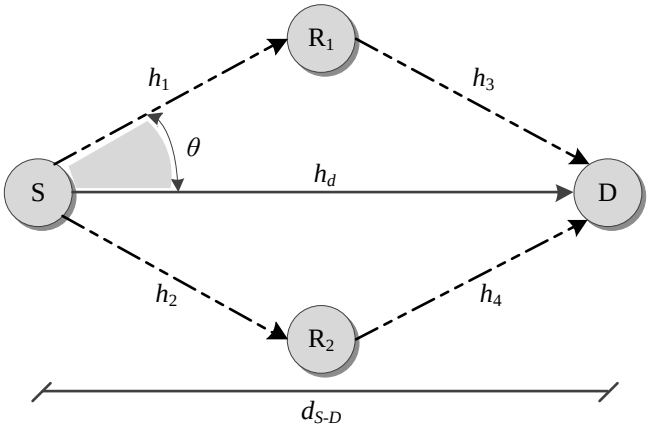

Figure 3-1: RA scheme with two relays and with the relative position of relays.

The generic expression of the received signal, for the analyzed schemes, associated with channel h and at k^{th} time slot, is given by

$$y_k = As_k h + n_k , \tag{3.1}$$

where s_k are the original symbols, which follow a complex Gaussian distribution given by $CN(0,1)$; A is the input signal amplitude; $x_k = As_k$ is the transmitted symbol in time slot *k*; and n_k refers to complex noise at the receiver, which follows the distribution $CN\left(0,\sigma_n^2\right)$. We assume that the receiving nodes have the same characteristics, and thus, statistics for receiver antennas are similar.

We consider that the channels are narrowband and time non-selective, i.e., flat-fading. Thus the approximation (3.1) is valid in each sample instant time. Furthermore, for multiple antennas and virtual MIMO systems, we consider that the channels are constant during the block coding duration (e.g., for Alamouti during two time slots). The total transmitted power is also maintained equal for all the systems and it is equally distributed by the transmit nodes. Consequently, if *N* nodes are transmitting, the average transmitted power in each node is P_T/N, where P_T is the total average transmitted power.

In our analysis, the channel h is decomposed as the product of fast fading and slow fading components, according to Section 2.2.2. Therefore the channel is given by $h = h_F \varphi_{PL}$, where φ_{PL} is attenuation due to path loss that affects the transmitted signals and h_F is the fast fading component, and they are respectively given by the following expressions:

$$\varphi_{PL} = \sqrt{\frac{k_0}{\left(d_t\right)^{\alpha}}} \tag{3.2}$$

and

$$h_F = a_R e^{j\phi}, \tag{3.3}$$

where k_0 is a constant dependent on frequency and antenna gains, from Friis Formula; d_t is the distance between the respective transmitter and receiver; α is the path loss exponent; a_R is the magnitude of fast-fading component, which is Rayleigh distributed and such that the absolute square value of the channel is unitary; and the argument ϕ is uniformly distributed between 0 and 2π.

This scheme has two types of links. The cooperative links, where a relay has the role of receiver or transmitter, are characterized by a channel model with similar path loss attenuations. On the other hand, the link that characterizes the DP between source and destination has a higher transmission distance, resulting in higher path loss attenuation. Consequently, characterization of the DP and cooperative path losses for each link can be defined by the following expressions, in function of the distance between the source and the destination, respectively:

$$\left|\varphi_{PL,d}\right|^2 = \frac{k_0}{d^\alpha} \tag{3.4}$$

and

$$\left|\varphi_{PL,c}\right|^2 = \frac{k_0}{\left(d/\left(2\cos\theta\right)\right)^\alpha}. \tag{3.5}$$

The path loss of the DP, φ_{PLd}, is related to the path loss of cooperative links, φ_{PLc}, by the expression

$$\left|\varphi_{PLd}\right|^2 = \frac{\left|\varphi_{PLc}\right|^2}{\left(2\cos\theta\right)^\alpha}. \tag{3.6}$$

Note that, the DP is just considered in some of the cooperative schemes. However, this relation of path loss attenuation between cooperative and direct links is used, since DP appears at least on the reference non-cooperative schemes.

For cooperative schemes, transmission of each block takes four time slots. This way, the cooperative system, compared with the equivalent non-cooperative system, with a multiple-antenna transmitter, will have half of the spectral efficiency. Moreover, we refer to time through k, taking the values $k = 1,2,3,4$. However, these four consecutive sample instants can occur in any moment. Thus, when we simply refer to instant k it is meant to be $t + kT_s$.

3.3 Link Equations and Equivalent Channel Matrices

3.3.1 RA Scheme with Two Relays and Without DP

The first cooperative scheme we analyze is the one with two relays, and considering no DP. Viewing the two relays as part of a MISO system, we implement Alamouti coding in the relays. The communication is divided into two phases. Assuming Alamouti is implemented in time domain, each phase has a two time slot duration. During the first two slots, two information symbols are broadcasted from source to relays R_1 and R_2, while during the last two they are retransmitted using Alamouti coding. Therefore, relays R_1 and R_2 act as elements of a virtual dual antenna array. Equivalent channel matrices and the main signal equations are derived separately for the different relay protocols.

3.3.1.1 AF and EF Relay Protocols

The general chain is specified next for AF and EF relay protocols. It shows several operations such as the multiplication of the input signals of a link by the channel contribution, the noise added in relays and destination receivers, and the processing done inside relays. For AF relays the only processing made is normalization, while for EF relays normalization and equalization are implemented. For AF relays the factor ξ_{Ri} represents the normalization factor, so that $\mu_{Ri} = \xi_{Ri}$, while for EF relays it is the product of normalization by equalization factors, i.e., $\mu_{Ri} = \eta_{Ri}\xi_{Ri}$. Thus, η_{Ri} is the instantaneous normalization factor derived from the power system constraints and ξ_{Ri} is the equalization factor, with which we can eliminate channel contributions until the relays.

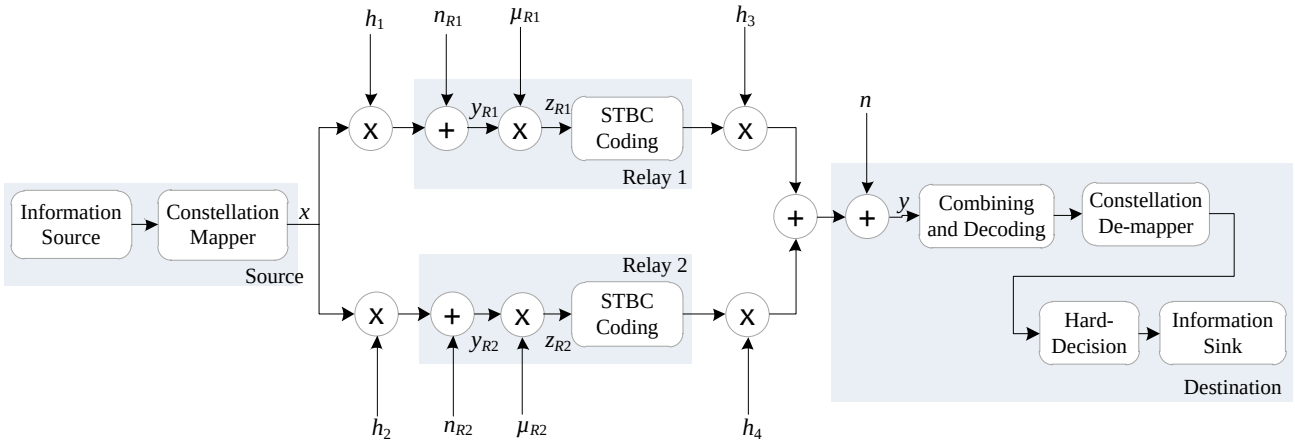

Figure 3-2: Block diagram for RA scheme with two relays and without DP, for AF and EF relays.

In a first phase, during the two first time slots, the source node broadcasts two symbols to the relays, with no space-time coding. In this first analysis we do not consider that the destination receives any useful signal during the first phase, i.e., we do not have a DP. Independently of the relay protocol, we consider that the signal transmitted by the relays has a power of $2/3P_T$ .The signals that arrive to the i^{th} relay node, in matrix form, are given by

$$\mathbf{y}_{Ri} = \sqrt{\frac{2}{3}} A \begin{bmatrix} s_1 \\ s_2 \end{bmatrix} h_i + \begin{bmatrix} n_{Ri,1} \\ n_{Ri,2} \end{bmatrix}, \tag{3.7}$$

where A is the square root of total transmitted power; the subscripts correspond to node identification and to time slot instants, respectively; and, the amplitude factor $\sqrt{2/3}$ comes from the constraint in transmitted power, so that all the considered systems have the same overall transmitted power. Then, we equalize and/or normalize the signal by the factor μ_{Ri}, which depends on the relay protocol, obtaining the following processed signal at relays

$$\mathbf{z}_{Ri} = \sqrt{\frac{2}{3}} A \mu_{Ri} \begin{bmatrix} s_1 \\ s_2 \end{bmatrix} h_i + \mu_{Ri} \begin{bmatrix} n_{Ri,1} \\ n_{Ri,2} \end{bmatrix}. \tag{3.8}$$

In the second phase the transmission from relays to destination occurs during the third and fourth time slots, while the source node does not transmit any information. In the destination, information received is processed and combined according to Alamouti decoding, assuming that CSI is known. This operation is also dependent on the relay protocol used.

In order to achieve diversity, the relays retransmit the received signals orthogonally by using an STBC at the relays. We choose to implement the Alamouti code that was initially employed in UMTS communications, being thus known as UMTS Alamouti. In this case, relay R_1 transmits z_1 and z_2, and relay R_2 the conjugates of $-z_2$ and z_1, in the third and fourth time slots. This slightly differs from the conventional Alamouti, but has the advantage that in one of the relays the retransmitted symbols are not changed. The cooperative algorithm for both phases is shown in Table 3.1. Concerning the normalization factors applied in relays, they are presented next for each relay protocol.

TABLE 3.1: TRANSMITTED INFORMATION BY EACH NODE OF THE RA SCHEME WITH TWO RELAYS, USING UMTS ALAMOUTI CODING.

	Source	**Relay 1**	**Relay 2**
Time slot 1	x_1	-	-
Time slot 2	x_2	-	-
Time slot 3	-	$z_{R1,1}$	$-z_{R2,2}^{*}$
Time slot 4	-	$z_{R1,2}$	$z_{R2,1}^{*}$

A. AF Relay Protocol

In AF relay protocol, since the relays do not need to know the CSI, it is an approximation of the exact one and is expressed independently of the relays as in the following expression

$$\mu_{Ri}\big|_{AF} = \xi_{Ri}\big|_{AF} = \left(\sqrt{1+\frac{3}{2}\frac{1}{SNR_T}}\right)^{-1}, \tag{3.9}$$

where SNR_T is the ratio between the transmitted power, P_T, and the noise power, σ_n^2.

Let y_3 and y_4 be the signals received at the destination in the third and fourth time slots respectively. Then, using a vector notation, the received signals coming from the two relays are given by

$$\mathbf{y} = \begin{bmatrix} y_3 \\ y_4 \end{bmatrix} = \frac{A\sqrt{2}}{\sqrt{3}}\mu \begin{bmatrix} H_1 s_1 - H_2 s_2^{*} \\ H_1 s_2 + H_2 s_1^{*} \end{bmatrix} + \mu \begin{bmatrix} n_{R1,1}h_3 - n_{R2,2}^{*}h_4 \\ n_{R1,2}h_3 + n_{R2,1}^{*}h_4 \end{bmatrix} + \begin{bmatrix} n_3 \\ n_4 \end{bmatrix}, \tag{3.10}$$

where $H_1 = h_1 h_3$ and $H_2 = h_2^{*} h_4$. At the receiver, Alamouti decoding is performed according to

$$\begin{cases} \hat{s}_1 = H_1^{*} y_3 + H_2 y_4^{*} \\ \hat{s}_2 = -H_2 y_3^{*} + H_1^{*} y_4 \end{cases}. \tag{3.11}$$

Then replacing (3.11) in (3.10), we get the final expressions for the soft-estimates of the decoded symbols

$$\begin{aligned} \hat{\mathbf{s}} = \begin{bmatrix} \hat{s}_1 \\ \hat{s}_2 \end{bmatrix} &= \frac{A\sqrt{2}}{\sqrt{3}}\mu\left(|H_1|^2 + |H_2|^2\right)\begin{bmatrix} s_1 \\ s_2 \end{bmatrix} \\ &+ \begin{bmatrix} H_1^{*}\left(\xi n_{R1,1}h_3 - \xi n_{R2,2}^{*}h_4 + n_3\right) + H_2\left(\xi n_{R1,2}^{*}h_3^{*} + \xi n_{R2,1}h_4^{*} + n_4^{*}\right) \\ -H_2\left(\xi n_{R1,1}^{*}h_3^{*} - \xi n_{R2,2}h_4^{*} + n_3^{*}\right) + H_1^{*}\left(\xi n_{R1,2}h_3 + \xi n_{R1,2}^{*}h_4 + n_4\right) \end{bmatrix}. \end{aligned} \tag{3.12}$$

B. EF Relay Protocol

Let us now consider the EF relay protocol. In this case the coefficient μ_{Ri}, represented in Figure 3-2, is the product of a normalization factor intended to provide constant output power and a factor intended to equalize the BS→RN channel. This type of relay is slightly more complex than the AF one, and requires that the relay knows the CSI through which signal is transmitted.

There are different types of equalizers that can be used, and we specifically consider the three following types:

- *Channel inversion* or *zero forcing*, with $\xi_{Ri} = \frac{1}{h_i}$;
- *Phase* equalization, with $\xi_{Ri} = h_i^*$;
- *Matched* equalization, with $\xi_{Ri} = \frac{h_i^*}{|h_i|^2}$.

The normalization factors corresponding to each of the mentioned equalization schemes are given by:

$$\eta_{Ri} = \begin{cases} \left(\sqrt{1+\frac{1}{|h_i|^2\, SNR}}\right)^{-1} & \text{, for channel inversion method} \\ \left(\sqrt{|h_i|^4+\frac{|h_i|^2}{SNR}}\right)^{-1} & \text{, for phase equalization method} \\ \left(\sqrt{1+\frac{3}{2}\frac{1}{|h_i|^2\, SNR_T}}\right)^{-1} & \text{, for matched equalization method} \end{cases} . \tag{3.13}$$

Consequently, we observe that the factor μ_{Ri} has the same expression for the three equalization types and is given by

$$\mu_{Ri}\big|_{EF} = \left(|h_i|^2 + \frac{3}{2}\frac{1}{SNR_T}\right)^{-1/2} . \tag{3.14}$$

After equalizing and normalizing the signals, the STBC of Table 3.1 is applied in the relays, similarly to the previous case. Then, the signals are re-transmitted to the destination. The received signal at the destination on the third and fourth time slots is shown next

$$\mathbf{y} = \begin{bmatrix} y_3 \\ y_4 \end{bmatrix} = \begin{bmatrix} z_{R1,1} - z_{R2,2}^* \\ z_{R1,2} + z_{R2,1}^* \end{bmatrix} \begin{bmatrix} h_3 \\ h_4 \end{bmatrix} + \begin{bmatrix} n_3 \\ n_4 \end{bmatrix} . \tag{3.15}$$

The general matrix equation of the received signals at the destination, which includes the noise component and the equivalent channel matrix, is given by

$$\begin{aligned}\begin{bmatrix} y_3 \\ y_4^* \end{bmatrix} &= \frac{A\sqrt{2}}{\sqrt{3}}\mathbf{H}\begin{bmatrix} s_1 \\ s_2^* \end{bmatrix} + \begin{bmatrix} n_{R1,1}\mu_{R1}h_3 - n_{R2,2}\mu_{R2}h_4 + n_3 \\ n_{R1,2}^*\mu_{R1}^*h_3^* + n_{R2,1}\mu_{R2}h_4^* + n_4^* \end{bmatrix} \\ &= \frac{A\sqrt{2}}{\sqrt{3}}\mu\begin{bmatrix} H_1 s_1 - H_2 s_2^* \\ H_1 s_2 + H_2 s_1^* \end{bmatrix} + \mu\begin{bmatrix} n_{R1,1}\mu_{R1}h_3 - n_{R2,2}^*\mu_{R2}^*h_4 \\ n_{R1,2}\mu_{R1}h_3 + n_{R2,1}^*\mu_{R2}^*h_4 \end{bmatrix} + \begin{bmatrix} n_3 \\ n_4 \end{bmatrix}\end{aligned}, \tag{3.16}$$

where now $H_1 = h_1\mu_{R1}h_3$ and $H_2 = h_2^*\mu_{R2}^*h_4$, while the equivalent channel matrix is given by

$$\mathbf{H} = \begin{bmatrix} h_1\mu_{R1}h_3 & -h_2^*\mu_{R2}^*h_4 \\ h_2\mu_{R2}h_4^* & h_1^*\mu_{R1}^*h_3^* \end{bmatrix}. \tag{3.17}$$

The same equations are used to obtain the decision symbols, similarly to the case of AF relays, according to (3.11), resulting in the following signals:

$$\begin{aligned}\hat{\mathbf{s}} = \begin{bmatrix} \hat{s}_1 \\ \hat{s}_2 \end{bmatrix} &= \frac{A\sqrt{2}}{\sqrt{3}}\left(|H_1|^2 + |H_2|^2\right)\begin{bmatrix} s_1 \\ s_2 \end{bmatrix} \\ &+ \begin{bmatrix} H_1^*\left(n_{R1,1}\mu_{R1}h_3 - n_{R2,2}^*\mu_{R2}^*h_4 + n_3\right) + H_2\left(n_{R1,2}^*\mu_{R1}h_3^* + n_{R2,1}\mu_{R2}h_4^* + n_4^*\right) \\ -H_2\left(n_{R1,1}^*\mu_{R1}^*h_3^* - n_{R2,2}\mu_{R2}h_4^* + n_3^*\right) + H_1^*\left(n_{R1,2}\mu_{R1}h_3 + n_{R2,1}^*\mu_{R2}^*h_4 + n_4\right) \end{bmatrix}.\end{aligned} \tag{3.18}$$

The normalization factor is applied to provide a constant average power at the output of the relays and it depends on the channel realization and on the power of the additive noise. With the AF relay protocol the relay does not need to know the CSI, and the normalization factor is given by (3.9). This factor depends on the expectation of the channel realizations and not on its instantaneous values. In the EF relay case, we are implicitly making an equalization of the channels between the source and the relays and its factor is in (3.14).

In Figure 3-3, mean and standard deviation statistics of those normalization factors are presented for different values of SNR, obtained using Monte Carlo simulations, through generation and then average of several channel realizations. We can observe differences in the mean values of the normalization factors. The mean of the normalization factor used in EF relays is higher than the one used in AF, with values up to 1.7, while for AF relays, it tends to 1 for high SNRs. The large variation in the normalization factor for EF relays arises because of the inverse channel factor, which can be highlighted manipulating (3.14):

$$E\left\{\mu_{Ri}\big|_{EF}\right\} = E\left\{\frac{1}{|h_i|}\left(\sqrt{1+\frac{3}{2}\frac{1}{|h_i|^2\,SNR_T}}\right)^{-1}\right\}. \tag{3.19}$$

The mean power of the inverse of a Rayleigh variable does not converge, which will lead to significant differences for distinct channel realizations. Therefore, this will have some impact in the system performances when using EF and AF, as it will be shown in the next sections.

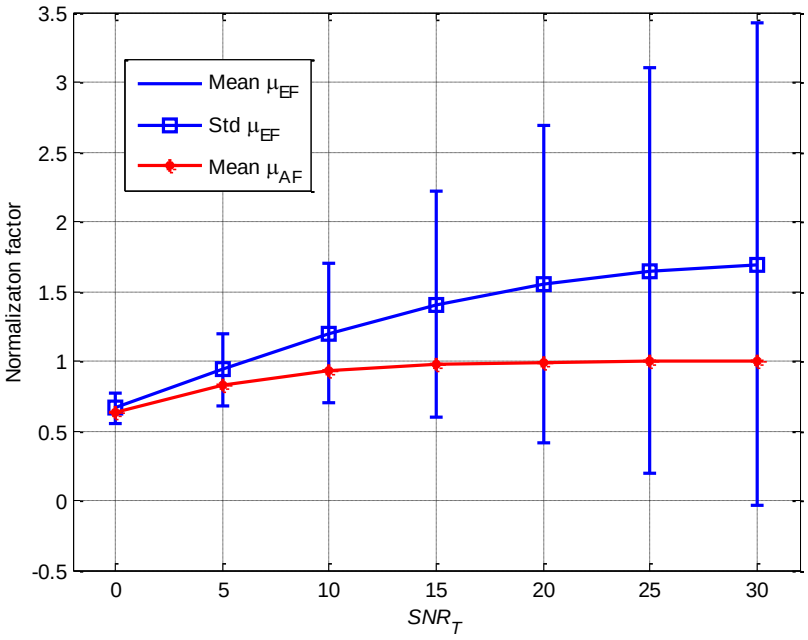

Figure 3-3: Relay normalization factor statistics, for the AF and EF relay protocols

3.3.1.2 DF Relay Protocol

When using DF relay protocol, the block diagram of the RA scheme, with two relays and no DP, is similar to the previous one. However, in this case, after the equalization, additional steps are followed, as schematized in Figure 3-4. The additional procedures are the de-mapping and hard-decision of the signals, followed by re-modulation. Then, space-time coding is applied in a similar way to the cases where other types of relay protocols are used.

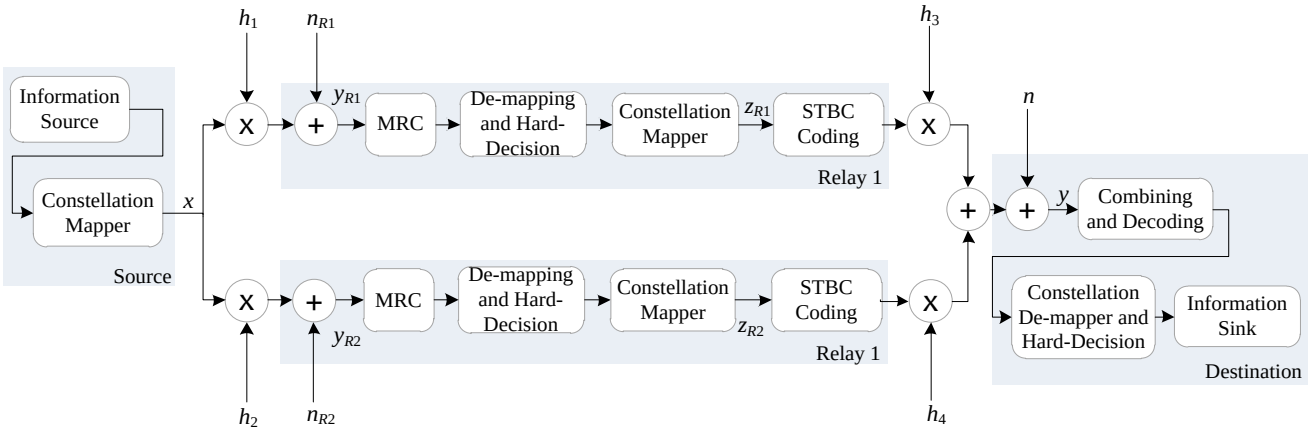

Figure 3-4: Block diagram for RA scheme with two relays and without DP, for DF relays.

The decoding block after equalization, followed by re-modulation, transforms the received signals in a sequence of estimated bits, and then again in modulated signals. If there are no bit errors in estimation during the first phase, we should have $\mathbf{z}_{Ri} = \mathbf{x}$, which does not always occur. A

more efficient relay protocol can be used, referred to as selective-DF, in which the cooperative signal is only used when no error is obtained during the first phase of transmission [LSSK09]. In the DF relay case, we are not concerned with the number of bit errors, thus we simply retransmit the modulated bits, which we call $\hat{s}_{Ri,k}$, where i represents the relay number and k the time slot. Afterwards, the estimated signal obtained in relays, before the Alamouti coding being applied, is given by

$$\mathbf{z}_{Ri} = \sqrt{\frac{2}{3}} A \begin{bmatrix} \hat{s}_{Ri,1} \\ \hat{s}_{Ri,2} \end{bmatrix}. \tag{3.20}$$

The space-time coding used is the Alamouti one, as shown in the next table, resulting in

$$\begin{cases} y_3 = \dfrac{A\sqrt{2}}{\sqrt{3}} \left(h_3 \hat{s}_{R1,1} + h_4 \hat{s}_{R2,2} \right) + n_3 \\ y_4 = \dfrac{A\sqrt{2}}{\sqrt{3}} \left(h_3 \hat{s}_{R1,2} - h_4 \hat{s}^*_{R2,1} \right) + n_4 \end{cases}. \tag{3.21}$$

TABLE 3.2: TRANSMITTED INFORMATION BY EACH NODE OF THE RA SCHEME WITH TWO RELAYS AND WITHOUT DP, USING ALAMOUTI CODING.

	Source	**Relay 1**	**Relay 2**
Time slot 1	x_1	-	-
Time slot 2	x_2	-	-
Time slot 3	-	$z_{R1,1}$	$z_{R2,2}$
Time slot 4	-	$z^*_{R1,2}$	$-z^*_{R2,1}$

If the hard-decision symbols after estimation in relays are equal to each other, i.e., $\overline{s}_{R1,k} = \overline{s}_{R2,k} = \overline{s}_{RN,k}$, we can obtain the final soft-estimates symbols in the destination as follows

$$\begin{aligned} \hat{\mathbf{s}} &= \frac{\sqrt{2}}{\sqrt{3}} \mathbf{H}^H \mathbf{H} \overline{\mathbf{s}}_{RN} + \mathbf{H}^H \mathbf{n} = \\ &= \frac{\sqrt{2}}{\sqrt{3}} \begin{bmatrix} |h_3|^2 + |h_4|^2 & 0 \\ 0 & |h_3|^2 + |h_4|^2 \end{bmatrix} \begin{bmatrix} \overline{s}_{RN,1} \\ \overline{s}_{RN,2} \end{bmatrix} + \begin{bmatrix} n_3 h_3^* - n_4^* h_4 \\ n_3 h_4^* + n_4^* h_3 \end{bmatrix}. \end{aligned} \tag{3.22}$$

If no errors result from the first phase of transmission, the estimated symbols are given by

$$\hat{\mathbf{s}} = \rho_h^2 \mathbf{I}_2 \mathbf{x} + \begin{bmatrix} n_3 h_3^* - n_4^* h_4 \\ n_3 h_4^* + n_4^* h_3 \end{bmatrix}, \tag{3.23}$$

where $\rho_h = \sqrt{|h_3|^2 + |h_4|^2}$ and $\mathbf{I}_2$ is the identity matrix. For this case, in which the signals are perfectly decoded in relays, it is predictable that their performances will be better, as the system becomes equivalent to the MISO one, with the advantage of having half of the distances.

3.3.2 RA Scheme with Two Relays and with DP

We now consider a cooperative scheme that makes use of two RNs cooperating with the source and the destination, similarly to the previous scheme, albeit with an extra link that allows the communication between those terminal nodes. Thus, the difference relatively to the previous scheme is that the destination receives the signal that the source transmits directly through the direct path. Therefore the capacity gains should be further improved if the destination can receive from this path.

Comparing this scheme with the mentioned in [NaBK04], it will correspond to protocol II, since in a first phase the source transmits to relays and destination, and no other node transmits. In a second phase, the relays transmit to the destination, while the source is idle in this phase. Each phase has a duration of two time slots, being necessary four time slots to transmit two symbols, so that the analyzed system has the same low spectral efficiency as the previous RA without direct path.

The distances of transmission are not the same for all the links, as seen in of Figure 3-1, being approximately the double for the direct path when compared with the other paths. Consequently, the propagation delay times may be substantially different. However, this is a problem of synchronization that does not concern our work and consequently is treated independently. Thus, we consider the propagation time very small in comparison with symbol duration.

3.3.2.1 AF and EF Relay Protocols

In order to transmit one third of the total mean power in each RN, we must normalize the signal by a factor dependent on the relay protocol. The normalization factors for AF and EF relays are the same as in the previous scheme, where their expressions are represented by (3.9) and (3.14), respectively. This new scheme is represented by the block diagram of Figure 3-5, which is similar to the one in Figure 3-2, but with an additional branch that corresponds to the direct path.

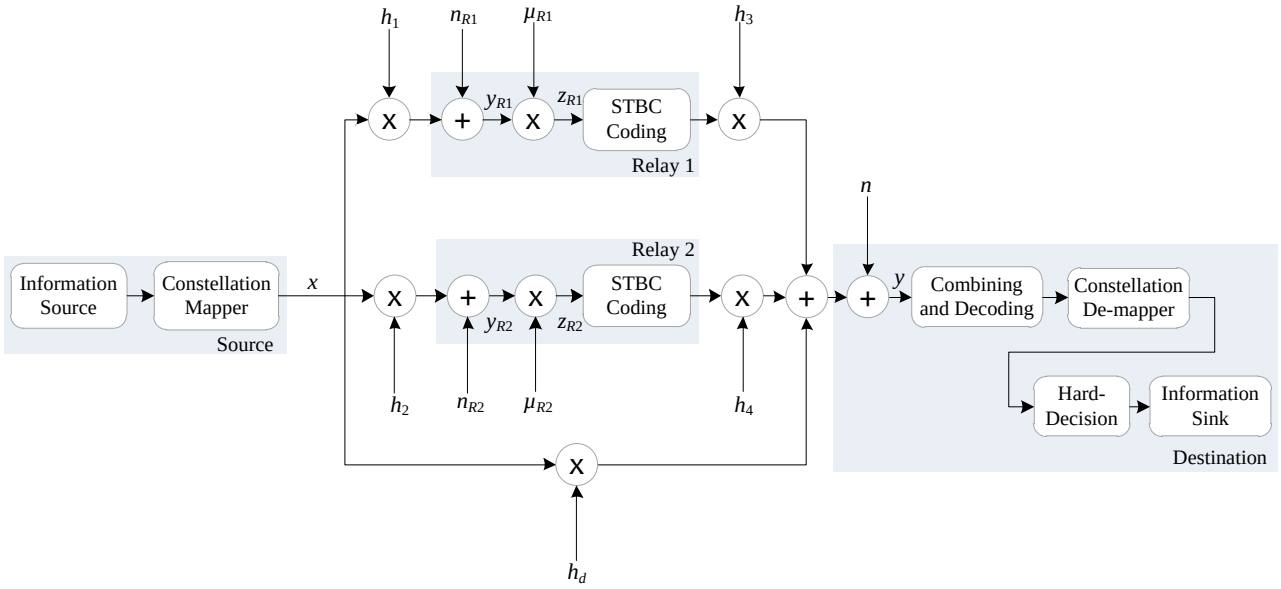

Figure 3-5: Block diagram of RA scheme with DP system, for AF and EF relays.

For both schemes, the source transmits x_1 and x_2 in the first and second time slots. These signals are received in relays and destination. Then, relay R_1 transmits $z_{R1,1}$ and $z_{R1,2}$ and relay R_2 transmits $-z_{R2,2}^{*}$ and $z_{R2,1}^{*}$, in the third and fourth time slots, according to Table 3.1, where $z_{Ri,k}$ is the signal received in the relay i in the k^{th} time slot, after some processing. The destination receives during the first two time slots the two symbols sent by the source and transmitted through channel h_d. In the following two time slots, it receives the information from relays. Afterwards, destination combines and decodes the two symbols in both phases. The signals that arrive at the destination for four consecutive time slots are given by:

$$\begin{cases} y_1 = \dfrac{A\sqrt{2}}{\sqrt{3}} h_d s_1 + n_1 \\ y_2 = \dfrac{A\sqrt{2}}{\sqrt{3}} h_d s_2 + n_2 \\ y_3 = \dfrac{A\sqrt{2}}{\sqrt{3}} \left(h_1 h_3 \mu_{R1} s_1 - h_2^{*} h_4 \mu_{R2} s_2^{*} \right) + n_{R1,1} \mu_{R1} h_3 + n_{R2,2}^{*} \mu_{R2} h_4 + n_3 \\ y_4 = \dfrac{A\sqrt{2}}{\sqrt{3}} \left(h_2^{*} h_4 \mu_{R2} s_1^{*} + h_1 h_3 \mu_{R1} s_2 \right) + n_{R1,2} \mu_{R1} h_3 + n_{R2,1}^{*} \mu_{R2} h_4 + n_4 \end{cases} . \tag{3.24}$$

The respective equivalent channel matrix is

$$\mathbf{H} = \begin{bmatrix} h_d & 0 \\ 0 & h_d \\ h_1 \mu_{R1} h_3 & h_2^{*} \mu_{R2} h_4 \\ -h_2^{*} \mu_{R2} h_4 & h_1 \mu_{R1} h_3 \end{bmatrix} . \tag{3.25}$$

As in the previous scheme, MRC is used to obtain the decoded symbols. Thus the decision symbols for the RA scheme with DP are obtained through

$$\begin{cases} \hat{s}_1 = g_0^* y_1 + g_1^* y_3 + g_2 y_4^* \\ \hat{s}_2 = g_0^* y_2 - g_2 y_3^* + g_1^* y_4 \end{cases}, \tag{3.26}$$

where $H_1 = \mu_{R1} h_1 h_3$ and $H_2 = \mu_{R2} h_2^* h_4$. The MRC gains are given by

$$g_i = \begin{cases} \dfrac{h_d}{\sigma_n^2} & ,i = 0 \\ \dfrac{H_i}{\left(\left|\mu_{R1}\right|^2 \left|h_3\right|^2 + \left|\mu_{R2}\right|^2 \left|h_4\right|^2 + 1 \right) \sigma_n^2} & ,i = 1,2 \end{cases}. \tag{3.27}$$

3.3.2.2 DF Relay Protocol

The block diagram for the RA scheme with two relays and DP when using the DF relay protocol in RNs can be obtained from the one for AF and EF relay protocols, in Figure 3-5, by changing the processing operations within each relay. These processing operations inside the relay nodes consist mainly of decoding, followed by re-modulation. If there were no bit errors in estimation on the relays, during the first phase, we should have $\mathbf{z}_{Ri} = \mathbf{x}$. The symbols retransmitted after being re-modulated are called $\overline{s}_{Ri,k}$. The estimated signal obtained at the relays, before the Alamouti coding being applied, is

$$\mathbf{z}_{Ri} = \sqrt{\frac{2}{3}} A \begin{bmatrix} \overline{s}_{Ri,1} \\ \overline{s}_{Ri,2} \end{bmatrix}. \tag{3.28}$$

Then, the space-time code of Table 3.2 is used. The signals received in the destination are given by

$$\begin{cases} y_1 = \dfrac{A\sqrt{2}}{\sqrt{3}} h_d s_1 + n_1 \\ y_2 = \dfrac{A\sqrt{2}}{\sqrt{3}} h_d s_2 + n_2 \\ y_3 = \dfrac{A\sqrt{2}}{\sqrt{3}} \left(h_3 \overline{s}_{R1,1} + h_4 \overline{s}_{R2,2} \right) + n_3 \\ y_4 = \dfrac{A\sqrt{2}}{\sqrt{3}} \left(h_4 \overline{s}_{R2,2}^* - h_3 \overline{s}_{R1,1}^* \right) + n_4 \end{cases}. \tag{3.29}$$

If the estimated signals in relays are equal, i.e., $\overline{s}_{R1,k} = \overline{s}_{R2,k} = \overline{s}_k$, the resultant signals in matrix form are given by

$$\begin{bmatrix} y_1 \\ y_2 \\ y_3 \\ y_4^* \end{bmatrix} = \frac{A\sqrt{2}}{\sqrt{3}} \begin{bmatrix} h_d & 0 \\ 0 & h_d \\ h_3 & h_4 \\ -h_4^* & h_3^* \end{bmatrix} \begin{bmatrix} \bar{s}_1 \\ \bar{s}_2 \end{bmatrix} + \begin{bmatrix} n_1 \\ n_2 \\ n_3 \\ n_4^* \end{bmatrix}. \tag{3.30}$$

We then obtain the estimation of symbols transmitted by relays, by multiplying the received symbol by the Hermitian of the equivalent channel matrix, resulting in

$$\begin{bmatrix} \hat{s}_1 \\ \hat{s}_2 \end{bmatrix} = \frac{A\sqrt{2}}{\sqrt{3}} \begin{bmatrix} |h_d|^2 + 2|h_3|^2 + 2|h_4|^2 & 0 \\ 0 & |h_d|^2 + 2|h_3|^2 + 2|h_4|^2 \end{bmatrix} \begin{bmatrix} \bar{s}_1 \\ \bar{s}_2 \end{bmatrix} + \begin{bmatrix} n_1 h_d^* + \sqrt{2} n_3 h_3^* - \sqrt{2} n_4^* h_4 \\ n_2 h_d^* + \sqrt{2} n_3 h_4^* + \sqrt{2} n_4^* h_3 \end{bmatrix}. \tag{3.31}$$

If the signals are perfectly decoded in relays during the first phase of transmission, i.e., $\bar{s}_k = s_k$, the estimated symbols on reception are given by

$$\hat{\mathbf{s}} = \rho_h^2 \mathbf{I_2 x} + \begin{bmatrix} n_1 h_d^* + \sqrt{2} n_3 h_3^* - \sqrt{2} n_4^* h_4 \\ n_2 h_d + \sqrt{2} n_3 h_4^* + \sqrt{2} n_4^* h_3 \end{bmatrix}, \tag{3.32}$$

with $\rho_h = \sqrt{|h_d|^2 + 2|h_3|^2 + 2|h_4|^2}$.

3.3.3 RA Scheme with One Relay

The scheme presented in this section corresponds to the RA scheme with a single relay and no space-time coding between these nodes. The corresponding transmitted signals in each time slot are shown in Table 3.3 and the block diagram is presented in Figure 3-6.

TABLE 3.3: TRANSMITTED INFORMATION BY EACH NODE OF THE RA SCHEME WITH ONE RELAY WITHOUT SPACE-TIME CODING.

	Source	**Relay 1**
Time slot 1	x_1	-
Time slot 2	x_2	-
Time slot 3	-	$z_{R,1}$
Time slot 4	-	$z_{R,2}$

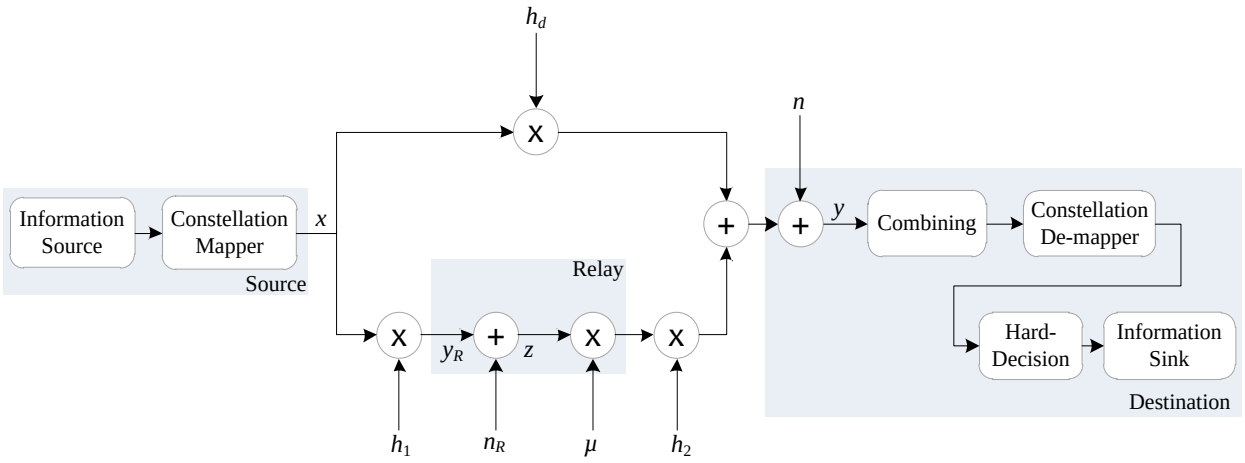

Figure 3-6: Block diagram of RA scheme with one relay and without space-time coding, for AF and EF relays.

For this scheme, in the first phase the source transmits at full power during T_s of the time. In the second phase or second time slot the relay can also transmit at full power to the destination, while the source does not transmit, as shown in Table 3.3, where x_k and $z_{R,k}$ are the signals transmitted by the source and relay, respectively. Note that there is no need to transmit in blocks of two symbols. However, aiming to have clear comparisons between the different schemes presented in this chapter and maintaining the expressions format similar to the ones of the previous schemes, we choose to consider all the transmissions in blocks of two symbols.

In this scheme each node transmits with a mean power of $P_T/2$ per time slot. As they just transmit in half of the time, instantaneous transmitted powers are P_T. The signal received in the destination is given by

$$\begin{cases} y_1 = Ah_d s_1 + n_1 \\ y_2 = Ah_d s_2 + n_2 \\ y_3 = Ah_2 z_{R,1} + n_3 \\ y_4 = Ah_2 z_{R,2} + n_4 \end{cases}, \tag{3.33}$$

where n_k is the AWGN noise introduced by the destination, which follows a distribution $CN\left(0,\sigma_n^2\right)$.

3.3.3.1 AF and EF Relay Protocol

The signals transmitted by the relays, when using AF or EF relay protocols, are defined as

$$\begin{bmatrix} z_1 \\ z_2 \end{bmatrix} = A\mu h_1 \begin{bmatrix} s_1 \\ s_2 \end{bmatrix} + \mu \begin{bmatrix} n_{R,1} \\ n_{R,2} \end{bmatrix}, \tag{3.34}$$

with the noise introduced by relays defined as $n_{R,k}$. The relay normalization factor, μ, depends on the relay protocol used and it is given by

$$\mu = \begin{cases} \dfrac{1}{\sqrt{|h_1|^2 + \dfrac{1}{SNR_T}}}, & \text{for EF relay protocol} \\ \dfrac{1}{\sqrt{1 + \dfrac{1}{SNR_T}}}, & \text{for AF relay protocol} \end{cases}. \tag{3.35}$$

For this space-time coding scheme the estimation symbols are obtained by

$$\begin{cases} \hat{s}_1 = y_1 g_0^* + y_3 g_1^* \\ \hat{s}_2 = y_2 g_0^* + y_4 g_1^* \end{cases}, \tag{3.36}$$

where g_j are the MRC factors, which include equalization, with the corresponding expression given by

$$g_j = \begin{cases} \dfrac{h_d}{\sigma_n^2}, & j = 0 \\ \dfrac{\mu h_1 h_2}{\left(1 + \mu^2 |h_2|^2\right)\sigma_n^2}, & j = 1 \end{cases}. \tag{3.37}$$

3.3.3.2 DF Relay Protocol

Similarly to the previous schemes, when using the DF relay protocol in RNs, the signals that are re-transmitted by the relay, after being decoded and re-modulated are given by

$$\mathbf{z} = A \begin{bmatrix} s_{R,1} \\ s_{R,2} \end{bmatrix}. \tag{3.38}$$

After that, the signals received in the destination are given by

$$\begin{cases} y_1 = A h_d s_1 + n_1 \\ y_2 = A h_d s_2 + n_2 \\ y_3 = A h_2 \overline{s}_{R,1} + n_3 \\ y_4 = A h_2 \overline{s}_{R,2}^* + n_4 \end{cases}. \tag{3.39}$$

If there are no bit errors in relay estimation, i.e., $\overline{s}_{R,k} = s_k$, then the resultant signals, in matrix form at destination, are given by

$$\begin{bmatrix} y_1 \\ y_2 \\ y_3 \\ y_4 \end{bmatrix} = A \begin{bmatrix} h_d & 0 \\ 0 & h_d \\ h_2 & 0 \\ 0 & h_2 \end{bmatrix} \begin{bmatrix} s_1 \\ s_2 \end{bmatrix} + \begin{bmatrix} n_1 \\ n_2 \\ n_3 \\ n_4 \end{bmatrix}. \tag{3.40}$$

We then obtain the estimation of symbols at the destination, by multiplying the received symbols by the Hermitian of the equivalent channel matrix, which, for the perfect detection in the relay, results in

$$\begin{bmatrix} \hat{s}_1 \\ \hat{s}_2 \end{bmatrix} = A \begin{bmatrix} |h_d|^2 + |h_2|^2 & 0 \\ 0 & |h_d|^2 + |h_2|^2 \end{bmatrix} \begin{bmatrix} s_1 \\ s_2 \end{bmatrix} + \begin{bmatrix} n_1 h_d^* + n_3 h_2^* \\ n_2 h_d^* + n_4 h_2^* \end{bmatrix}. \tag{3.41}$$

3.3.4 RA Scheme with One Relay and with STBC

For the RA scheme with just a single relay and using an STBC in relay, during the first phase of transmission, the source transmits at full power for T_s of the time. During the second phase, or second time slot, the relay can also transmit at full power to the destination, while the source does not transmit as shown in Table 3.4. The corresponding block diagram is in Figure 3-7, including the additional space-time coding block.

TABLE 3.4: TRANSMITTED INFORMATION BY EACH NODE FOR OF THE RA SCHEME WITH ONE RELAY, WITH ALAMOUTI CODING.

	Source	**Relay**
Time slot 1	x_1	-
Time slot 2	x_2	-
Time slot 3	x_2	$-z_{R,2}^*$
Time slot 4	x_1	$z_{R,1}^*$

Thus, the source transmits in both phases of communication. The relay re-transmits its information just in the second phase to the destination. Once more, the same total transmitted power is ensured in this scheme like in the previous ones, and it is distributed so that each node has in mean a power of $P_T/2$. Consequently, the signals received in the destination are now given by

$$\begin{cases} y_1 = \dfrac{A}{\sqrt{2}} h_d s_1 + n_1 \\ y_2 = \dfrac{A}{\sqrt{2}} h_d s_2 + n_2 \\ y_3 = \dfrac{A}{\sqrt{2}} h_d s_1 - h_2 z_2^* + n_3 \\ y_4 = \dfrac{A}{\sqrt{2}} h_d s_2 + h_2 z_1^* + n_4 \end{cases} . \tag{3.42}$$

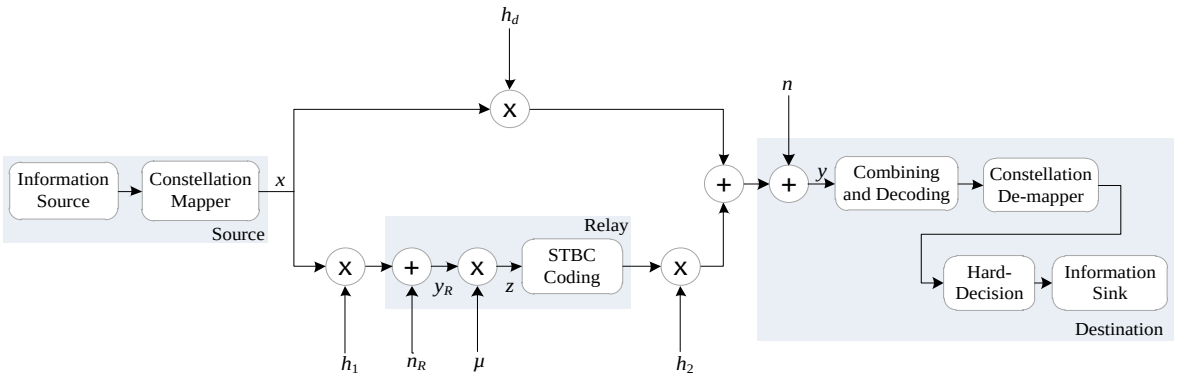

Figure 3-7: Block diagram of RA scheme with one relay and without space-time coding, for AF and EF relays.

The signals transmitted by the relay are defined as follows

$$\begin{bmatrix} z_1 \\ z_2 \end{bmatrix} = \frac{A}{\sqrt{2}} \mu h_1 \begin{bmatrix} s_1 \\ s_2 \end{bmatrix} + \mu \begin{bmatrix} n_{R,1} \\ n_{R,2} \end{bmatrix}, \tag{3.43}$$

where the normalization factors for the EF and AF relay protocols are given by

$$\mu = \begin{cases} \dfrac{1}{\sqrt{\dfrac{|h_1|^2}{2} + \dfrac{1}{SNR_T}}} & \text{, for EF relay protocol} \\ \dfrac{1}{\sqrt{\dfrac{1}{2} + \dfrac{1}{SNR_T}}} & \text{, for AF relay protocol} \end{cases} . \tag{3.44}$$

The soft-estimated signals are then obtained and given by the expression

$$\begin{cases} \hat{s}_1 = y_1 g_0^* + y_3 g_1^* + y_4^* g_2 \\ \hat{s}_2 = y_2 g_0^* - y_3^* g_2 + y_4 g_1^* \end{cases}, \tag{3.45}$$

with the corresponding MRC factors:

$$g_j = \begin{cases} \dfrac{h_d}{\sigma_n^2} & , j = 0 \\ \dfrac{h_d}{\left(1+\mu^2\left|h_2\right|^2\right)\sigma_n^2} & , j = 1 \\ \dfrac{\mu h_1^* h_2}{\left(1+\mu^2\left|h_2\right|^2\right)\sigma_n^2} & , j = 2 \end{cases}. \tag{3.46}$$

3.3.4.1 DF Relay Protocol

For the DF relay protocol case, the signal after the decoding and re-modulation in the relay is given by

$$\mathbf{z} = \frac{A}{\sqrt{2}}\begin{bmatrix} \overline{s}_{R,1} \\ \overline{s}_{R,2} \end{bmatrix}. \tag{3.47}$$

Then, an STBC is applied to those signals at the relay, according to the Table 3.4. The signals received in the destination are then given by

$$\begin{cases} y_1 = \dfrac{A}{\sqrt{2}} h_d s_1 + n_1 \\ y_2 = \dfrac{A}{\sqrt{2}} h_d s_2 + n_2 \\ y_3 = \dfrac{A}{\sqrt{2}} h_d s_1 - h_2 \overline{s}_{R,2}^* + n_3 \\ y_4 = \dfrac{A}{\sqrt{2}} h_d s_2 + h_2 \overline{s}_{R,1}^* + n_4 \end{cases}. \tag{3.48}$$

The estimated resultant signals are given by (3.45), with the corresponding combining factors as follows

$$g_j = \begin{cases} \dfrac{h_d}{\sigma_n^2} & , j = 0 \\ \dfrac{h_d}{\left(1+\mu^2\left|h_2\right|^2\right)\sigma_n^2} & , j = 1 \\ \dfrac{h_2}{\left(1+\mu^2\left|h_2\right|^2\right)\sigma_n^2} & , j = 2 \end{cases}. \tag{3.49}$$

3.4 Capacity Analysis

3.4.1 Average and Outage Capacities

In order to improve our study analysis and to know the limits of the RA schemes defined previously, we use ergodic average and outage capacities as primary performance measures. Average capacity is the theoretical maximum rate that can be achieved arbitrarily and reliably. It is obtained by averaging the capacity through several channel realizations.

Traditional information theory for fading channels has often been devoted to finding the mean capacity for a given channel. However, it is also interesting to know how often the capacity of a system is above some required rate. For any given rate *R*, there exists a nonzero probability for which the instantaneous channel capacity falls below *R*, considering that channel realizations have a finite time duration. Hence rate *R* cannot be achieved reliably in an arbitrary way. Thus, it makes sense to examine capacity through outage characteristics. Outage capacity for a given failure probability, P_{out}, is the maximum rate that can be supported by the channel with probability $1-P_{out}$. Outage or failure probability for a given rate *R* is the probability of the instantaneous capacity falling below *R*, and can be expressed as follows

$$C_o \triangleq \lim_{P_{out}\to 0} \sup\left(R; \Pr\left(C(h) < R\right) < P_{out}\right). \tag{3.50}$$

Outage capacity of low failure probability is of practical interest, considered as a realistic performance measure in [GaSa00], [SuBa08].

Average and outage capacities in MIMO systems are not solvable in a closed form due to the nonlinear logarithm function in the definition of Shannon capacity limit. Some approximations to the MIMO capacity over flat Rayleigh fading channels were introduced by Dohler and Aghvami, in [DoAg05]. Moreover, capacity of RA systems cannot be exactly determined. Outer bounds for these systems were found by Meulen and Sato, in [Meul71] and [Sato76], and for the case of degraded channels by Cover and Gamal in [CoGa79]. Other studies of upper bounds of the capacity of virtual MIMO systems were done in [ScGa00] and [RoZL06]. In the last reference, the authors reduce the overall multilink to a AWGN channel and then used the Shannon capacity,

$$C = \frac{1}{2}\ln\left(1 + SNR_R\right), \tag{3.51}$$

where $SNR_R = \dfrac{P_R}{\sigma_n^2}$ with P_R and σ_n^2 being average signal and noise powers at the receiver, respectively. In our derivations the same approach is followed.

3.4.2 Capacity Expressions

As the power received in the destination is related to the total transmitted power, P_T, instantaneous capacity can be given in function of the SNR_T, which can be seen as the SNR viewed from the transmitter in the point-to-point communication, for the system *j*:

$$C^{(j)} = \log_2\left(1+\left|\beta_{eq}^{(j)}\right|^2 SNR_T\right), \tag{3.52}$$

where $\left|h_{eq}\right|^2$ is the equivalent channel attenuation;, $\left|n_{eq}\right|^2$ is the equivalent noise power; $SNR_T = P_T/\sigma_n^2$; and, $\left|\beta_{eq}\right|^2$ is the equivalent attenuation factor given by

$$\left|\beta_{eq}\right|^2 = \frac{\left|h_{eq}\right|^2}{\left|n_{eq}\right|^2}\sigma_n^2 . \tag{3.53}$$

Characterization of multiple antennas or virtual MIMO schemes through the general expression in (3.52) can be seen as an attempt to approximate them to an equivalent SISO system, which is represented in Figure 3-8.

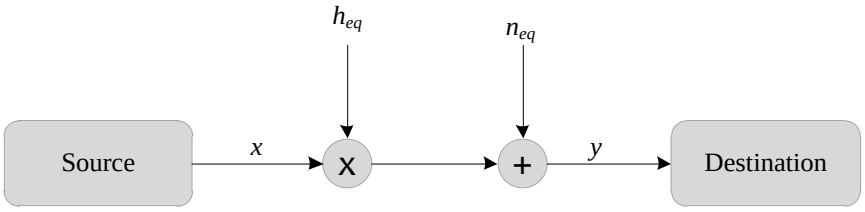

Figure 3-8: Equivalent SISO system to obtain capacity expressions for MISO and RA systems.

Capacity expressions are obtained for RA schemes with AF and EF relay protocols, since they are the simplest protocols. Moreover, they are the best option in comparison with DF, since this one has only good performances for the cases where the first cooperative hop has a high quality.

3.4.2.1 Non-Cooperative Schemes

We start by analyzing the non-cooperative schemes SISO and 2×1 MISO. The SNR in the destination depends on the system we are analyzing, since they have different transmitted powers. The corresponding expression for both schemes are shown in the following expressions:

$$SNR_R^{(SISO)} = SNR_T\left|h\right|^2 \tag{3.54}$$

and

$$SNR_R^{(MISO-2ant)} = SNR_T\frac{\left|h_1\right|^2+\left|h_2\right|^2}{2} . \tag{3.55}$$

The equivalent attenuation factors for SISO and MISO schemes are given by

$$\beta_{eq}^{(SISO)} = |h| \tag{3.56}$$

and

$$\beta_{eq}^{(MISO-2ant)} = \sqrt{|h_1|^2 + |h_2|^2}\,. \tag{3.57}$$

If we consider the existence of path loss attenuation, expressions (3.54) and (3.55) will become as follows, depending on the path loss power $|\varphi_{PLc}|^2$ and fast-fading channel contribution h_F:

$$SNR_R^{(SISO)} = SNR_T\,|h_F|^2\,|\varphi_{PLc}|^2\,(2\cos\theta)^{-\alpha} \tag{3.58}$$

and

$$SNR_R^{(MISO-2ant)} = SNR_T\,\frac{|h_{F,1}|^2 + |h_{F,2}|^2}{2}|\varphi_{PLc}|^2\,(2\cos\theta)^{-\alpha}\,. \tag{3.59}$$

Path loss power is normalized for all systems in relation to cooperative links of RA systems. The relation between the path loss powers of cooperative and direct links is in (3.6). Since the fading channel is defined as a sum of two Gaussian variables in quadrature, i.e., $h_{F,i} = a_i + jb_i$, with $a_i, b_i \sim CN\left(0, \sigma_n^2\right)$, the variable $|h_{F,i}|$ follows a Rayleigh distribution, i.e., $|h_{F,i}| \sim R\left(\sigma\sqrt{\frac{\pi}{2}}, \frac{4-\pi}{2}\sigma^2\right)$, while $|h_{F,i}|^2$ follows a Chi-square distribution with 4 degrees of freedom, i.e., $|h_{F,i}|^2 \sim \chi^2(4)$.

Therefore, we obtain the instantaneous capacity for both systems:

$$C^{(SISO)} = \log_2\left(1 + |h_F|^2\,|\varphi_{PLc}|^2\,(2\cos\theta)^{-\alpha}\,SNR_T\right) \tag{3.60}$$

$$C^{(MISO-2ant)} = \log_2\left(1 + \frac{1}{2}\left(|h_{F,1}|^2 + |h_{F,2}|^2\right)|\varphi_{PLc}|^2\,(2\cos\theta)^{-\alpha}\,SNR_T\right). \tag{3.61}$$

In the theoretical limit, for $\theta = 90^{\circ}$, SISO and MISO capacities will tend to be infinite, due to the fact that these expressions are normalized in relation to the RA system.

3.4.2.2 RA Scheme with Two Relays and Without DP

Similarly to the non-cooperative scheme cases, the SNR viewed from the receiver, in function of SNR_T, for the RA scheme with two RNs and not considering the DP, is given by

$$SNR_R^{(RA-2RN-NDP)} = \frac{2}{3}SNR_T\left|\beta_{eq}^{(RA-2RN-NDP)}\right|^2. \tag{3.62}$$

The equivalent attenuation factor for this scheme, with AF and EF relays, can be extracted from (3.18):

$$\beta_{eq}^{(RA-2RN-NDP)} = \frac{\mu_{R1}^2 |h_1|^2 |h_3|^2 + \mu_{R2}^2 |h_2|^2 |h_4|^2}{\mu_{R1}^2 |h_3|^2 + \mu_{R2}^2 |h_4|^2 + 1}, \tag{3.63}$$

where μ_{Ri} is the normalization factor that depends on the relay protocol and is given by (3.9) and (3.14) for AF and EF cases, respectively.

Therefore, we can obtain the corresponding instantaneous capacity, which includes the large-scale effect of path loss:

$$C^{(RA-2RN-NDP)} = \frac{1}{2}\log_2\left(1+\frac{2}{3}\frac{\mu_{R1}^2 |h_{F,1}|^2 |h_{F,3}|^2 + \mu_{R2}^2 |h_{F,2}|^2 |h_{F,3}|^2}{\mu_{R1}^2 |h_{F,3}|^2 + \mu_{R2}^2 |h_{F,4}|^2 + 1} |\varphi_{PLc}|^2 SNR_T\right). \tag{3.64}$$

The factor of $1/2$ in (3.64) arises from the fact that two consecutive time slots are used to transmit a frame.

Average capacity is then computed over the variables related with fast fading, depending on Rayleigh pdf in (2.14), with $a_{Ri} = |h_{F,i}|$, through expression

$$C_{av}^{(VM)} = \iiiint \frac{1}{2}\log_2\left(1+\frac{2}{3}\frac{\left(\mu_{R1}^2 a_{R1}^2 a_{R3}^2 + \mu_{R2}^2 a_{R2}^2 a_{R4}^2\right)}{\mu_{R1}^2 a_{R3}^2 + \mu_{R2}^2 a_{R4}^2 + 1} |\varphi_{PLc}|^2 SNR_T\right) \prod_{i=1}^{4} p_R(a_{Ri}) da_{R1} da_{R2} da_{R3} da_{R4} \tag{3.65}.$$

Due to the fact that it is not possible to get a closed expression of the expectations, because of the four-dimensional integration in (3.65), capacity, for this scheme and for all the others, was computed resorting to Monte Carlo simulations. We generate several realizations of the channels according to the required statistics, thus evaluating the instantaneous capacity. We then compute the required metrics after multiple realizations.

3.4.2.3 RA Scheme with Two Relays and DP

In the same way we obtained the instantaneous capacity for the RA scheme without a DP, we start by getting the expression of the SNR viewed in destination, for the scheme with the same number of RNs but considering communication through the DP. This is done by consulting the expressions derived in Subsection 3.3.2.1, particularly (3.26), obtaining the following expression

$$SNR_R = \frac{1}{3}\left(|h_d|^2 + \frac{\mu_{R1}^2 |h_1|^2 |h_3|^2 + \mu_{R2}^2 |h_2|^2 |h_4|^2}{1 + \mu_{R1}^2 |h_3|^2 + \mu_{R2}^2 |h_4|^2}\right) SNR_T. \tag{3.66}$$

Consequently, the equivalent attenuation factor and instantaneous capacity expressions with path loss attenuation, are given respectively by

$$\beta_{eq}^{(RA-2RN-DP)} = |h_{F,d}|^2 |\varphi_{PLd}|^2 + H_{eq} |\varphi_{PLc}|^2 \tag{3.67}$$

and

$$C^{(RA-2RN-DP)} = \frac{1}{2}\log_2\left(1+\frac{2}{3}\left|\varphi_{PLc}\right|^2\left(\left|h_{F,d}\right|^2\left(2\cos\theta\right)^{-\alpha}+H_{eq}\right)SNR_T\right). \tag{3.68}$$

The factor H_{eq} is given by

$$H_{eq} = \frac{\mu_{R1}^2\left|h_{F,1}\right|^2\left|h_{F,3}\right|^2+\mu_{R2}^2\left|h_{F,2}\right|^2\left|h_{F,4}\right|^2}{1+\mu_{R1}^2\left|h_{F,3}\right|^2+\mu_{R2}^2\left|h_{F,4}\right|^2} \tag{3.69}$$

and the relay normalization factors are in (3.9) and (3.14), for AF or EF relay protocols, respectively.

3.4.2.4 RA Scheme with One Relay and Without Space-Time Coding

The equivalent attenuation factor for the RA scheme with a single relay and without space-time coding can be obtained through (3.36) and is given by

$$\beta_{eq}^{(RA-1RN-Ncod)} = \left|h_d\right|^2+\frac{\mu^2\left|h_1\right|^2\left|h_2\right|^2}{1+\mu^2\left|h_1\right|^2} \tag{3.70}$$

As a result, the instantaneous capacity expression, with the path loss propagation effect included, is

$$C^{(RA-1RN-Ncod)} = \frac{1}{2}\log_2\left(1+\left|\varphi_{PLc}\right|^2\left(\left|h_{F,d}\right|^2\left(2\cos\theta\right)^{-\alpha}+\frac{\mu^2\left|h_{F,1}\right|^2\left|h_{F,2}\right|^2}{1+\mu^2\left|h_{F,1}\right|^2}\right)SNR_T\right), \tag{3.71}$$

where μ is defined in (3.35) for the AF and EF relay protocols case.

3.4.2.5 RA Scheme with One Relay and with Space-Time Coding

The equivalent attenuation factor for cooperative scheme with a single RN and with an STBC, is derived from (3.45) and is given by

$$\beta_{eq}^{(RA-1RN-cod)} = \frac{1}{2}\left|h_{F,d}\right|^2\left|\varphi_{PLd}\right|^2+\left|\varphi_{PLc}\right|^2\frac{\left|h_{F,d}\right|^2+2\mu^2\left|h_{F,1}\right|^2\left|h_{F,2}\right|^2}{2+2\mu^2\left|h_{F,1}\right|^2}, \tag{3.72}$$

where μ is defined in (3.35). In the same way as in the previous cases, the instantaneous capacity for this scheme is given as follows

$$C^{(RA-1RN-cod)} = \frac{1}{2}\log_2\left(1+\left|\varphi_{PLc}\right|^2\left(\frac{\left|h_{F,d}\right|^2}{2}\left(2\cos\theta\right)^{-\alpha}+\frac{\left|h_{F,d}\right|^2\left(2\cos\theta\right)^{-\alpha}+2\mu^2\left|h_{F,1}\right|^2\left|h_{F,2}\right|^2}{2+2\mu^2\left|h_{F,1}\right|^2}\right)SNR_T\right). \tag{3.73}$$

3.5 Numerical Results and Analysis

3.5.1 Assumptions and Constraints

We consider that CSI is only available at the receivers and that all nodes are similar, with isotropic antennas. Moreover, the transmitted power is normalized at each node so that the total transmitted power of each scheme is maintained the same. Moreover, in our system analysis, for simplicity, we suppress any interaction among signals in the processing for channel estimation and synchronization. Actually, it seems unlikely that a model general enough to evaluate all these interactions and tradeoffs will be tractable [FiKa06].

When analyzing the behavior of cooperative communications using different strategies and algorithms, it is of extreme importance to observe it in different propagation scenarios. One of the options is to consider relative distances between terminal nodes. However, path loss exponent and shadowing parameters should be defined separately, accordingly to Section 2.2.2, giving different results for different combinations of these values. Another option is to characterize propagation aspects as a whole, including the effects of path loss, shadowing, scattering and others, assuming that there are different link quality combinations, quantifying link quality in terms of different SNRs. In this chapter we use the first option and in the following ones the second option is considered.

In this section average and outage capacities are evaluated for the referred cooperative and non-cooperative systems, for several values of the angle θ, which represent different positions of RNs, and for different channel propagation conditions, i.e., having different values of the path loss exponent α.

First, we start by comparing the capacity performances of the two RA schemes with two RNs. Further comparisons of these schemes with the reference non-cooperative ones are also made. Secondly, we focus on a general comparison between all the RA schemes previously defined in this chapter, also for different scenarios. Regarding outage capacity, results are presented in two different ways:

- Outage capacity as a function of SNR_T;
- Outage capacity as a function of path loss exponent.

Concerning both situations above, we consider an initial scenario with fixed characteristics, named as scenario 1. The angle θ is fixed at 30º, while the outage level, P_{out}, is set to 5%, since this is a practical value in wireless communication networks [ZhDa04]. For the case in which the study is made in function of SNR_T, the path loss exponent is fixed at 5, since it is a likewise reasonable value in practice for a moderate intensity fading environment. For the case where the SNR_T is

fixed, despite the large number of values that can be selected, 10 dB was chosen as it is in the middle of the range of SNR that we chose to use. Other scenarios are derived from this one by varying these variables. Since average capacity is not the most realistic tool, its results are also referred to, but just for comparison purposes with the outage capacity measure tool.

Despite considering particular values for the distances between nodes, we define relative distances between the cooperative links and the direct link in order to characterize the path loss factor. The cooperative link distances are equal, since the relays are half way from terminal nodes. The path loss of links S-R_i and R_i-D is considered to be unitary, since these are the shortest links. Thus, according to Figure 3-1 the path loss expressions for cooperative and direct path links are given respectively by

$$\left|\varphi_{PLc}\right|^2 = 1 \tag{3.74}$$

and

$$\left|\varphi_{PLd}\right|^2 = \left(2\cos\theta\right)^{-\alpha}. \tag{3.75}$$

3.5.2 RA Schemes with Two Relays

In this sub-section we compare the RA scheme with two RNs with and without considering the DP with the 2×1 MISO and SISO. Figure 3-9 shows the performance of these schemes in scenario 1 when varying SNR_T. The relay protocols considered are AF and EF.

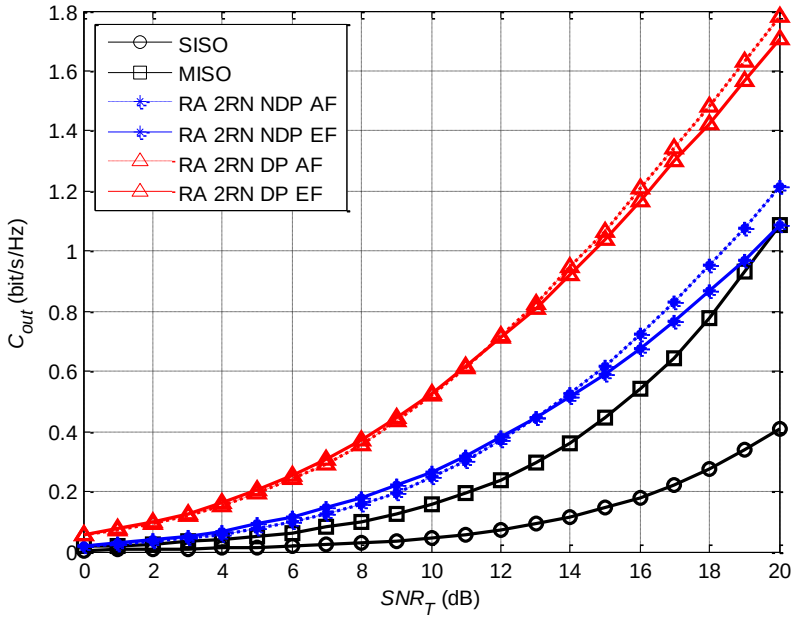

Figure 3-9: Outage capacity of non-cooperative and cooperative schemes with two relays in function of SNR_T, with θ=30º, α=5 and outage level of 5%.

Clearly, RA and MISO systems achieve diversity, outperforming the reference SISO case. Comparing the RA NDP scheme with the MISO one, we conclude that the virtual MIMO scheme has a better performance for low to moderate values of SNR. When using the EF relay protocol, the crossover point, from which this scheme is better than MISO, is 20 dB of SNR_T, while when using the AF relay protocol the crossover point is about 22 dB, for the specified path loss exponent. Some high values of SNR were intentionally not shown in the figure in order to be in the same line with the next figures. The crossover points increase with the path loss exponent. That trend can be explained by the low spectral efficiency of RA schemes, as they need twice as much time to transmit the same information, which is also visible in the factor ½ that is applied to the logarithm function in the capacity of cooperative schemes, as for example in (3.64) . The capacity gain of RA with EF against MISO is 0.15 bit/s/Hz, which is 61% more than the MISO rate for $SNR_T = 12$ dB.

In addition, as expected, the direct path in cooperative schemes strongly increases outage capacity. In comparison with RA NDP, the same trends were obtained, albeit with an upper shift. For $SNR_T = 12$ dB, RA DP has 200% and 89% more capacity in comparison with MISO and RA NDP, respectively. Note that in this case MISO does not outperform the RA scheme, at least at realistic values of SNR.

Concerning the two relay protocols studied for RA schemes, we observe that AF relays are better than EF relays for SNR_T higher than 12 dB, concerning outage measurements. This is due to the differences resulting from the normalization power made in relays. The crossover point, from which EF relay protocols become worse than AF, is approximately the same for all the schemes. For values of SNR_T lower than 12 dB, the EF case is the best option, having a maximum gain of 15% as compared to the AF for this scenario. For low values of SNR_T, slightly better performances occur when using the AF relay protocol.

The same curves in terms of average capacity can be seen in Figure 3-10. In general, we observe the same trend for both average and outage capacity performances, although the SISO system comes closer to cooperative schemes. Another difference is that AF relays are always slightly better than EF. However, as previously seen, outage capacity is a more realistic measurement. Thus, this is the measurement tool selected for further analysis.

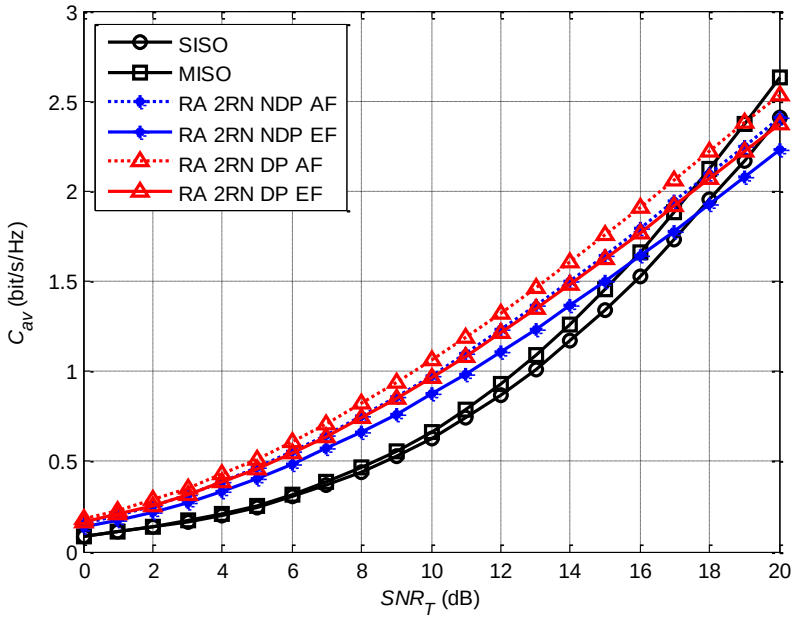

Figure 3-10: Average capacity of non-cooperative and cooperative schemes with two relays in function of SNR_T, with θ=30º, α=5 and outage level of 5%.

Until now we have only considered the case in which the angle θ is equal to 30º. Some differences can be seen in terms of capacity for low to moderate values of that angle in Figure 3-11 and Figure 3-12, for $\theta = 0^{\circ}$ and $\theta = 60^{\circ}$, respectively. In fact, it is easy to verify from (3.60) or (3.61) that, for high SNR, this accounts for a vertical shift of the curves of $-\alpha \log_2(2\cos\theta)$. In turn, it results in a variation of 0.2 α bit/s/Hz by changing the angle from 0 to 30º. Regarding these figures, we conclude that as the angle amplitude between source and relays decreases, the difference between the virtual antenna and the MISO schemes increases, due to the decrease in the transmission distance and the resulting lower path loss attenuation.

The case of θ=0º can be considered as a limit approach, for the situation when the distance between the terminal nodes is so far that this angle is approximately zero. This situation represents the best angle so that the maximum advantage for cooperative schemes is achieved, since it corresponds to the shortest distance between terminal nodes and relays and, thus, there is less path loss attenuation. In conclusion, the higher the angle between the source node and the relays, the smaller the advantage obtained with the virtual MIMO schemes.

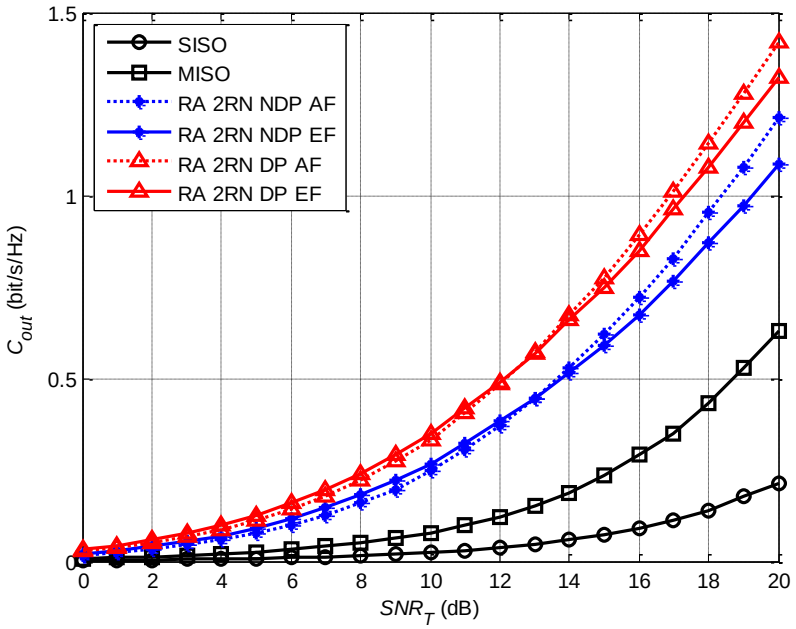

Figure 3-11: Outage capacity of non-cooperative and cooperative schemes with two relays in function of SNR_T, with θ=0º, α=5 and outage level of 5%.

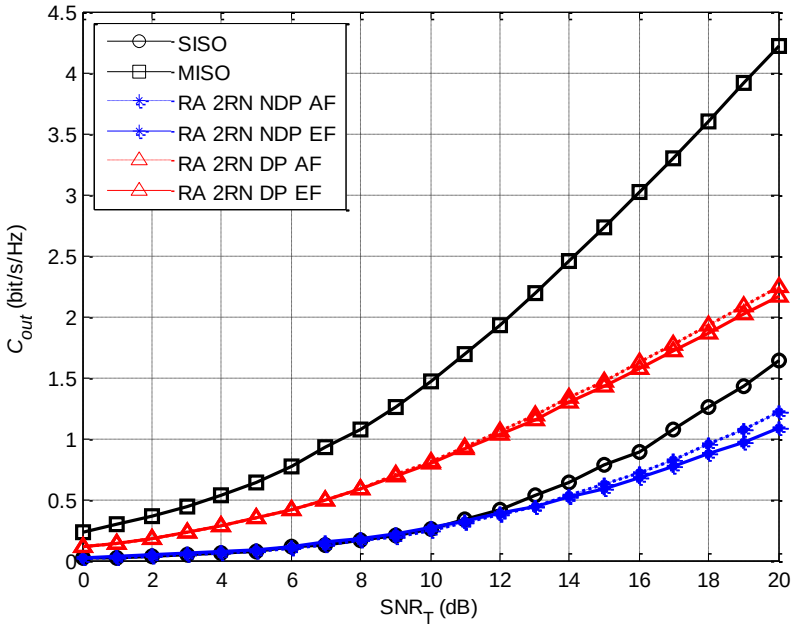

Figure 3-12: Outage capacity of non-cooperative and cooperative schemes with two relays in function of SNR_T, with θ=60º, α=5 and outage level of 5%.

Another limit to outage probability can also be used, such as $P_{out}=10\%$. Outage capacities of the same schemes for this outage level are presented in Figure 3-13. Comparing this scenario with the one in Figure 3-9, where the outage level is of 5 %, all the capacity rates slightly increase.

However, the relations between the different schemes are maintained, including the crossover points. The opposite happens if the failure limit decreases with the reduction of capacity rates.

Figure 3-14 shows outage capacity performances as a function of the path loss exponent, considering the scenario 1. Once more RA schemes have higher capacities for all the SNRs than the simplest SISO scheme. Comparing the cooperative scheme with the MISO one, we conclude that the MISO scheme is better for low path loss exponents, while for higher values of this exponent the opposite is true. For example, for a free space scenario, where $\alpha = 2$, MISO just has a rate gain of 12.5% in comparison with RA DP EF, while for $\alpha = 4$ the capacity of RA DP EF is 70.4% more than MISO capacity. The crossover point from which the RA schemes are advantageous in relation to MISO depends on the scheme considered and the relay protocol used. The crossover points are of $\alpha = 4$ using EF relays and $\alpha = 4.1$ using AF relays for RA NDP, and of $\alpha = 2.4$ for RA DP scheme in both relay protocols. Thus, the cooperative schemes are beneficial in most propagation scenarios representative of mobile communications.

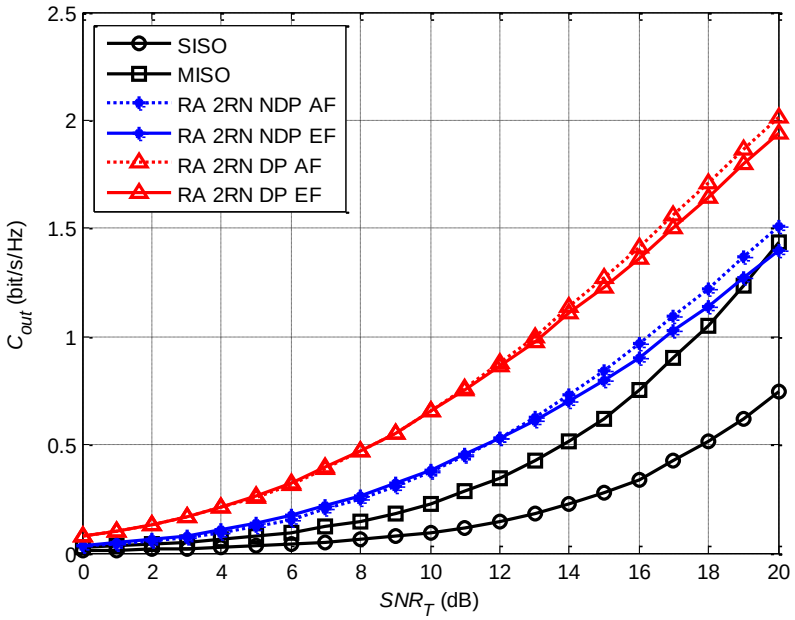

Figure 3-13: Outage capacity of non-cooperative and cooperative schemes with two relays in function of SNR_T, with θ=30º, α=5 and outage level of 10%.

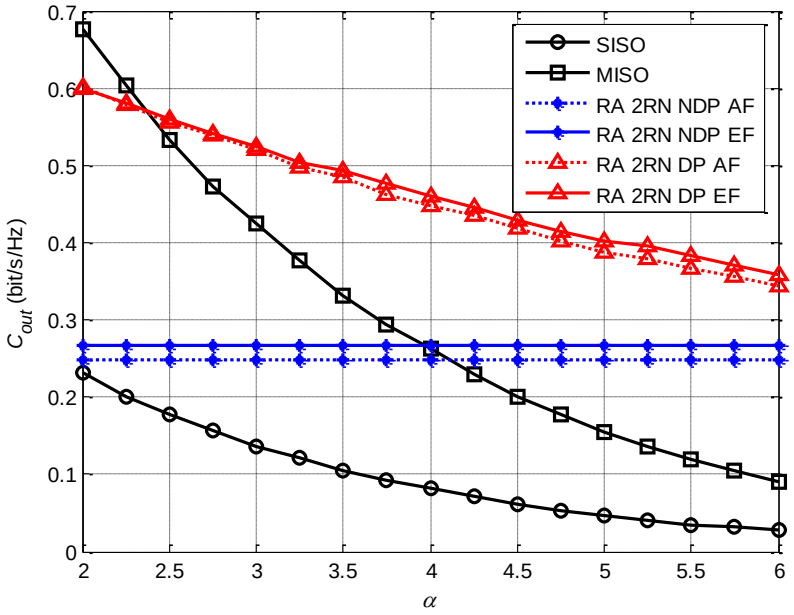

Figure 3-14: Outage capacity of non-cooperative and cooperative schemes with two relays in function of the path loss exponent, with θ=30º, SNR_T=5 dB and outage level of 5%.

3.5.3 RA Schemes with One and Two Relays

In Figures 3-15 to 3-18, the performance of all the cooperative schemes with one and two relays previously referred to is presented, considering the use of the EF relay protocol, since this is better than the AF for low to moderate SNR values.

The outage capacity of these schemes for scenario 1 is stated in Figure 3-15. In order to easily quantify the differences between schemes for this scenario, Table 3.5 shows the gains in dBs obtained with each pair of schemes for the target outage capacity of 0.4 bit/s/Hz.

For this propagation scenario, we observe that all the cooperative schemes outperform the conventional SISO and MISO systems, when using the EF relay protocol. We can observe a gain of approximately 11.6 dB and 6.1 dB for RA-2RN DP based scheme, against the SISO and MISO systems respectively, considering C_{out}=0.4 bit/s/Hz. The best scheme is the cooperative one, with two relays and with DP, followed by the RA-1RN scheme with space-time coding, with a difference between them of 2.8 dB, for C_{out}=0.4 bit/s/Hz. This is due to the use of the DP, which avoids an additional noise point that interferes in the useful signal. However, in some situations it is not possible to use the DP due to the poor link quality, for example.

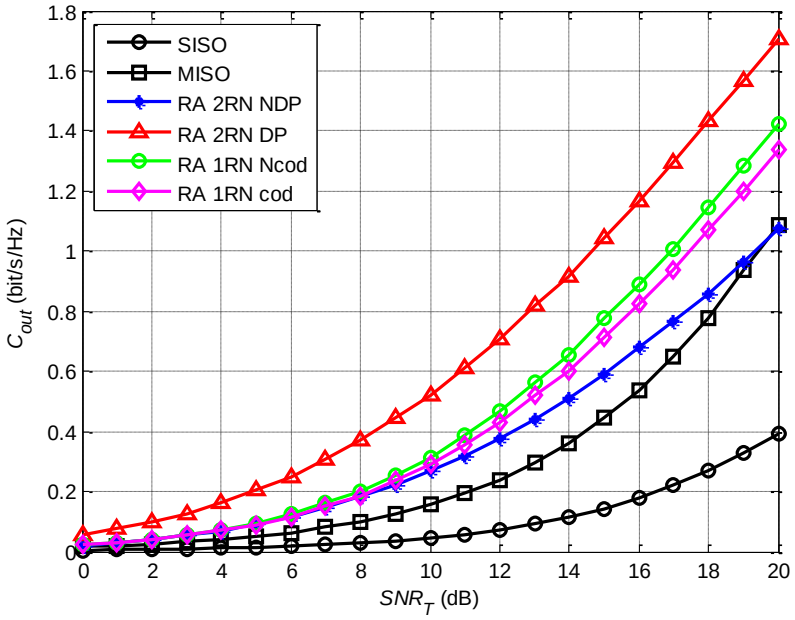

Figure 3-15: Outage capacity for cooperative and non-cooperative schemes with EF relay protocols for θ=30º, α=5 and outage level of 5%, for the EF relay protocol.

TABLE 3.5: GAIN IN DBS OBTAINED FOR EACH SCHEME OF THE FIRST COLUMN WHEN COMPARED WITH EACH SCHEME OF THE FIRST LINE, FOR C_{OUT}=0.4 BIT/S/HZ, WHEN USING EF RELAY PROTOCOL AND FOR SCENARIO 1.

Gain in dBs	SISO	MISO	RA-2RN NDP	RA-1RN cod	RA-1RN Ncod
RA-2RN DP	7.6	2.1	-	-	-
RA-1RN cod	8.4	2.9	0.8	-	-
RA-1RN Ncod	8.8	3.3	1.2	0.4	-
RA-2RN DP	11.6	6.1	4.0	3.2	2.8

Comparing the two investigated schemes with two relays, they differ in about 4 dB, for C_{out}=0.4 bit/s/Hz. In the RA-2RN DP, additional space diversity and also a virtual array gain are achieved, due to the DP. This *virtual array gain* is similar to the array gain achieved by the co-located MIMO systems. It arises from the effect of combining coherently multiple channels at the receiver, transmitter or both. However, in this case, the received signals are coherently combined in multiple instants of time instead of in multiple antennas. Furthermore, from the same performance results, we observe that the RA-2RN DP based scheme outperforms the RA schemes with a single

relay. All the schemes achieve virtual array gain, but the first one has an additional double-Rayleigh channel and thus some additional diversity is achieved.

Concerning the schemes with just a single RN, the one with STBC is slightly outperformed by the one with no space-time coding, resulting in more 0.5 dB, in the same conditions. This is justified by the different virtual antenna gains for each scheme. These differences are evident in capacity expressions and in the instantaneous transmitted power in the source, which are lower since the source transmits continuously in this scheme.

An interesting observation is that the RA schemes with a single relay are better than those with two relays and without DP. The latter has one more RN, which introduces more noise and decreases the transmitted power per node. Moreover, in opposite to the RA schemes with a single relay, this one does not have virtual antenna gain. Furthermore, its spatial diversity gain is slightly lower than in the scheme with a single relay, since double-Rayleigh fading channels have lower order diversity than single-Rayleigh channels. The lower path losses result from the fact that the additional relay is not enough to compensate for these disadvantages.

If we consider a scenario with a low path loss exponent, e.g., with α=3, which is close to a free space environment, we still have better capacity rates with RA-2RN DP and RA-1RN than with the other non-cooperative schemes for $SNR_T < 15$ dB, although the differences are not higher than 1 dB. Performances for those schemes in such a scenario are shown in Figure 3-16.

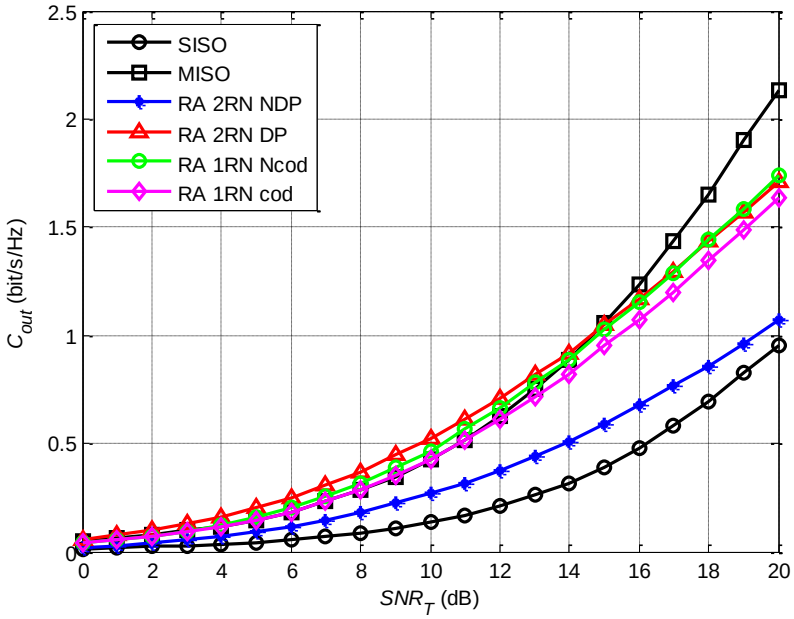

Figure 3-16: Outage capacity for cooperative and non-cooperative schemes with EF relay protocols for θ=30º, α=3 and outage level of 5%, for the EF relay protocol.

Some results for scenarios with different positions of the RNs are also obtained. With the decrease in the position angle of the relays, all the cooperative schemes will have even higher capacity gains. This is equivalent to increasing the distance between terminal nodes. The lower the angle, the higher is the advantage of cooperative schemes in relation to non-cooperative, since the relative path loss effect of the DP will be higher.

Changing the angle position of the relays to 0º, the cooperative schemes will all have higher capacity gains, in comparison with SISO and MISO, as it can be seen in Figure 3-17. For example the RA-2RN DP scheme achieves near 7.2 dB of gain in relation to MISO scheme, for C_{out}=0.2 bit/s/Hz. This theoretical limit scenario represents the situation when the relays are far away enough, so that we may consider them in the same line as the source-to-destination direction. This is the most advantageous relay position for cooperative schemes.

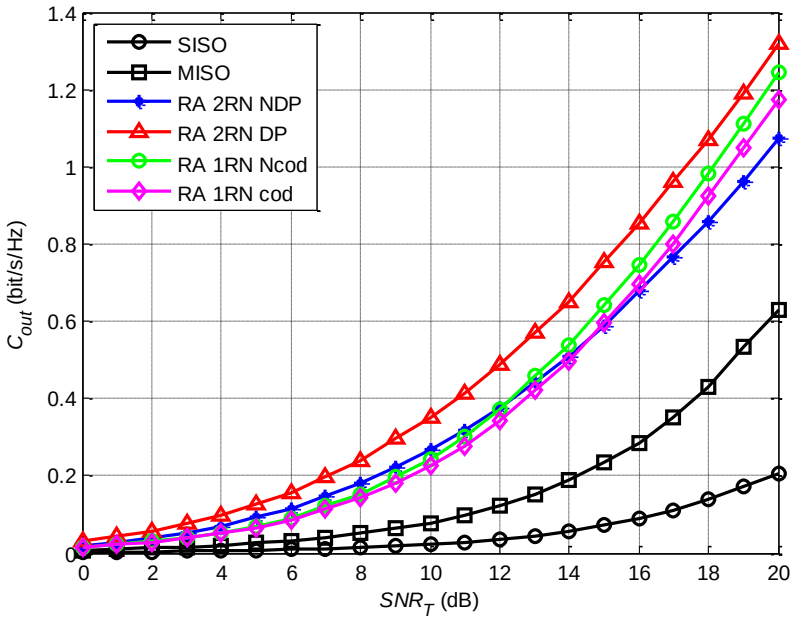

Figure 3-17: Outage capacity for cooperative and non-cooperative schemes with EF relay protocols for θ=0º, α=5 and outage level of 5%, for the EF relay protocol.

On the other hand, for higher angles all the cooperative schemes have lower capacity rates than the MISO system. In these scenarios, path loss reduction in the cooperative system is not enough to compensate for the half spectral efficiency, the additional noise introduced by the relays and the higher diversity order of the co-located antenna system. For example, if we change the angle θ to 60º, as it can be seen in Figure 3-18, there is no advantage in using RA schemes, in terms of capacity rates.

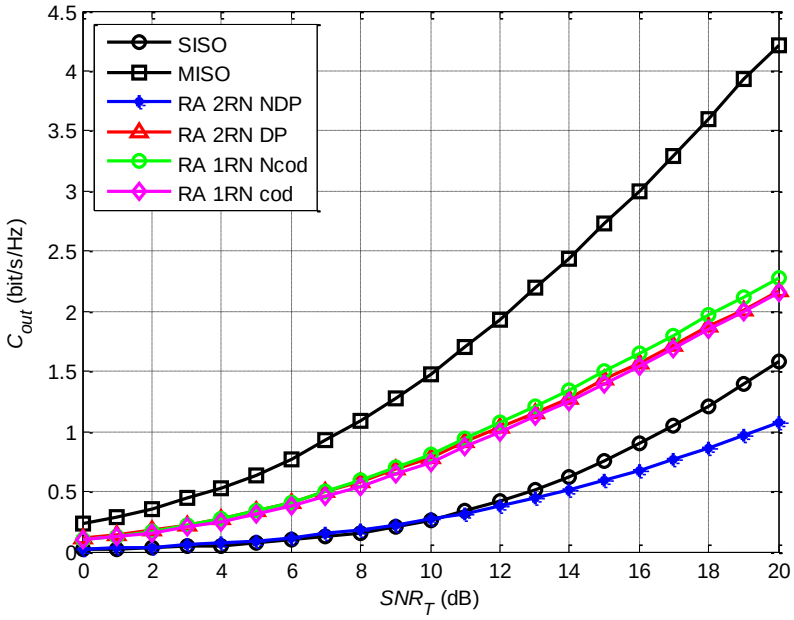

Figure 3-18: Outage capacity for cooperative schemes with EF relay protocols for θ=60º, α=5 and outage level of 5%, for the EF relay protocol.

Figure 3-19 compares the reference non-cooperative systems with the best single relay assisted scheme and both two-relay assisted schemes, considering the AF and EF relay protocols. In this scenario, all cooperative schemes outperform the SISO and the co-located MISO systems, even with the AF relay protocol. In the single relay assisted scheme, the use of the EF relay protocol brings advantages in comparison with the use of the AF one, even for high SNR_T values, achieving, for example, 27.9% of extra gain comparatively, for 15 dB of SNR_T. For the two-relay schemes this gain is very low and occurs just for low values of SNR_T, as it was mentioned previously.

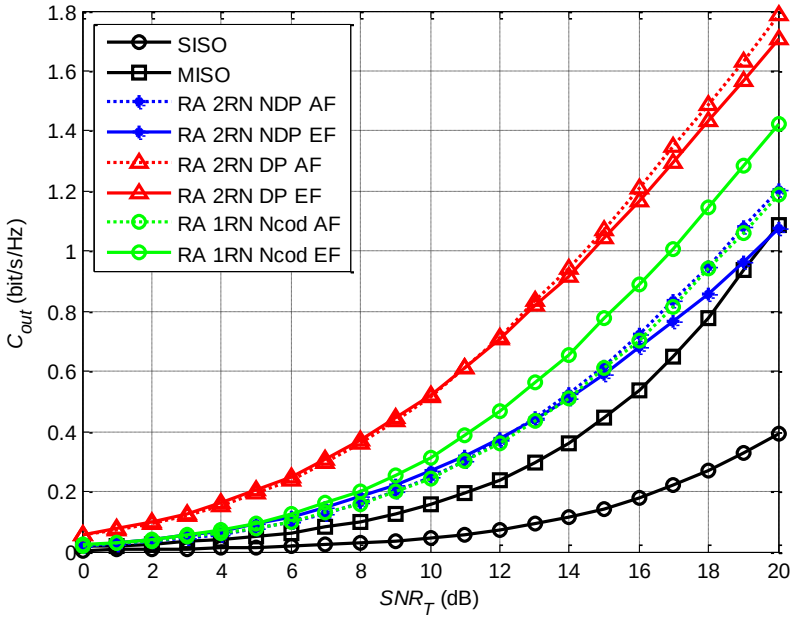

Figure 3-19: Outage capacity for cooperative schemes and non-cooperative for θ=30º, α=5 and outage level of 5%, for AF and EF relay protocols.

3.6 Conclusions

In this chapter RA schemes were analyzed and their performances were compared with basis on the study of their theoretical capacity. We observed that, for scenarios in which a low path loss exponent characterizes the propagation channel, the use of co-located antennas has advantages when compared with the RA scheme with two relays and no DP. However, for moderate to high-loss propagation scenarios, the RA scheme presents considerable capacity gains, with both EF and AF relay protocols, considering reasonable values of SNR, thus overcoming its lower spectral efficiency. The crossover point in the path loss exponent was about 4, considering the SNR at the transmitter as 10 dB. Moreover, this means that the cooperative schemes may achieve better capacity results than multi-antenna systems depending on the relative position of relays and on the density of channels and terminals. This is justified by the cooperative diversity achieved and the path loss reduction obtained when using the RA schemes.

Capacity gains were higher using the EF relay protocol, as compared to the AF one, for all the SNRs in the RA-1RN scheme and for low values of SNR in the other schemes. This is mainly due to the way relay equalization affects noise power.

The results for capacities also showed that, in the cases where it is possible to use the DP, such system performances increase. The scheme with the best capacity results is the one with two

RNs and DP, achieving 6.1 dB of improvement in relation to MISO, for C_{out}=0.4 bit/s/Hz, in the scenario with α=5 and θ=30º. This was justified by the high diversity order obtained with the additional path, besides the high virtual antenna gain. This cooperative scheme was better than the corresponding MISO in almost all the situations, even for a path loss factor of 3, except for acute short transmission distances. The low spectral efficiency and the additional noise introduced by the relays were compensated by the lower path loss effect and higher diversity order introduced by them. Therefore, the capacity gains were improved due to the exploration of this path by the destination receiver.

The single relay schemes considered were shown to have different performances, depending on the processing made in relays, since the combination of space-time coding and transmitted power constraints changes the values of virtual antenna gain. Furthermore we observed that the simplest scheme with a single relay outperforms the more resource-consuming RA scheme with two relays without the DP. Therefore, we can conclude about the importance of the algorithm chosen to implement a RA communication, including the distributed code used.

In conclusion, RA schemes are beneficial mainly in dense urban mobile communications scenarios, achieving spatial diversity, while reducing the path loss attenuation in comparison with the co-located systems, with the advantage of ensuring low power requirements in almost all the cases and less equipment relatively to the conventional MISO with co-located antennas.

4 Distributed SFBC RA Scheme for OFDM Systems

4.1 Introduction

In the previous chapter several schemes were considered and their capacity was analyzed. We concluded about the importance of the choice of the algorithm and the code used in the final capacity gain. In this chapter the classical three relay-node-assisted schemes are studied in more detail, based on OFDM technology and considering practical scenarios, since most of the recently proposed relaying schemes are not targeting OFDM based systems and are assessed under simplified scenarios. Thus, the aim of the study presented in this chapter is to propose and evaluate the performance of two DL OFDM based RA schemes with a single relay and using a distributed SFBC. The system definition is presented in Section 4.2. Both schemes have a UT with a single antenna and a BS with a two-antenna array. The schemes differ on the number of antennas equipping the relay, which can be one or two. Four half-duplex relay protocols are analyzed, in the following two sections, for both schemes: amplify-and-forward, equalize–and-forward, decode-and-forward and selective decode-and-forward. The performance is evaluated under realistic scenarios, such as correlated antennas, precise channel models and Doppler effects. Typical pedestrian scenarios based on LTE specifications and channel turbo coding are considered in the realistic simulations evaluated, emulating possible 4G system conditions. BER and FER performance metrics are obtained through Monte Carlo simulation and analyzed and compared with reference non-cooperative systems in Section 4.5 and the main conclusions are presented in Section 4.6.

4.2 System Definition

Let us consider a general 4G cooperative communication system, for a downlink transmission. The rates required for downlink transmissions are generally higher than for the uplink, and therefore cooperation will be more beneficial when applied to the downlink, reason why we focus on this case. This RA system includes different configurations with different numbers of nodes and antennas. Thus, this system will also be used in the next chapter for other configurations. The generic scheme has *L* RNs cooperating with a BS and a UT, as shown in Figure 4-1.

The system nodes can have multiple transmitter or receiver antennas, specially the BS. The BS and UT are equipped with N_B and N_U antennas, respectively. The RNs are seen as dedicated and strategically located relays and are equipped with N_R antennas. In addition, relays are considered to be half-duplex. When *L* is zero, the system is considered to be non-cooperative. In this case, if $N_B > 1$ or $N_U > 1$, we have a co-located multiple antenna system. When at least one RN is cooperating with the point-to-point communication, the system can be referred to as RA or VAA system. As different cooperative schemes can be considered by changing the number of antennas in each terminal, their designation can be simplified to the form RA *L* RN $N_B \times N_R \times N_U$. Similarly, the non-cooperative systems can be named non-relay-assisted (NRA) schemes with N_B and N_U antennas at the BS and UT, respectively, which can be generically referred to as NRA $N_B \times N_U$.

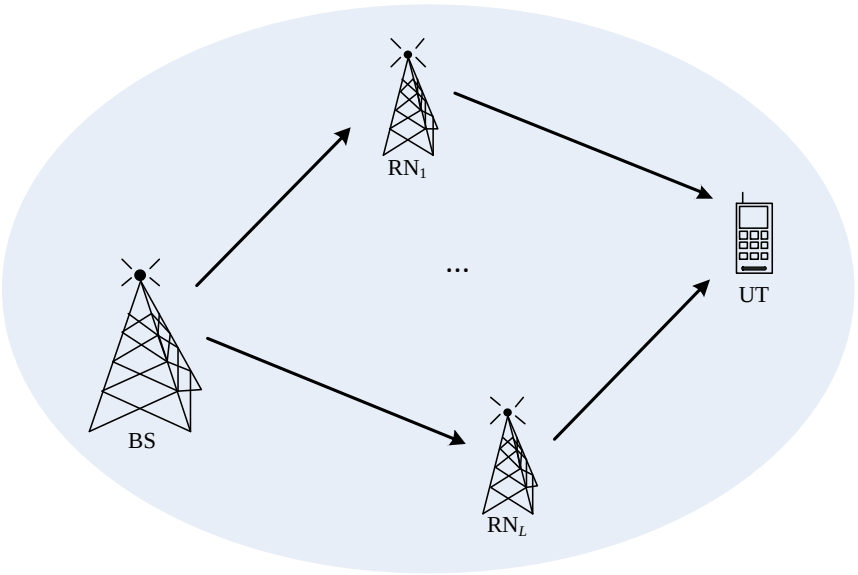

Figure 4-1: General downlink system with *L* relays cooperating with one BS and one UT.

In this chapter we consider the cooperative schemes where cooperation is assisted by one RN, as represented in Figure 4-2. Three main links can be identified: BS→UT represented by channels $h_{bu\_q_b}$, with $q_b \in \{1,...,N_B\}$; BS→RN formed by channels $h_{br\_q_b\_q_r}$, with $q_r \in \{1,...,N_R\}$; and,

RN→UT represented by channels h_{ru,q_r}. Moreover, for each subcarrier, channels are modeled by Rayleigh flat-fading channels. The BS is equipped with an antenna array with two elements, i.e., $N_B = 2$. The RN can have one or two antennas, i.e., $N_R \in \{1,2\}$, as presented in Figure 4-3 and Figure 4-4, severally. These schemes are referred to as RA 1RN 2×1×1 and RA 1RN 2×2×1 respectively, according to the previously mentioned.

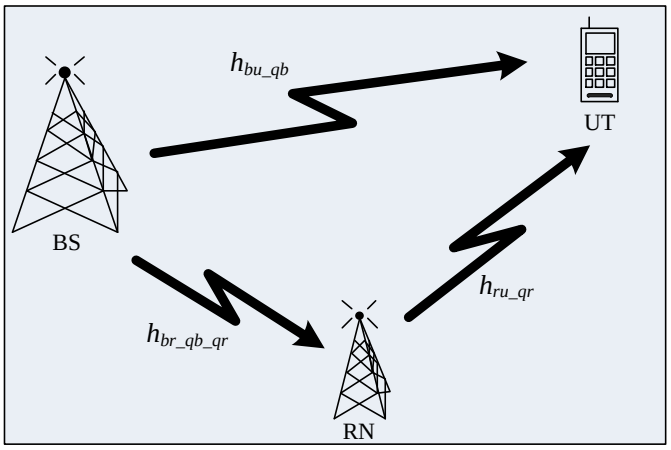

Figure 4-2: RA scheme with one RN and correspondent links between nodes.

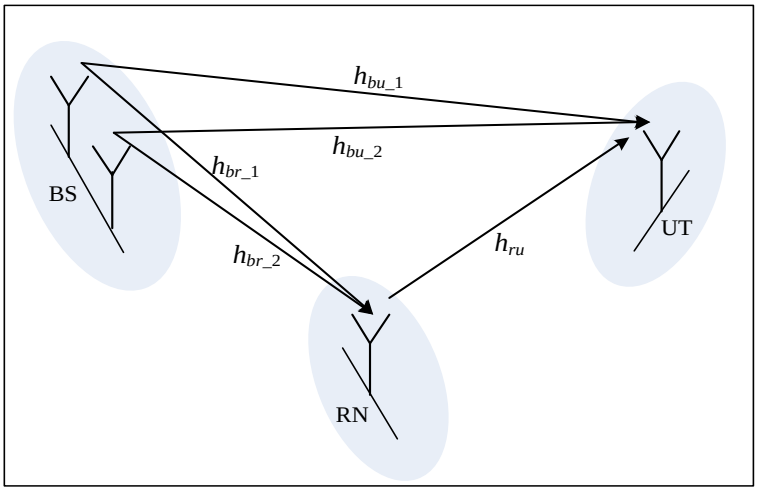

Figure 4-3: RA scheme with one RN equipped with a single antenna (RA 1RN-2×1×1).

The communication process, in both schemes, consists of two time phases, each with a time slot duration, which was defined by Nabar and Bölcskei, in [NaBK04], as Protocol II. The BS communicates with the RN and UT during the first time slot, while the relay is idle. In the second time slot, only the relay terminal communicates with the UT. This protocol realizes a maximum degree of broadcasting and exhibits no receive collision. The degree of broadcasting is given by the number of nodes that are listening to the source node simultaneously, i.e., in the same time slot. Thus, it will have the value 2 if both RN and UT are listening, or 1 if only the RN or the UT is

listening. Moreover, receive collision is said to be maximum if the destination node receives information simultaneously from both the BS and the RN.

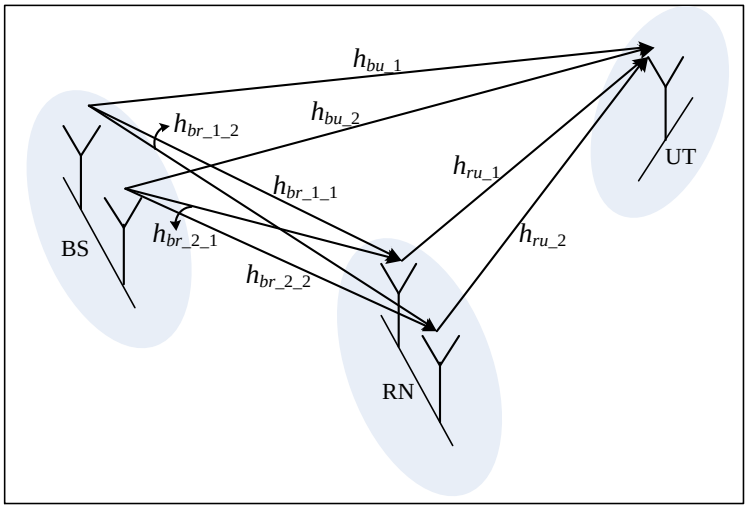

Figure 4-4: RA scheme with one RN equipped with two antennas (RA 1RN 2×2×1).

As we have no receive collision with the proposed RA scheme, since we have orthogonal transmission between nodes, no space-time coding is needed for the single antenna terminals. However, in the nodes equipped with two antennas we shall use an STBC or SFBC, so that we have the maximum spatial diversity. As we consider an OFDM communication, we use the space-frequency code Alamouti, with code rate 1, already defined in previous schemes, which is shown in Table 4.1, where s_p is the data symbol transmitted by the p^{th} subcarrier and the complex conjugate operator is denoted by $(\bullet)^*$. This code is implemented in the BS for both schemes and in the RN in the distributed SFBC RA scheme with two antennas at the RN.

TABLE 4.1: SFBC MAPPING SCHEME FOR THE TWO-ANTENNA NODES.

	Antenna 1	**Antenna 2**
Subcarrier *p*	s_p	$-s_{p+1}^*$
Subcarrier *p*+1	s_{p+1}	s_p^*

We can also analyze the relay protocols considered in terms of complexity. In Table 4.2 the availability of CSI from the BS to the RNs and the decision that is made in RNs are summarized. The relay protocols presented are in order from the less to the more complex ones: AF, EF, DF and SDF. The detailed description of each relay protocol is made in Section 2.4.4. The AF relay protocol

is the simplest one, as observed in the table, with no information needed about the channels and with no operation besides the power normalization. The SDF one is the more complex, since besides the two parameters analyzed in this table, demands a method that allows the RNs to verify if the detection done is correct or not.

TABLE 4.2: CSI AND DECISION NEEDED IN RNS FOR AF, EF AND DF RELAY PROTOCOLS.

	CSI at RN	**Decision in RN**
AF	No	None
EF	Yes	Soft-Decision
DF	Yes	Hard-Decision
SDF	Yes	Hard-Decision

4.3 Protocols for a Single-Antenna RA Scheme

4.3.1 General Scheme Description

The algorithm for the RA 1RN 2×1×1 scheme is described in this section. The algorithm depends on the processing at the RN. The first phase of the communication is common to all the relay protocols, being firstly described independently from the protocol used.

During the first phase the BS transmits at full power for a time slot duration, T_s. Thus, the received signals at the UT, at instant k and on subcarrier p and p+1, are given by

$$\begin{cases} y_{UT,k,p} = \dfrac{1}{\sqrt{2}}\left(s_{k,p}h_{bu\_1,k,p} - s^{*}_{k,p+1}h_{bu\_2,k,p}\right) + n_{UT,k,p} \\ y_{UT,k,p+1} = \dfrac{1}{\sqrt{2}}\left(s_{k,p+1}h_{bu\_1,k,p+1} + s^{*}_{k,p}h_{bu\_2,k,p+1}\right) + n_{UT,k,p+1} \end{cases}, \tag{4.1}$$

where $s_{k,p}$ is the data symbol of the p^{th} subcarrier, with unit power; $h_{bu\_q_b,k,p}$ with $q_b \in \{1,2\}$, represents the complex Rayleigh flat fading non-cooperative channel on subcarrier p between the q_b^{th} BS antenna and the UT; and, $n_{UT,k,p}$ and $n_{UT,k,p+1}$ are the zero mean complex additive white Gaussian noise samples with variance of $\sigma^2_{n_d}$, at instant k and on subcarrier p and p+1, respectively. The factor $1/\sqrt{2}$ arises from the unitary transmitted power normalization, which is made for each node.

On the other hand, the received signals at the RN, at instant k, on subcarrier p and p+1, are given by

$$\begin{cases} y_{RN,k,p} = \dfrac{1}{\sqrt{2}}\left(s_{k,p}h_{br\_1,k,p} - s^{*}_{k,p+1}h_{br\_2,k,p}\right) + n_{RN,k,p} \\ y_{RN,k,p+1} = \dfrac{1}{\sqrt{2}}\left(s_{k,p+1}h_{br\_1,k,p+1} + s^{*}_{k,p}h_{br\_2,k,p+1}\right) + n_{RN,k,p+1} \end{cases}, \tag{4.2}$$

where $h_{br\_q_b,k,p}$ represents the complex Rayleigh flat fading cooperative channel, between the BS and RN, on subcarrier p or p+1, related to the q_b^{th} BS antenna; $n_{RN,k,p}$ and $n_{RN,k,p+1}$ are the zero mean complex AWGN samples on the RN, with variance of $\sigma^2_{n_{c2}}$, on subcarrier p and $p+1$, respectively.

The OFDM systems are usually designed so that the subcarrier separation may be significantly lower than the coherence bandwidth of the channel. Therefore, as these algorithms are designed for OFDM communications, the fading in two adjacent subcarriers can be considered flat, i.e., we can consider $h_{\Phi,k,p} = h_{\Phi,k,p+1}$, with $\Phi \in \{'bu','br','ru'\}$.

During the second phase, or second time slot, the relay can also transmit at full power to the UT, while the BS does not transmit. The signals transmitted by the relays during this phase depend on the processing done in this node. Thus, description of protocols is made separately from this point on for AF, DF and SDF protocols.

4.3.2 Amplify-and-Forward Protocol

In the AF relay protocol the relay just normalizes the received signals and retransmits them, as mentioned previously in Sub-section 3.3.1.1. The received signals at the UT at instant $k+1$, on a pair of adjacent subcarriers, are then given by the following expressions

$$\begin{cases} y_{UT,k+1,p} = \dfrac{1}{\sqrt{2}}\mu h_{ru\_1,k+1,p}\left(s_{k,p}h_{br\_1,k+1,p} - s^{*}_{k,p+1}h_{br\_2,k,p}\right) + \mu h_{ru\_1,k+1,p}n_{RN,k,p} + n_{UT,k+1,p} \\ y_{UT,k+1,p+1} = \dfrac{1}{\sqrt{2}}\mu h_{ru\_1,k+1,p}\left(s_{k,p+1}h_{br\_1,p} + s^{*}_{k,p}h_{br\_2,k,p}\right) + \mu h_{ru\_1,k+1,p+1}n_{RN,k,p+1} + n_{UT,k+1,p+1} \end{cases}, \tag{4.3}$$

where $h_{ru\_1,k,p}$ represents the complex flat fading cooperative Rayleigh channel between the RN and UT, on subcarrier p or p+1; $n_{UT,k+1,p}$ and $n_{UT,k+1,p+1}$ are the zero mean complex AWGN samples, with variance of $\sigma^2_{n_{c2}}$, at instant $k+1$ and on subcarrier p and p+1, correspondingly. The normalization constant, μ, which was already mentioned for the system defined in Chapter 3, is used to constrain to one the average transmitted power by the relay on each subcarrier. It is given in this case by

$$\mu = \sqrt{\frac{1}{1+\sigma^2_{n_{c1}}}}. \tag{4.4}$$

Defining $h_{eq\_1,k+1,p} = \frac{1}{\sqrt{2}} \mu h_{br\_1,k,p} h_{ru\_1,k+1,p}$ and $h_{eq\_2,k+1,p} = \frac{1}{\sqrt{2}} \mu h_{br\_2,k,p} h_{ru\_1,k+1,p}$, (4.3) can be re-written as

$$\begin{cases} y_{UT,k+1,p} = \left(s_{k,p} h_{eq\_1,k+1,p} - s^*_{k,p+1} h_{eq\_2,p} \right) + \mu h_{ru\_1,k,p} n_{RN,k,p} + n_{UT,k+1,p} \\ y_{UT,k+1,p+1} = \left(s_{k,p+1} h_{eq\_1,k+1,p} + s^*_{k,p} h_{eq\_2,p} \right) + \mu h_{ru\_1,k+1,p} n_{RN,k,p+1} + n_{UT,k+1,p+1} \end{cases} . \quad (4.5)$$

At the UT, MRC is used to combine the received signal from the direct link and the two-hop path. Thus, the final estimated symbol for an arbitrary pair of adjacent subcarriers, which were transmitted during time slots k and $k+1$, is obtained by the correspondent space-frequency decoding. Thus, the estimation of $s_{k,p}$ is given by

$$\begin{cases} \hat{s}_{k,p} = \sum_{j=0}^{1} g^*_{1,k+j,p} y_{UT,k+j,p} + g_{2,k+j,p} y^*_{UT,k+j,p+1} \\ \hat{s}_{k,p+1} = \sum_{j=0}^{1} g^*_{1,k+j,p} y_{UT,k+j,p+1} - g_{2,k+j,p} y^*_{UT,k+j,p} \end{cases} . \quad (4.6)$$

The equalization coefficients are presented as

$$g_{q_r,k+j,p} = \begin{cases} \frac{1}{\sqrt{2}} \frac{h_{bu\_q_r,k,p}}{\sigma^2_{n_d}} & , j = 0 \\ \frac{h_{eq\_q_r,k+1,p}}{\sigma^2_{n_c,k+1,p}} & , j = 1 \end{cases} \quad (4.7)$$

and we consider that $g_{j,q_r,k,p} = g_{j,q_r,k,p+1}$, with j=0,1 due to the previous channel assumption. The equivalent noise power of the signals obtained through cooperation, which is dependent on subcarrier p or p+1 and on time slot $k+1$, is referred to as $\sigma^2_{n_c,k+1,p}$ and is given by

$$\sigma^2_{n_c,k+1,p} = \mu^2 \left| h_{ru\_1,k+1,p} \right|^2 \sigma^2_{n_{c1}} + \sigma^2_{n_{c2}} . \quad (4.8)$$

Since this total noise power depends on the factor $\left| h_{ru\_1,k,p} \right|^2$, it must be estimated for all the used subcarriers. Then, the expanded expression for each estimated symbol, on a generic subcarrier p, is given by

$$\begin{aligned} \hat{s}_{k,p} = & \left(\frac{1}{2} \frac{\left| h_{bu\_1,k,p} \right|^2}{\sigma^2_{n_1}} + \frac{1}{2} \frac{\left| h_{bu\_2,k,p} \right|^2}{\sigma^2_{n_1}} + \frac{\left| h_{eq\_1,k+1,p} \right|^2}{\sigma^2_{n_t,p}} + \frac{\left| h_{eq\_2,k+1,p} \right|^2}{\sigma^2_{n_c,k,p}} \right) s_{k,p} \\ & + \frac{1}{\sqrt{2}} \frac{h^*_{bu\_1,k,p}}{\sigma^2_{n_1}} n_{UT,k,p} + \frac{1}{\sqrt{2}} \frac{h_{bu\_2,k,p}}{\sigma^2_{n_1}} n^*_{UT,k,p+1} + \mu \frac{h^*_{eq\_1,k+1,p}}{\sigma^2_{n_c,k,p}} h_{ru\_1,k+1,p} n_{RN,k,p} \\ & + \mu \frac{h^*_{eq\_2,k+1,p}}{\sigma^2_{n_c,k,p}} h^*_{ru\_1,k+1,p} n^*_{RN,k,p+1} + \frac{h^*_{eq\_1,k+1,p}}{\sigma^2_{n_c,k,p}} n_{UT,k+1,p} + \frac{h^*_{eq\_2,k+1,p}}{\sigma^2_{n_c,k,p}} n^*_{UT,k+1,p+1} \end{aligned} . \quad (4.9)$$

4.3.3 Decode-and-Forward Protocol

For DF relay protocol, the relay first demodulates and decodes the received information, according to Sub-section 2.4.4. After that, the RN re-encodes the data and forwards it to the UT. Thus, the received signal, on the adjacent subcarriers p and p+1 and at instant $k+1$, can be written as follows

$$\begin{cases} y_{UT,k+1,p} = \overline{s}_{RN,k,p} h_{ru\_1,k+1,p} + n_{UT,k+1,p} \\ y_{UT,k+1,p+1} = \overline{s}_{RN,k,p+1} h_{ru\_1,k+1,p+1} + n_{UT,k+1,p+1} \end{cases}, \tag{4.10}$$

where $\overline{s}_{RN,k,p}$ is the symbol obtained after hard-decision at the RN. At the UT, the received signals are also combined using the MRC criterion, and the resulting soft-decision variable on the p^{th} subcarrier is given by

$$\begin{aligned} \hat{s}_{k,p} = \frac{1}{2}\left(\left|h_{bu\_1,k,p}\right|^2 + \left|h_{bu\_2,k,p}\right|^2\right) s_{k,p} + \left|h_{ru\_1,k+1,p}\right|^2 \overline{s}_{RN,k,p} + \frac{1}{\sqrt{2}} h^*_{bu\_1,k,p} n_{UT,k,p} \\ + \frac{1}{\sqrt{2}} h_{bu\_2,k,p} n^*_{UT,k,p+1} + h^*_{ru\_1,k+1,p} n_{UT,k+1,p} \end{aligned}. \tag{4.11}$$

When the data is successfully detected at the RN, $\overline{s}_{RN,k,p}$ is equal to the original data transmitted by the BS, s_p. It is possible to conclude, from (4.11), that, in that specific case, the soft-decision variable on the p^{th} subcarrier position is expressed by

$$\begin{aligned} \hat{s}_{k,p} = \left(\frac{1}{2}\left(\left|h_{bu\_1,k,p}\right|^2 + \left|h_{bu\_2,k,p}\right|^2\right) + \left|h_{ru\_1,k+1,p}\right|^2\right) s_{k,p} + \frac{1}{\sqrt{2}} h^*_{bu\_1,k,p} n_{UT,k,p} \\ + \frac{1}{\sqrt{2}} h_{bu\_2,k,n} n^*_{UT,k,p+1} + h^*_{ru\_1,k+1,p} n_{UT,k+1,p} \end{aligned}. \tag{4.12}$$

For this specific case, this cooperative scheme yields a diversity gain of 3, for perfect transmission conditions until the relay.

4.3.4 Selective Decode-and-Forward Protocol

Fixed DF transmission does not offer diversity gains for low SNR values, since the imperfect information decoding at the relay limits its performance, in comparison with the equivalent non-cooperative system [LaTW04]. The SDF relay protocol can be used to overcome the shortcomings of the fixed DF protocol. In this protocol, the relay first demodulates and decodes the received signals. Only upon success, does it re-encode the data and forwards it to the UT, by using one of the different strategies previous explained in Sub-section 2.4.4. At this terminal, the received signals at the two instants are combined using the MRC criterion. The soft-decision variable on a generic subcarrier p is given by

$$\hat{s}_{k,p} = \left(\frac{1}{2}\left|h_{bu\_1,k,p}\right|^2 + \frac{1}{2}\left|h_{bu\_2,k,p}\right|^2 + \left|h_{ru\_1,k+1,p}\right|^2 \right) s_{k,p} + \frac{1}{\sqrt{2}} h^*_{bu\_1,k,p} n_{UT,k,p} + \frac{1}{\sqrt{2}} h_{bu\_2,k,p} n_{UT,k,p+1} + h^*_{ru\_1,k+1,p} n_{UT,k+1,p} \quad . \tag{4.13}$$

In the outage case, where the relay fails to decode the data correctly, the RN cannot help the BS→UT communication, during the cooperation phase. In this case, the UT only uses the signal received directly from the BS and thus, the soft-decision variable is given by

$$\hat{s}_{k,p} = \frac{1}{2}\left(\left|h_{bu\_1,k,p}\right|^2 + \left|h_{bu\_2,k,p}\right|^2 \right) s_{k,p} + \frac{1}{\sqrt{2}} h^*_{bu\_1,k,p} n_{UT,k,p} + \frac{1}{\sqrt{2}} h_{bu\_2,k,p} n^*_{UT,k,p+1}, \tag{4.14}$$

which is the same expression given by the classical non-cooperative 2×1 scheme.

4.4 Algorithm for a Two-Antenna Relay Node

4.4.1 General Algorithm Description

We now describe the algorithm proposed for the RA 1RN 2×2×1, in which the relay is equipped with two antennas. This algorithm is also formed by two time phases. The same relay protocols are considered and, similarly to the previous scheme, the first phase of communication is common to all the protocols and it is, then, firstly described. During this phase of communication the BS transmits with full power. The received signals at the UT, at instant k, on subcarrier p and p+1, are given by the same expression as in the RA 1RN 2×1×1, represented in (4.1). The received signals at the q_r^{th} antenna of the RN, at the same instant and on subcarriers p and p+1, are given by

$$\begin{cases} y_{RN\_q_r,k,p} = \frac{1}{\sqrt{2}}\left(s_{k,p} h_{br\_1\_q_r,k,p} - s^*_{k,p+1} h_{br\_2\_q_r,k,p} \right) + n_{RN\_q_r,k,p} \\ y_{RN\_q_r,k,p+1} = \frac{1}{\sqrt{2}}\left(s_{k,p+1} h_{br\_1\_q_r,k,p+1} + s^*_{k,p} h_{br\_2\_q_r,k,p+1} \right) + n_{RN\_q_r,k,p+1} \end{cases}, \tag{4.15}$$

where $h_{br\_q_b\_q_r,k,p}$, with $q_r \in \{1,2\}$ and $q_b \in \{1,2\}$, represents the complex Rayleigh flat fading cooperative channel between the q_b^{th} and the q_r^{th} antennas in the BS and the RN, respectively, on subcarrier p or p+1; $n_{RN\_q_r,k,p}$ is the noise introduced by the q_r^{th} antenna of the RN on subcarrier p, with variance of $\sigma^2_{n_d}$.

During the second phase the relay can also transmit at full power to the UT, while the BS does not transmit. Algorithm description is made separately in the following sub-sections, depending on the relay protocols used.

4.4.2 Equalize-and-Forward Protocol

In the single-antenna relay case previously analyzed, the AF protocol is equivalent to the EF protocol. In this scheme the relay has two antennas, thus we need to equalize and estimate the received data at the relay and only after that we retransmit the space-frequency encoded data. However, no hard decision is made at the RN. The received signals at the q_r^{th} antenna of the RN, at instant k, for subcarriers p and p+1, are given by

$$\begin{cases} y_{RN\_q_r,k,p} = \dfrac{1}{\sqrt{2}}\left(s_{k,p}h_{br\_1\_q_r,k,p} - s^*_{k,p+1}h_{br\_2\_q_r,k,p}\right) + n_{RN\_q_r,k,p} \\ y_{RN\_q_r,k,p+1} = \dfrac{1}{\sqrt{2}}\left(s_{k,p+1}h_{br\_1\_q_r,k,p+1} + s^*_{k,p}h_{br\_2\_q_r,l,k,p+1}\right) + n_{RN\_q_r,k,p+1} \end{cases}, \tag{4.16}$$

where $n_{RN\_q_r,k,p}$ and $n_{RN\_q_r,k,p+1}$ are the zero mean complex AWGN samples on the RN, with variance of $\sigma^2_{n_{c1}}$, on subcarrier p and p+1, respectively.

Consequently, the relay equalizes the received signal, after space-frequency decoding, and the soft-decision variable corresponding to the relay is expressed as

$$\begin{cases} \hat{s}_{RN,k,p} = \sum_{q_r=1}^{2}\left(g^*_{RN\_1\_q_r,k,p}y_{RN\_q_r,k,p} + g_{RN\_2\_q_r,k,p}y^*_{RN\_q_r,k,p+1}\right) \\ \hat{s}_{RN,k,p+1} = \sum_{q_r=1}^{2}\left(g^*_{RN\_1\_q_r,k,p}y_{RN\_q_r,k,p+1} - g_{RN\_2\_q_r,k,p}y^*_{RN\_q_r,k,p}\right) \end{cases}, \tag{4.17}$$

where the equalization coefficients, $g_{RN\_q_b\_q_r,k,p}$, are defined as

$$g_{RN\_q_b\_q_r,k,p} = \frac{h_{br\_q_b\_q_r,k,p}}{\sum_{i_1=1}^{2}\sum_{i_2=1}^{2}\left|h_{br\_i_1\_i_2,k,p}\right|^2}\ . \tag{4.18}$$

After this processing, the RN retransmits $\hat{s}_{RN,k,p}$ according to the SFBC mapping scheme in Table 4.1 and sends it to the UT. Thus, the signals received in the UT, at instant k and on subcarriers p and p+1, are given by

$$\begin{cases} y_{UT,k+1,p} = h_{ru\_1,k+1,p}\,\hat{s}_{RN,k,p} - h_{ru\_2,k+1,p}\,\hat{s}^*_{RN,k,p+1} + n_{UT,k+1,p} \\ y_{UT,k+1,p+1} = h_{ru\_2,k+1,p+1}\hat{s}^*_{RN,k,p} + h_{ru\_1,k+1,p+1}\,\hat{s}_{RN,k,p} + n_{UT,k+1,p+1} \end{cases}. \tag{4.19}$$

At the UT, MRC is used to combine the received signal from the direct and from the cooperative paths. The estimated signal for an arbitrary pair of adjacent subcarriers, at instant k is also given by (4.6), where the equalization coefficients are defined as

$$g_{q_r,k+j,p}=\begin{cases}\dfrac{1}{\sqrt{2}}\dfrac{h_{bu\_q_r,k,p}}{\sigma^2_{n_d}} & ,j=0\\ \dfrac{1}{\sqrt{2}}\dfrac{h_{ru\_q_r,k+1,p}}{\sigma^2_{n_c,k+1,p}} & ,j=1\end{cases}. \tag{4.20}$$

The equivalent noise power obtained through the cooperation path, received on subcarrier p or p+1, is given by

$$\sigma^2_{n_c,k,p}=\left(\frac{\sum_{q_r=1}^{2}\left|h_{ru\_q_r,k+1,p}\right|^2}{\sum_{i_1=1}^{2}\sum_{i_2=1}^{2}\left|h_{br\_i_1\_i_2,k,p}\right|^2}\right)\sigma^2_{n_{c1}}+\sigma^2_{n_{c2}}. \tag{4.21}$$

The resultant estimated signal is in the following expression

$$\hat{s}_p=\frac{1}{2}\left(\frac{1}{\sigma^2_{n_d}}\sum_{q_b=1}^{2}\left|h_{bu\_q_b,k,p}\right|^2+\frac{1}{\sigma^2_{n_c,k,p}}\sum_{q_r=1}^{2}\left|h_{ru\_q_r,k+1,p}\right|^2\right)s_{k,p}+\psi, \tag{4.22}$$

where ψ is the noise term contribution, formed by the addition of the noise contribution introduced by the RN given by

$$\begin{aligned}\psi_1=&\frac{1}{\sqrt{2}\sigma^2_{n_c,k,p}\sum_{i_1=1}^{2}\sum_{i_2=1}^{2}\left|h_{br\_i_1\_i_2,k,p}\right|^2}\\ &\left[\left(\begin{array}{l}h^*_{br\_1\_1,k,p}n_{RN\_1,k,p}+h_{br\_2\_1,k,p}n^*_{RN\_1,k,p+1}+\\ \qquad h^*_{br\_1\_2,k,p}n_{RN\_2,k,p}+h_{br\_2\_2,k,p}n^*_{RN\_2,k,p+1}\end{array}\right)h^*_{ru\_1,k+1,p}\right.\\ &\left.+\left(\begin{array}{l}h^*_{br\_1\_1,k,p}n_{RN\_1,k,p+1}-h_{br\_2\_1,k,p}n^*_{RN\_1,k,p}+\\ \qquad h^*_{br\_1\_2,k,p}n_{RN\_2,k,p+1}-h_{br\_2\_2,k,p}n^*_{RN\_2,k,p}\end{array}\right)h_{ru\_2,k+1,p}\right]\end{aligned} \tag{4.23}$$

and the noise contribution of the UT given by

$$\psi_2=\frac{1}{\sqrt{2}\sigma^2_{n_c,k,p}}\left(h^*_{ru\_1,k+1,p}n_{UT,k+1,p}+h_{ru\_2,k+1,p}n^*_{UT,k+1,p+1}\right). \tag{4.24}$$

For modulations with higher order than QPSK, this relation should be normalized.

4.4.3 Decode-and-Forward Protocol

In this case, during the second phase, the relay demodulates and decodes the received information. The decision in relay, for the p^{th} subcarrier, is based on

$$\begin{aligned}\hat{s}_{RN,k,p}=&\frac{1}{\sqrt{2}}s_{k,p}\left(\sum_{q_b=1}^{2}\sum_{q_r=1}^{2}\left|h_{br\_q_b\_q_r,k,p}\right|^2\right)+h^*_{br\_1\_1,k,p}n_{RN\_1,k,p}+h_{br\_2\_1,k,p}n^*_{RN\_1,k,p+1}\\ &+h^*_{br\_1\_2,k,p}n_{RN\_2,k,p}+h_{br\_2\_2,k,p}n^*_{RN\_2,k,p+1}\end{aligned}. \tag{4.25}$$

After that, the RN re-encodes the data and forwards it to the UT, and the received signals are given by

$$\begin{cases} y_{UT,k+1,p} = \frac{1}{\sqrt{2}}\left(\bar{s}_{k,p} h_{ru\_1,k+1,p} - \bar{s}^{*}_{k,p+1} h_{ru\_2,k+1,p}\right) + n_{UT,k+1,p} \\ y_{UT,k+1,p+1} = \frac{1}{\sqrt{2}}\left(\bar{s}_{k,p+1} h_{ru\_1,k+1,p+1} + \bar{s}^{*}_{k,p} h_{ru\_2,k+1,p+1}\right) + n_{UT,k+1,p+1} \end{cases}, \tag{4.26}$$

where $\bar{s}_{k,p}$ is the symbol transmitted by the relay after hard-decision on subcarrier *p*. Signals are then combined using the MRC criterion and the data is estimated resulting in the final expression, which is represented as follows

$$\begin{aligned} \hat{s}_{k,p} = \frac{1}{\sqrt{2}}\Bigg(& s_{k,p} \sum_{q_b=1}^{2} \left| h_{bu\_q_r,k,p} \right|^2 + \bar{s}_{k,p} \sum_{q_r=1}^{2} \left| h_{ru\_q_r,k+1,p} \right|^2 \Bigg) + h^{*}_{bu\_1,k,p} n_{UT,k,p} \\ & + h_{bu\_2,k,p} n^{*}_{UT,k,p+1} + h^{*}_{ru\_1,k+1,p} n_{UT,k+1,p} + h_{ru,2,k+1,p} n^{*}_{UT,k+1,p+1} \end{aligned}. \tag{4.27}$$

The optimum situation occurs when the data is successfully detected at the RN, so that $\bar{s}_{k,p}$ is equal to the original data transmitted by the BS, $s_{k,p}$.

4.4.4 Selective Decode-and-Forward Protocol

In this protocol, the relay just forwards the received information if the data is successfully decoded. Thus, according to (4.27), in the case of a successful transmission during the first cooperative phase, the soft-decision variable in UT results in

$$\begin{aligned} \hat{s}_{k,p} = \frac{1}{\sqrt{2}} s_p \Bigg(& \sum_{q_b=1}^{2} \left| h_{bu\_q_b,k,p} \right|^2 + \sum_{q_r=1}^{2} \left| h_{ru\_q_r,k+1,p} \right|^2 \Bigg) + h^{*}_{bu\_1,k,p} n_{UT,k,p} \\ & + h_{bu\_2,k,n} n^{*}_{UT,k,p+1} + h^{*}_{ru\_1,k+1,p} n_{UT,k+1,p} + h_{ru\_2,k+1,p} n^{*}_{UT,k+1,p+1} \end{aligned}. \tag{4.28}$$

In the outage case, where the relay does not perfectly decode the received data, the relay cannot help the BS→UT communication and the soft-decision variable is as follows

$$\hat{s}_{k,p} = \frac{1}{\sqrt{2}} s_{k,p} \sum_{q_b=1}^{2} \left| h_{bu\_q_b,k,p} \right|^2 + h^{*}_{bu\_1,k,p} n_{UT,k,p} + h_{bu\_2,k,p} n^{*}_{UT,k,p+1}. \tag{4.29}$$

4.5 Numerical Results

4.5.1 Assumptions and Conditions

The performances of the two distributed SFBC schemes, previously defined for different relay protocols, are evaluated and presented in this section. We considered a typical pedestrian scenario, based on LTE specifications, where the main parameters are defined in Table 4.3 [3GPP07].

TABLE 4.3: PARAMETERS OF SIMULATED SCENARIOS ACCORDING TO LTE STANDARD.

LTE general signal definitions	FFT size:	1024
	Number of available subcarriers:	300
	Sampling frequency:	15.36 MHz
	Useful symbol duration:	66.6 μs
	Cyclic prefix duration:	5.21 μs
	Overall OFDM symbol duration:	71.86 μs
	Sub-carrier separation:	15 kHz
	Number of OFDM symbols per block:	12
Channel model	ITU pedestrian model B	
	Tap delays modified accordingly to the sampling frequency defined for LTE systems	
UT velocity	3km/h	

We consider that the UT has just one antenna ($N_U = 1$), the BS has two transmit antennas (N_B =2) and that the relay can have either one or two antennas (N_R =1 or 2). We further assume perfect CSI on at both RN and UT and the overall transmitted power is normalized to the unit. We use a spatial transmitter correlation matrix for all the multiple transmit antennas (at the BS or UT) with the average angle of departure (AoD) of 50°, the standard deviation of AoD set to 8°. A spatial receiver matrix is used in all the multiple receive antenna nodes (at the UT when equipped with an antenna array) with the average angle of arrival (AoA) set to 67.5º, the standard deviation of AoA set to 68° and the antenna spacing at both transmitter and receiver set to 0.5 wavelength, according to CODIV group channel scenario specifications [CBVS08]. Thus, the spatial transmitter and receiver correlation matrixes for all the taps are given by

$$R_{Tx} = \begin{pmatrix} 1 & -0.7013 - 0.6590i \\ -0.7013 + 0.6590i & 1 \end{pmatrix} \tag{4.30}$$

and

$$R_{Rx} = \begin{pmatrix} 1 & -0.4833 - 0.2850i \\ -0.4833 + 0.2850i & 1 \end{pmatrix}. \tag{4.31}$$

With the objective of having the same spectral efficiency between both cooperative and non-cooperative schemes, we use two different modulations: for the RA schemes we use QPSK; for the non-cooperative schemes we use BPSK. In the evaluation of the referred schemes we consider two cases in which concerns channel coding: uncoded data transmission; and, usage of convolutional turbo code (CTC), following the specifications in Table 4.4 according to the modulation used. In this latter case we use a Max Log MAP algorithm with eight iterations.

TABLE 4.4: MODULATION AND THE CORRESPONDING CODING SCHEMES WHEN USING CTC.

	Modulation	**Code rate**	**CTC code size**
Modulation and coding schemes for CTC	BPSK	$1/2$	(7200, 3600);
	QPSK	$1/2$	(3600, 1800)

Since the aim is to evaluate both RA schemes, we find it useful to consider different propagation scenarios. In order to characterize propagation aspects as a whole, including the effects of path loss, shadowing, scattering and others, we consider different link quality combinations, quantifying it in terms of SNR. Thus, we define different SNRs for each link: SNR_d for the link BS→UT, SNR_b for the link BS→RN, and SNR_r for the link RN→UT.

Three propagation scenarios are considered, with different link SNRs, as shown in Table 4.5. In scenario 1 we assume that all the links have the same quality conditions, i.e., $SNR_d = SNR_b = SNR_r$. However due to the mobility of the mobile terminals and of the surrounding environment, the relative SNRs can vary and we therefore define two additional scenarios with different relative SNRs. Hence, we define scenario 2 similarly to the scenario 1, with the difference that the link between the BS and the RN has a SNR 10 dB higher than the other two links, i.e., $SNR_d = SNR_r$ and $SNR_b = SNR_d + 10\text{dB}$. Scenario 3 is the best cooperative scenario that we consider, where the entire cooperative path, formed by two links, has better transmission quality conditions than the direct path, i.e., $SNR_b = SNR_r = SNR_d + 10\text{dB}$. In fact as the simulations will show, cooperation is more effective when the direct link is poor and the use of relays is essential to achieve the required quality of service.

The cooperative systems that are analyzed are the following:

- The RA scheme cooperating with a single-antenna relay (RA 1RN 2×1×1);
- The RA scheme cooperating with a two-antenna relay (RA 1RN 2×2×1).

As non-cooperative reference systems we consider:

- The point-to-point communication with a single antenna at both the BS and UT terminals (NRA 1×1);
- The equivalent non-cooperative system, with two antennas in the BS and one antenna at the UT, using the same distributed SFBC (NRA 2×1);
- The non-cooperative system with two co-located antennas in both BS and UT, again with a distributed SFBC (NRA 2×2).

The numerical results are presented in terms of the average BER as a function of E_b/N_0, where E_b is the received energy per bit at the UT through the direct link (BS→UT) and N_0 is the noise power spectral density. Average FER results were also obtained for the referred schemes. However, as the conclusions drawn from those curves are the same as the ones resulting from BER performances, they are not in the main text for simplicity. Annex B contains such curves, in case they are of interest for future research.

TABLE 4.5: PROPAGATION SCENARIOS CONSIDERED FOR MONTE CARLO SIMULATIONS OF RA SCHEMES.

	SNR_d	SNR_b	SNR_r
Scenario 1	SNR_d	SNR_d	SNR_d
Scenario 2	SNR_d	SNR_d +10 dB	SNR_d
Scenario 3	SNR_d	SNR_d +10 dB	SNR_d +10 dB

4.5.2 RA Scheme with Single-Antenna Relay Node

In Figure 4-5 BER performances of the proposed RA with AF, DF and SDF relay protocols and of the non-cooperative schemes are shown. These results were obtained for scenario 1, when all the links have the same quality conditions, i.e., $SNR_d = SNR_b = SNR_r$. In this scenario we see that the proposed RA schemes outperform the non-cooperative SISO and MISO ones, independently of the protocol used. Considering the protocol AF, for BER=10^{-3}, we have improvements of 4.7 dB and 3.6 dB in comparison with SISO and MISO systems, respectively.

When comparing the cooperative schemes, the AF protocol has the best performance in this scenario. A gain of approximately 3 dB is achieved comparatively with the DF protocol and 0.7 dB with the SDF one, for BER=10^{-3}. This is justified by the fact that in the AF protocol information is only decoded at the UT, after combining the signals received by the two independent links BS→UT and RN→UT, thus increasing the overall system performance. Moreover, in the SDF protocol the relay does not decode all the information successfully. Consequently in those cases, the relay does

not cooperate with the BS, contrarily to what happens in the AF protocol, where the relay is always cooperating.

On the other hand, the SDF cooperative scheme outperforms the DF one as it only re-transmits to the UT the frames that are successfully decoded at the relay. This means that if the channels between the BS and the RN are in outage, the scheme with the relay using the SDF does not retransmit the information, avoiding a considerable number of errors due to the cooperative transmission, in comparison with the relay using the DF protocol.

In this scenario cooperative schemes cannot achieve the performance given by the reference MIMO 2×2 as expected. This happens because, as the relay is equipped with a single antenna, the maximum diversity achieved would be of 3. Furthermore, additional noise is introduced in the two-phase cooperative schemes.

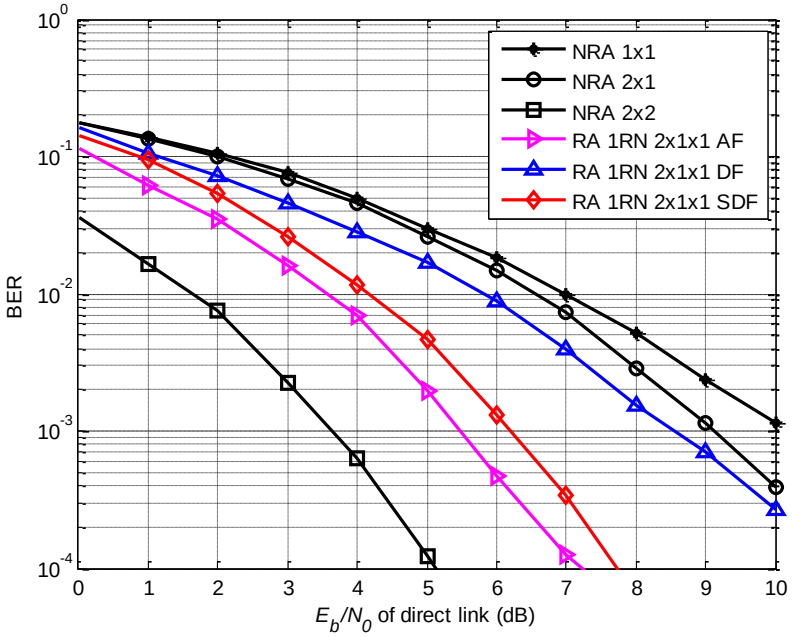

Figure 4-5: BER performances of RA 1RN 2×1×1 and reference schemes for scenario 1.

In Figure 4-6 the performance of the same schemes is presented, with the difference that the link between the BS and the RN has a SNR 10 dB higher than the other two links (scenario 2). The choice of this scenario derives from the fact that, as said previously, in more real situations the cooperative link has higher transmission quality conditions than the direct link. We observe that the performances of RA schemes are improved in comparison with the previous scenario, independently of the relay protocol used, achieving more 6.9 dB than SISO and more 5.8 dB than MISO systems, for BER=10^{-3} and using DF relay protocol. For best visualization purposes, the non-cooperative curve is not completely shown in the plot for these measurements.

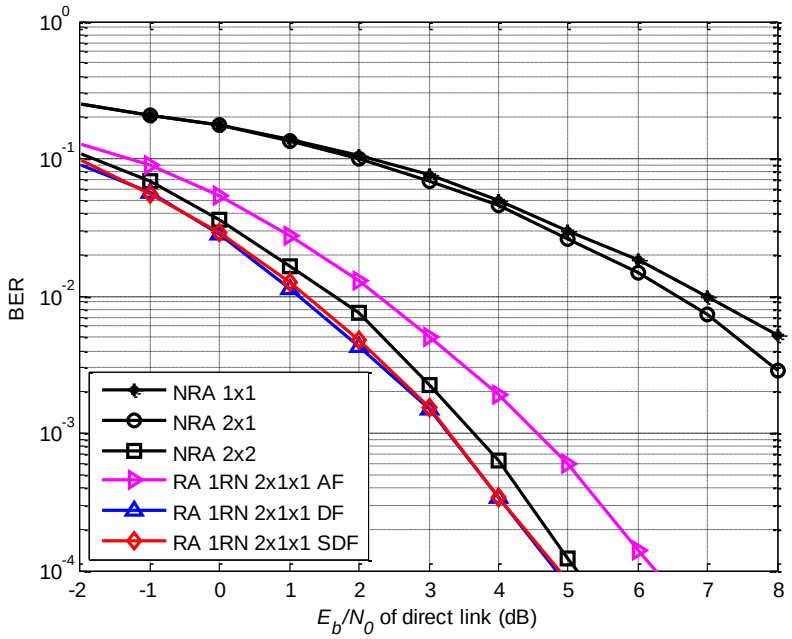

Figure 4-6: BER performances of RA 1RN 2×1×1 and reference schemes for scenario 2.

In this scenario the scheme with the AF protocol is outperformed by the ones with DF and SDF protocols. This is justified by the fact that when the link between the BS and the RN has higher quality, the information detection is improved at the RN. The scheme with DF protocol has the same performance as the one with SDF, again because almost all the detections at the relay are successful.

Furthermore, we observe that the performances of the reference MIMO and the RA schemes are quite close. The schemes with DF and SDF relays outperform the one with co-located antennas achieving improvements of about 0.4 dB, for BER=10^{-3}, which was already expected for this scenario. Despite the successful detection of almost all information at the relay node, we particularly note that in the reference MIMO case the channels of the two receiver antennas are strongly correlated, while for the relay-based systems the channels corresponding to the links RN→UT and BS→UT are uncorrelated, increasing the diversity order and thus the overall system performance of the relay cases. The scheme with the AF relay protocol is still worse than the 2×2 co-located system, differing 0.9 dB for the same BER.

In Figure 4-7 we consider the best cooperative scenario, where the entire cooperative path, formed by two links, has better transmission quality conditions than the direct path, i.e., scenario 3.

This is a realistic scenario, since when using a relay to cooperate in a point-to-point transmission, the cooperative node is chosen due to its better quality links than the direct link between the terminal nodes. This aspect of relay selection can be solved with different solutions already outlined in Sub-section 2.4.3, which is not the object of study of this work.

The advantages of cooperation are evident in scenarios like this. In this case, a gain of 4.5 dB is obtained with the DF relay protocol in comparison with the MIMO system, for BER=10^{-2}. Comparing to the MISO and the SISO systems we have a difference of 9.6 dB and 10 dB, respectively, for the same BER.

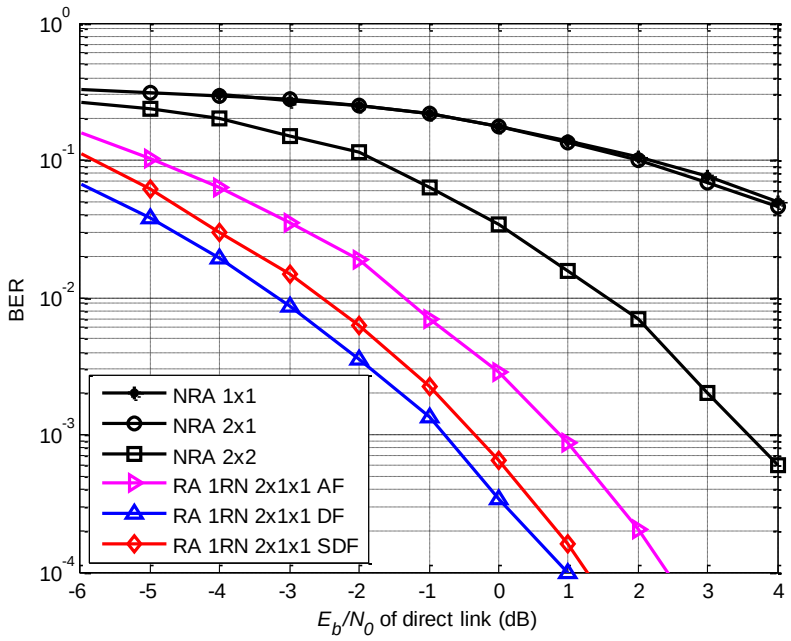

Figure 4-7: BER performances of RA 1RN 2×1×1 and reference schemes for scenario 3.

4.5.3 RA Scheme with Two-Antenna Relay Node

In this section the performances of the RA scheme with a two-antenna relay are presented and analyzed in terms of BER results. Figure 4-8 shows the results for the non-cooperative and cooperative schemes with the two-antenna relay, for scenario 1, i.e., $SNR_d = SNR_b = SNR_r$. For this scenario, the best cooperative schemes are the ones with DF and SDF relay protocols, reaching improvements of 6.5 dB and 5.6 dB, for BER=10^{-3}, in comparison with the SISO and the MISO. Moreover, we observe that, even when the quality is the same among links, this two-antenna relay scheme has a similar performance to the co-located 2x2 MIMO system, for high SNRs ($E_b/N_0 > 2$ dB).

The use of the DF relay protocol outperforms the use of the EF one, in opposition to the single-antenna relay scheme, where the best relay protocol was the AF one. This is justified by the fact that relay detection does not have significant errors and does not propagate further errors to the RN→UT link. The difference is of 0.7 dB, for BER=10^{-3}.

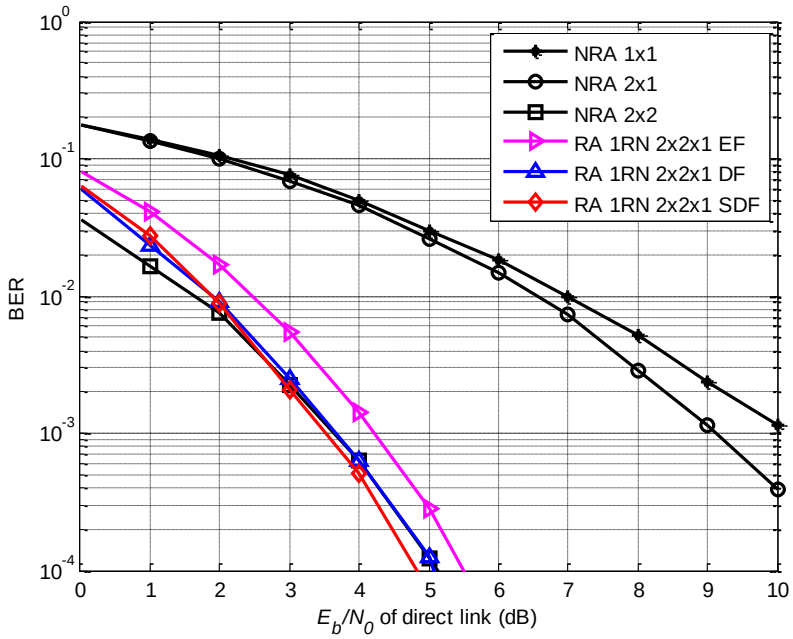

Figure 4-8: BER performances of RA 1RN 2×2×1 and reference schemes for scenario 1.

In Figure 4-9 we show the performance of the same cooperative scheme for scenario 2. In this case, cooperative schemes slightly outperform the MIMO system, achieving 0.5 dB of gain, for BER=10^{-3}. All the protocols have similar performances in this case.

Figure 4-10 illustrates the results for scenario 3, i.e., $SNR_b = SNR_r = SNR_d + 10\text{dB}$. The cooperative schemes have improvements in comparison with the previous scenarios, having an enhancement of 6.5 dB between scenarios 1 and 3 for the DF protocol case and for BER=10^{-3}. Moreover, the difference between this scheme and the non-cooperative MIMO 2×2 one is higher in this scenario than in the previous ones, with a gain of 6.6 dB for the same conditions. Following the results obtained in all of the previous scenarios, the DF relay protocol scheme outperforms the EF one.

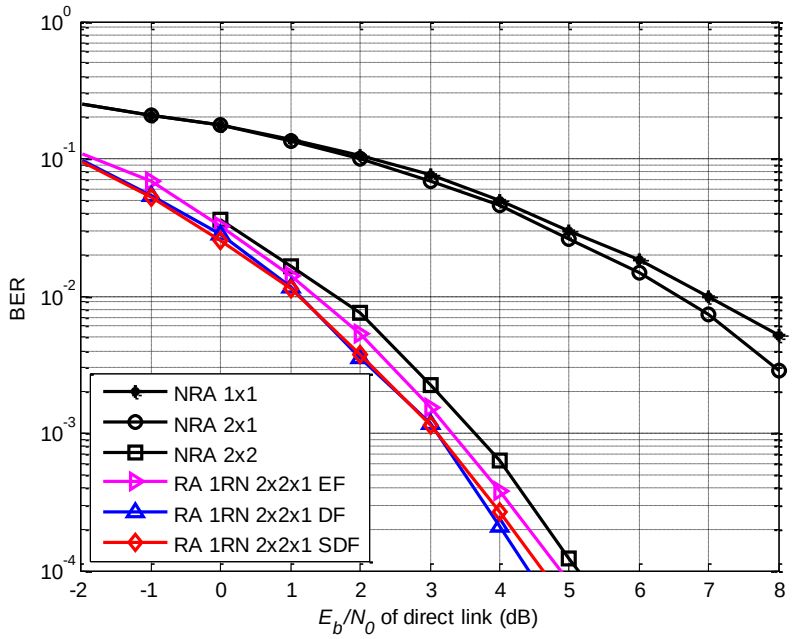

Figure 4-9: BER performances of RA 1RN 2×2×1 and reference schemes for scenario 2.

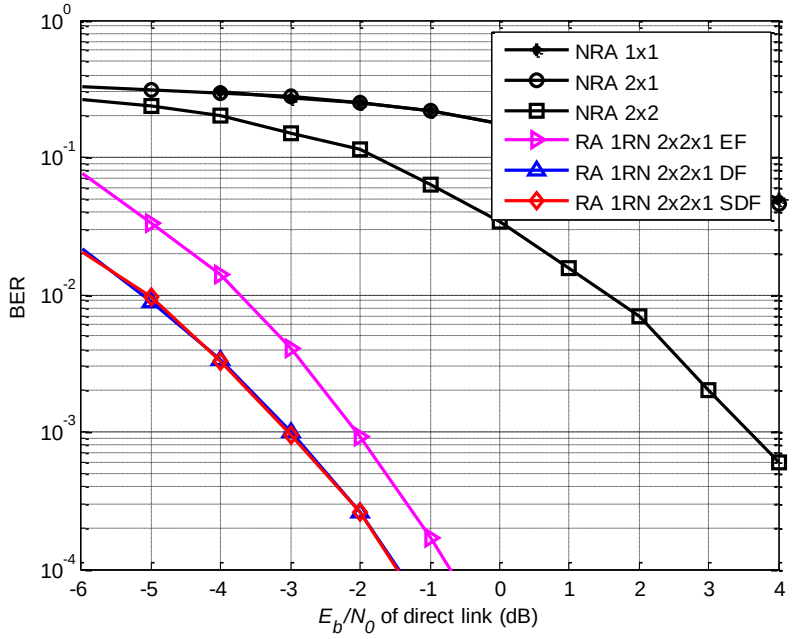

Figure 4-10: BER performances of RA 1RN 2×2×1 and reference schemes for scenario 3.

4.5.4 Comparison Between RA Schemes with One- and Two-Antenna RNs

In this section we compare the BER performances for the RA 2RN 2×1×1 and RA 2RN 2×2×1 schemes. The results are shown in Figures 4-11 to 4-16. For simplicity and readability the plots do not consider the SDF relay protocol, since we have verified the performances are very similar to the ones obtained with the scheme using the DF relay protocol for almost all the cases, except for scenario 1 in the RA 1RN 2×1×1, which was reported in Figure 4-5.

The two-antenna relay scheme has the best performance, for scenario 1 and 3, when using the DF relay protocol, as seen in Figures 4-11 to 4-13, respectively. In scenario 2 all cooperative schemes have a similar behavior, with performances close to the reference MIMO 2×2 system.

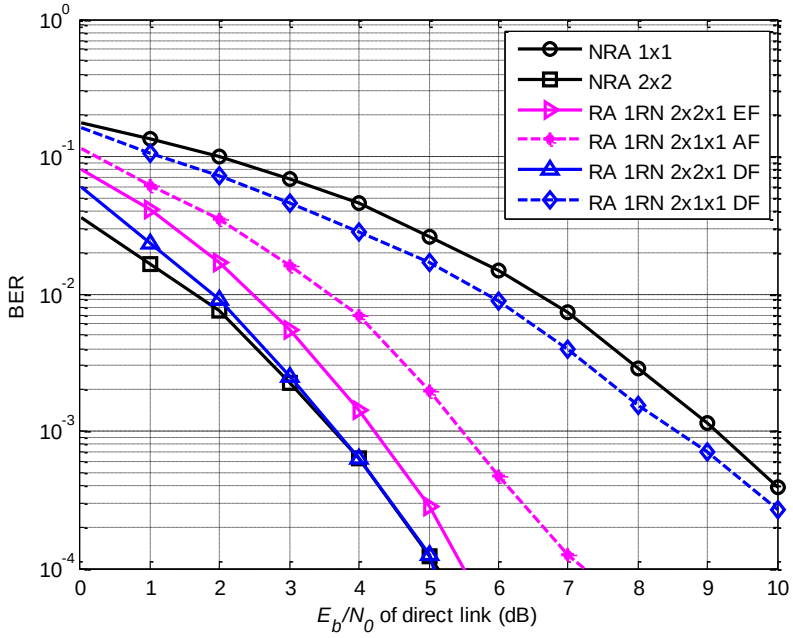

Figure 4-11: Comparison between both cooperative schemes with one and two antennas at relays for scenario 1.

In scenario 2 the two-antenna scheme has a small gain in comparison with the first scenario, in the order of 0.6 dB for the scheme with DF relay protocol and for BER=10^{-3}, as we observe in Figure 4-12. In contrast, the single-antenna scheme achieves more 5.3 dB than in the previous scenario, for the same conditions. The curves for both schemes, using the DF relay protocol, get close to each other. In this scenario, there is no advantage in using an additional antenna at relay with the DF relay protocol, since the BS→RN link already has a low BER. Note also that in the RN→UT link, where most of the errors occur, the schemes behave as a 1×1 for the single-antenna relay scheme and as a 2×2 for the two-antenna relay scheme. As these schemes have similar performances for low SNRs (for SNR<6 dB these curves do not differ more than 0.3 dB), the RA scheme error rates are close to each other.

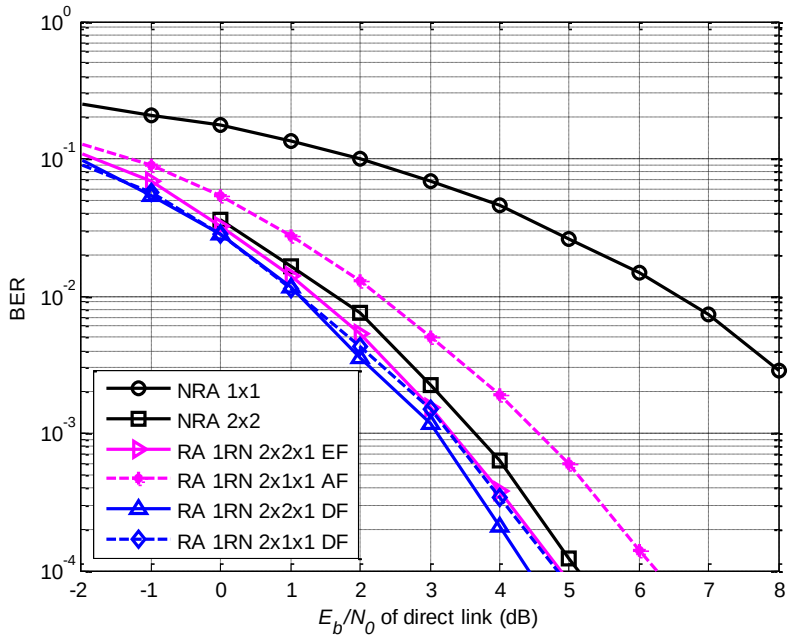

Figure 4-12: Comparison between both cooperative schemes with one and two antennas at relays for scenario 2.

In scenario 3, the two-antenna relay scheme has a better performance than that of the single-antenna case (Figure 4-13). They differ by 2.2 dB or 3 dB, with the DF and the AF/EF protocols, respectively. Despite the fact that both have a lower error rate in relay detection, as previously mentioned, they have a good quality of transmission in the second hop of the cooperative path, increasing the difference in the generation of errors relatively to the case of RA 1RN 2×1×1. The link RN→UT also contributes for this difference, since 1×1 and 2×2 system performances are different for high SNRs. For example, for BER=10^{-3} they differ by 1.2 dB.

Moreover, the performances of the same schemes, but considering no channel coding, are presented next. The BER curves for the proposed RA schemes are shown in Figures 4.14, 4.15 and 4.16 for scenarios 1, 2 and 3 respectively. Similar conclusions can be drawn in relation to the use of these cooperative schemes in comparison with the non-cooperative ones. However, when comparing the relay protocols used in the distributed SFBC schemes without channel coding some differences can be seen in comparison with the one with CTC. The DF relay protocol has lower relative performances comparatively to the AF one for this case. This is justified by the lower performance of the link until the relay node in this case without channel coding comparatively to the simulations with CTC. Thus, the performance of the scheme, when using AF relay protocol, is never outperformed by the one with DF relay protocol, except for scenario 2 in the single-antenna case.

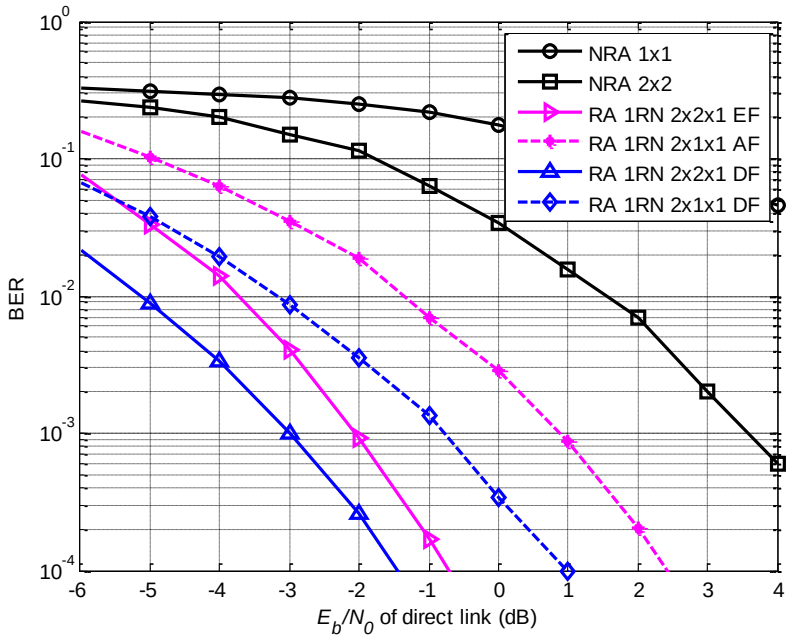

Figure 4-13: Comparison between both cooperative schemes with one and two antennas at relays for scenario 3.

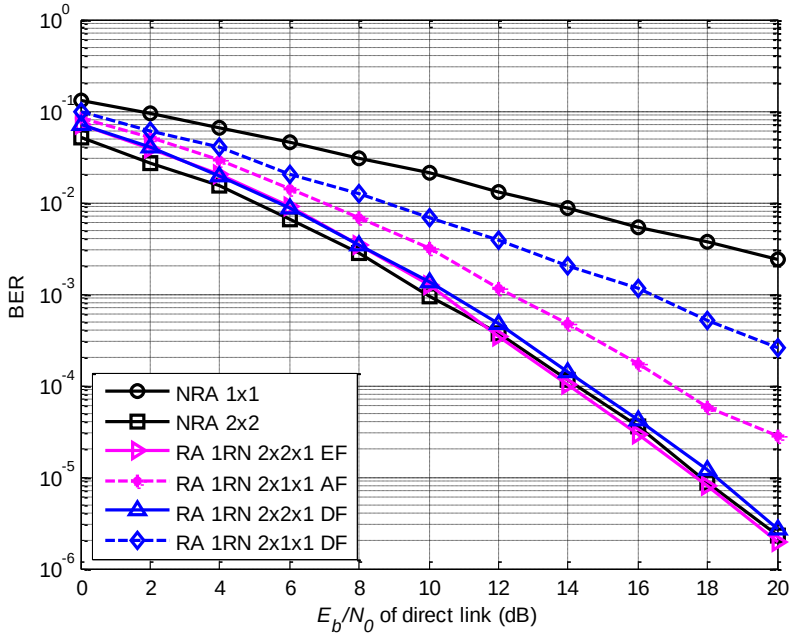

Figure 4-14: Comparison between both cooperative schemes with one and two antennas at relays for scenario 1, for simulations without CTC.

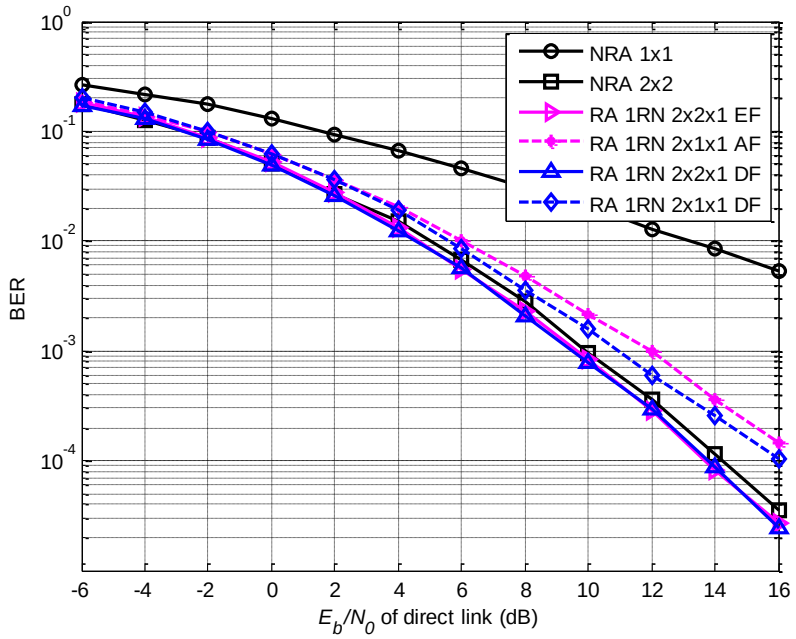

Figure 4-15: Comparison between both cooperative schemes with one and two antennas at relays for scenario 2, for simulations without CTC.

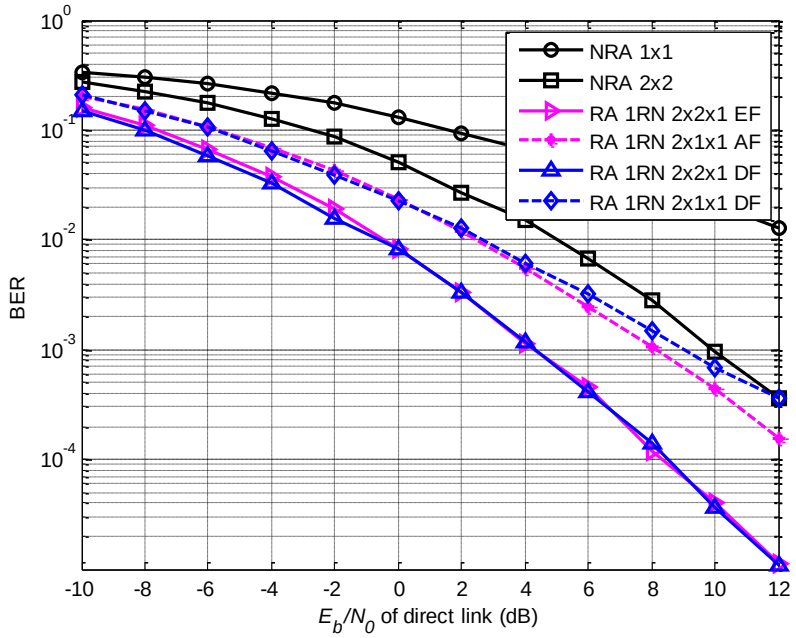

Figure 4-16: Comparison between both cooperative schemes with one and two antennas at relays for scenario 3, for simulations without CTC.

4.6 Conclusions

In this chapter we proposed and evaluated two RA schemes designed for distributed DL SFBC OFDM based systems. The results obtained during the research and here presented, showed that the performance of the proposed RA scheme with just one antenna at the relay is higher than that of the non-cooperative SISO 1×1 and MISO 2×1 systems. This difference is more evident for the case when the cooperative links have higher quality than the direct link, with an enhancement of more than 12 dB, for the scenario with an improvement of 10 dB in the link quality and for $\mathrm{BER} = 10^{-3}$. For this specific scenario the performances of the cooperative schemes outperform those of the reference MIMO 2×2 system for low values of E_b/N_o, achieving 4.5 dB of improvement for the same BER. Note that, for RA schemes, the UT terminal is just equipped with a single antenna, contrarily to the conventional MIMO system. Moreover, for this scenario, the performance of all the relay protocols for this RA scheme is quite similar.

We observed that the schemes with SDF and DF relay protocols have similar behaviors when the first cooperative link has good quality, since a high amount of data is successfully decoded. Otherwise the use of the DF protocol is even worse than the EF and AF ones. Thus, concerning the complexity of the relay protocols and the results they provide, the SDF protocol should be used in detriment of the DF one, since it has better results and almost the same complexity as the DF. The AF or EF relay protocols are a good choice for situations when it is not possible to implement processing operations such as decoding or correction of the received signals at relays, with performances close to the ones with SDF and lower complexity.

The RA scheme with two antennas in the relay outperforms the scheme using a single antenna, even when the propagation transmission conditions are identical for both hops of the cooperative path. When using two antennas at the relay, the RA scheme is never outperformed by the co-located MIMO 2×2 system. In fact, when the cooperative path has a SNR 10 dB higher than that of the direct path, we show that this scheme has a gain of 6.6 dB, comparing to MIMO and using the DF protocol, for BER=10^{-3}. Besides that, in the RA scheme, a single antenna in the BS is considered, oppositely to the non-cooperative scheme, with two antennas in the source. Concerning the FER results (in Annex B), the same trends were observed, but with higher error rates for the same values of E_b/N_0.

Moreover, we concluded that when the link until the relay, i.e., BS→RN, has the same quality as the second hop cooperative link, i.e., RN→UT, the two-antenna cooperative scheme always achieves a better performance than the single-antenna scheme. Thus, despite the additional complexity and equipment in the relay with two antennas, this scheme provides advantages for these scenarios.

The aforementioned results suggest that the RA schemes are severely limited by the relative quality of the cooperative links, specially the BS→RN link. Thus, the success of the cooperative schemes lies upon the choice of the relay in the network. Ideally, it should be chosen so that the BS→RN link is highly reliable.

Further results were extended for uplink relay-assisted systems, where we observed improvements when using the proposed cooperative schemes comparatively to the reference non-cooperative ones, in all the scenarios considered [MTSG08], [MTSG10]. Additionally, simulations of the RA schemes with two relays were evaluated for OFDM based-systems. Such schemes were already defined in Chapter 3 in a general way, where we considered the transmission or non-transmission through the direct path. Other modulations besides QPSK, such as 16-QAM and 64-QAM, were also considered [TMSG10]. Similar conclusions were obtained with the results attained with other modulations. Moreover, we accomplished other conclusions such as that RA schemes are limited by the worst BS→RN link, thus being useful to place relays so that both links of the first cooperative hop are highly reliable. We also showed that cooperative schemes should use DP for transmission in situations when its transmission quality is at least equal to the quality of the worst cooperative link. Otherwise, communication through the direct link should be neglected.

5 Data-Precoded Algorithm for Relay-Assisted Schemes

5.1 Introduction

The RA schemes require the use of constellations with higher cardinality in comparison with the continuous link transmission from the BS to the UT, when this is available. This is due to the half-duplex constraint in relay nodes. Despite achieving full diversity, these schemes cannot achieve full spectral efficiency, since they use two phases for transmission, thus achieving half of the bandwidth efficiency of the equivalent non-cooperative systems. Consequently, the use of constellations with more symbols is considered in these cases as a mean to achieve the same transmission rates of the non-cooperative ones, but it leads to a power efficiency penalty. Some examples of these proposed RA schemes use distributed orthogonal algorithms such as the ones in [JiHa06], [YiKi07], [SrCR08] and the ones presented in Chapter 4.

Capacity for a RA system with one and two RNs with single-antenna terminals was studied in Chapter 3. There we found out that the use of relays to assist a communication, with the objective of increasing its capacity, is only effective in high path loss scenarios, because of the half-duplex constraint of RA schemes. We also concluded that RA schemes that do not have transmission through the DP have lower performances than similar ones having such contribution, when the DP has a good transmission quality. For example, non-orthogonal protocols for cooperative systems with two or more relays, were developed with the objective of increasing capacity or diversity order of cooperative systems [RaRa06], [KrGB07]. These proposals require

the existence of the DP, therefore, in situations with poor direct link conditions, their performances are significantly degraded and, in case of outage of one relay, some information can be lost. Motivated by the fact that it is common to have large objects or other hindrances affecting the direct path, the proposal of a new algorithm for these situations that brings RA performances close to the continuous link transmission is done in this chapter.

The proposed data precoded RA scheme is presented for a system cooperating with two relays, each equipped with either a single antenna or a two-antenna array, in Section 5.2. In Section 5.3 and 5.4 a precoded algorithm for relays with one and two antennas is presented, respectively. The algorithm proposed explores the relation between QPSK and 16-QAM, by alternately transmitting through the two relays, achieving full diversity, while significantly reducing the power penalty resulting from the half-duplex constraint. In this algorithm, we perform precoding of the data symbols prior to transmission, and post decoding at the UT. Two decoding methods are applied: decision feedback (DeF) and Viterbi algorithm.

The precoded algorithm is then extended for a general number of RNs and for one or two antennas in each relay in Section 5.5. Analytical derivation of the PEP of the proposed algorithm for each scheme is made and confirmed with numerical results. The performance improvements of the precoded schemes, relatively to the equivalent distributed SFBC schemes employing higher order modulations, are also analytically derived for a generic RA scheme. Numerical results for the proposed scheme are then computed for two- and three-relay schemes for several scenarios with different link qualities in Section 5.6 and the main conclusions are drawn in the last section.

5.2 Systems Definition

The system considered in this chapter is a particular case of the one in Figure 4-1, consisting of one BS, one UT and two RNs. The BS is equipped with N_B antennas and the UT with a single antenna, whereas the RNs have N_R antennas each, with $N_R \in \{1,2\}$, being referred to as RA 2RNs $N_B \times N_R \times 1$ (Figure 5-1). Channels are modeled by Rayleigh flat-fading channels and are represented by $h_{br\_q_b\_l\_q_r}$ for the link formed between the q_b^{th} antenna of the BS and the q_r^{th} antenna of the RN$_l$, and by $h_{ru\_l\_q_r}$ for the link between the q_r^{th} antenna of the RN$_l$ and the UT, with q_b =1,2, l=1,2 and q_r =1,..., N_R.

In practical systems the BS is usually equipped with multiple antennas, since the size, cost and other physical problems are much less stringent than in the UTs. This generally leads to lower bit error rates for the links between the BS and the RNs. As we consider a DL transmission and that the RNs are dedicated, relays are strategically located so that they have a good quality link to the

BS, as in the system considered in the previous chapter. Furthermore we can assume to have an SDF relay protocol by considering that each RN is capable of deciding whether or not it has decoded correctly. If a RN decodes correctly, it will forward the BS data in the second phase, otherwise it remains idle. This can be achieved through the use of cyclic redundancy check codes. This decision can also be approximated by setting a SNR threshold at both RNs; the RN will only forward the source data if the received SNR is larger than that threshold, as seen in Sub-section 2.4.4 [JiHa06].

For simplification purposes, we consider for all the theoretical derivations and for most of the simulated scenarios that BS→RN channels are error-free and thus the number of antennas at the BS is irrelevant. Furthermore, we focus our efforts on the special case where the direct link transmission is strongly affected by large-scale losses, such as due to shadowing, and thus no DP is considered for communication.

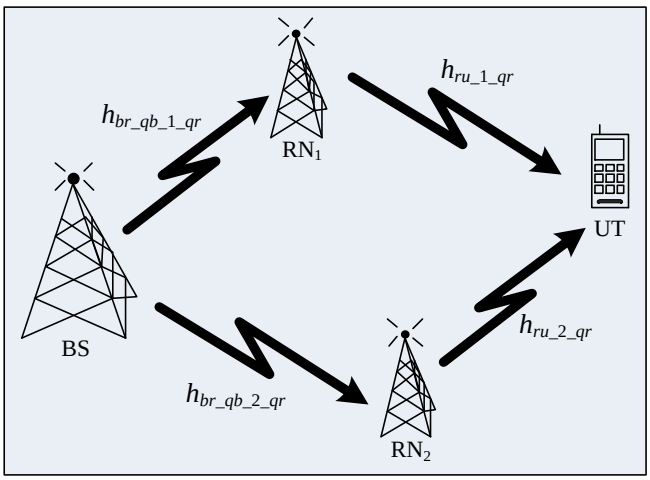

Figure 5-1: System model for the RA scheme with two RNs and N_R antennas at each relay (RA 2RN $N_B \times N_R \times 1$).

The fact that we have two independent paths from the relays to the destination allows us to achieve diversity. As in the previous chapters, we consider the case in which the relays are half-duplex, i.e., they cannot transmit and receive at the same time. Considering their half-duplex nature, we may have several options.

The relay nodes are allowed to simultaneously transmit over the same channel by emulating a space-frequency code. Concerning the scheme with single antenna relays, i.e., RA $N_B \times 1 \times 1$ system, Alamouti coding can be implemented in a distributed fashion by the two RNs [Alam98], as presented in Table 5.1. Considering the scheme with two antennas in each relay, the distributed quasi-orthogonal SFBC (QO-SFBC) proposed in [TiBH00] can also be implemented in a distributed manner.

TABLE 5.1: TRANSMITTED (LIGHTER CELLS) AND RECEIVED (DARKER CELLS) SIGNALS CORRESPONDING TO EACH TERMINAL OF THE ALAMOUTI RA N_BX1X1 SCHEME.

T_s	$2k$-1	$2k$
BS	$\left(s_{2k-1}^{p}; s_{2k-1}^{p+1}\right)$	
RN_1	$\left(s_{2k-1}^{p}; s_{2k-1}^{p+1}\right)$	$\left(s_{2k-1}^{p}; s_{2k-1}^{p+1}\right)$
RN_2	$\left(s_{2k-1}^{p}; s_{2k-1}^{p+1}\right)$	$\left(-s_{2k-1}^{p+1*}; s_{2k-1}^{p*}\right)$
UT		$\left(y_{2k}^{p}; y_{2k}^{p+1}\right)$

Another case occurs when the relays receive and transmit alternately and the source is transmitting continuously, firstly sending the information to the RN_1 and then repeating it to the RN_2. In this approach, diversity is achieved without need for any extra processing at the relays and using MRC at the UT.

In the two approaches above spatial diversity can be achieved, but because of the half-duplex constraints of relays, the information has to be transmitted in half of the time that would be needed in the case of a continuous link available from the source to the destination. This means that, assuming that a modulation scheme carrying m bits per symbol could be used in the case when the continuous direct link is available, one would need to switch towards a modulation carrying $2m$ bits per symbol (if the symbol duration was kept identical). Thus, in this case, in which two RNs are available, we need to switch from QPSK to 16-QAM modulations. As a major consequence, increasing modulation order leads to a decrease of power efficiency.

Another option is when the relays receive and transmit alternately, while the source is transmitting continuously different symbols in each instant, maintaining spectral efficiency and modulation as compared to the non-cooperative scheme. However, no diversity can be achieved in this case. In order to get both full spectral efficiency and diversity, we propose a novel algorithm where the data symbols are precoded, prior to the transmission from the source to the RNs. The RA schemes that use this precoding are referred to precoded RA (PRA). The data information received and transmitted in each time slot is exemplified in Table 5.2, for the case of single antenna RNs (PRA $N_B \times 1 \times 1$). Precoding was chosen so that diversity can be achieved without the need of exact duplication of the signal. Furthermore the relation between 16-QAM and QPSK defines an inherent trellis structure that is used in the precoding algorithm aiming to bring the performance closer to the one that would be obtained with the most power efficient modulation scheme. This proposed algorithm is defined for the OFDM technology and thus, for the two-antenna relays scheme (PRA $N_B \times 2 \times 1$), the signals transmitted by the two antennas are space-frequency encoded using the

Alamouti coding. Assuming uncorrelated antenna channels, a diversity order of 4 can be achieved. The rate of the proposed scheme is $N_l/(N_l+1)$, where N_l is the number of symbols transmitted, which is close to 1 for large values of N_l.

TABLE 5.2: TRANSMITTED (LIGHTER CELLS) AND RECEIVED (DARKER CELLS) SIGNALS CORRESPONDING TO EACH NODE OF THE RA N_BX1X1 SCHEME WITH ALTERNATE TRANSMISSION/RECEPTION IN RNS.

T_s	1	2	3	4	5	…	$2k$-1	$2k$
BS	s_1	s_2	s_3	s_4	s_5		s_{2k-1}	s_{2k}
RN_1	s_1	s_1	s_3	s_3	s_5		s_{2k-2}	s_{2k}
RN_2		s_2	s_2	s_4	s_4		s_{2k-1}	s_{2k-1}
UT		y_2	y_3	y_4	y_5		y_{2k-1}	y_{2k}

5.3 Precoded Algorithm for Two Single-Antenna Relays

5.3.1 Algorithm Description

Let us assume that the source produces a sequence of symbols $\{x_k\}$, each one carrying m information bits. The BS transmitter precodes successive pairs of symbols $\{x_k, x_{k-1}\}$, using a bijective function $F(x_k, x_{k+1})$. The precoded symbols, s_k, are alternately transmitted to the two relays, allowing each symbol to reach the UT through two independent links. When one of the links fails, the bijectivity allows the recover of the original symbols QPSK, as shown in Figure 5-2.

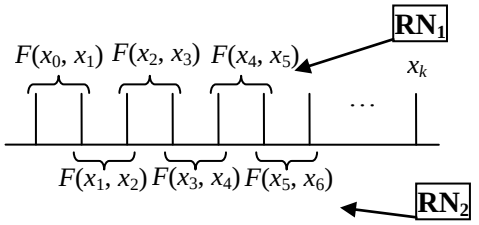

Figure 5-2: Pairs of symbols alternately transmitted to each relay, according to a bijective function $F(x_k, x_{k+1})$.

In the case that original symbols are QPSK, one can use a simple precoding operation that relates QPSK and 16-QAM, obtaining the symbols transmitted by the BS given by

$$s_k = \mu\left(x_k + \frac{1}{2}x_{k+1}\right), \tag{5.1}$$

where x_k is the k^{th} QPSK symbol of the original sequence information, with unitary power; and μ is a normalization factor, so that the average transmitted power is unitary. In this case the value is $\mu = 2/\sqrt{5}$. From (5.1), we can easily recognize that each symbol s_k is a 16-QAM symbol. However, the receiver will interpret it as a sum of two QPSK symbols, allowing to bring the performance close to the one that would be achieved if the QPSK symbols were transmitted continuously, because of the fact that each QPSK symbol is received through two paths.

In the data-precoded algorithm, while BS continuously transmits data to the RNs, relays transmit and receive alternately: RN_1 transmits in even time slots, or symbol duration, while RN_2 receives; RN_2 transmits in odd time slots, during the reception period of RN_1 , as can be seen in Table 5.2. The received signals at UT, when we have a single-antenna at each relay, in time slots 2*k* and 2*k*+1, are given by

$$\begin{cases} y_{2k} = \mu h_{ru\_1\_1,2k}\left(x_{2k-1} + \frac{1}{2}x_{2k}\right) + n_{2k} \\ y_{2k+1} = \mu h_{ru\_2\_1,2k+1}\left(x_{2k} + \frac{1}{2}x_{2k+1}\right) + n_{2k+1} \end{cases}, \tag{5.2}$$

where $h_{ru\_l\_1,k} = \sqrt{\varphi_{l,1}}h_{F,ru\_l\_1,k}$ represents the cooperative channel for links $RN_l \rightarrow UT$; $h_{F,ru\_l\_1,k}$ is the complex flat-fading Rayleigh channel realization for time slot *k*, with unit average power; $\varphi_{l,1}$ representing the long-term channel power; and, n_{2k+1} and n_{2k+2} are the zero mean complex additive white Gaussian noise samples with a variance of σ_n^2.

5.3.2 Decoding Methods

At the UT two decoding methods, to separate the QPSK data symbols, are considered: decision feedback and Viterbi [Vite67] algorithms, which are described below.

5.3.2.1 Decision Feedback Decoding

The decision feedback detection method is represented through the scheme in Figure 5-3, where $\hat{x}_k$ is the soft-decision of the symbol x_k. In order to recover symbol x_k, we first add two consecutive MRC symbols $\hat{y}_k$, according to the figure, given by

$$\hat{y}_k = h^*_{ru\_i\_1,k} y_k \tag{5.3}$$

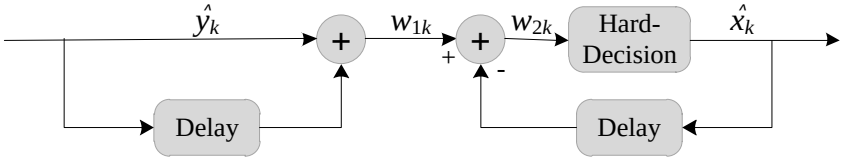

Figure 5-3: Block diagram of detection at UT for DeF algorithm.

Thus, the estimated symbol is derived from

$$\begin{aligned} w_{2,k} &= w_{1,k} - \mu \left| h_{ru\_3i-1\_1\_k-1} \right|^2 \hat{x}_{k-1} = \\ &= \mu \left(\left| h_{ru\_i\_1,k} \right|^2 + \frac{1}{2} \left| h_{ru\_3-i\_1,k-1} \right|^2 \right) x_k + \mu \left| h_{ru\_3-i\_k,k-1} \right|^2 \left(x_{k-1} - \hat{x}_{k-1} \right), \\ &+ \frac{1}{2} \mu \left| h_{ru\_i\_1,k} \right|^2 x_{k+1} + h^*_{ru\_i\_1,k} n_k + h^*_{ru\_3-i\_1,k-1} n_{k-1} \end{aligned} \tag{5.4}$$

where $w_{i,k}$, with i=1,2, are intermediate signals in the communication, as can be seen in the block diagram. We observe that each recovered symbol will have an interference due to the symbol x_{k+1} and to the errors obtained in the estimation of x_{k-1}. This interference can be constructive or destructive.

5.3.2.2 Viterbi Algorithm

The Viterbi algorithm is a maximum likelihood technique that explores the repetitive structure of tree codes, using a constant number of algebraic operations in each iteration of the algorithm. This is the most used method of convolutional decoding when its constraint length is not very large and it has the best performance in comparison with other decoding methods. This algorithm is used to look for the sequence $\hat{\mathbf{u}}$, such that:

$$\Pr[\hat{\mathbf{u}} \mid \mathbf{y}] \geq \Pr[\mathbf{u} \mid \mathbf{y}], \forall \mathbf{u}, \tag{5.5}$$

where $\Pr[\mathbf{u} \mid \mathbf{y}]$ is the probability of the information sequence $\mathbf{u}$ conditioned to the observation of $\mathbf{y}$ [Vite67].

The precoding performed in the proposed algorithm can be seen as a convolutional code with the corresponding encoder given in Figure 5-4. The code rate is 1/1 since it has one decoded symbol for each information symbol received. The number of symbol blocks on which each output block is dependent is *m* and is referred to as code memory. For our precoding method the code memory is 1.

In our strategy we consider that samples are not regenerated before entering the decoder, which is referred to as Viterbi with soft-decision algorithm. The soft-decision method is expected to have a better performance than the hard-decision one, since it does not destroy any information

that could be helpful in detection. For non-regenerated samples of y_k the conditioned probability is given by

$$\Pr[u_k \mid y_k] = \frac{1}{\sigma\sqrt{2\pi}} \exp(-\frac{1}{2\sigma^2}(y_k - u_k)^2). \tag{5.6}$$

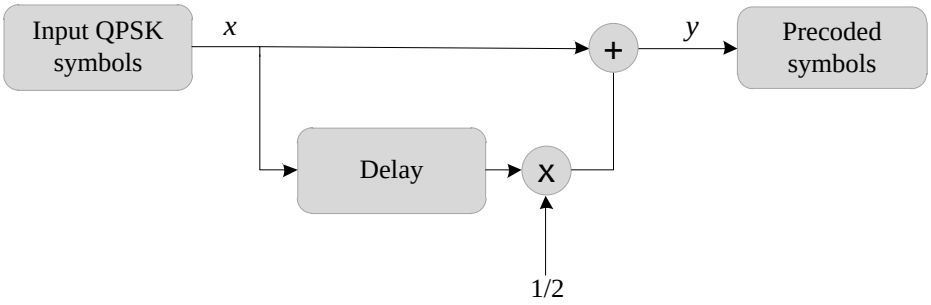

Figure 5-4: Convolutional encoder for the precoding algorithm of the RA schemes with two relays.

It is easy to see that the proposed algorithm has a trellis structure for the transmission of the QPSK symbols x_k. The corresponding trellis code of the proposed algorithm is represented in Figure 5-5. According to (5.1), we have defined four states, $u_k \in U$, $U = \{(0,0);(1,0);(0,1);(1,1)\}$, which are basically the QPSK symbols, whereas the transmitted QPSK symbols x_k are simply the scaled bipolar versions of u_k, so that they have the required power.

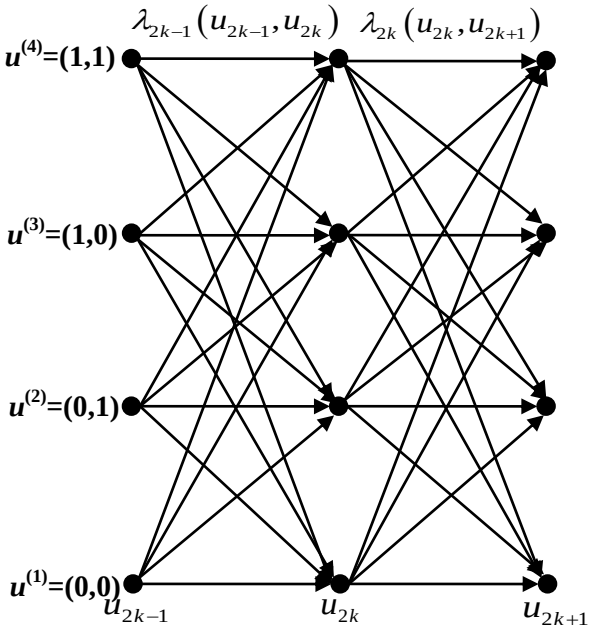

Figure 5-5: Trellis code structure for precoded algorithm.

The weight associated with a state transition from u_{k-1} to u_k is defined as $\lambda_{k-1}(u_{k-1},u_k)$. As we have alternate transmission through RN_1 and RN_2, the weights depend on the instant *k* and are given by

$$\lambda_{k-1}(u_{k-1},u_k)=\mu h_{ru\_l\_1,k}\left(\breve{u}_{k-1}+\frac{1}{2}\breve{u}_k\right), \tag{5.7}$$

with *l*=1 if *k* is even and *l*=2 if *k* is odd; $\breve{u}_k$ represents the QPSK soft-symbol associated with u_k, i.e.,

$$\breve{u}_k=\frac{1}{\sqrt{2}}\left[(-1)^{u_k(1)}+j(-1)^{u_k(2)}\right]. \tag{5.8}$$

For each state, there are four branches arriving at each symbol. The Viterbi algorithm is then used to find the most probable sequence. Thus, the most probable sequence is the one with the minimum Euclidean squared distance, which is given by

$$\nu(u_k,u_{k+1})=\left|y_k-\lambda_k(u_k,u_{k+1})\right|^2. \tag{5.9}$$

As the code is linear we can assume that the symbol $u^{(1)}$ is transmitted. An error event can be recovered in two steps as shown in Figure 5-6. The bits represented in each branch correspond to the output bits of each transition. The squared distance for the path that will erroneously recover $u^{(i)}$ instead of $u^{(1)}$ is given by

$$d^2_{\mathrm{PRA}}=\mu^2 d^2\left(u^{(1)},u^{(i)}\right)\left(\frac{\left|h_{ru\_l\_1,k}\right|^2}{4}+\left|h_{ru\_(3-l)\_1,k}\right|^2\right), \tag{5.10}$$

where $d\left(u^{(1)},u^{(i)}\right)$ is the distance between the QPSK symbols $u^{(1)}$ and $u^{(i)}$, as we observe in Figure 5-7**.** We observe that the proposed code has three paths where the error is recovered during two iterations. However, two of them have a minimum Hamming distance, through symbols $u^{(2)}$ and $u^{(3)}$. Thus, the distance between symbols $u^{(1)}$ and $u^{(i)}$, for $i=2,3$ is given by

$$d\left(u^{(1)},u^{(i)}\right)=2\sqrt{E_b}, \tag{5.11}$$

which is equal to the minimum QPSK distance ($d_{\min_{\mathrm{QPSK}}}$) and can be attained through the QPSK constellation represented in Figure 5-8.

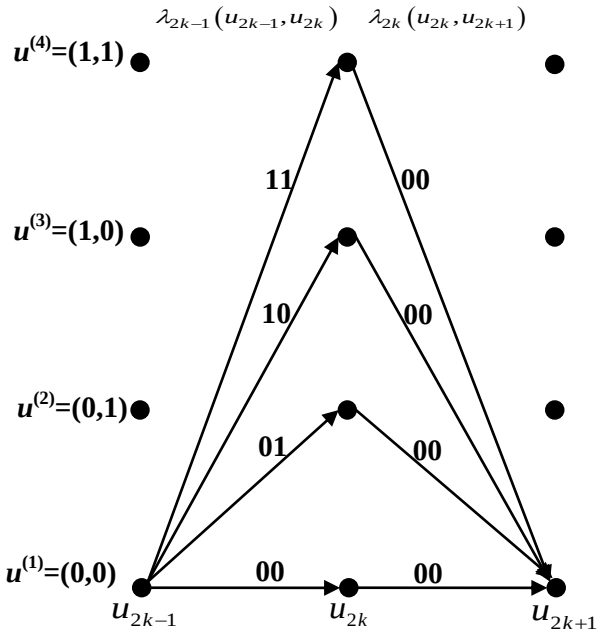

Figure 5-6: Trellis code for the precoded algorithm between symbol $u^{(1)}$ and the other possible symbols.

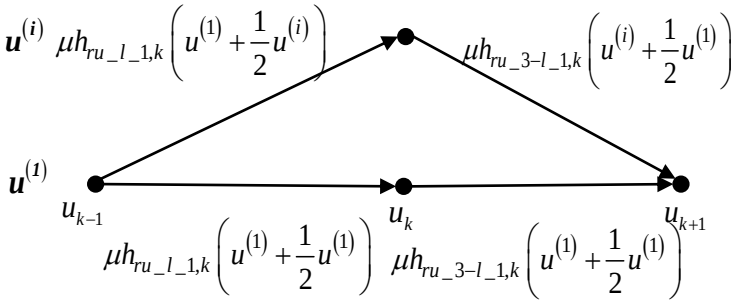

Figure 5-7: Trellis code for the RA precoded algorithm between symbols $u^{(1)}$ and $u^{(i)}$, for L=2.

As the error events can start at an odd or even time slot, the squared minimum distance is given by

$$d^2_{\min_{\text{PRA}}} = \mu^2 d^2_{\min_{\text{QPSK}}} \min\left(\left(\frac{\left|h_{ru\_l\_1,k}\right|^2}{4}+\left|h_{ru,(3-l)1,k}\right|^2\right),\left(\left|h_{ru\_l\_1,k}\right|^2+\frac{\left|h_{ru\_(3-l)\_1,k}\right|^2}{4}\right)\right). \quad (5.12)$$

Let ρ_m be the ratio between the minimum and maximum of the channel power gains, i.e.,

$$\rho_m = \frac{\min\left(\left|h_{ru\_l\_1,k}\right|^2,\left|h_{ru\_(3-l)\_1,k}\right|^2\right)}{\max\left(\left|h_{ru\_l\_1,k}\right|^2,\left|h_{ru\_(3-l)\_1,k}\right|^2\right)}. \quad (5.13)$$

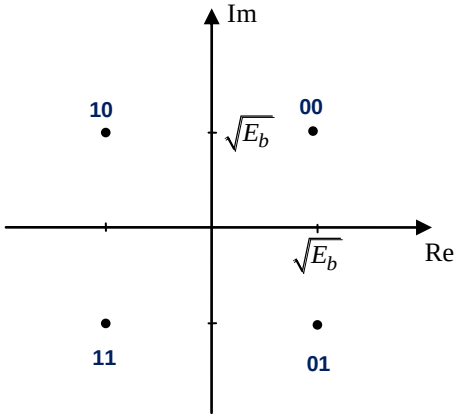

Figure 5-8: Constellation map of QPSK symbols.

Then, when the channel power gains exhibit an asymmetry with ratio ρ_m, the asymptotic coding power gain of the proposed algorithm, relatively to the distributed Alamouti, is given by

$$G = 10\log\left(\frac{1+4\rho_m}{1+\rho_m}\right). \tag{5.14}$$

Therefore, the proposed algorithm asymptotically achieves the performance of QPSK, in the case of high SNR and when the channels have equal average power gain, i.e., an improvement of 4 dB relatively to 16-QAM; taking ρ_m to 0, the performance will be that of distributed Alamouti, as we only have one path, reducing to a 16-QAM demodulation situation. The gain, as a function of the channel power gain ratio, is represented in Figure 5-9.

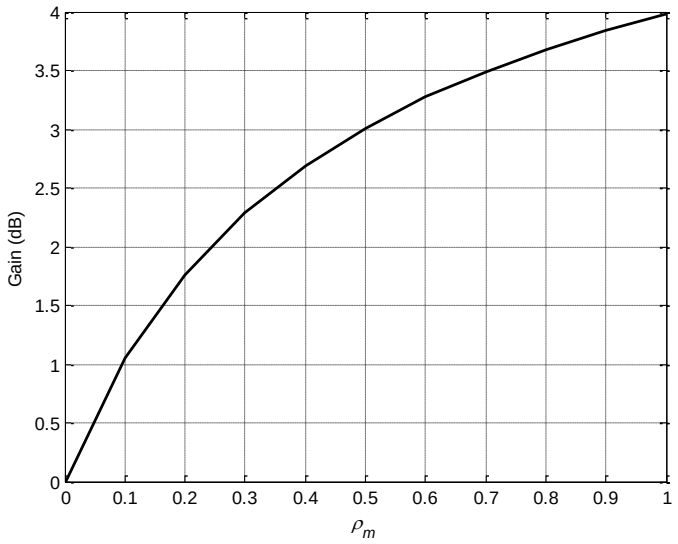

Figure 5-9: Coding gain obtained with PRA in relation to RA Alamouti, for N_B×1×1 system.

5.3.3 Error Probability and Diversity Gain Analysis

The proposed data precoding is equivalent to have a convolutional code characterized by the block diagram in Figure 5-4. At the receiver side, Viterbi algorithm is the best decoding strategy and starts by associating each combination of encoder memory states with a code state. This way, the encoding operation can be thought of as a series of transitions through the different states where each transition is driven by an input data bit and results in a number of coded bits. All the possible transitions over time are expressed in the trellis diagram, represented in Figure 5-5. The decoder, then, uses the bits of the received codeword to estimate the most likely path through the trellis. A decoding error occurs when the decoder picks a path that does not correspond to the one followed by the encoder during the encoding process. This occurs when one or more incorrect state transitions are calculated [LiSa09].

Let us compute the probability of an error event with basis on Figure 5-7, i.e., assuming that the transmitted symbols correspond to the all-zero path. The probability is obtained considering that, in the decoding, an incorrect path is taken at time *k* and remerges at time *k*+2. This represents a lower-bound on the actual probability of error, which is accurate for medium to high SNRs. Dropping, for simplicity, the subscripts ru_1,k in $h_{ru\_l\_1,k}$ and assuming, without loss of generality, that $h_1 \geq h_2$, the minimum distance between the two segments is given by

$$d_{\min}^2 = \mu^2 d_{\min_{\text{QPSK}}}^2 \left(|h_1|^2 / 4 + |h_2|^2 \right). \tag{5.15}$$

For high SNR regime, the pairwise error probability for convolutional codes can be asymptotically approached by [Glav07]:

$$PEP \simeq \frac{N_{\min}}{2} erfc\left(\frac{d_{\min}}{2\sqrt{N_0}} \right), \tag{5.16}$$

where $N_{\min}$ is the number of paths with the minimum distance and the complementary error function is

$$erfc(z) = \frac{2}{\sqrt{\pi}} \int_z^{+\infty} e^{-u^2} du \, . \tag{5.17}$$

Consequently, as there are two minimum paths, the PEP for the proposed algorithm, under perfect synchronization, is given by

$$PEP = erfc\left(\frac{d_{\min}}{2\sqrt{N_0}} \right). \tag{5.18}$$

Since the two minimum paths have a Hamming distance of one and have the same weight, the conditioned bit error probability for the RA 1RN $N_B \times 1 \times 1$ scheme is obtained by replacing (5.15) in (5.18), thus obtaining the following expression

$$P_{b|h_1,h_2} = \frac{1}{2} erfc\left(\sqrt{\frac{\mu^2 E_b\left(|h_1|^2/4 + |h_2|^2\right)}{N_0}}\right) = \frac{1}{2} erfc\left(\sqrt{\nu_1 + \nu_2}\right), \tag{5.19}$$

where $\nu_1 = |h_1|^2 \frac{\gamma}{4}$, $\nu_2 = |h_2|^2 \gamma$ and $\gamma = \mu^2 \frac{E_b}{N_0}$. The variables ν_i are i.i.d. and follow an exponential distribution with the respective means of $\bar{\nu}_1 = \frac{\gamma}{4}$ and $\bar{\nu}_2 = \gamma$. The pdf of such variables is given as follows

$$f_{\nu_i}(\bar{\nu}_i) = \begin{cases} \frac{1}{\bar{\nu}_i} e^{-\frac{\nu_i}{\bar{\nu}_i}} & ,\nu_i \geq 0 \\ 0 & ,\nu_i < 0 \end{cases}. \tag{5.20}$$

For the proposed algorithm we then get the unconditioned probability of error, as can be seen in the following expression

$$P_b = \frac{1}{2} \int_0^{+\infty} \int_0^{+\infty} erfc\left(\sqrt{\nu_1 + \nu_2}\right) f_{\nu_1}(\nu_1) f_{\nu_2}(\nu_2) d\nu_1 d\nu_2, \tag{5.21}$$

which, with the replacement of the pdf expressions of ν_1 and ν_2 in (5.21), can be simplified to the expression

$$P_b = \frac{2}{\gamma^2} \int_0^{+\infty} \int_0^{+\infty} erfc\left(\sqrt{\nu_1 + \nu_2}\right) e^{-\frac{4\nu_1 + \nu_2}{\gamma}} d\nu_1 d\nu_2. \tag{5.22}$$

Integrating (5.22), the final expression for the bit error probability of the proposed algorithm is extracted:

$$\begin{aligned} P_b &= \frac{1}{2\gamma}\left(\gamma - \gamma\sqrt{\frac{\gamma}{1+\gamma}} - \sqrt{\frac{\gamma}{4+\gamma}}\left(\frac{\gamma\sqrt{4+\gamma}}{3\sqrt{1+\gamma}} - \frac{1}{3}\right)\right) = \\ &= \frac{1}{2}\left(1 - \frac{4}{3}\sqrt{\frac{\gamma}{1+\gamma}} + \frac{1}{3}\sqrt{\frac{\gamma}{4+\gamma}}\right) \end{aligned}. \tag{5.23}$$

Re-writing the error probability expression as a function of $x = \gamma^{-1}$, a simplified expression is obtained

$$P_b = \frac{1}{2} - \frac{2}{3}(1+x)^{-\frac{1}{2}} + \frac{1}{6}(1+4x)^{-\frac{1}{2}}. \tag{5.24}$$

Expanding this expression as a Mac-Laurin series up to order 2, (5.24) is reduced to

$$P_e = \frac{3}{4}x^2 + r_2(x), \tag{5.25}$$

where $r_2(x)$ is the remainder term of order 2 [JBDS01].

For the high SNR regime, i.e., for $\gamma \to \infty$, we obtain an approximated expression for the proposed error probability

$$P_b \approx \frac{3}{4}\gamma^{-2}. \tag{5.26}$$

Diversity order is an important measure and is defined as the absolute values of the slopes of the error probability curve plotted on a log-log scale in a high SNR regime, [SiAl05], i.e.,

$$D \triangleq \lim_{\gamma\to\infty} \frac{-\log(P_e)}{\log(\gamma)}. \tag{5.27}$$

From (5.26) we can see that the error probability decays as γ^{-2}, which means that the scheme with our algorithm achieves diversity order of 2.

5.4 Precoded Algorithm for Two-Antenna Relays

5.4.1.1 Algorithm Description

For the case of RNs equipped with two antennas (N_R=2), the signals transmitted by each relay are encoded in space-frequency using Alamouti code. The received signals at UT, in time slot *k*, for adjacent subcarrier *p* and *p*+1, are given by

$$\begin{cases} y_{k,p} = \frac{1}{\sqrt{2}}\left(s_{k-1,p}h_{ru\_l\_1,k,p} - s^*_{k-1,p+1}h_{ru\_l\_2,k,p}\right) + n_{k,p} \\ y_{k,p+1} = \frac{1}{\sqrt{2}}\left(s_{k-1,p+1}h_{ru\_l\_2,k,p} + s^*_{k-1,p}h_{ru\_l\_1,k,p}\right) + n_{k,p+1} \end{cases}, \tag{5.28}$$

with *l*=1 in odd time slots and *l*=2 in even time slots, where $h_{ru\_l\_q_r,k,p}$ represents the complex flat-fading cooperative channel of the q_r^{th} antenna of RN$_l$ and UT, at time slot *k* and on p^{th} subcarrier position. Channels are considered flat for adjacent subcarriers, i.e., we assume that the subcarrier separation is significantly lower than the coherence bandwidth of the channel.

At the UT, the SFBC decoding is performed, using coefficients $g_{l\_q_r,k,p} = h_{ru\_l\_q_r,k,p}$, as follows

$$\begin{cases} \hat{y}_{k,p} = g^*_{l\_1,k,p}y_{k,p} + g_{l\_2,k,p}y^*_{k,p+1} \\ \hat{y}_{k,p+1} = -g_{l\_2,k,p}y^*_{k,p} + g^*_{l\_1,k,p}y_{k,p+1} \end{cases}. \tag{5.29}$$

Thus, the obtained soft-decision symbols are given by

$$\begin{cases} \hat{y}_{k+1,p} = \dfrac{\mu}{\sqrt{2}}\left(\left|h_{ru\_l\_1,k+1,p}\right|^2 + \left|h_{ru\_l\_2,k+1,p}\right|^2\right)\left(x_{k,p} + \dfrac{1}{2}x_{k+1,p}\right) \\ \qquad\qquad + \left(n_{k+1,p}h^*_{ru\_l\_1,k+1,p} + n^*_{k+1,p+1}h_{ru\_l\_2,k+1,p}\right) \\ \hat{y}_{k+1,p+1} = \dfrac{\mu}{\sqrt{2}}\left(\left|h_{ru\_l\_1,k+1,p}\right|^2 + \left|h_{ru\_l\_2,k+1,p}\right|^2\right)\left(x_{k,p+1} + \dfrac{1}{2}x_{k+1,p+1}\right) \\ \qquad\qquad + \left(-n^*_{k+1,p}h^*_{ru\_l\_2,k+1,p} + n^*_{k+1,p+1}h_{ru\_l\_1,k+1,p}\right) \end{cases}, \tag{5.30}$$

and are then object of Viterbi decoding, so that the most probable sequence can be found, similarly to the previous scheme, with the corresponding trellis code weights for time slot *k* given by

$$\lambda_{k,p}\left(u_{k,p}, u_{k,p+1}\right) = \frac{\mu}{\sqrt{2}}\left(\left|h_{ru\_l\_1,k,p}\right|^2 + \left|h_{ru\_l\_2,k,p}\right|^2\right)\left(\breve{u}_{k,p} + \frac{1}{2}\breve{u}_{k,p}\right), \tag{5.31}$$

and with $\breve{u}_k$ represented in (5.8).

In this case we intend to minimize the probability given by

$$\Pr\left[u_k \mid y_k\right] = \frac{1}{\sigma\left|g_k\right|\sqrt{2\pi}}\exp\left(-\frac{1}{2\sigma^2\left|g_k\right|^2}\left(y_k - u_k\right)^2\right), \tag{5.32}$$

which is equivalent to minimize $\sum_{i=0}^{N-1}\frac{(y_i - \lambda_i)^2}{g_i}$, with $g_k = \left|h_{ru\_l\_1,k,p}\right|^2 + \left|h_{ru\_l\_2,k,p}\right|^2$.

The squared minimum distance for this scheme is

$$d^2_{\min_{\text{PRA}}} = \mu^2 d^2_{\min_{\text{QPSK}}}\left(\left(\left|h_1\right|^2 + \left|h_2\right|^2\right)/8 + \left(\left|h_3\right|^2 + \left|h_4\right|^2\right)/2\right), \tag{5.33}$$

when simplifying the representation of the four channels between relays and the UT for a specific transmission as h_i, with *i*=1,2,3,4 and where $\left|h_1\right|^2 + \left|h_2\right|^2 > \left|h_3\right|^2 + \left|h_4\right|^2$. This is equivalent to having an equivalent channel with power equal to the sum of the powers of each two channels that form the link.

For the distributed QO-SFBC we have inter-symbol interference between each two symbols, due to the code design that is not fully orthogonal. However, we can get the expression for the squared minimum distance for a high SNR regime, where that interference is null for ML decoding, which is given by

$$d^2_{\min_{4\text{x}1,16\text{–QAM}}} = d^2_{\min_{16\text{–QAM}}}\frac{\left|h_1\right|^2 + \left|h_2\right|^2 + \left|h_3\right|^2 + \left|h_4\right|^2}{4} = \frac{\mu^2 d^2_{\min_{\text{QPSK}}}}{8}\left(\left|h_1\right|^2 + \left|h_2\right|^2 + \left|h_3\right|^2 + \left|h_4\right|^2\right). \tag{5.34},$$

Then, when the channel power gains exhibit asymmetry with ratio ρ_m, the asymptotic channel power gain from the proposed algorithm considered relatively to the distributed SFBC is given by

$$\rho_m = \frac{\min\limits_{\substack{i\in\{1,\ldots,L-1\}\\ i\neq j}}\left(\min\limits_{j\in\{1,\ldots,L-1\}}\left(|h_i|^2+|h_j|^2\right)\right)}{\max\limits_{\substack{i\in\{1,\ldots,L-1\}\\ i\neq j}}\left(\max\limits_{j\in\{1,\ldots,L-1\}}\left(|h_i|^2+|h_j|^2\right)\right)}, \tag{5.35}$$

which is the same as in the previous scheme with $N_R = 1$, when the equivalent channels have the same power in both cases.

5.4.1.2 PEP derivation

The PEP expression for this scheme with two relays, each equipped with two antennas, is the same as the previous one, since the algorithm has the same trellis code. However trellis paths have different weights, as referred to in the previous sub-section. Thus, the corresponding error probability, conditioned to channel realizations, is given by

$$P_{b|h_1,h_2} = \frac{1}{2}erfc\left(\sqrt{\frac{E_b\mu^2\left(\left(\left|h_{ru\_l\_1,k}\right|^2+\left|h_{ru\_l\_2,k}\right|^2\right)/8+\left(\left|h_{ru\_(3-l)\_2,k+1}\right|^2+\left|h_{ru\_(3-l)\_2,k+1}\right|^2\right)/2\right)}{\sigma_n^2}}\right). \tag{5.36}$$

Let us consider i.i.d. exponential random variables following a Chi-square distribution, i.e., $\nu_i \sim \chi^2\left(\bar{\nu}_i, k\right)$ given as

$$\nu_i = \begin{cases} \dfrac{|h_1|^2+|h_2|^2}{4}\gamma & ,i=1 \\ \left(|h_3|^2+|h_4|^2\right)\gamma & ,i=2 \end{cases}, \tag{5.37}$$

with means $\bar{\nu}_1 = \gamma/4$ and $\bar{\nu}_2 = \gamma$, each with two degrees of freedom, and where $\gamma = \mu^2\dfrac{E_b}{2N_0}$.

According to [SiAl05], the pdf of a Chi-square variable with *k* degrees of freedom is given by

$$f_{\nu_i}\left(\bar{\nu}_i, k\right) = \frac{\nu_i^{\,k-1}e^{-\frac{\nu_i}{\bar{\nu}_i}}}{(k-1)!\bar{\nu}_i^{\,k}}. \tag{5.38}$$

Consequently the bit error probability of the algorithm is simplified to the expression that follows:

$$P_b = \frac{1}{2}\int_0^{+\infty}\int_0^{+\infty} erfc\left(\sqrt{\sum_{i=1}^{2}\nu_i}\right)\prod_{i=1}^{2} f_{\nu_i}\left(\nu_i, 2\right)d\nu_2 d\nu_1. \tag{5.39}$$

Integrating the previous expression we achieve our goal, obtaining the final bit error probability expression

$$P_b = \frac{1}{2} - \frac{4}{9}\sqrt{\frac{\gamma}{1+\gamma}}\left(\frac{2}{3}+\frac{1}{1+\gamma}\right) - \frac{1}{18}\sqrt{\frac{\gamma}{4+\gamma}}\left(\frac{11}{3}+\frac{2}{4+\gamma}\right). \tag{5.40}$$

This expression can also be represented as

$$P_b = \frac{1}{2}\left(1 - \frac{8}{27} f_1\left(\gamma^{-1}\right) - \frac{4}{9} f_2\left(\gamma^{-1}\right) - \frac{11}{54} f_1\left(4\gamma^{-1}\right) - \frac{1}{36} f_2\left(4\gamma^{-1}\right)\right), \tag{5.41}$$

where the functions $f_1(x)$ and $f_2(x)$ are expressed by

$$f_i(x) = \begin{cases} (1+x)^{-\frac{1}{2}} & , i = 1 \\ x(1+x)^{-\frac{3}{2}} & , i = 2 \end{cases}. \tag{5.42}$$

Their corresponding Mac-Laurin series are

$$f_i(x) = \begin{cases} \sum_{n=0}^{+\infty} (-1)^n \frac{(2n-1)!!}{2^n} x^n = 1 - \frac{1}{2}x + \frac{3}{8}x^2 - \frac{5}{16}x^3 + \frac{35}{128}x^4 + \ldots & , i = 1 \\ \sum_{n=0}^{+\infty} (-1)^n \frac{(2n-1)!!}{2^{n-1}(n-1)!} x^n = x - \frac{3}{2}x^2 + \frac{5}{8}x^3 - \frac{35}{16}x^4 + \ldots & , i = 2 \end{cases}. \tag{5.43}$$

Replacing the previous series approaches up to order 4, we reach the upper bound expression for bit error probability of this scheme, represented as follows:

$$P_b = \frac{35}{16}\gamma^{-4}. \tag{5.44}$$

The diversity order of this scheme, as expected, and according to (5.26) is of 4.

5.5 Precoded Algorithm for a Multiple Relay-Assisted Scheme

5.5.1 Algorithm Description

The proposed cooperative algorithm for a two-relay scheme can be extended to a generic number of relays. Thus, similarly to the previous case, the relation between *M*-QAM and QPSK defines an inherent trellis structure that can be used to bring the performance closer to the one that would be obtained with the conventional distributed algorithms, which demand for the use of constellations with higher cardinality schemes. Note that a distributed space-time/frequency code should be implemented in each relay with more than one antenna and there are only codes fully orthogonal and with unitary rate for a maximum of two antennas. Thus, only when the number of antennas at the relays is less or equal to two, is it possible to achieve full diversity. As previously mentioned, the relays receive and transmit alternately. The source is transmitting continuously, sending firstly information to RN_1 and then repeating it to RN_2, and then successively until RN_L. Diversity is achieved by using a precoding at the BS. There is no need for any extra processing at the relays, and decoding at the UT is obtained by using MRC, followed by a decoding based on Viterbi algorithm. The nodes that are transmitting and receiving in each instant are exemplified in Table 5.3, where A→B represents the transmission from the node A to node B.

TABLE 5.3: ACTIVE LINKS IN EACH TIME SLOT FOR THE PRECODED RA SCHEME.

T_s	L-1	L	L+1	L+2
Active links	BS→RN_L RN_{L-1}→UT	BS→RN_{L+1} RN_L→UT	BS→RN_{L+2} RN_{L+1}→UT	BS→RN_{L+3} RN_{L+2}→UT

The source produces a sequence of symbols $\{x_k\}$, each one carrying m information bits. The BS transmitter precodes successive groups of symbols $\{x_k, x_{k-1,\ldots,} x_{k-L}\}$, using a bijective function $F(x_k, x_{k-1,\ldots,} x_{k-L})$. The precoded symbols, s_k, are alternately transmitted to the relays, allowing each symbol, when all paths are available, to reach the UT through L independent links. When one of the links fails, the bijectivity allows the recovery of the original symbols QPSK. The groups of original symbols that are joined in a single precoded symbol are shown in Figure 5-10, considering the scheme with three RNs.

In the case that original symbols are QPSK, we can use a simple precoding operation that relates QPSK and M-QAM, obtaining the symbols transmitted by the BS, given by

$$s_k = \mu \sum_{i=0}^{L-1} 2^{-i} x_{k+i} \,, \tag{5.45}$$

where x_k is the k^{th} QPSK symbol of the original sequence information, with unitary power; μ is the normalization factor for a generic number of relays, which is independent of the number of antennas in each relay, and is given by

$$\mu = \sqrt{\frac{4^{L-1}}{\sum_{i=0}^{L-1} 4^i}} \,. \tag{5.46}$$

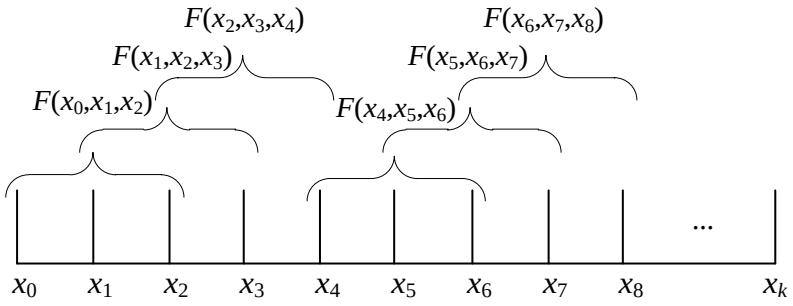

Figure 5-10: Groups of symbols alternately transmitted to each relay, according to a bijective function $F(x_k, x_{k+1}, x_{k+2})$ for the case of L=3.

From (5.45), we easily recognize each symbol s_k as a M-QAM symbol. However, the receiver will interpret it as a sum of L QPSK symbols, thus bringing the performance close to the one that would be achieved if the QPSK symbols were transmitted continuously, because of the

fact that each QPSK symbol is received through L paths. When L_f of the links fails, with $L_f < L$, it is possible to recover the original symbols QPSK from the L-L_f available links, although the diversity is reduced to L-L_f.

In this algorithm, while BS transmits data continuously to the RNs, relays transmit and receive alternately, as shown in Table 5.3. Thus, the received signals at UT, in time slots $Lk+l$, with $l=1,...,L$ and $k \in \mathbb{N}$, are given respectively by

$$y_{Lk+l} = \begin{cases} \mu^2 h_{ru\_l\_1,Lk+l} \sum_{i=0}^{L-1} 2^{-i} x_{Lk+l-1+i} + n_{Lk+l} & , N_R = 1 \\ \frac{\mu^2}{2}\left(\left|h_{ru\_l\_1,k,p}\right|^2 + \left|h_{ru\_l\_2,k,p}\right|^2\right) \sum_{i=0}^{L-1} 2^{-i} x_{Lk+l-1+i} + n_{Lk+l} & , N_R = 2 \end{cases}, \tag{5.47}$$

where $h_{ru\_l\_q_r,k} = \sqrt{\varphi_{l,q_r}} h_{F,ru\_l\_q_r,k}$ represents the cooperative channel for the link between the q_r^{th} antenna of RN$_l$ and the UT; $h_{F,ru\_l\_q_r,k}$ is the complex flat fading Rayleigh channel realization for time slot k, with unit average power; and, φ_{l,q_r} represents the long-term channel power.

As referred previously the proposed algorithm has a trellis structure for the transmission of the QPSK symbols. As the code is linear an error event can be recovered in L steps. We get the squared minimum distance of the proposed algorithm for relays equipped with one antenna, resulting in

$$d^2_{\min_{\text{PRA}}} = \mu^2 d^2_{\min_{QPSK}} \min_{j \in J} \left(\sum_{i=0}^{L-1} 4^{-i} \left|h_{ru\_i+L\_1,k}\right|^2 \right) \tag{5.48}$$

with $J \in \{1,2,...,L\}$ and assuming that $h_{ru\_l\_q_r,k} = h_{ru\_l+L\_q_r,k}$.

Let us define ρ_{mi} as the channel power gains of each link comparatively to the maximum channel power gain. Assuming, without loss of generality, that $\left|h_{ru\_1\_1,k}\right|^2 \geq \left|h_{ru\_2\_1,k}\right|^2 \geq ... \geq \left|h_{ru\_L\_1,k}\right|^2$, we obtain the channel power gain for each link for relays with one antenna and for $i=1,...,L-1$:

$$\rho_{mi} = \frac{\left|h_{ru\_i+1\_1,k}\right|^2}{\left|h_{ru\_1\_1,k}\right|^2}. \tag{5.49}$$

Thus, using the variables of channel power gains, (5.48) can be simplified to

$$d^2_{\min_{PRA}} = \mu^2 d^2_{\min_{QPSK}} \left(\sum_{i=1}^{L-1} 4^i \rho_{mi} + 1 \right) \left|h_{ru\_i\_1,k}\right|^2. \tag{5.50}$$

Similarly, for the case of relays equipped with two antennas, we can assume that $\left|h_{ru\_1\_1,k}\right|^2 + \left|h_{ru\_1\_2,k}\right|^2 \geq \left|h_{ru\_2\_1,k}\right|^2 + \left|h_{ru\_2\_2,k}\right|^2 \geq ... \geq \left|h_{ru\_L\_1,k}\right|^2 + \left|h_{ru\_L\_2,k}\right|^2$, and thus obtain the corresponding channel power gains for $i=1,...,L-1$ in

$$\rho_{mi} = \frac{\left|h_{ru\_i+1\_1,k}\right|^2 + \left|h_{ru\_i+1\_2,k}\right|^2}{\left|h_{ru\_1\_1,k}\right|^2 + \left|h_{ru\_1\_2,k}\right|^2} \tag{5.51}$$

and the squared minimum distance in

$$d^2_{\min_{\text{PRA}}} = \frac{\mu^2}{2} d^2_{\min_{\text{QPSK}}} \left(\sum_{i=1}^{L-1} 4^i \rho_{mi} + 1 \right) \left(\left|h_{ru\_l\_1,k}\right|^2 + \left|h_{ru\_l\_2,k}\right|^2 \right). \tag{5.52}$$

It is important to evaluate the performance achieved with the data-precoded algorithm comparatively to the one we get using conventional cooperative algorithms. First we compare the precoded algorithm with one using distributed SFBCs, with unitary multiplexing rate. For the cases of having more than two transmitting antennas, the SFBCs are not fully orthogonal, thus resulting in lower performances. We present the theoretical minimum distance for the cases that a DSFBC is applied to the RA scheme with L relay nodes, although neglecting the quasi-orthogonal impact on the final performance, which are derived in Annex C. Thus, the gain obtained is a lower-bound, because of the non-achievement of full orthogonality, if we consider $N_R > 2$. The asymptotic gain from the proposed algorithm considered relatively to the SFBC, for $L \in \mathbb{N} \setminus \{1\}$ and $N_R \in \{1,2\}$, is given for

$$G_L = 10\log\left(\frac{15L\left(\sum_{i=1}^{L-1} 4^i \rho_{mi} + 1 \right)}{2\left(4^L - 1\right)\left(\sum_{i=1}^{L-1} \rho_{mi} + 1 \right)} \right), \tag{5.53}$$

where the channel gains ρ_{mi} are defined in (5.49) for the case of a single antenna at the relays and in (5.51) for the two-antenna case. Detailed derivation is in Annex C. Considering the example of the scheme with four RNs equipped with single antennas, the gain we obtain in comparison with the equivalent distributed SFBC is given by

$$G_{L=4} = 10\log\left(\frac{2}{17} \frac{64\rho_{m3} + 16\rho_{m2} + 4\rho_{m1} + 1}{\rho_{m3} + \rho_{m2} + \rho_{m1} + 1} \right). \tag{5.54}$$

In the asymptotic case of high SNR values, and when channels have equal power gains, the gain tends to a constant irrespective of the number of relays, L, given by

$$\lim_{SNR\to\infty} G_L = 10\log\left(\frac{15L\dfrac{4^L - 1}{3}}{2\left(4^L - 1\right)L} \right) = 10\log\left(\frac{5}{2} \right). \tag{5.55}$$

An alternative scheme for comparison with the proposed one is a cooperative scheme, also with a unitary rate, though fully orthogonal. This cooperative scheme can use the Alamouti code multiple times according to the number of elements and is referred to as distributed compound

Alamouti (DCA) algorithm. This algorithm requires more time for transmission, which depends on the number of relays. Thus, for the case of single antenna relays, it takes twice the time to transmit as compared to the time that the continuous link would take if available for the two-relay case, and thrice the time for three- and four-relay cases and so forth. The final expression for the gain obtained when using the precoded algorithm instead of a DCA one, derived in Annex C, is given by

$$G_L = \begin{cases} 10\log\left(\dfrac{\dfrac{1}{4^L-1}\left(\sum_{i=1}^{L-1}4^i\rho_{mi}+1\right)}{\dfrac{(L+2)}{4\left(4^{\frac{L}{2}+1}-1\right)}\left(\sum_{i=1}^{L-1}\rho_{mi}+1\right)}\right), & L \text{ is even} \wedge N_R=1 \\ 10\log\left(\dfrac{\dfrac{1}{4^L-1}\left(\sum_{i=1}^{L-1}4^i\rho_{mi}+1\right)}{\dfrac{(L+3)}{4\left(4^{\frac{L+3}{2}}-1\right)}\left(\sum_{i=1}^{L-1}\rho_{mi}+1\right)}\right), & L \text{ is odd} \wedge N_R=1 \\ 10\log\left(\dfrac{\dfrac{1}{4^L-1}\left(\sum_{i=1}^{L-1}4^i\rho_{mi}+1\right)}{\dfrac{3L}{2\left(4^L-1\right)}\left(\sum_{i=1}^{L-1}\rho_{mi}+1\right)}\right), & N_R=2 \end{cases} . \quad (5.56)$$

In the case of high SNR values and when channels have equal power gain, we have an improvement, for a generic system with L relays, using the proposed algorithm against the DCA algorithm, given by

$$\lim_{SNR\to\infty} G_L = \begin{cases} 10\log\left(\dfrac{4\left(4^{\frac{L}{2}+1}-1\right)}{3L\left(L+2\right)}\right) & , L \text{ is even} \wedge N_R=1 \\ 10\log\left(\dfrac{4\left(4^{\frac{L+3}{2}}-1\right)}{3L\left(L+3\right)}\right) & , L \text{ is odd} \wedge N_R=1 \\ 10\log\left(\dfrac{2\left(4^{L}-1\right)}{L^2}\right) & , N_R=2 \end{cases} . \quad (5.57)$$

Thus, the asymptotic gain that the precoded algorithm achieves relatively to the DCA one, when the channels have equal power gains, depends on the number of RNs and on the number of antennas in each one. This gain in dBs in function of the number of relays is shown in Figure 5-11.

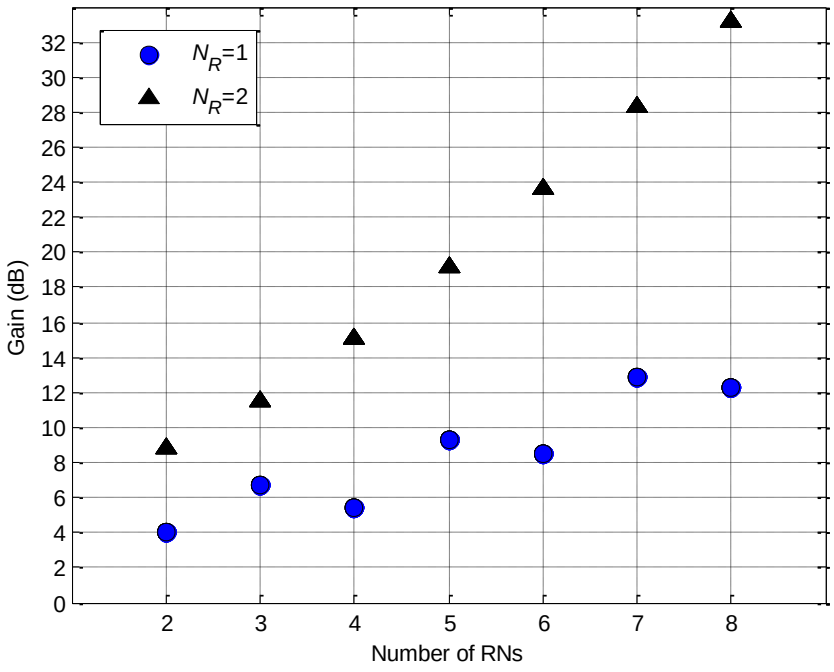

Figure 5-11: Coding gain obtained with the precoded algorithm in comparison to the DCA one, for a high SNR regime, for equal channel power gains.

When the number of antennas in each relay is two, the gain increases with the number of relays, since Alamouti code is implemented in each relay. However, in the case of the single-antenna relay the gain decreases when the number of RNs goes from 3 to 4 or from 5 to 6. Note that in those situations we are increasing the cardinality of modulation in a factor of 4, because of

the lower spectral efficiency of this scheme, since in those cases we need an additional time phase for another Alamouti code implementation. When ρ goes to 0, the performance is reduced to a *M*-QAM demodulation.

5.5.2 PEP Derivation for a Multiple Number of Relays and Antennas

In this section, the bit error probability for a general number of relays, designated as *L*, and for a general number of antennas equipping each relay, designated as N_R, is derived. Similarly to the previous particular case, where (5.21) was obtained, we reach the expression

$$P_b = \underbrace{\int_0^{+\infty} \cdots \int_0^{+\infty}}_{LN_R} Q\left(\sqrt{2\sum_{i=1}^{LN_R} \nu_i}\right) \prod_{i=1}^{LN_R} f_{\nu_i}(\nu_i) d\nu_1 \ldots d\nu_{LN_R}, \tag{5.58}$$

where the pdf of ν_i is in (5.20), and function Q is defined as [Gold05]

$$Q\left(\sqrt{2\varphi}\right) = \frac{1}{\pi} \int_0^{\frac{\pi}{2}} e^{-\frac{\varphi}{\sin^2\phi}} d\phi. \tag{5.59}$$

Replacing (5.59) in (5.58), we start by presenting an alternative expression for the bit error probability, given by

$$P_b = \frac{1}{\pi} \int_0^{\frac{\pi}{2}} \prod_{i=1}^{LN_R} \frac{\sin^2\phi}{\sin^2\phi + \overline{\nu}_i} d\phi. \tag{5.60}$$

For the case of *L* relays and N_R antennas, the LN_R variables of the product referred to as ν_i can be divided as *L* variables with different means, each one repeated N_R times. Consequently, the previous expression can be presented as

$$P_b = \frac{1}{\pi} \int_0^{\frac{\pi}{2}} \prod_{i=1}^{L} \left(\frac{\sin^2\phi}{\sin^2\phi + \overline{\nu}_i} \right)^{N_R} d\phi. \tag{5.61}$$

By solving this integral, we obtain the final expression for the bit error probability given, for a general scheme, by

$$P_b = \frac{1}{2} \sum_{i=1}^{L} \sum_{k=1}^{N_R} A_{k_i} \left[1 - \sqrt{\frac{\overline{\nu}_i}{1+\overline{\nu}_i}} \sum_{j=0}^{k-1} \binom{2j}{j} \frac{1}{\left[4\left(1+\overline{\nu}_i\right)\right]^j} \right], \tag{5.62}$$

where each variable mean $\overline{\nu}_i$ is given through $\overline{\nu}_i = \frac{\gamma}{N_R 4^{i-1}}$; the signal to noise ratio is $\gamma = \mu^2 \frac{E_b}{N_0}$; $\binom{n}{k}$ is the *k*-combination of a set of *n* elements; and, the auxiliary variable A_{k_i} is obtained based on [SiAl05] and it is defined as

$$A_{k_i} = \frac{1}{(N_R-k)!(\bar{\nu}_i)^{N_R-k}} \left\{ \frac{d^{N_R-k}}{dx^{N_R-k}} \prod_{\substack{j=1 \\ j\neq i}}^{L} \left(\frac{1}{1+\bar{\nu}_j x} \right)^{N_R} \right\} \Bigg|_{x=-\frac{1}{\bar{\nu}_i}} . \tag{5.63}$$

By replacing N_R and L in (5.62) with the values used in Sections 5.3 and 5.4, we get the expressions (5.23) and (5.41), previously derived through other methods, thus verifying the validity of these expressions. Additionally, we can get the correspondent bit error probabilities for all sets of combinations of L and N_R, as for example for $L=3$ and $N_R=1$, which results in the following

$$P_b = \frac{1}{2}\left(1 - \frac{64}{45}\sqrt{\frac{\gamma}{1+\gamma}} + \frac{4}{9}\sqrt{\frac{\gamma}{4+\gamma}} - \frac{1}{45}\sqrt{\frac{\gamma}{16+\gamma}} \right). \tag{5.64}$$

As mentioned previously, full diversity is just possible for the case of having two or less antennas in each relay, since in this case the SFBC implemented in each relay is not full orthogonal. However, for the situations where there are more than two antennas in each relay, i.e., $N_R > 2$, this expression can be seen as a lower-bound of the bit error probability.

In order to obtain an approximation to the error probability for high SNR regime, considering a general number of relays and antennas equipping each relay, we try to simplify the bit error expression in (5.60). For a high SNR, it is reasonable to assume $\nu_i \gg \sin^2\phi$. This simplification approximates (5.60) to an upper bound based on [GRJZ00]

$$P_b \approx \frac{(2N_R L-1)!!}{2^{N_R L+1}\cdot(N_R L)!} \prod_{i=1}^{L} \left(4^{i-1}\right)^{N_R} \cdot \left(\frac{\gamma}{N_R} \right)^{-N_R \cdot L} , \tag{5.65}$$

dependent of the double factorial operator, defined as

$$n!! = \begin{cases} n(n-2)...5\cdot 3\cdot 1, n>0 \text{ and odd} \\ n(n-2)...6\cdot 4\cdot 2, n>0 \text{ and even} \\ 1 \qquad\qquad\quad ,n=-1,0 \end{cases} . \tag{5.66}$$

A diversity order of LN_R can be achieved with the proposed algorithm, as can be confirmed by (5.65).

By replacing the variable that characterizes the number of relays by three and the number of antennas at each relay by one in the previous derived expression, we reach the upper bound expression for P_b of the proposed algorithm for the scheme PRA 3RN $N_B \times 1 \times 1$, represented by

$$P_b = 10\gamma^{-3}. \tag{5.67}$$

The diversity order of this scheme, as expected, is of 3.

5.5.3 Validation of Bit Error Probability Analysis

In this section the analytical derivation of the error probability of the proposed algorithm is corroborated by the BER performance obtained through Monte Carlo simulations, for the RA scheme with one antenna in each relay, assuming error free transmission between the BS and the RNs. Theoretical and simulated BER curves are shown in Figure 5-12, including the theoretical upper-bound approximation for high SNR regime derived previously. The simulation curve has approximately the same behavior as the one given by the theoretical expression provided in (5.23), only differing for low SNRs. At low SNRs error events may correspond to paths that do not have the minimum distance, which results in the differences between the theoretical and the simulated curves. These are, nonetheless, lower than 1 dB for $E_b/N_0 \geq 12$ dB and, thus, negligible for high SNR values. We can also observe that the simulated curve has the same linear decay as the asymptotic curve given by (5.26) for high SNRs, confirming the diversity order of 2.

Regarding the simulated performance obtained for the RA with the proposed algorithm for two relays, each one equipped with two antennas, it is compared with the theoretical expression derived and shown in Figure 5-13. Again, the curves are close to each other, not differing more than 1 dB for any value of the SNR. Moreover, the asymptotic curve confirms the order diversity of 4, which was assessed in (5.44).

Another simulated scheme, in order to validate the error probability expression derived previously, is the RA with three RNs, all equipped with a single antenna. The curves with the theoretical and simulated results are presented in Figure 5-14, with the theoretical expression shown in (5.64). As in the previous cases, the curves approach one another as SNR increases. Again, the small discrepancy is due to the approximation done in the theoretical expressions derivation. These expressions are obtained assuming the recovery of each bit error through one of the minimum distance paths. Furthermore, the slope derived by the approximated expression for high-SNR regime in (5.82) is of order 3, as can be confirmed in the figure below.

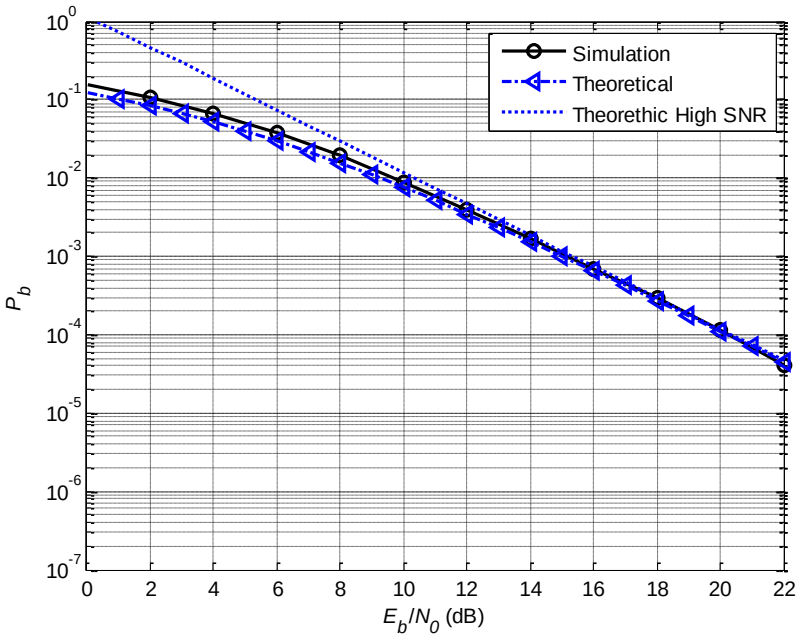

Figure 5-12: Theoretical and simulated error probability for RA precoded scheme with L=2 N_R=1.

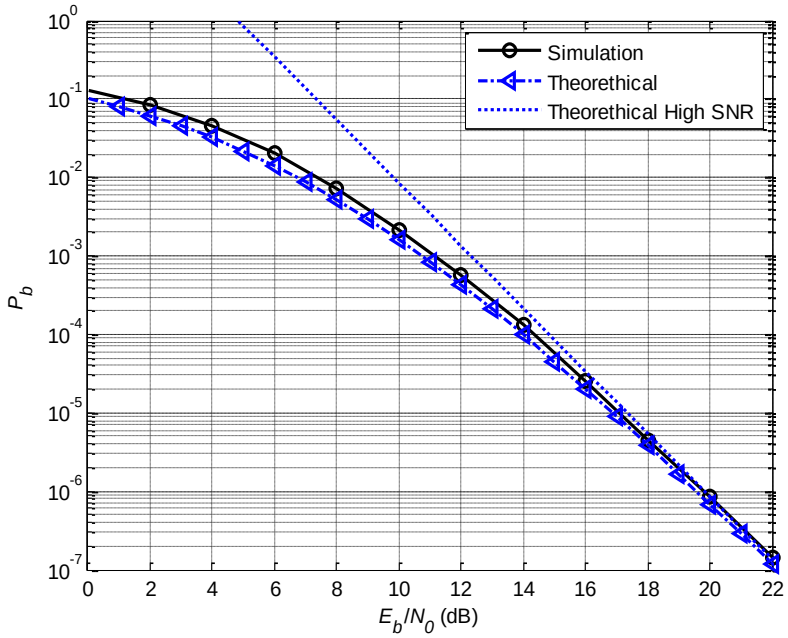

Figure 5-13: Theoretical and simulated error probability for RA precoded scheme with L=2 N_R=2.

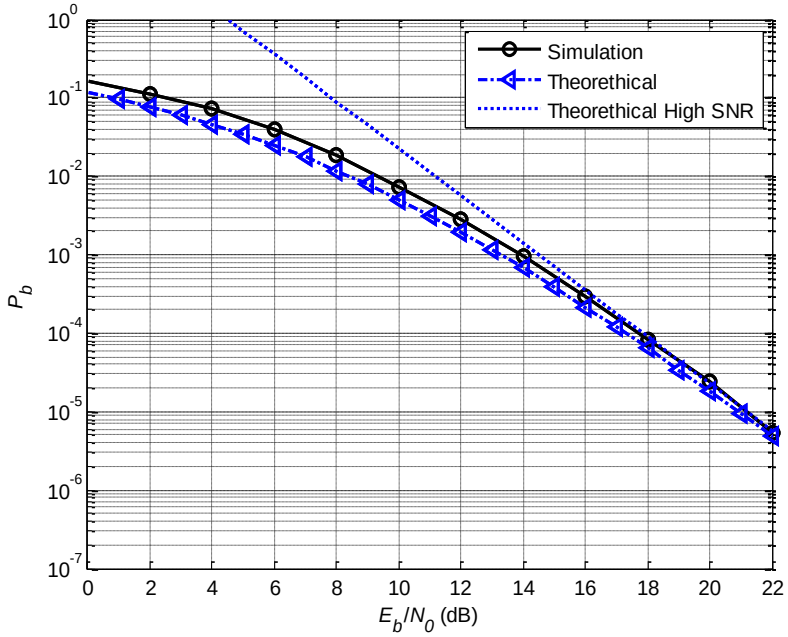

Figure 5-14: Theoretical and simulated error probability for RA precoded scheme with L=3 N_R=1.

5.6 Numerical Results

5.6.1 Assumptions and Conditions

Some assumptions already considered in Chapter 4 are also considered in this chapter simulations, such as: perfect CSI at the relays and at the UT; normalization of the transmitted power per time slot to one; and distance between antenna elements of each BS and RN far apart to assume uncorrelated antenna propagation channels. The block length used in the simulations, N_l, is of 3600 symbols. In all the considered systems, two information bits are transmitted per symbol interval, and thus all of them have the same spectral efficiency.

In order to characterize propagation aspects as a whole, including the effects of path loss, shadowing, scattering and others, we consider again different link quality combinations, as in Chapter 4, quantifying them in terms of SNR, given, for each link, by the ratio between received and noise powers. We define different SNRs for the second-hop cooperative links $RN_i \rightarrow UT$ for i=1,…,L, referred to as SNR_{ci}, and for the direct link (the alternative link between the BS and the UT of the non-cooperative systems) as SNR_d. For simplicity, as we assume perfect detection in relays, we do not refer to SNR differences in the first cooperative hop.

Three propagation scenarios are accounted for, differing in the link SNRs mentioned above, for the schemes with two relays cooperating, as shown in Table 5.4, similarly to what was done in Sub-section 4.5.1. In scenario 2.1 we assume that all the links have the same quality

conditions, i.e., $SNR_d = SNR_{c1} = SNR_{c2}$. We then define scenario 2.2 where the link between RN_1 and UT has a SNR 10 dB higher than the other two links, i.e., $SNR_{c2} = SNR_d$ and $SNR_{c1} = SNR_d + 10$ dB. In scenario 2.3, $RN_1 \rightarrow$UT and $RN_2 \rightarrow$UT cooperative paths have better transmission quality conditions than the direct path, i.e., $SNR_{c1} = SNR_{c2} = SNR_d + 10$ dB. The value for the increment in SNR links was chosen as 10 dB, though the same results would be obtained if other values for this increment were chosen, as for example 5 dB. These results were obtained and are shown in Annex D, since they can be useful for reference in future works.

For the RA schemes assisted by three RNs, we can have four scenarios, according to Table 5.4. The difference between the two schemes is in the extra cooperative path through the additional RN, which results in the four different scenarios that include all the link combinations: the first scenario is similar to the first one of the previous scheme; scenario 3.2 just considers one link with higher quality of transmission; scenario 3.3 considers two cooperative links with 10 dB more; and, scenario 3.4 is the case where all the cooperative links have a good quality of transmission.

TABLE 5.4: PROPAGATION SCENARIOS CONSIDERED IN MONTE CARLO SIMULATIONS FOR L=2.

	SNR_d	SNR_{c1}	SNR_{c2}
Scenario 2.1	SNR_d	SNR_d	SNR_d
Scenario 2.2	SNR_d	SNR_d +10 dB	SNR_d
Scenario 2.3	SNR_d	SNR_d +10 dB	SNR_d +10 dB

TABLE 5.5: PROPAGATION SCENARIOS CONSIDERED IN MONTE CARLO SIMULATIONS FOR L=3.

	SNR_d	SNR_{c1}	SNR_{c2}	SNR_{c3}
Scenario 3.1	SNR_d	SNR_d	SNR_d	SNR_d
Scenario 3.2	SNR_d	SNR_d +10 dB	SNR_d	SNR_d
Scenario 3.3	SNR_d	SNR_d +10 dB	SNR_d +10 dB	SNR_d
Scenario 3.4	SNR_d	SNR_d +10 dB	SNR_d +10 dB	SNR_d +10 dB

We consider a typical pedestrian scenario based on LTE specifications, following the system configurations in Table 4.3 [3GPP07]. Concerning correlation between channels we consider two options, one with independent channels and another with the correlation used in CODIV group channel scenario specifications, with the correlation matrices given by (4.30) and (4.31) [CBVS08].

In systems where a space-frequency code is needed for two transmitting antennas, the well-known Alamouti coding is implemented [Alam98]. For the three antennas case the implemented distributed QO-SFBC is the one proposed by Li, Park and Kim (LPK) [LiPK08]. In systems with four antennas transmitting simultaneously, we implement the QO-SFBC proposed by Tirkkonen, Boariu and Hottinen (TBH) in a distributed manner [TiBH00].

The schemes considered in our evaluation are presented in the list below. The first two bullets correspond to the proposed schemes and the remaining schemes are used as references:

- RA scheme with the proposed algorithm, using precoded QPSK symbols, for two relays with one and two antennas (PRA 2RN-N_B ×1×1 and PRA 2RN-N_B ×2×1, respectively);
- RA scheme with the precoded algorithm, for three relay nodes, each one equipped with one antenna (PRA 3RN-N_B×1×1);
- Distributed RA (DRA) scheme for two relays with one and two antennas, using an SFBC and 16-QAM modulation (DRA 2RN-N_B×1×1 and DRA 2RN-N_B ×2×1, respectively) [TiBH00];
- Distributed RA scheme, using a QO-SFBC applied to three relays, with 16-QAM modulation (DRA 3RN-N_B×1×1) [LiPK08];
- Non-cooperative 4x1 QPSK with a QO-SFBC with a continuous link available (NRA QO-SFBC 4×1) [TiBH00];
- Non-cooperative 2x1 QPSK Alamouti coding with a continuous link available (NRA 2×1).

The results of the cooperative and non-cooperative schemes are presented in terms of BER as a function of E_b/N_0.

5.6.2 Decoding Method and Precoding Algorithm

Figure 5-15 shows the performance results for the precoded algorithm with the two proposed decoding methods for scenario 2.1: DeF and Viterbi decoding methods. For all the scenarios, Viterbi decoding has a better performance than the DeF one for all the values of the SNR considered. When comparing both methods for the symmetric scenarios (scenarios 2.1 and 2.3), an approximately constant difference of 2 dB is observed. The difference between these methods for scenario 2.2 is slightly higher, approaching the 2.8 dB for BER=10^{-3}.

In Figure 5-16, the performance of the schemes with the proposed method and a Gray precoding method is presented. That alternative precoding mapping we consider is based on a 16-QAM Gray code and is described in Annex E. We observe that the proposed code leads to higher gains than the one with the Gray code. These gains for the BER target of 10^{-3} are approximately

1.5 dB for all the scenarios. This precoding does not bring any advantage, since it has a minimum distance higher than the one proposed.

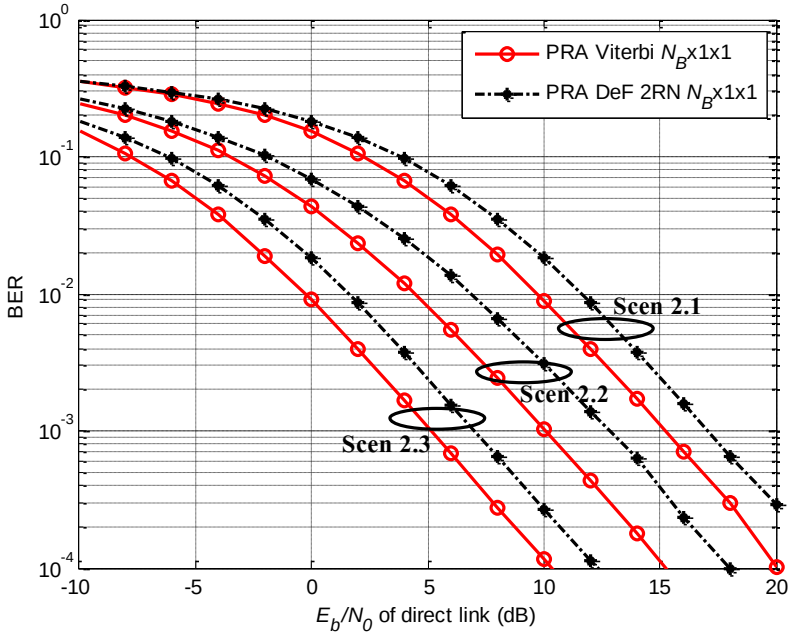

Figure 5-15: BER of PRA 2RN-N_B×1×1 with Viterbi and decision feedback decoded methods.

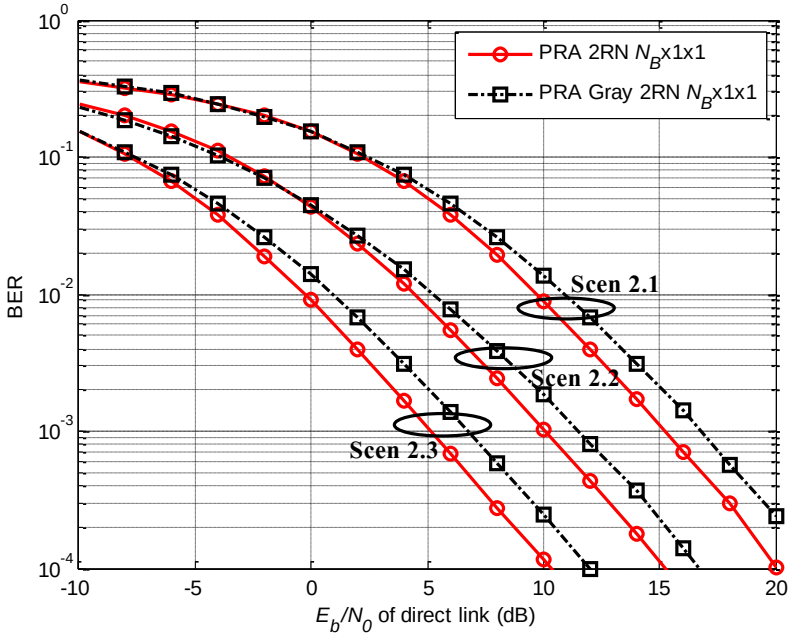

Figure 5-16: BER of PRA 2RN-N_B×1×1 with proposed precoding and Gray precoded algorithms.

5.6.3 Numerical Results for Two-Relay Schemes

5.6.3.1 Schemes with Single Antennas in each Relay

Cooperative and reference system performances are shown in Figure 5-17 for scenario 2.1, for the case of the having two RNs are cooperating, each equipped with a single antenna. In this case, the reference systems presented are the non-cooperative NRA 2×1 and DRA N_B×1×1 ones, both using Alamouti code.

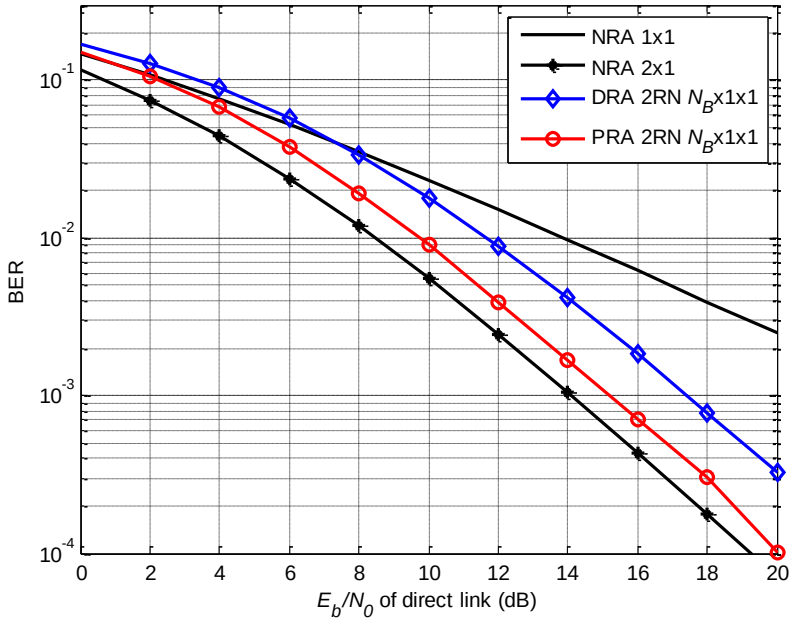

Figure 5-17: BER of cooperative systems with two single-antenna relays and BER of reference systems for scenario 2.1.

When comparing the PRA scheme against DRA, we observe an improvement of 2.2 dB, for BER=10^{-3}. This, in turn, derives from the precoding used in the proposed scheme, which mitigates some of the penalty resulting from the half-duplex constraint at the relays, avoiding the use of a higher modulation order.

The proposed cooperative scheme has a penalty of about 1 dB from the best reference, i.e., 2×1 QPSK Alamouti coding with a continuous link available, for the same BER conditions. It is, however, worthwhile pointing out that in our reference we assume independence between the channels. In practice, the use of co-located antennas inevitably leads to some correlation between the channels, in fact reducing such 1 dB of penalty, or even outperforming it in the case of high correlation. This situation is analyzed next in Figure 5-20.

In Figure 5-18, the performance of the same schemes in scenario 2.2 is shown. Under this scenario conditions, the proposed precoded scheme outperforms the equivalent non-cooperative system. Improvements of 4 dB are obtained in comparison with 2×1 Alamouti, for BER=10^{-3}.

However, the RA Alamouti scheme is still worse than the non-cooperative scheme with two antennas in the BS. The coding gain between the precoded scheme and the RA Alamouti is of 6 dB for the same BER conditions, which is higher than in the previous scenario. On account of this, we extrapolate that, when we have quality asymmetry in cooperative links, we have more benefits in using the precoded Viterbi scheme than the other presented schemes.

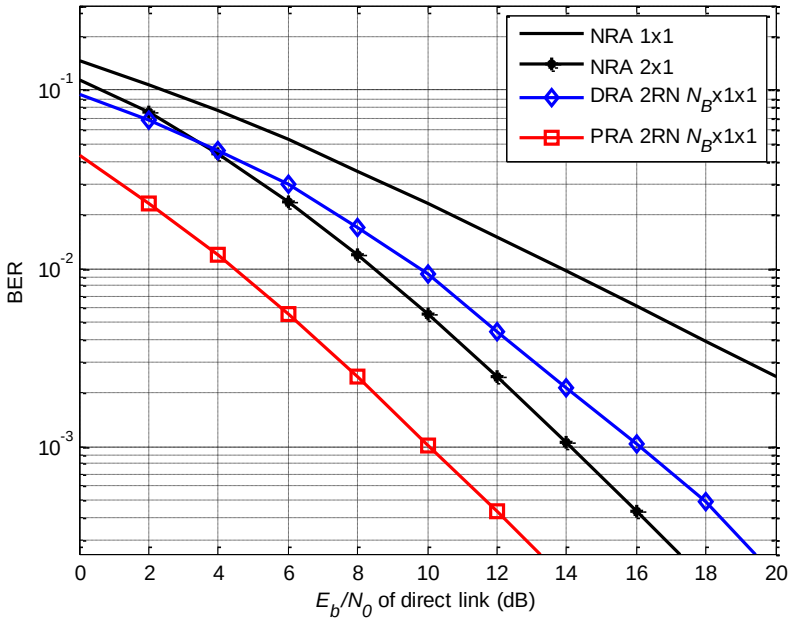

Figure 5-18: BER of cooperative systems with two single-antenna relays and of reference systems for scenario 2.2.

In Figure 5-19, both links between relays and UT have SNRs 10 dB higher than the direct link (Scenario 2.3). In this case, the cooperative schemes have the same behavior concerning results as in the previous scenarios, although the cooperative schemes achieve better performances, as expected. The difference between non-cooperative 2×1 and the PRA schemes is now more than 8 dB, for BER=10^{-3} (for best visualization purposes, the non-cooperative 2x1 curve is not completely shown in the plot). Compared to the DRA using Alamouti, we have an improvement of about 2.2 dB with the proposed code, for BER=10^{-3}, which is the same difference as in Scenario 2.1.

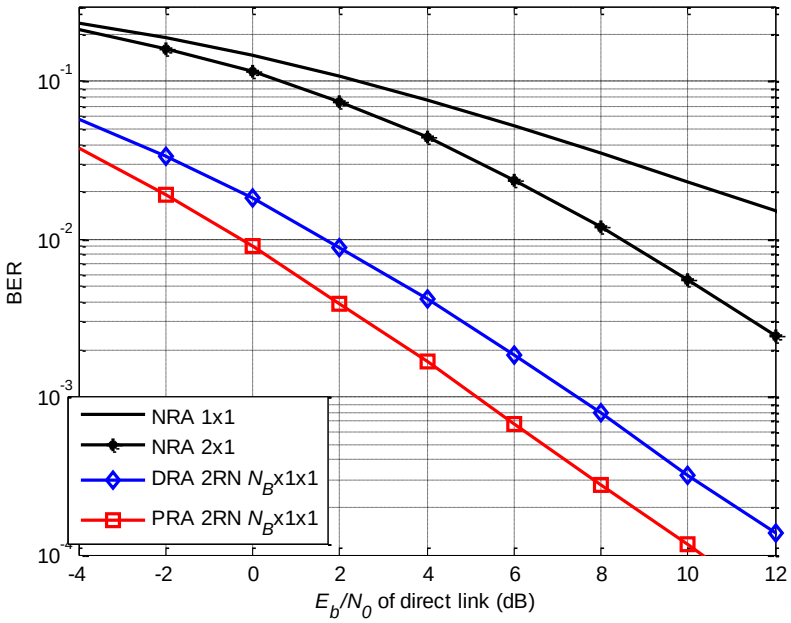

Figure 5-19: BER of cooperative systems with two single-antenna relays and of reference systems for scenario 2.3.

For the case where the antenna channels are correlated, higher gains were obtained for the cooperative schemes with two relays. The results for the three scenarios previously considered are shown in Figures 5-20, 5-21 and 5-22. The relays are again equipped with one and two antennas. We observe that the proposed RA scheme has better performances than the non-cooperative 2×1 system for all the scenarios. This happens because the non-cooperative system uses co-located antennas with correlation, while the precoded scheme achieves diversity through two non-correlated antennas located in each relay. The difference between the non-cooperative 2×1 and the PRA scheme is of about 7.2 dB and 17.4 dB for scenarios 2.1 and 2.3 respectively, considering $N_R = 2$ and BER=10^{-3}.

When comparing the PRA scheme to the DRA one, we observe that higher improvements are also obtained. For example, gains of 9.8 dB and 14.7 dB are obtained for scenarios 2.1 and 2.3 respectively, considering $N_R = 2$ and BER=10^{-3}.

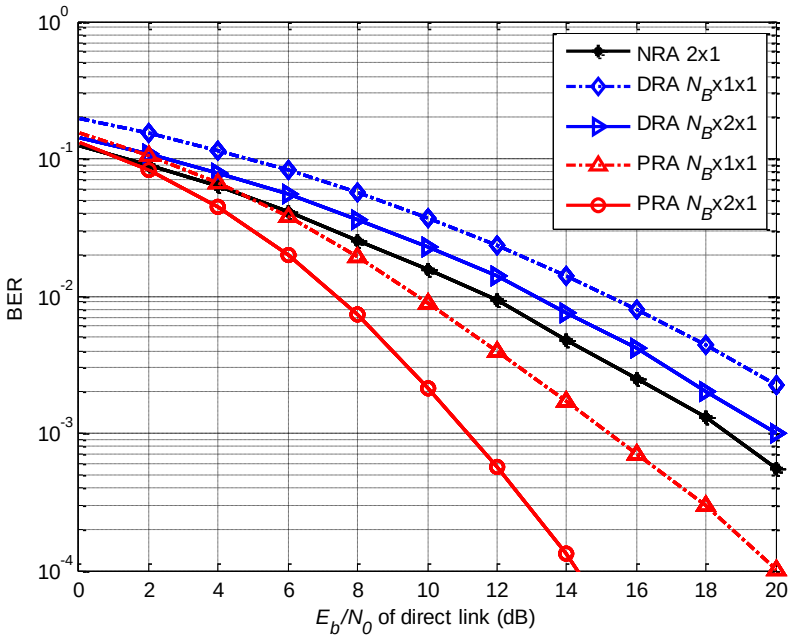

Figure 5-20: BER of cooperative systems with two single-antenna relays and of reference systems for scenario 2.1 with correlation.

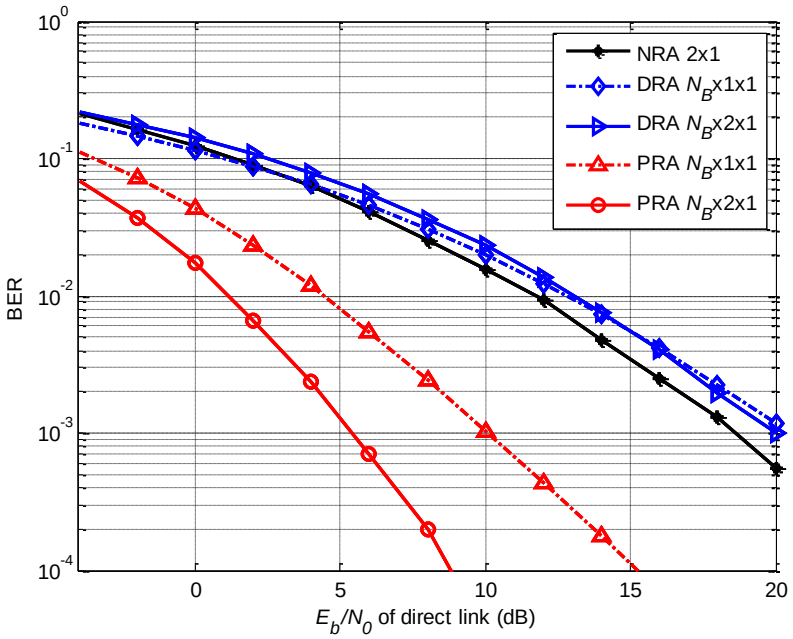

Figure 5-21: BER of cooperative systems with two single-antenna relays and of reference systems for scenario 2.2 with correlation.

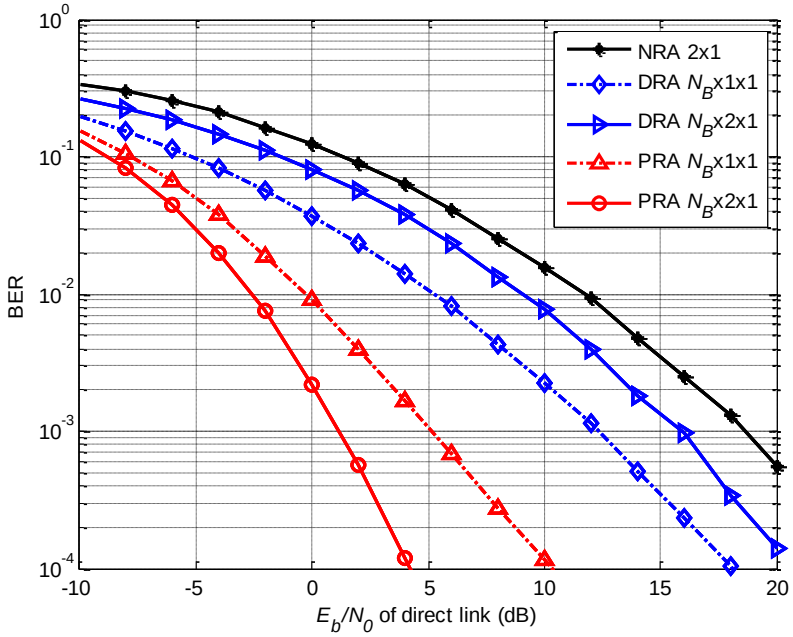

Figure 5-22: BER of cooperative systems with two single-antenna relays and of reference systems for scenario 2.3 with correlation.

In order to observe the improvement obtained with the proposed algorithm in a more realistic situation, where the cooperative first-hops are not considered error-free, a further scenario is considered. It includes correlation between channels and the links between the BS and the RNs have a quality of transmission 10 dB higher than the direct link, since relays are often selected in such way that at least those links have high-quality. The other links have the same relations defined for each of the scenarios 2.1, 2.2 and 2.3. The resulted performances are presented in Figure 5-23. We observe that differences between this case and assuming error-free links until the relays do not have large differences, differing less than 1.5 dB, for BER=10^{-3}, independently of the considered scenario.

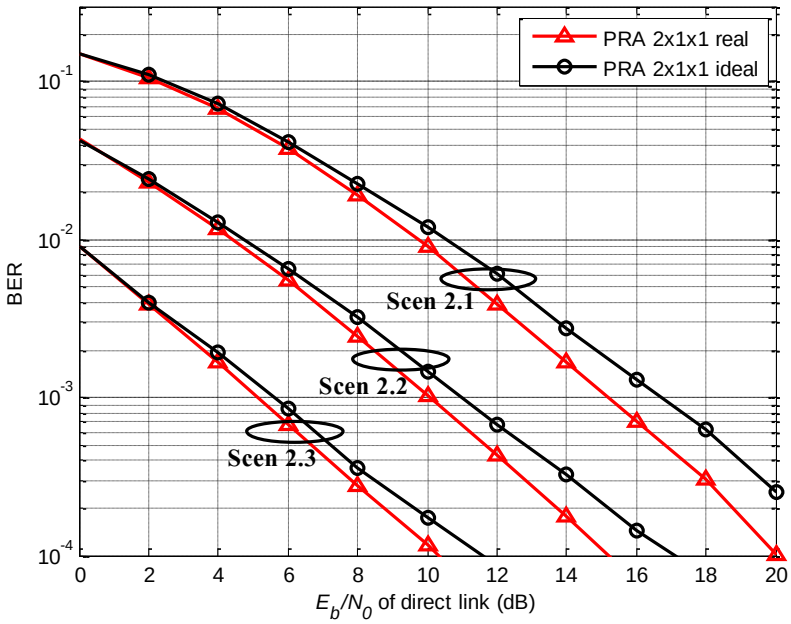

Figure 5-23: BER of cooperative systems with two single-antenna relays and of reference systems for a realistic scenario.

5.6.3.2 Schemes with Two Antennas in each Relay

In this sub-section we assume the two RNs cooperative scheme, with both RNs equipped with two antennas. The considered reference systems are: the non-cooperative 2×1 and 4×1 systems, using Alamouti and TBH codes respectively; and, the RA scheme with the TBH code applied to the RNs.

The results shown in Figure 5-24 were obtained considering that all the links have the same transmission conditions. In this scenario, higher coding gains are obtained with the proposed algorithm than in Figure 5-17, as expected, since we have two antennas in each relay. An enhancement of about 5 dB is achieved with the PRA scheme, compared to the distributed cooperative scheme using TBH code, for BER=10^{-3}. Comparing to the non-cooperative systems, the proposed scheme outperforms the NRA 2×1 system by about 3 dB, for the same BER. The performance of the new algorithm also outperform the non-cooperative system 4×1 for high SNRs, specifically for $E_b/N_0 > 9$ dB. This happens because, contrarily to the Alamouti coding, space-time codes for four antennas are not fully orthogonal, thus not achieving full diversity.

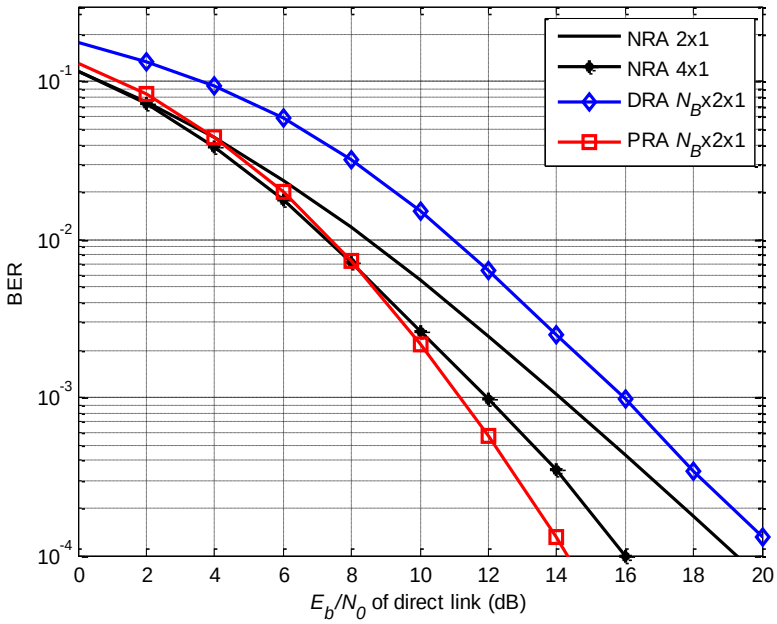

Figure 5-24: BER of cooperative systems with two relays, each equipped with two antennas per relay, and BER of reference systems for scenario 2.1.

For scenario 2.2, as expected, the difference between the RA and non-cooperative systems is higher than in the previous scenario, as can be seen in Figure 5-25. The precoded RA scheme has improvements of 7.2 dB and more than 16 dB in comparison with the non-cooperative 2×1 and 4×1 systems, respectively, for BER=10^{-3}. As in the RA N_B×1×1, the difference between the algorithms used in cooperative schemes is higher than in the first scenario, differing about 8.4 dB, for BER=10^{-3}.

For scenario 2.3, even higher coding gains are obtained with cooperative systems, when compared to the non-cooperative ones, as observed in Figure 5-26. For example, the proposed algorithm, in comparison with the equivalent non-cooperative 4×1 system, has a gain higher than 10 dB. The difference between both RA schemes is similar to the one in scenario 2.1.

Further scenarios are considered, as for example with gains of 5 dB instead of 10 dB in scenarios 2.2 and 2.3, which we refer to as scenarios 2.4 and 2.5. These results are in Annex D.

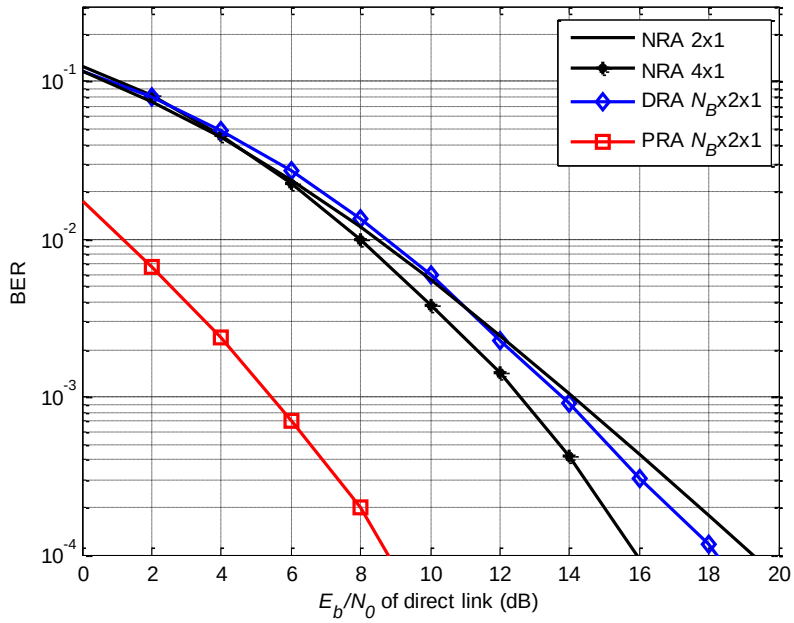

Figure 5-25: BER of cooperative systems with two relays, each equipped with two antennas per relay, and of reference systems for scenario 2.2.

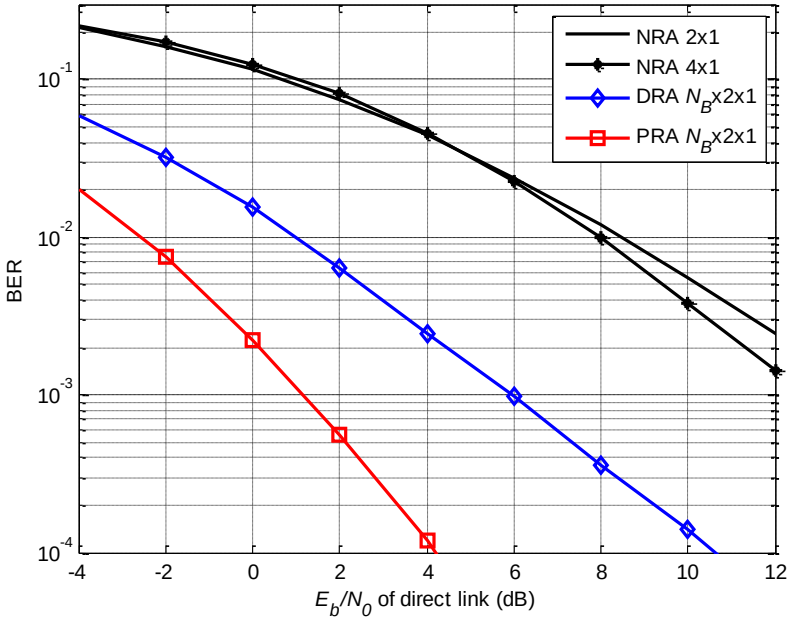

Figure 5-26: BER of cooperative systems with two relays, each equipped with two antennas per relay, and of reference systems for scenario 2.3.

5.6.4 Numerical Results for Three-Relay Schemes

In this section the performance of cooperative schemes with three single-antenna RNs are analyzed. The schemes considered are the PRA schemes with the precoded algorithm, for two and three RNs, the DRA with the distributed QO-SFBC LPK and the non-cooperative systems 2×1 and 3×1, using Alamouti and LPK codes, respectively. Figure 5-27 shows the performance results for the first scenario.

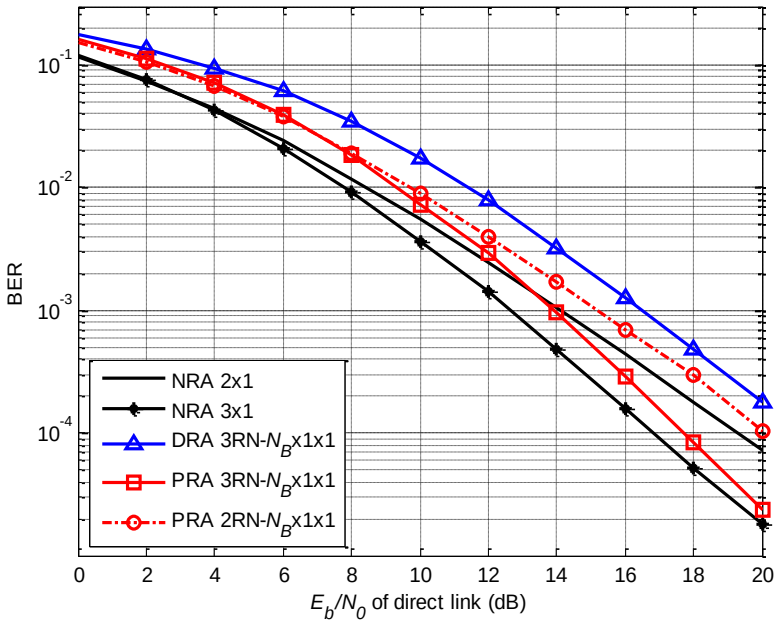

Figure 5-27: BER of cooperative systems with two and three single-antenna relays and BER of reference systems for scenario 3.1.

When comparing the PRA scheme to DRA, we observe an improvement of 2.5 dB for BER=10^{-3}. This gain is due to the precoding used in the proposed scheme, which avoids the use of a higher modulation order. Moreover, the proposed scheme achieves a diversity order of 3, while the SFBC applied to the three relays does not achieve full diversity, since for the three transmitting antennas, the orthogonality is relaxed in order to maintain a unitary rate.

The proposed cooperative scheme has a penalty of about 1.3 dB from the best reference, i.e., NRA 3×1 scheme with a continuous link available, for the same BER=10^{-3}. It is however worthwhile pointing out that we assume independence between the channels. In practice using co-located antennas inevitably leads to some correlation between the channels, in fact reducing such penalty, or even outperforming it in the case of high correlation.

The additional relay brings advantage for moderate-to-high SNR values. The gain increases with SNR, achieving about 2 dB for BER=10^{-4}.

Figure 5-28 and Figure 5-29 represent the scenarios when only one link and two cooperative links have 10 dB more than the other links, respectively, exemplifying a situation where we do not have the same propagation conditions in either relays.

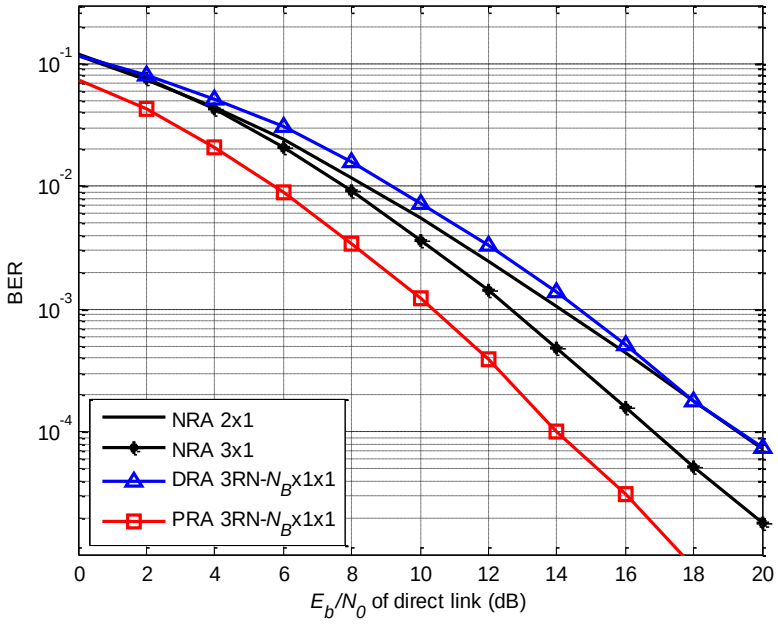

Figure 5-28: BER of cooperative systems with three single-antenna relays and BER of reference for scenario 3.2.

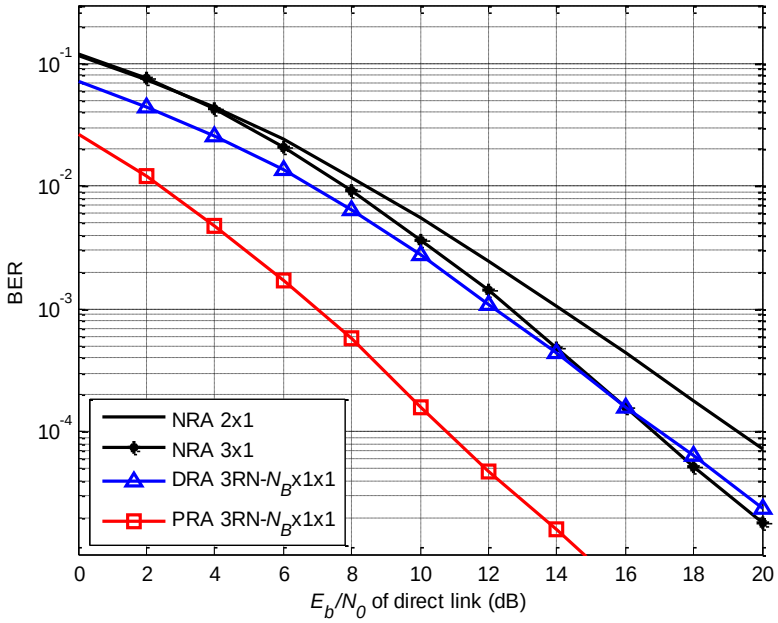

Figure 5-29: BER of cooperative systems with three single-antenna relays and BER of reference for scenario 3.3.

In scenario 3.2, just one of the cooperative links has better quality of transmission than the direct link, which is sufficient condition for the precoded scheme to outperform both non-cooperative systems for the whole SNR range. Improvements of 2.3 dB and 4 dB were obtained in comparison with non-cooperative 3×1 and 2×1 systems, respectively, for BER=10^{-3}. However DRA scheme is still worse than the non-cooperative reference systems.

In this case, the difference between PRA scheme and the equivalent cooperative scheme is higher than in the previous scenario. For example, the gain in using it instead of DRA is of 4.3 dB, while in the first scenario it was of 2.5 dB, for the same BER condition.

For scenario 3.3 the DRA scheme outperforms the 3×1 non-cooperative one just for $E_b/N_0 > 14$ dB, while the PRA scheme incurs in a gain of approximately 6 dB. The difference between both RA schemes is even higher, resulting in 5.2 dB. From this, we can extrapolate that when we have quality asymmetry in cooperative links, we have more benefits in using the data-precoded algorithm than the distributed ones.

In Figure 5-30 performances of the presented schemes are shown when the SNR of all the links between relays and UT have 10 dB more than the direct link. In this scenario the cooperative schemes have the same behavior as in the previous scenarios, although cooperative schemes achieve better performances, as expected. The difference between non-cooperative 2×1 and 3×1 schemes and PRA scheme is now of about 10.1 dB and 8.6 dB, respectively, for BER=10^{-3}.

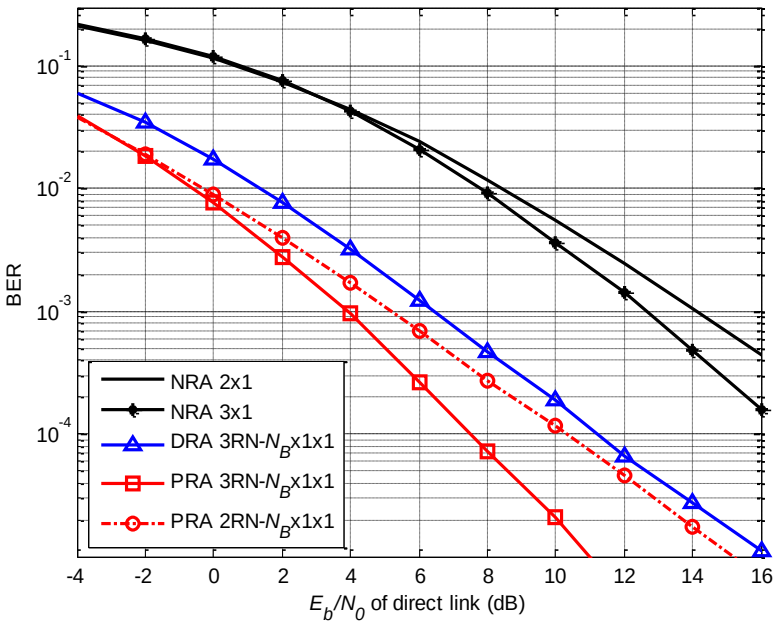

Figure 5-30: BER of cooperative systems with two and three single-antenna relays and BER of reference for scenario 3.4.

Comparing with the DRA, we have the same gain in using the proposed algorithm as in the first scenario. We thus infer that improvements are fixed for the cases where all the cooperative links have the same quality of transmission.

We can also observe that having two and three RNs, in both cases with single-antenna relays, result in different performances, as it is evident in this scenario. The difference between them can be of 5.4 dB for BER=10^{-4}.

5.7 Conclusions

We proposed a data-precoded algorithm for RA schemes, which ensures spatial diversity for cooperative systems with more than two relays, while maximizing spectral efficiency. The algorithm mitigates some of the penalty resulting from the half-duplex constraint at the relays and asymptotically achieves the same performance as the one obtained when a direct continuous link is available.

We observed that the gain obtained with the precoded algorithm relatively to the distributed one increases with the number of RNs in a non-linear way. Concerning the two decoding methods considered at the UT, we observed that Viterbi decoding outperforms the DeF, for all the studied scenarios, with higher difference in scenarios with differing quality between cooperative links. We also concluded that the code used in precoding at the BS is better than the code using a Gray 16-QAM mapping scheme, since the first has a lower minimum distance between precoded symbols. The difference between these schemes is independent of the scenario considered.

The implemented precoding brings the performance very close to the one achieved when a direct continuous link is available and SFBC coding is used at the BS. Actually, for the case of two antennas in each relay, the precoded scheme outperforms the non-cooperative one for the high SNR regime, due to the non-orthogonality of space-frequency codes for four transmitting antennas. Improvements are obtained for scenarios where cooperative links have higher quality than the direct link, being more pronounced as the quality of the cooperative links increases.

When considering correlation between antenna arrays, we obtained better performances for the precoded algorithm than for the continuous direct link transmission, even when having the same quality of transmission for all links. This is justified by the lower correlation between relay channels than between channels of the BS antennas.

Moreover, we concluded that, independently of the propagation scenario, the precoded schemes outperform the equivalent distributed SFBC cooperative schemes, achieving better performance due to the coding gain obtained with precoding. Even for the most probable situation of asymmetric quality conditions between cooperative links, results show that the proposed scheme

is better than the reference cooperative ones. In these cases, the difference between the two cooperative schemes is higher.

We also observed that the extra antenna in each relay leads to a considerable improvement in the overall system performance, which is at least of 4 dB for BER=10^{-3}, for the case of independent channels. Furthermore, the performance difference between the precoded schemes and the respective equivalent DRA schemes is higher for the case of having two antennas in each relay.

The performance of the PRA scheme was also obtained for three RNs, confirming the previous conclusions for two relays. The performance of this scheme, as expected, outperforms that of the scheme with two relays, both with single antennas equipping the relays, especially for scenarios with high-quality links. Furthermore, with the precoded algorithm, there is no need to transmit through the direct link, which is beneficial for most scenarios, since the direct link is usually most strongly affected by path loss or shadowing.

6 Conclusions and Future Work

6.1 Final Conclusions

The point-to-point or point-to-multipoint paradigms of classical cellular networks will be replaced or enhanced by cooperative systems in the future 4G systems. The future wireless networks will involve relay nodes that cooperate with one another in order to improve the performance of their own communication and that of the global network, due to the need of optimizing the usage of resources. Relay-assisted communications have emerged as a promising approach to increase spectral and power efficiency, network coverage, and reduce outage probability. Similarly to multi-antenna transceivers, relays provide diversity by creating multiple replicas of the signal of interest.

The main objective of this thesis was to contribute to the threefold objective of advancing the understanding of cooperative transmission, developing new algorithms for cooperative communications and evaluating these systems for realistic scenarios. This research work has contributed with original high-performance algorithms for RA schemes and included the multicarrier signal processing technique OFDM. The investigated algorithms included systems with different configurations, considering multiple relays and multiple antenna configurations, and were emulated so that they can be used in different real life situations.

In order to grasp the overall contribution of this study, it is important to bear in mind the major contributions of each chapter as well the most relevant conclusions resulting from the overall work.

Regarding Chapter 2, "Fundamentals of Cooperative Communications", we presented the channel models commonly used in wireless communications and their main characteristics. The basis about cooperative systems was put forward, starting by the definition of cooperative diversity. This included the introduction of the fundamental elements of cooperative systems, as well as of the main state-of-the-art techniques and algorithms, setting forth the main points of relay-assisted schemes related to this thesis. The detection modes of a point-to-point communication were revised, asserting the main signal expression, besides some summarized description of the detection modes for the RA schemes.

In Chapter 3, "Theoretical Capacity of Relay-Assisted Schemes", some distributed algorithms were introduced and studied for different numbers of RNs, with focus on one and two relays. This included the case where there is no direct path available between the terminal nodes. The equations of such systems were derived, considering relays of the type amplify-and-forward and equalize-and-forward. The integrals of instantaneous capacity expressions of those algorithms were found to be too complex and of high order. This problem was circumvented by emulating such algorithms in RA schemes and measuring outage and average capacities, which led to some conclusions about distributed algorithms for RA schemes. Fast-fading and path loss effects were taken into account for channel characterizations and the schemes were studied for different propagation scenarios. Some of the main conclusions extracted from this chapter were:

- The studied RA schemes, when compared to the non-cooperative ones with co-located antennas, despite the disadvantages of having a lower spectral efficiency and additional noise introduced by the relays, usually benefit in terms of path loss effect, since RNs are between the source and the destination.
- The cooperative schemes presented may achieve better capacity results than multi-antenna systems depending on the relative position of relays and on the density of terminals.
- Performance measurements were realized for different propagation scenarios. For scenarios where a low path loss exponent characterizes the propagation channel, the use of co-located antennas may have a slight advantage when compared to the RA scheme. However, for moderate to high-loss propagation scenarios, the RA scheme presents significant capacity gains considering reasonable values of SNR, thus overcoming its lower spectral efficiency caused by its half-duplex constraint.
- EF and AF relay protocols were compared in terms of outage capacity, when applied to the RA schemes. Their performances were close to each other, just differing for low

values of SNR, where the EF relay protocol is slightly better. This is mainly due to the way relay equalization affects noise power.

- The results for capacities also show that in the cases where it is possible to use the DP, such system performances increase. It is possible to use the DP whenever the quality of that path is not lower than that of the cooperative links. This improves diversity order and the virtual antenna gain of the system.
- RA schemes can have different performances, depending on the algorithms implemented and on the relay protocol, since the combination of coding and transmitted power constraints changes the values of virtual antenna gain. For example, the simplest scheme with a single relay outperforms the more resource-consuming RA scheme with two relays but without the DP.

As most of the relaying schemes considered in the literature are not targeting OFDM based systems and have been assessed under unrealistic scenarios, another contributions of this thesis was, in Chapter 4, "Distributed SFBC RA for OFDM Scheme", the proposal of two algorithms to be applied in OFDM based RA schemes. The schemes were assisted by one RN and designed for downlink, making use of SFBCs. Both schemes have a UT with a single antenna and a BS with a two-antenna array. Four half-duplex relay protocols were analyzed: amplify-and-forward, equalize–and-forward, decode-and-forward and selective decode-and-forward. BER and FER performance metrics were obtained through Monte Carlo simulations and analyzed and compared with the reference non-cooperative systems. The performance of these schemes was evaluated under realistic scenarios, according to LTE specifications and including channel turbo coding. The main conclusions concerning this chapter were:

- Further conclusions were obtained in relation to relay protocols. The schemes with SDF and DF relay protocols have similar behaviors when the first cooperative link has a good quality, since most of the data is successfully decoded. If high reliability in the source to relay links is not guaranteed the performance of the DF protocol is even worse than the EF and AF ones. Thus, the SDF protocol should be used in detriment of the DF one, since it has better results for all scenarios and almost the same complexity as the DF. The AF or EF relay protocols are a good choice for situations when it is not possible to implement processing operations such as decoding or correction of the received signals at relays.
- The cooperative schemes with the proposed algorithm outperform the reference non-cooperative ones, both SISO 1×1 and MISO 2×1, for all the scenarios considered, even for those where the cooperative links have the same quality as the direct link.

This shows the advantages of these schemes for practical scenarios, which are consistent with the conclusions of Chapter 3. For the case in which each relay has two antennas, the RA scheme is never outperformed by the co-located MIMO 2×2 system either.

- When the link BS→RN has the same quality as the second-hop cooperative link, the two-antenna cooperative scheme always achieves a better performance than the single-antenna scheme. Thus, despite the additional complexity and equipment in the relay with two antennas, the usage of an additional antenna provides advantages for these scenarios.
- The RA schemes are severely limited by the relative quality of the cooperative links, specially the BS→RN link. Thus, the success of the cooperative schemes lies upon the choice of the relay in the network. Ideally, it should be chosen so that the BS→RN link is highly reliable.
- The cooperative schemes should use the direct link for transmission in situations when their transmission quality is at least equal to the quality of the worst cooperative link. Otherwise, communication through the direct link should be neglected.

A novel algorithm was presented in Chapter 5, "Data-Precoded Algorithm for Relay-Assisted Schemes". It ensures spatial diversity for cooperative systems with two relays, and mitigates some of the penalty resulting from the half-duplex constraint at the relays. This algorithm arose mainly to address some of the shortcomings of the conventional cooperative schemes, such as the degradation caused by the outage of one relay or poor direct link condition. We derived the theoretical expressions for the gain obtained with the precoded algorithm relatively to the distributed one, as well as the expressions for the bit error probability for a generic scheme with a multiple number of relays and antennas in each relay. Numerical results for OFDM RA schemes using the precoded algorithm were computed for two and three RNs in scenarios with different link quality conditions. Practical parameters were used, based on LTE specification. Performances were obtained for the cases of each RN being equipped with either one or two antennas. At the user terminal, we considered two decoding methods: Viterbi and DeF methods. The main conclusions obtained were:

- The data-precoded algorithm is beneficial for most scenarios, since the direct link is usually most strongly affected by path loss or shadowing and this algorithm was specifically constructed for the scenarios where direct link quality has high vulnerability.

- Another advantage of this algorithm is that it adds high reliability and full diversity to the implemented cooperative scheme maintaining the same bandwidth efficiency as the non-cooperative systems.
- Viterbi decoding outperforms the DeF, for all the studied scenarios, with higher differences in the scenarios where the cooperative links have different transmission quality.
- The code used in data-precoding at the BS outperforms the scheme with Gray 16-QAM code. The difference between these schemes is independent of the scenario considered.
- The precoding implemented in the data-precoded scheme brings the performance very close to the one achieved when a direct continuous link is available and SFBC is used at the BS. In fact, if there are two antennas in each relay, the data-precoded scheme will outperform the non-cooperative one in high SNR regime, due to the non-orthogonality of space-frequency codes for four transmitting antennas, for the case where all the links have the same quality. Moreover, the direct continuous link performance is always outperformed by the precoded scheme when correlation between aggregated antennas is taken into consideration. These improvements increase for scenarios in which cooperative links have higher quality than the direct link.
- Independently of the propagation scenario, schemes with two RNs using the data-precoded algorithm outperform the equivalent distributed SFBC cooperative schemes, achieving better performances due to the coding gain obtained with precoding. Even for the most probable situation of asymmetric quality conditions between cooperative links, the results showed that the scheme with the proposed algorithm is better than the reference cooperative ones.
- An additional antenna in each relay, included in the two-antenna RA scheme, leads to a considerable improvement in the overall system performance, leading to a higher difference between the precoded RA schemes. Moreover, the performance of these schemes increases with the number of relay nodes.

To summarize, we can draw the following overall conclusions:

- The proposed cooperative schemes can be used to extend the coverage mainly in scenarios where the quality of the direct link is poor, as it is the case of cluttered urban

environments, thus achieving full diversity, with moderate or no degradation relatively to the case where a continuous link is available.

- The good performances obtained with the proposed algorithms anticipate the relay capabilities, and suggest that they are very good solutions to be integrated in future 4G wireless communications, since they can provide improved flexibility, reliability and efficiency to the system.
- RA schemes are beneficial mainly in dense urban mobile communication scenarios, since they reduce the path loss attenuation in comparison with the co-located systems. They achieve spatial diversity, with the advantage of ensuring low power requirements in almost all the cases and requiring less equipment relatively to the conventional scheme with co-located antennas. They can be useful in a large number of applications such as cellular and sensor networks.

6.2 Future Research

In this study of cooperative communications some open problems can be identified as interesting matters and subjects for future research.

Although our research work has shown that the code we use in the data-precoding at the BS achieves good performances for RA schemes, an exhaustive study can be done to verify if there is any code which results in even better performances. The best code should ensure the minimum distance in destination detection in comparison with the same scheme using other codes.

In the case of the proposed precoding algorithm, some interference can also occur in the RNs or in the destination, since the relays transmit alternately to the destination, and the BS also transmits simultaneously for a specific RN. The effect of this interference is worthwhile being investigated, despite having been included in this thesis in a general way, since we considered different channel scaling factors for each link, when on defining the proposed scenarios. In addition, a solution to cancel this interference can be investigated.

The evaluation of the algorithms proposed for cooperative systems has been based so far on some ideal assumptions, such as synchronization constraints between the relay nodes or the availability of perfect CSI at the resource allocation unit. It is important to study these two aspects so that solutions can be found to minimize the impact these issues have in practical scenarios, with the proposed schemes. Both intra- and inter-cell interferences of other nodes in the proposed cooperative scheme are interesting issues for future work.

The combination of relay selection with space-time signaling schemes, has been noted by several researchers, but much work remains to be done in this area, thus being a worthy subject for

future research. It seems relevant to combine the proposed algorithms with the two relay selection algorithms in [YuKY06] and [AmAT10]. The algorithm where the relay selection is done at the destination, in [YuKY06], is based on the maximum receiver SNR, and the second-hop of cooperative paths has a good quality of transmission. In the other algorithm all the cooperative paths through each relay have high-quality conditions.

Moreover, scheduling algorithms that take into account QoS requirements of different users (e.g., BER, delay or data rate) and their current state (e.g., the current battery level) can be studied to be applied in the proposed RA schemes. This would be helpful for the particular problem of relay selection, so that at least the first cooperative path has high link quality.

It is also of interest to integrate the data-precoded algorithm in an incremental relay transmission scheme. In this scheme, relays help to forward the data only under the condition that incorrect decoding occurs at the destination after the source transmission. For these situations, hybrid automatic repeat request (H-ARQ) protocols are used in the multi-hop communication [ZhVa05]. The combination of these three strategies, together with an optimal relay selection, can bring even more advantages, by achieving an order of diversity that equals the aggregated number of source and relays, without penalty in spectral efficiency.

Finally, real-life wireless communication systems are composed of several interfering cells with complex handover and radio resource management algorithms, serving UTs that travel at different speeds or that might suddenly change from one propagation environment to another. These factors somehow affect the performance of the proposed algorithms. It is of interest to evaluate the impact of relays using the proposed algorithms at the system level, such as the user throughput or efficiency and fairness of an algorithm, thus calling for a method to test implementation conditions in a context as real as possible.

References

[3GPP] Third Generation Partnership Project, http://www.3gpp.org.

[3GPP07] 3GPP TS 36.201 V8.1.0, *3rd Generation Partnership Project*, Technical Specification Group Radio Access Network; Evolved Universal Terrestrial Radio Access (E-UTRA); LTE Physical Layer - General Description, Nov. 2007.

[3GPP99] 3GPP TR 25.924 V1.0.0, *3rd Generation Partnership Project*, Technical Specification Group Radio Access Network, Opportunity Driven, Apr. 1999.

[802.16] IEEE 802.16's 802.16, Task Group m (TGm), http://ieee802.org/16/tgm.

[AdYa06] A. Adinoyi and H. Yanikomeroglu, "On the performance of cooperative wireless fixed relays in asymmetric channels," in *Proc. of the IEEE Globecom '06*, San Francisco, CA, pp. 1-5, Dec. 2006.

[Alam98] S. M. Alamouti, "A simple transmit diversity technique for wireless communications," *IEEE Journal on Selected Areas in Communications*, vol. 16, no. 8, pp. 1451-1458, Oct. 1998.

[AlPB10] G. C. Alexandropoulos, A. Papadogiannis, and K. Berberidis, "Performance analysis of cooperative networks with relay selection over Nakagami-m fading channels," *IEEE Signal Processing Letters*, vol. 17, no. 5, pp. 441-444, May 2010.

[AmAT10] G. Amarasuriya, M. Ardakani and C. Tellambura, "Output-threshold multiple-relay-selection scheme for cooperative wireless networks," *IEEE Transactions of Vehicular Technology*, vol. 59, no.6, pp. 3091-3097, July 2010.

[AzGS05] K. Azarian, H. Gamal, and P. Schniter, "On the achievable diversity-multiplexing tradeoff in half duplex cooperative channels," *IEEE Transaction of Information Theory*, vol. 51, no. 12, pp. 4152-4172, Dec. 2005.

[Bala97] C. Balanis, *Antenna Theory*, John Wiley & Sons, Inc., 1997.

[BaRW04] B. Badic, M. Rupp, and H. Weinrichter, "Extended Alamouti codes in correlated channels using partial feedback," in *Proc. of the IEEE International Conference on Communications (ICC'04)*, Paris, France, vol. 2, pp. 896–900, June 2004.

[BGQS01] A. Bria, F. Gessler, O. Queseth, R. Stridh, M. Unbehaun, J. Wu and J. Zander, "4th-generation wireless infrastructure: scenarios and research challenges," *IEEE Personal Communications*, vol. 8, no. 6, pp. 25-31, Dec. 2001.

[BKRL06] A. Bletsas, A. Khisti, D. Reed, and A. Lippman, "A simple cooperative diversity method based on network path selection," *IEEE Journal on Selected Areas in Communications*, vol. 24, no. 3, pp. 659–672, Mar. 2006.

[BlKW06] A. Bletsas, A. Khisti, and M. Z. Win, "Low complexity virtual antenna arrays using cooperative relay selection," in *Proc. of the International Conference on Wireless Communications and Mobile Computing (ICWMC'06)*, British Columbia, Canada, pp. 461-466, July 2006.

[BPST10] V. Bota, A. Polgar, A. Silva, S. Teodoro, M. P. Stef, A. Moço, A. Botos, and A. Gameiro, "Combined distributed turbo coding and space frequency block coding techniques," *EURASIP Journal on Wireless Communications and Networking*, vol. 2010, Article ID 327041, 14 pages, 2010.

[CBVS08] D. Castelain, V. Bota, M. Varga, and M.P. Stef, "Structure and Calibration of the Simulation Chain," *Internal Note of Codiv Project*, Sep. 2008.

[CEUC97] Committee on Evolution of Untethered Communications, National Research Council, *The evolution of untethered communications*, Washington D.C., USA, National Academy Press, 1997.

[Chts01] B. Chatschik, "An overview of the Bluetooth wireless technology," *IEEE Communication Magazine*, vol. 39, no. 12, pp. 86-94, Dec. 2001.

[ChVa09] B. K. Chalise and L. Vandendorpe, "MIMO relay design for multipoint-to-multipoint communications with imperfect channel state information," *IEEE Transactions on Signal Processing*, vol. 57, no. 7, pp. 2785-2796, July 2009.

[ChYX05] W. Chen, Y. Yuan, C. Xu, K. Liu, and K. Yang, "Virtual MIMO protocol based on clustering for wireless sensor network," in *Proc. of the 10th IEEE Symposium on Computers and Communications (ISCC'05),* La Manga, Spain, pp. 335-340, June 2005.

[Cimi85] L. J. Cimini, "Analysis and simulation of a digital mobile channel using orthogonal frequency division multiplexing," *IEEE Transactions on Communications*, vol. COM-33, no. 7, pp. 665-675, July 1985.

[CoGa79] T. M. Cover and A. A. E. Gamal, "Capacity theorems for the relay channel," *IEEE Transactions on Information Theory*, vol. 25, no. 5, pp. 572-584, Sep.1979.

[DaGC07] D. Lai, B. Gui, and L. Cimini, "Selective relaying in OFDM multi-hop cooperative networks," in *Proc. of IEEE the Wireless Communications and Networking Conference (WCNC '07)*, Hong Kong, pp. 963-968, Mar. 2007.

[DoAg05] M. Dohler and H. Aghvami, "On the approximation of MIMO capacity," *IEEE Transactions on Wireless Communications*, vol. 4, no. 1, pp. 30-34, Jan. 2005.

[Dohl03] M. Dohler, *Virtual Antenna Arrays*, Ph. D. Thesis, King's College London, University of London, London, UK, Nov. 2003.

[DoLA02] M. Dohler, E. Lefranc, and H Aghvami, "Space-time block codes for virtual antenna arrays," in *Proc. of the 13th IEEE International Symposium on Personal, Indoor and Mobile Radio Communications (PIMRC'02)*, Lisbon, Portugal, pp. 414-417, Sep. 2002.

[DSGA01] M. Dohler, A. Gkelias, A. Ghorashi, and H. Aghvami, *Improvements in or relating to electronic data communication systems*, Patent Public no. WO 03/003672, June 2001.

[DuYP10] D. Duan, L. Yang, and J. C. Principe, "Cooperative diversity of spectrum sensing for cognitive radio systems," *IEEE Transactions on Signal Processing*, vol. 58, no. 6, pp. 3218-3227, June 2010.

[ETSI09a] ETSI Technical Specification TS 136 201 v8.3.0, *LTE; Evolved universal terrestrial radio access (E-UTRA); Long Term Evolution (LTE) physical layer; General description*, Apr. 2009.

[ETSI09b] ETSI Technical Report 136 913 V8.0.1, *LTE; Requirements for further advancements for Evolved Universal Terrestrial Radio Access (E-UTRA) (LTE Advanced)*, Apr. 2009.

[ETSI99] ETSI HIPERLAN/2 TS 101 475, *Broadband Radio Access Networks HIPERLAN Type 2, Functional Specification-Part 1: Physical Layer*, Sep. 1999.

[FFFK06] F. H. P. Frattasi, H. Fathi, F. H. P. Fitzek, M. Katz, and R. Prasad, "Defining 4G technology from the user perspective," *IEEE Network Magazine*, vol. 20, no. 1, pp. 35-41, Fev. 2006.

[FiKa06] F. H. P. Fitzek and M. D. Katz, *Cooperation in Wireless Networks: Principles and Applications*, Springer, Dordrechi, The Netherlands, 2006.

[FoGa98] G. J. Foschini and M. J. Gans, "On limits of wireless communications in a fading environment when using multiple antennas," *Wireless Personal Communications Magazine*, vol. 6, no. 3, pp. 311-335, Mar. 1998.

[Fosc96] G. J. Foschini, "Layered space-time architecture for wireless communication in a fading environment when using multiple antennas," *Bell Labs Technical Journal*, vol. 1, no. 2, pp. 41-59, Autumn 1996.

[GaSa00] A. Ganesan and A. M. Sayeed, "A virtual MIMO framework for multipath fading channels," in *Proc. of the 34th Asilomar Conference on Signals, Systems and Computers*, Pacific Grove, Calif, USA, vol. 2, pp. 537-541, Nov. 2000.

[Glav07] A. Glavieux, *Channel coding in communication networks- From theory to Turbo codes*, Digital Signal and Image Processing Series, ISCTE, London, UK, 2007.

[Gold05] A. Goldsmith, *Wireless communications*, Cambridge University Press, New York, NY, USA, 2005.

[GRJZ00] I. S. Gradshteyn, I. M. Ryzhik, A. Jeffrey, and D. Zwillinger, *Table of integrals, series, and products*, Sixth edition, Academic Press, London, UK, July 2000.

[GrTs02] M. Grossglauser and D. Tse, "Mobility increases the capacity of ad hoc wireless networks," *IEEE/ACM Transactions on Networking*, vol. 10, no. 4, pp. 477-486, Aug. 2002.

[GSMA] GSM Association, "GSM World Subscriber Statistics," <http:/www.gsmworld.com/news/statistics/substats.shtml>.

[GuKu00] P. Gupta and P. R. Kumar, "The capacity of wireless networks," *IEEE Transactions on Wireless Communications*, vol. 46, no. 2, pp. 388-404, Mar. 2000.

[GuKu03] P. Gupta and P. R. Kumar, "Towards an information theory of large networks: an achievable rate region," *IEEE Transactions on Wireless Communications*, vol. 49, no. 8, pp. 1877-1894, Aug. 2003.

[HaAl04] M. O. Hasna and M. S. Alouini, "A performance study of dual-hop transmissions with fixed gain relays," *IEEE Transactions on Wireless Communications*, vol. 3, no. 6, pp. 1963-1968, Nov. 2004.

[Haen04] M. Haenggi, "Routing in ad-hoc – a wireless perspective," in *Proc. of the 1st IEEE International Conference on Broadband Networks (BroadNets'04)*, San Jose, California, CA, USA, vol. 1, pp. 652-660, Oct. 2004.

[HaNi00] T. J. Harrold and A. R. Nix, "Capacity enhancement using intelligent relaying for future personal communication system," in *Proc. of the 52nd IEEE Vehicular Technology Conference (VTC'00 Fall)*, Boston, MA, USA, vol. 5, pp. 2115-2120, Sep. 2000.

[HaRa09] J. Harshan and B. S. Rajan, "High-rate, single-symbol ML decodable precoded DSTBCs for cooperative networks," *IEEE Transactions on Information Theory*, vol. 55, no. 05, pp. 2004-2015, May. 2009.

[HiSL05] T. Himsoon, W. Su, and K. Liu, "Differential transmission for amplify-and-forward cooperative communications," *IEEE Signal Processing Letters*, vol. 12, no. 9, pp. 597–600, Sep. 2005.

[HMRS00] B. M. Hochwald, T. L. Marzetta, T. J. Richardson, W. Sweldens, and R. Urbanke, "System design of unitary space-time constellations," *IEEE Transactions on Information Theory*, vol. 46, no. 6, pp. 1962-1973, Sep. 2000.

[HoMa00] B. M. Hochwald and T. L. Marzetta, "Unitary space-time modulation for multiple-antenna communications in Rayleigh flat fading," *IEEE Transactions on Information Theory*, vol. 46. no. 2, pp. 543-564, Mar. 2000.

[HoSW00] W. Hochwald and W. Sweldens, "Differential unitary space-time modulation," *IEEE Transactions on Communications*, vol. 48, no.12, pp. 2041-2052, Dec. 2000.

[HuSN06] T. E. Hunter, S. Sanayei, and A. Nosratinia, "Outage analysis of coded cooperation," *IEEE Transactions on Information Theory*, vol. 52, no. 2, pp. 375-391, Feb. 2006.

[IkAh08] S. Ikki and M. H. Ahmed, "Performance of selection combining in cooperative relaying networks over Rayleigh fading channel," in *Proc. of the Canadian Conference on Electrical and Computer Engineering*, Niagara Falls, NO, pp. 831-836, May 2008.

[ITUR03] ITU-R Recommendation M.1645, *Framework and overall objectives of future development for IMT-2000 and systems beyond IMT-2000*, http://www.itu.int/ITU-R/publications/index.html, 2003.

[Jafa01] H. Jafarkhani, "A quasi-orthogonal space-time block code," *IEEE Transactions on Information Theory*, vol. 49, no. 1, pp. 1-4, Jan. 2001.

[Jake74] W. C. Jakes, *Microwave Mobile Communications*, IEEE Press, New York, NY, USA, 1974.

[JBDS01] G. James, D. Burley, P. Dyke, J. Searl, D. Clements, and J. Wright, *Modern engineering mathematics*, Third Edition, Prentice Hall, Harlow, England, 2001.

[JiHa06] Y. Jing and B. Hassibi, "Distributed space time coding in wireless relay networks," *IEEE Transactions on Wireless Communications*, vol. 5, no. 12, pp. 3524-3536, Dec. 2006.

[Kahn77] R. E. Kahn, "The organization of computer resources into a packet radio network," *IEEE Transactions on Communications*, vol. 25, no. 1, pp.169-178, Jan. 1977.

[KaKu03] V. Kawadia and P. R. Kumar, "Power control and clustering in ad hoc networks," in *Proc. of the 2nd IEEE Computer and Communications Societies (INFOCOM'03)*, San Francisco, California, CA, USA, vol. 1, pp. 459-469, Apr. 2003.

[KlSS96] A. Klein, B. Steiner, and A. Steil, "Known and novel diversity approaches as a powerful means to enhance the performance of cellular mobile radio systems," *IEEE*

Journal on Selected Areas in Communications, vol. 14, no. 9, pp.1784-1795, Dec. 1996.

[KrGB07] G. M. Kraidy, N. Gresset, and J. J. Boutros, "Coding for the non-orthogonal amplify-and-forward cooperative channel," in *Proc. of the IEEE Information Theory Workshop (ITW'07)*, Lake Tahoe, California, pp. 626-631, Sep. 2007.

[KuBr04] A. H. Kupetz and K. T. Brown, "4G-A look into the future wireless communications," *Rollins Business Journal*, pp. 1-5, Jan./Mar. 2004.

[Lane02] J. N. Laneman, *Cooperative diversity in wireless networks: algorithms and architectures*, Ph.D. Thesis, Massachusetts Institute of Technology, Cambridge, Massachusetts, MA, USA, Aug. 2002.

[LaTW04] J. N. Laneman, D. N. C. Tse, and G. W. Wornell, "Cooperative diversity in wireless networks: efficient protocols and outage behavior," *IEEE Transactions on Information Theory*, vol. 50, no. 12, pp. 3062-3080, Dec. 2004.

[LaUL04] R. Laroia, S. Uppala, and J. Li, "Designing a mobile broadband wireless access network," *IEEE Signal Processing Magazine*, vol. 21, no. 5, pp. 20-28, Sep. 2004.

[LaWo00] J. N. Laneman and G. Wornell, "Energy-efficient antenna sharing and relaying for wireless networks," in *Proc. of the IEEE Wireless Communications and Networking Conference (WCNC'00)*, Chicago, IL, USA, pp. 7-12, Sep. 2000.

[LaWo03] J. N. Laneman and G. Wornell, "Distributed space-time-coded protocols for exploiting cooperative diversity in wireless networks," *IEEE Transactions on Information Theory*, vol. 49, no. 10, pp.2415-2425, Oct. 2003.

[LiKL07] L. Liu, S. Kim, and M. Lim, "An efficient selective receiver for STBC scheme", in *Proc. of the IEEE International Conference on communications (ICC'07)*, Glasgow, pp.4196-4200, June 2007.

[LiLi05] H. Liu and G. Li, *OFDM-based broadband wireless networks*, Wiley-Interscience, New York, NY, USA, 2005.

[LiPK08] J. Li, U. Park, and S. Kim, "An efficient rate one STBC scheme with 3 transmit antennas," in *Proc. of the 4th International Conference on Wireless Communications, Networking and Mobile Computing (WiCOM'08)*, Dallian, China, pp. 1-4, Oct. 2008.

[LiSa09] K. J. R. Liu, A. K. Sadek, W. Su, and A. Kwasinski, *Cooperative Communications and Networking*, Cambridge University Press, New York, USA, 2009.

[LiVu08] Y. Li and B. Vucetic, "On the performance of a simple adaptative relaying protocol for wireless relay networks," in *Proc. of the 67th IEEE Vehicular Technology Conference (VTC'08 Spring)*, Singapore, pp. 2400-2405, May 2008.

[LSSK09] K. J. R. Liu, A. K. Sadek, W. Su, and A. Kwasinski, *Cooperative communications and networking*, Cambridge University Press, Cambridge, New York, USA, 2009.

[Maho03] B. Mahon, *The man who changed everything: the life of James Clerck Maxwell*, John Chichester, England, Wiley & Sons, 2003.

[Matl00] Matlab, *The Language of Technical Computing*, Version 6.0, The MathWorks, Inc, 2000, http://www.mathworks.com/.

[Meul71] E. C. van der Meulen, "Three-terminal communication channels," *Advances in Applied Probability*, vol. 3, no.1, pp. 120-154, 1971.

[MTSG08] A. Moço, S. Teodoro, A. Silva, and A. Gameiro, "Relay-assisted cooperative schemes for the UL OFDMA based systems," in *Proc. of the 4th International Conference on Wireless and Mobile Communications (ICWMC'08)*, Athens, Greece, Aug. 2008, pp. 71-76.

[MTSG10] A. Moço, S. Teodoro, A. Silva, H. Lima, and A. Gameiro, "Single and multiple antenna, relay-assisted techniques for uplink and downlink OFDM systems," *IARIA International Journal on Advances in Systems and Measurements*, vol.3, no. 1&2, pp. 22-34, Sep. 2010.

[MuUy08] H. Muhaidat and M. Uysal, "Cooperative diversity with multiple-antenna nodes in fading relay channels," *IEEE Transactions on Wireless Communications*, vol. 7, no. 8, pp. 3036-3046, Aug. 2008.

[NaBK04] R. U. Nabar, H. Bolcskei, and F. W. Kneubuhler, "Fading relay channels: performance limits and space-time signal design," *IEEE Journal Selected Areas* Communications, vol. 22, no. 6, pp. 1099-1109, Aug. 2004.

[NaTW99] A. Narula, M. D. Trott, and G. W. Wornell, "Performance limits of coded diversity methods for transmitter antenna arrays," *IEEE Transactions on Information Theory*, vol. 45, no. 7, pp. 2418-2433, Nov. 1999.

[NeKT09] T. Nechiporenko, P. Kalansuriya, and C. Tellambura, "Performance of optimum switching adaptative M-QAM for amplify-and-forward relays," *IEEE Transactions on Vehicular Technology*, vol. 58, no. 5, pp. 2258-2268, June 2009.

[NoHH04] A. Nosratnia, T. Hunter, and A. Hedayat, "Cooperative communication in wireless networks," *IEEE Communications Magazine*, vol. 42, no. 10, pp. 74–80, Oct. 2004.

[NRSG09] D. Neves, C. Ribeiro, A. Silva, and A. Gameiro, "A time domain channel estimation scheme for equalize-and-forward relay-assisted systems," in *Proc. of the 72nd IEEE Vehicular Technology Conference (VTC'10 Fall)*, Ottawa, Canada, pp. 1-5, Sep. 2010.

[PDFJ08] S. Parkvall, E. Dahlman, A. Furuskar, Y. Jading M. Olsson, S. Wanstedt, and K. Zangi, "LTE-advanced - evolving LTE towards IMT-advanced," in *Proc. of the 68th IEEE Vehicular Technology Conference (VTC '08),* Calgary, Alberta, pp. 1–5, Sep. 2008.

[PeHe09] S. Peters and R. Heath, "The future of WiMAX: multihop relaying with IEEE 802.16j," *IEEE Communications Magazine*, vol. 47, no. 1, pp. 104-111, Jan. 2009.

[PPTH09] S. W. Peters, A. Panah, K. Truong, and R. Heath., "Relay architectures for 3GPP LTE-Advanced," *EURASIP Journal on Wireless Communication and Networking*, vol. 2009, May 2009.

[Proa01] J. G. Proakis, *Digital Communications*, McGraw-Hill Edition, New York, NY, USA, 2001.

[PWSH04] R. Past, B. Walke, D. Schultz, P. Herhold, H. Yanikomeroglu, S. Mukherjee, H. Viswanathan, M. Lott, W. Zirwas, M. Dohler, H. Aghvami, D. Falconer, and G. Fettweis, "Relay-based deployment concepts for wireless and mobile broadband radio," *IEEE Communications Magazine*, vol. 42, no. 9, pp. 80-89, Sep. 2004.

[Rapp96] T. Rappaport, *Wireless Communications: Principles and Practice*, Upper Saddle River, New Jersey, USA, Prentice Hall, 1996.

[RaRa06] G. S. Rajan and B. S. Rajan, "A non-orthogonal distributed space-time coded protocol, Part-I: signal model and design criteria," in *Proc. of the IEEE Information Theory Workshop (ITW'06)*, Chegdu, China, pp. 385-389, Oct. 2006.

[RoZL06] H. Rong, Z. Zhang, and P. Larsson, "Cooperative relaying based on Alamouti diversity under aggregate relay power constraints," in *Proc. of the 63rd IEEE Vehicular Technology Conference (VTC'06 Spring)*, Melbourne, Australia, pp. 2563-2567, May 2006.

[Sato76] H. Sato, "Information transmission through a channel with relay," *Technical Report ALOHA SYSTEM B76-7*, University of Hawaii, Honolulu, Mar. 1976.

[ScGa00] B. Schein and R. Gallager, "The Gaussian parallel relay network," in *Proc. of the International Symposium on Information Theory (ISIT'00)*, Sorrento, Italy, pp. 22, June 2000.

[SCHG11] S. Sugiura, S. Chen, H. Haas, P. Grant, and L. Hanzo, "Coherent versus non-coherent decode-and-forward relaying aided cooperative space-time shift keying," *IEEE Transactions on Communications*, vol. 59, no. 6, pp. 1707–1718, June 2011.

[SeEA03a] A. Sendonaris, E. Erkip, and B. Aazhang, "User cooperation diversity - Part I: System description," *IEEE Transactions on Communications*, vol. 51, no. 11, pp. 1927-1938, Nov. 2003.

[SeEA03b] A. Sendonaris, E. Erkip, and B. Aazhang, "User cooperation diversity - Part II: Implementation aspects and performance analysis," *IEEE Transactions on Communications*, vol. 51, no. 11, pp. 1939-1948, Nov. 2003.

[SeEA98] A. Sendonaris, E. Erkip, and B. Aazhang, "Increasing uplink capacity via user cooperation diversity," in *Proc. of the International Symposium on Information Theory (ISIT'98)*, Cambridge, MA, USA, pp. 156, Aug. 1998.

[SeWi93] N. Seshadri and J. H. Winters, "Two signaling schemes for improving the error performance of frequency-division-duplex transmission systems using transmitter

antenna diversity," in *Proc. of the 43rd IEEE Vehicular Technology Conference (VTC'93 Spring),* Secaucus, NJ, USA, pp. 508-511, May 1993.

[ShPa93] N. Sharma and C. Papadias, "Improved quasi-orthogonal codes through constellation," in *Proc. of the IEEE International Conference on Acoustics, Speech, and Signal Processing (ICASSP'93)*, Minneapolis, MN, USA, pp. 3968-3971, Apr. 1993.

[SiAl05] M. K. Simon and M. S. Alouini, *Digital communication over fading channels*, Second Edition, Wiley-Interscience, New Jersey, 2005.

[SiMV10] S. Simoens, O. M. Medina, and J. Vidal, "Compress-and-forward cooperative MIMO relaying with full channel state information," *IEEE Transactions on Signal Processing*, vol. 58, no. 2, pp.781-791, Feb. 2010.

[SrCR08] D. Sreedhar, A. Chockalingam, and S. Rajan, "Single-symbol ML decodable distributed STBCs for partially-coherent cooperative networks," in *Proc. of the IEEE International Symposium on Information Theory (ISIT'08)*, Toronto, Canada, pp. 1029-1033, July 2008.

[Stee92] R. Steele, *Mobile Radio Communications*, Wiley-Pentech Publication, IEEE Press, New York, NY, USA, 1992.

[StEr05] A. Stefanov and E. Erkip, "Cooperative space-time coding for wireless networks," *IEEE Transactions on Communications*, vol. 53, no. 11, pp. 1804-1809, Nov. 2005.

[SuBa08] J. Sung and J. Barry, "Approaching the zero-outage capacity of MIMO OFDM without water-filling," *IEEE Transactions on Information Theory*, vol. 54, no. 4, pp. 1423-1436, Apr. 2008.

[SuKS09] H. A. Suraweera, G. J. Karagiannidis, and P. J. Smith, "Performance analysis of the dual-hop asymmetric channels," *IEEE Transactions on Wireless Communications*, vol. 8, no. 6, pp. 2783-2788, June 2009.

[SuXi04] W. Su and X. G. Xia, "Signal constellations for quasi-orthogonal space time block codes with full diversity," *IEEE Transactions on Information Theory*, vol. 50, no. 10, pp. 2331–2347, Oct. 2004.

[TaHu07] X. Tang and Y. Hua, "Optimal design of non-regenerative MIMO wireless relays," *IEEE Transactions on Wireless Communications*, vol. 6, no. 4, pp. 1398-1407, Apr. 2007.

[TaJC99] V. Tarokh, H. Jafarkhani, and A. Calderbank, "Space time block codes from orthogonal design," *IEEE Transactions on Information Theory*, vol. 45, no. 5, pp. 1456-1467, July 1999.

[TaSC98] V. Tarokh, N. Seshadri, and A. Calderbank, "Space time codes for high data rate wireless communication: performance criterion and code construction," *IEEE Transactions on Information Theory*, vol. 44, no. 2, pp. 744-756, Mar. 1998.

[Tela99] E. Telatar, "Capacity of multi-antenna Gaussian channels," *European Transactions on Telecommunication*, vol. 10, no. 6, pp. 585-595, Dec. 1999.

[TiBH00] O. Tirkkonen, A. Boariu, and A. Hottinen, "Minimal non-orthogonality rate 1 space-time block code for 3+Tx antennas," in *Proc. of the 6th IEEE International Symposium on Spread-Spectrum Techniques and Applications* (*ISSSTA'00)*, New Jersey, USA, pp. 429-432, Sep. 2000.

[TiHo02] O. Tirkkonen and A. Hottinen, "Square-matrix embeddable space–time block codes for complex signal constellations," *IEEE Transactions on Information Theory*, vol. 48, no. 2, pp. 384-395, Feb. 2002.

[TMSG10] S. Teodoro, A. Moço, A. Silva, and A. Gameiro, "Performance evaluation of a distributed SFBC relay-assisted scheme for OFDM systems," in *Proc. of the Future Network and Mobile Summit 2010*, Florence, Italy, pp.1-10, June 2010.

[ToHA10] M. Torabi, D. Haccoun, and W. Ajib, "Performance analysis of cooperative diversity with relay selection over non-identically distributed links," *IET Communications*, vol. 4, no. 5, pp. 596–605, Mar. 2010.

[TSGG08] S. Teodoro, A. Silva, J. M. Gil, and A. Gameiro, "Capacity comparison between Alamouti and cooperative VAA with EF and AF relays," in *Proc. of the 17th International Conference on Telecommunications (ICT-Mobile Summit'08)*, Stockholm, Sweden, pp.1-10, June 2008.

[TSGG09a] S. Teodoro, A. Silva, J. M. Gil, and A. Gameiro, "Capacity comparison of relay-assisted schemes with and without direct path," in *Proc. of the 18th International Conference on Telecommunications (ICT-Mobile Summit'09)*, Santander, Spain, pp.1-10, June 2009.

[TSGG09b] S. Teodoro, A. Silva, J. M. Gil, and A. Gameiro, "Virtual MIMO schemes for downlink space-frequency coding OFDM systems," in *Proc. of the 20th IEEE Personal, Indoor and Mobile Radio Communications (PIMRC'09),* Tokyo, Japan, pp. 1322-1326, Sep. 2009.

[TSGG09c] S. Teodoro, A. Silva, J. M. Gil, and A. Gameiro, "Distributed space-frequency block coding for a 2-antenna relay in downlink OFDM systems," in *Proc. of the 9th IEEE International Symposium on Communication and Information Technology (ISCIT'09)*, Incheon, Korea, pp. 853-858, Sep. 2009.

[TSGG10a] S. Teodoro, A. Silva, J. M. Gil, and A. Gameiro, "Distributed space-time code using precoding for cellular systems," in *Proc. of* the *72nd IEEE Vehicular Technology Conference (VTC'10 Fall)*, Ottawa, Canada, pp. 1-5, Sep. 2010.

[TSGG10b] S. Teodoro, A. Silva, J. M. Gil, and A. Gameiro, "Data precoded relay-assisted scheme for cellular systems," in *Proc. of the 21st IEEE Personal, Indoor and Mobile Radio Communications (PIMRC'10)*, Istanbul, Turkey, pp. 2413-2418, Sep. 2010.

[TSGG10c] S. Teodoro, A. Silva, J. M. Gil, and A. Gameiro, "Precoded multiple relay-assisted scheme for cellular systems," in *Proc. of the 13th International Symposium on Wireless Personal Multimedia Communications (WPMC'10)*, Recife, Brazil, pp. 1-5, Oct. 2010.

[TSGG10d] S. Teodoro, A. Silva, J. M. Gil, and A. Gameiro, "Novel precoded relay-assisted algorithm for cellular systems," *EURASIP Journal on Wireless Communications and Networking*, vol. 2010, Article ID 414657, 10 pages, 2010.

[TsVi05] D. Tse and P. Viswanath, *Fundamentals of Wireless Communications*, Cambridge University Press, New York, NY, USA, 2005.

[TsVZ04] D. Tse, P. Viswanat, and L. Zheng, "Diversity multiplexing tradeoff in multiple access channels," *IEEE Transactions on Information Theory*, vol. 50, no. 9, pp. 1859-74, Sep. 2004.

[Unge82] G. Ungerboeck, "Channel coding with multilevel/phase signals," *IEEE Transactions on Information Theory*, vol. 28, no. 1, pp. 55-67, Jan. 1982.

[Vite67] A. J. Viterbi, "Error bounds on convolutional codes and an asymptotically optimum decoding algorithms," *IEEE Transactions on Information Theory*, vol. 13, no. 2, pp. 260-269, Apr. 1967.

[ViTH10] Q. Vien, L. Tran, and E. Hong, "Distributed space-time block code over mixed Rayleigh and Rician frequency-selective fading channels," *EURASIP Journal on Wireless Communications and Networking*, vol. 2010, Article ID 385872, 9 pages, 2010.

[VuYu03] B. Vucetic, J. Yuan, *Space-Time Coding*, John Wiley & Sons, Inc., 2003.

[WeRS10] Y. Wei, F. Richard, and M. Song, "Distributed optimal relay selection in wireless cooperative networks with finite-state Markov channels," *IEEE Transactions on Vehicular Technology*, vol. 56, no. 5, pp.2149-2158, June 2010.

[WiRa03] A. Wittneben and B. Rankov, "Impact of cooperative relays on the capacity of rank-deficient MIMO channels," in *Proc. of the 12th IST Summit on Mobile and Wireless Communications*, Aveiro, Portugal, pp.421-425, June 2003.

[YiKi07] Z. Yi and I. Kim, "Single-symbol ML decidable distributed STBCs for cooperative networks," *IEEE Transactions on Information Theory*, vol.53, no. 8, pp. 2977-2985, Aug. 2007.

[YuEr06] M. Yuksel and E. Erkip, "Diversity-multiplexing tradeoff in multiple-antenna relay systems," in *Proc. of the International Symposium on Information Theory*, Seattle, USA, pp. 1154-1158, July 2006.

[YuKY06] Y. Yu, S. Keroueden, and J. Yuan, "Closed-loop extended orthogonal space-time block codes for three and four transmit antennas," *IEEE Signal Processing Letters*, vol. 13, no. 5, pp. 273–276, May. 2006.

[YuKY06] Y. Yu, S. Keroueden, and J. Yuan, "Closed-loop extended orthogonal STBC for three and four transmit antennas," *IEEE Signal Processing Letters*, vol. 13, no. 5, May 2006.

[ZhDa04] H. Zhang and H. Dai, "On the capacity of distributed MIMO systems," *Conference on Information Sciences and Systems*, Princeton University, Princeton, NJ, Mar. 2004.

[ZhLi05] Q. Zhao and H. Li, Member, "Performance of differential modulation with wireless relays in Rayleigh fading channels," *IEEE Communication Letters*, vol. 9, no. 4, pp. 343-345, Apr. 2005.

[ZhTs03] L. Zheng and D. N. C. Tse, "Diversity and multiplexing: A fundamental trade-off in multiplexing antennas," *IEEE Transactions on Information Theory*, vol. 49, no. 5, pp.1073-1095, May 2003.

[ZhVa05] B. Zhao and M. C. Valenti, "Practical relay networks: a generalization of hybrid-ARQ," *IEEE Journal on Selected Areas in Communications*, vol. 23, no. 1, pp. 7-18, Jan. 2005.

[ZhWL10] D. Zhang, Y. Wang, and J. Lu, "QoS aware relay selection and subcarrier and power allocation in cooperative OFDM systems," *IEEE Communication Letters*, vol.14, no. 4, pp. 294-296, Apr. 2010.

Annexes

A. STBCs and Reference Non-Cooperative Schemes

Along this thesis we commonly refer to non-cooperative schemes with the objective of comparing them to the cooperative ones, as in Sections 3.5, 4.5 and 5.6. This non-cooperative systems are formed by two terminal nodes (source and destination), each equipped with a different number of antennas. In the cases of multiple transmitting antennas, we consider the use of STBCs, which are also described in this annex. The objective of this annex is therefore to present these reference schemes and the STBCs used in this thesis.

The simplest non-cooperative scheme is the SISO one, represented in Figure A-1, formed by a continuous communication link between the source and the destination, both with a single antenna. A simple block diagram for SISO system is represented in Figure A-2.

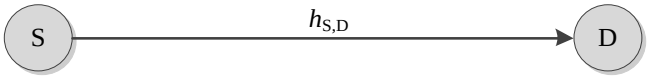

Figure A-1: SISO system model.

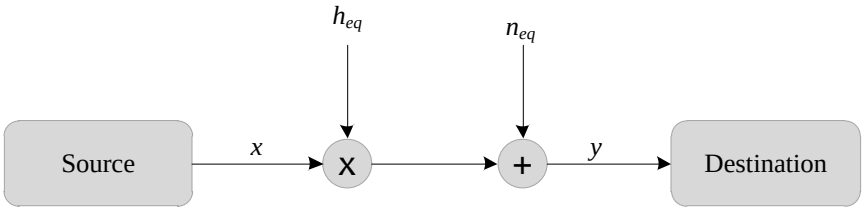

Figure A-2: Block diagram of SISO system transmission.

The first operation performed in this system is the convolution of the input signal by the channel between the two nodes. After this operation, thermal noise, *n*, is added in reception, after which the signal is equalized and recovered. The output of a simple channel transmission is given by

$$y(t,\tau) = h(t,\tau) * x(t) + n(t), \tag{A.1}$$

where $x(t)$ is the input signal and $n(t)$ is the thermal noise introduced in reception, both dependent on instant time *t*, where $h(t,\tau)$ is the impulse response of the channel.

For simplicity, let us assume a flat- fading model where the channel can be represented by a single discrete-time complex filter *h*. The received signal at the antenna element associated at k^{th} time slot is, therefore, given by

$$y_k = As_k h + n_k, \tag{A.2}$$

where s_k is the transmitted symbol assumed to have unitary variance, *A* is the input signal amplitude and n_k refers to complex noise $CN(0,\sigma_n^2)$ at the receiver.

MISO systems are formed by multiple antennas at the transmitter and a single antenna at the receiver. An example of a MISO system is the scheme with two antennas at the source, which form two channels between the two terminal nodes, as can be seen in Figure A-3. In this scheme, the well-known Alamouti code can be used, considered as an optimal code to decrease error rate [Alam98]. This code makes use of spatial diversity, more specifically antenna diversity, obtained through the two different channels. The code is presented in Table A.1 and consists in antenna 1 transmitting s_1 and s_2^* symbols in the first and second time slots, respectively, through $h_{S1,D}$, and antenna 2 transmitting s_2 and $-s_1^*$ symbols in first and second time slots, respectively, through $h_{S2,D}$.

The block diagram of this system is presented in Figure A-4, where the input vector signal $\mathbf{x} = A/\sqrt{2}\left[s_1 \; s_2\right]^T$ is coded, as explained before, and transmitted by the two source antennas. After passing through the channels, the thermal noise is added to the signals, forming vector **y**. Then the

two signals are decoded/equalized resulting in recovered symbols in the vector $\hat{\mathbf{x}}$, which corresponds to the estimation of symbols $\mathbf{x}$.

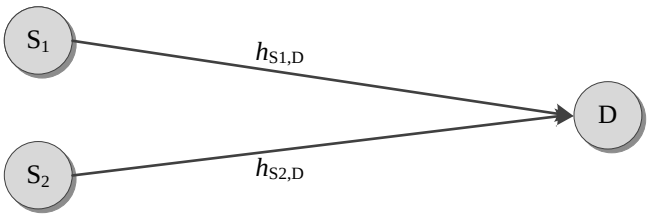

Figure A-3: MISO system model with two transmitting antennas.

TABLE A.1: TRANSMITTED INFORMATION BY EACH ANTENNA FOR ALAMOUTI CODING.

	Antenna 1	**Antenna 2**
Time slot 1	s_1	s_2
Time slot 2	s_2^*	$-s_1^*$

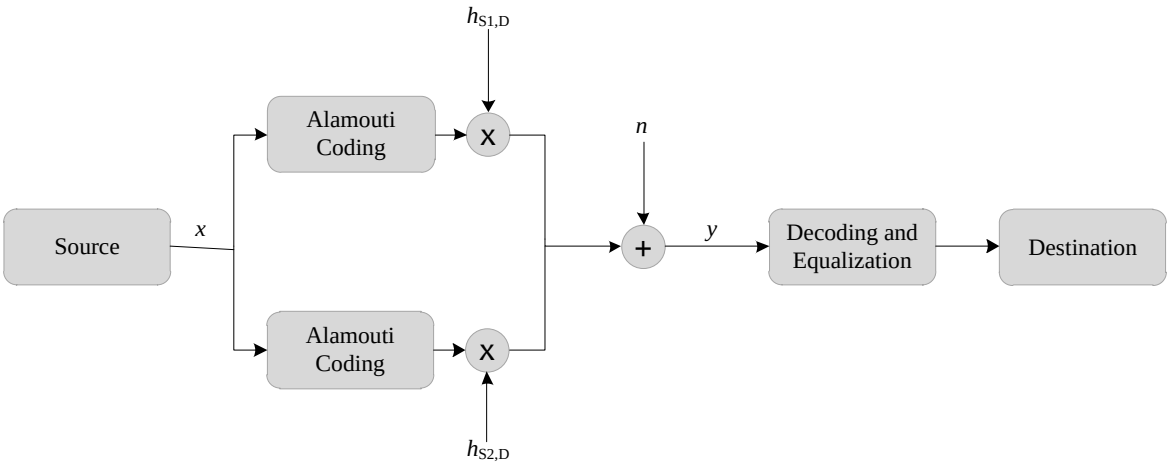

Figure A-4: Block diagram of MISO system.

The corresponding transmitting matrix is given by

$$C_x = \begin{bmatrix} x_1 & x_2 \\ x_2^* & -x_1^* \end{bmatrix}, \tag{A.3}$$

where the number of rows corresponds to the number of symbols needed for code precoding (in this case two) and the number of columns is the number of antennas.

An equivalent channel matrix, $\mathbf{H}$, can be performed by means of characterizing the channel where system information passes through. For example, in Alamouti code the equivalent channel matrix is given by

$$\mathbf{H} = = \begin{bmatrix} h_{S1,D} & h_{S2,D} \\ -h_{S2,D}^{*} & h_{S1,D}^{*} \end{bmatrix}, \tag{A.4}$$

which can be taken by the received signals expression

$$\begin{bmatrix} y_1 \\ y_2^{*} \end{bmatrix} = \frac{1}{\sqrt{2}} \mathbf{H} \begin{bmatrix} s_1 \\ s_2 \end{bmatrix} + \begin{bmatrix} n_1 \\ n_2^{*} \end{bmatrix}. \tag{A.5}$$

The receiver structure is a matched filter, also called a maximal ratio combiner, which weighs the received signal in each branch in proportion to the signal strength and also aligns the phases of the signals in the summation to maximize the output SNR. In case the Alamouti code is applied, if we multiply the output vector, with the received words through the several paths, by the Hermitian of the equivalent channel matrix and the inverse module of that matrix, we obtain the input signal by the following expression

$$\hat{\mathbf{x}} = \mathbf{H}^{H}\mathbf{y} = \mathbf{H}^{H}\mathbf{H}\mathbf{x} + \mathbf{H}^{H}\mathbf{n} = \left\|\mathbf{H}\right\|^{2}\mathbf{x} + \mathbf{H}^{H}\mathbf{n}, \tag{A.6}$$

where $\left\|\mathbf{H}\right\|^{2}$ is a diagonal matrix with each diagonal element equal to $\left|h_{S1,D}\right|^{2} + \left|h_{S2,D}\right|^{2}$. Thus, we have an equivalent scalar detection problem with noise $\mathbf{H}^{H}\mathbf{n} \sim CN\left(0, \sigma_n^{2}\right)$.

For MISO schemes with more than two transmit antennas, it is not possible to design encoding schemes that are orthogonal and have an unitary rate. O-STBCs were proposed for more than two antenna systems, ensuring diversity equal to the number of transmitting antennas and a linear maximal likelihood detection [TJCa99]. However, these codes have rates lesser than one.

With the objective of achieving a full rate code, for more than two transmit antennas, QO-STBCs were developed, as for example in [Jafa01], [TSCa98], [ShPa02], [TBHo00]. These quasi-orthogonal coding schemes are generally more complex, especially for decoding, which can be done with ML decoding by searching pairs of symbols.

In the case where there are three transmit antennas, we can implement the QO-STBC, with full rate, described in [LiPK08]. The corresponding transmission matrix is the following:

$$C_x = \begin{bmatrix} x_2 & x_3 & x_4 \\ x_1^{*} & -x_4^{*} & x_3^{*} \\ x_4 & x_1 & x_2 \\ x_3^{*} & -x_2^{*} & x_1^{*} \end{bmatrix}, \tag{A.7}$$

where the columns correspond to the signal transmitted by each antenna and the lines to the time slots; x_k are the transmit symbols corresponding to time slot *k* already normalized so that $x_k = \frac{1}{\sqrt{3}} s_k$. Estimated symbols can be obtained by

$$\begin{bmatrix} \hat{x}_1 \\ \hat{x}_2 \\ \hat{x}_3 \\ \hat{x}_4 \end{bmatrix} = \mathbf{H}^H \begin{bmatrix} y_1 \\ y_2^* \\ y_3 \\ y_4^* \end{bmatrix} + \mathbf{H}^H \begin{bmatrix} n_1 \\ n_2^* \\ n_3 \\ n_4^* \end{bmatrix}, \tag{A.8}$$

with the equivalent matrix given by

$$\mathbf{H} = \begin{bmatrix} 0 & h_1 & h_2 & h_3 \\ h_1^* & 0 & h_3^* & -h_2^* \\ h_2 & h_3 & 0 & h_1 \\ h_3^* & -h_2^* & h_1^* & 0 \end{bmatrix}. \tag{A.9}$$

An equation relating to the estimated symbols with the original ones can be obtained by (A.8) and (A.9), resulting in

$$\begin{bmatrix} \hat{x}_1 \\ \hat{x}_2 \\ \hat{x}_3 \\ \hat{x}_4 \end{bmatrix} = \begin{bmatrix} a & 0 & b & 0 \\ 0 & a & 0 & b \\ b & 0 & a & 0 \\ 0 & b & 0 & a \end{bmatrix} \begin{bmatrix} x_1 \\ x_2 \\ x_3 \\ x_4 \end{bmatrix} + \mathbf{H}^H \begin{bmatrix} n_1 \\ n_2^* \\ n_3 \\ n_4^* \end{bmatrix}, \tag{A.10}$$

where $a = \sum_{i=1}^{3} |h_i|^2$ and $b = h_1 h_3^* + h_3 h_1^*$. This detection method has interference between symbols: x_1 interferes with x_3 estimation, and x_2 interferes with x_4 and vice-versa, leading to the low diversity gain obtained when using this code.

Let us consider the situation with four transmit antennas. An example of QO-STBC with rate one for this case, can be the one described in [TBHo00]. The corresponding transmission matrix is

$$C_x = \begin{bmatrix} \xrightarrow{\text{space}} & & & \\ x_1 & x_2 & x_3 & x_4 \\ -x_2^* & x_1^* & -x_4^* & x_3^* \\ x_3 & x_4 & x_1 & x_2 \\ -x_4^* & x_3^* & -x_2^* & x_1^* \end{bmatrix} \begin{matrix} \\ \\ \\ \\ \downarrow \text{time/frequency} \end{matrix}, \tag{A.11}$$

where columns correspond to the signal transmitted by each antenna and lines to the time slots; and $x_k = \frac{1}{2} s_k$. The corresponding equivalent matrix is given by

$$\mathbf{H} = \begin{bmatrix} h_1 & h_2 & h_3 & h_4 \\ h_2^* & -h_1^* & h_4^* & -h_3^* \\ h_3 & h_4 & h_1 & h_2 \\ h_4^* & -h_3^* & h_2^* & -h_1^* \end{bmatrix}. \tag{A.12}$$

and the operations to get the estimated symbols are

$$\begin{bmatrix} \hat{x}_1 \\ \hat{x}_2 \\ \hat{x}_3 \\ \hat{x}_4 \end{bmatrix} = \mathbf{H}^H \begin{bmatrix} y_1 \\ y_2^* \\ y_3 \\ y_4^* \end{bmatrix} + \mathbf{H}^H \begin{bmatrix} n_1 \\ n_2^* \\ n_3 \\ n_4^* \end{bmatrix}. \tag{A.13}$$

Thus, soft-estimated symbols can be represented as function of the original ones, as

$$\begin{bmatrix} \hat{x}_1 \\ \hat{x}_2 \\ \hat{x}_3 \\ \hat{x}_4 \end{bmatrix} = \begin{bmatrix} a & 0 & b & 0 \\ 0 & a & 0 & b \\ b & 0 & a & 0 \\ 0 & b & 0 & a \end{bmatrix} \begin{bmatrix} x_1 \\ x_2 \\ x_3 \\ x_4 \end{bmatrix} + \mathbf{H}^H \begin{bmatrix} n_1 \\ n_2^* \\ n_3 \\ n_4^* \end{bmatrix}. \tag{A.14}$$

In this case, the estimation, also based on conventional linear STBC detection method, has interference between symbols x_1 and x_4, and between x_2 and x_3. The interference factors are given by $a = \sum_{i=1}^{4} |h_i|^2$ and $b = h_1 h_4^* + h_4 h_1^* + h_2 h_3^* + h_3 h_2^*$.

SIMO systems are also often used. In these cases, antenna diversity is obtained through combination of signals received by each receiver antenna. MIMO systems combine the benefits of both SIMO and MISO systems. For example, a communication scheme between two antenna nodes in transmitter and receiver is represented in Figure A-5. Alamouti code can be applied to the transmit antennas and after that the MRC is made in destination according to the signals received in both receiver antennas. This scheme will have a maximum diversity order of 4, when considering independence between links.

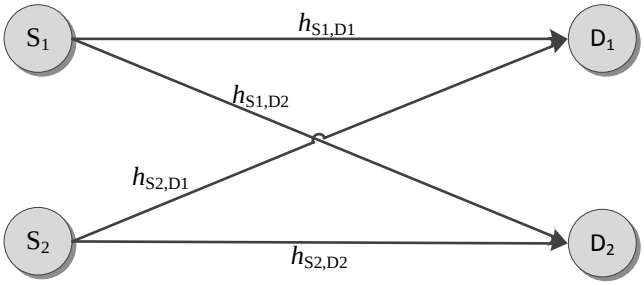

Figure A-5: MIMO system model with two transmit and two receive antennas.

B. FER Performances for OFDM RA Schemes with Distributed SFBC

The FER performances of the two distributed SFBC schemes, previously defined in Chapter 4, are evaluated and presented in this annex for relay protocols AF, DF and SDF. We considered a typical pedestrian scenario, based on LTE specifications, where the main parameters are defined in Table 4.3 [3GPP07]. The drawn conclusions are the same as the ones obtained by BER performances, though these results are shown in this annex since can be of interest, as reference, in future works.

FER performances of the proposed RA with the mentioned protocols and of the non-cooperative schemes are shown in Figure B-1. These results were obtained for scenario 1, when all the links have the same quality conditions, i.e., $SNR_d = SNR_b = SNR_r$. The same trends previously observed in BER performances in Chapter 4, are obtained in terms of FER, but with higher error rates for the same E_b/N_0. For this scenario, the differences between the scheme with the AF protocol and SISO and MISO ones is of 4.2 dB and 3 dB, respectively, for FER=10^{-2}. The difference is of 3 dB, when using the DF relay protocol instead of the AF one, for the same FER.

Figures B-2 and B-3 show the results for the single-antenna RA scheme for scenarios 2 and 3, respectively. Similar behaviors are observed in FER results, where the schemes have the same qualitative behavior, albeit differing in the relative gains among schemes. For example, in scenario 3, the DF and SDF relay protocols produce the same amount of error frames, while with the AF one an higher error rate is obtained, differing in about 1.8 dB, for FER=10^{-2}. This indicates that when

the relay selection is appropriate, so that the cooperative links have higher quality than the direct link, we have advantages in using the DF or SDF relay protocols instead of the AF one.

The performances of the RA scheme with a two-antenna relay are also presented and analyzed in terms of FER results. In, Figures B-4, B-5 and B-6 the results for the non-cooperative and cooperative schemes with the two-antenna relay are shown for scenarios 1, 2 and 3, respectively. Again, the FER results confirm the analysis and conclusions of the BER results, which have similar behaviors.

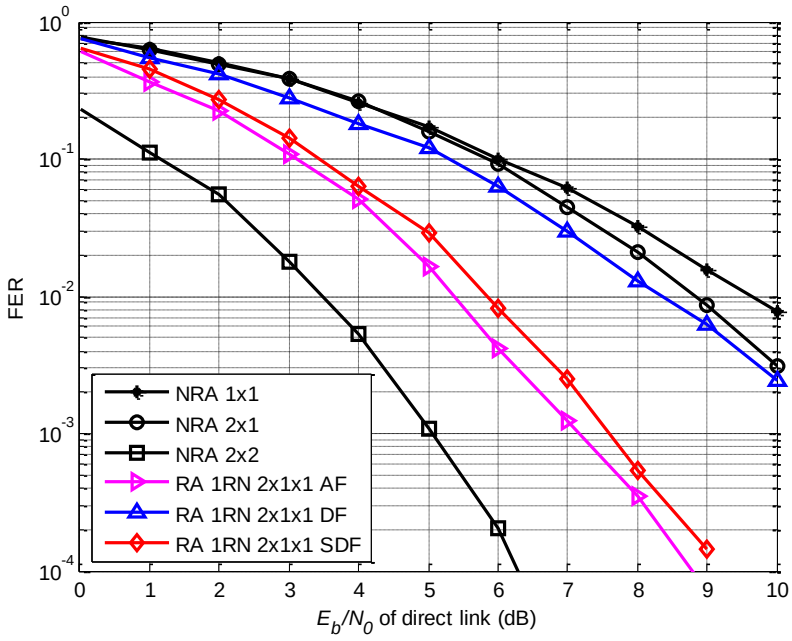

Figure B-1: FER performances of RA 1RN 2×1×1 and reference schemes for scenario 1.

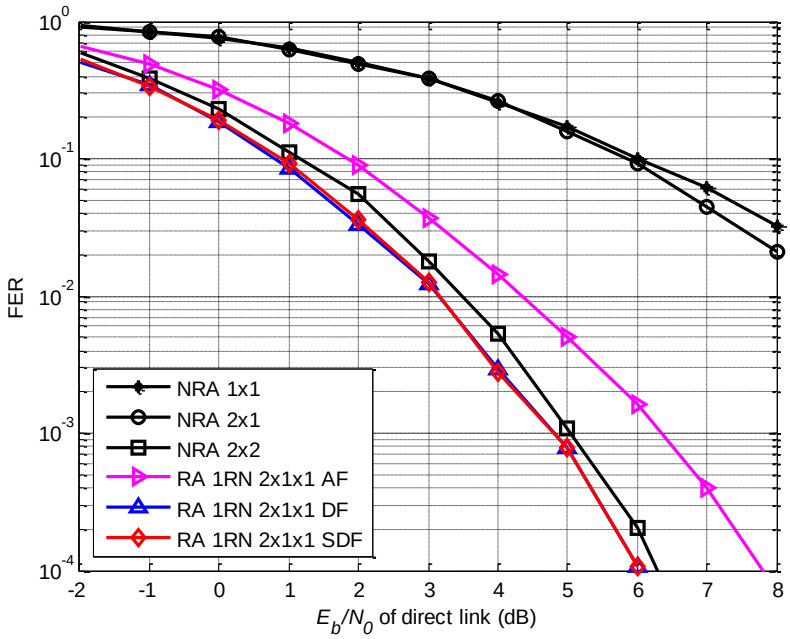

Figure B-2: FER performances of RA 1RN 2×1×1 and reference schemes for scenario 2.

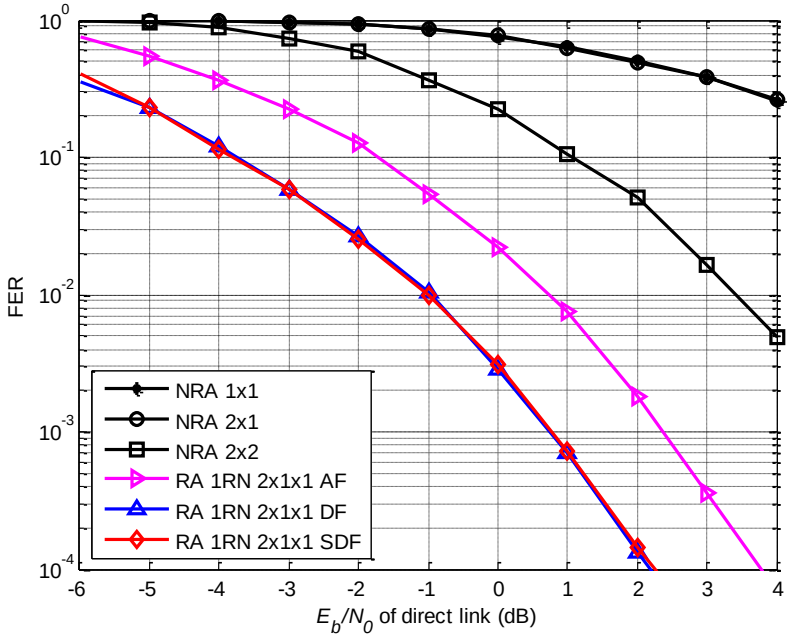

Figure B-3: FER performances of RA 1RN 2×1×1 and reference schemes for scenario 3.

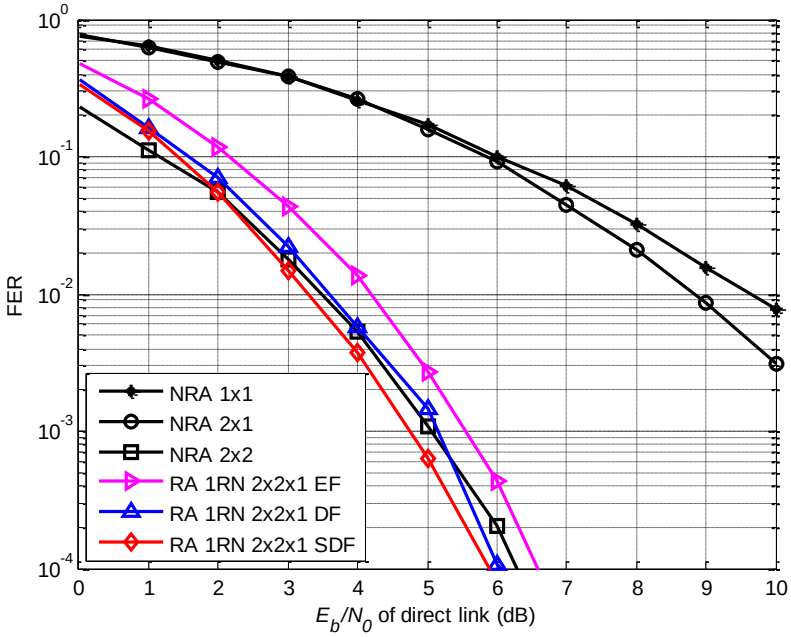

Figure B-4: FER performances of RA 1RN 2×2×1 and reference schemes for scenario 1.

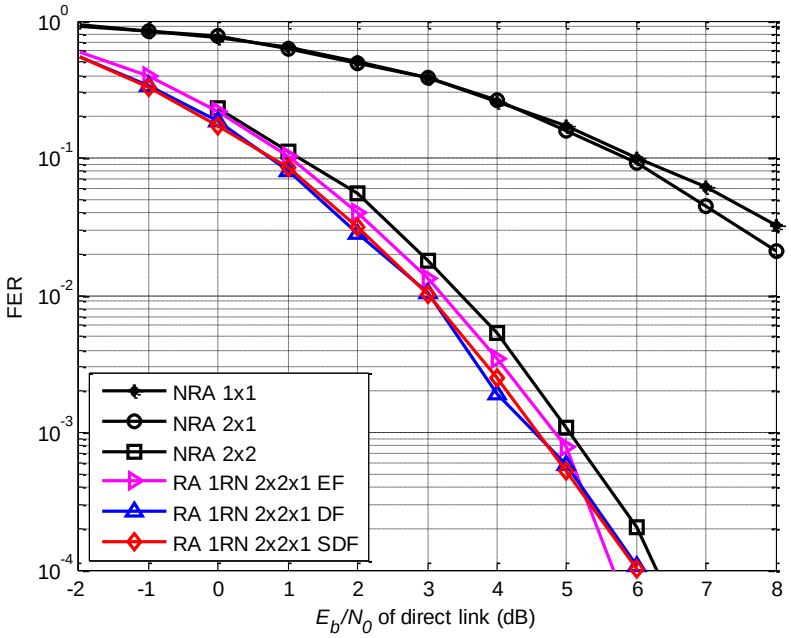

Figure B-5: FER performances of RA 1RN 2×2×1 and reference schemes for scenario 2.

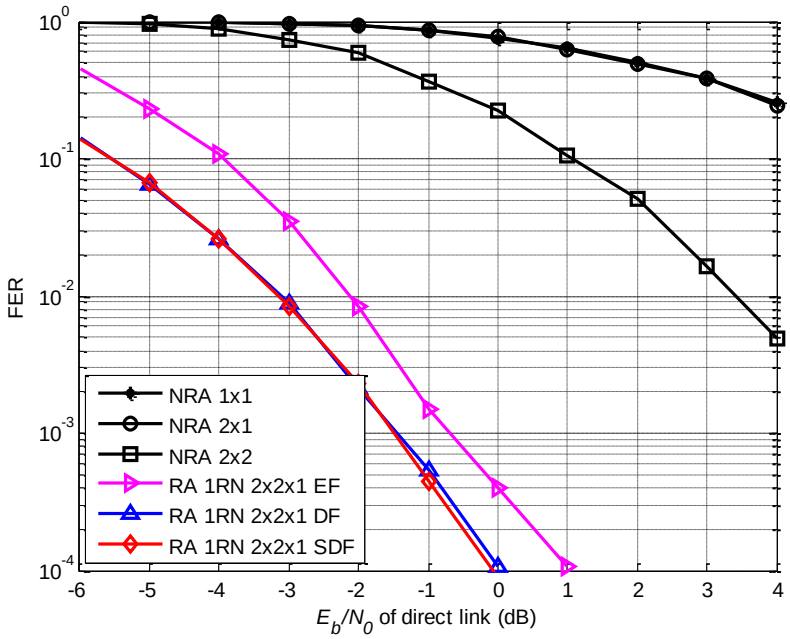

Figure B-6: FER performances of RA 1RN 2×2×1 and reference schemes for scenario 3.

C. Gain Derivation for Precoded Algorithm

In Chapter 5 the data PRA algorithm was compared against reference cooperative algorithms in terms of asymptotic gain. In this annex we derive the expressions for the minimum distances that were used for derivation of that gain. Two reference RA schemes are considered for comparison with the data-precoded schemes. In the first case, the reference RA scheme with distributed SFBC is used for comparison. It has a 16-QAM modulation, since it needs two phases for communication: in the first one the source broadcasts its information to the relays and in the second one the relays forward that information to the UT using a QO-SFBC. In the cases where there are two antennas at the RNs, instead of one, we use a DSFBC designed for 2*L* transmitters, maintaining the same modulation. The squared minimum distance expression for the RA algorithm with SFBC is given by

$$d^2_{\min_{\text{RA-SFBC}}} = \frac{d^2_{\min_{\text{16-QAM}}}}{N_R L} \sum_{i=0}^{L-1} g_{N_R,i,k} \,, \tag{C.1}$$

where the variable with the equivalent link channel gain is given by

$$g_{j,i,k=} \begin{cases} \left|h_{ru\_i\_1,k}\right|^2 & , j=1 \\ \left|h_{ru\_i\_1,k}\right|^2 + \left|h_{ru\_i\_2,k}\right|^2 & , j=2 \end{cases}. \tag{C.2}$$

The ratio between the minimum distance of a *M*-QAM modulation and of a QPSK modulation, named as normalization factor for *M*-QAM modulation, is given by [Gold05]

$$\alpha_{M-\text{QAM}} = \frac{d_{\min_{M-\text{QAM}}}}{d_{\min_{\text{QPSK}}}} = \sqrt{\frac{3\log_2 M}{2(M-1)}}. \tag{C.3}$$

Thus, we can simplify the expression of the squared minimum distance for the RA with distributed SFBC, expressed in (C.1), into the one given by

$$d^2_{\min_{\text{RA-SFBC}}} = d^2_{\min_{\text{QPSK}}} \frac{2}{5L}\left(\sum_{i=1}^{L-1}\rho_{mi}+1\right) g_{N_R,1,k}, \tag{C.4}$$

where the channel gains ρ_{mi} are exhibited in (5.49) for the case of a single antenna at the relays and in (5.51) for the two-antenna case. Note that for more than two RNs, there are not fully orthogonal SFBC, thus resulting in lower performances. The final gain is then a lower-bound approximation, for these cases.

The asymptotic gain from the proposed algorithm considered relatively to the RA with distributed SFBC is obtained through the ratio of the minimum distances of both algorithms in (5.50), (5.52) and (C.4), which results in

$$G_L = 10\log\left(\frac{\frac{1}{\sum_{i=0}^{L-1}4^i}\left(\sum_{i=1}^{L-1}4^i\rho_{mi}+1\right)}{\frac{2}{5L}\left(\sum_{i=1}^{L-1}\rho_{mi}+1\right)}\right). \tag{C.5}$$

We can consider $\sum_{i=0}^{L-1}4^i$ as a sum of the first *L* terms of a geometric progression of ratio 4 and initial value 1, which is equivalent to having

$$\sum_{i=0}^{L-1}4^i = \frac{1-4^L}{1-4} = \frac{4^L-1}{3}. \tag{C.6}$$

Thus, the gain for $L \in \mathbb{N}\setminus\{1\}$ and $N_R \in \{1,2\}$ will be given by (5.53).

An alternative scheme for comparison with the proposed one is an equivalent cooperative scheme, fully orthogonal and with a unitary rate. This cooperative scheme can use the Alamouti code multiple times according to the number of elements and is named DCA algorithm. This algorithm will need more time for transmission, which depends on the number of relays. Thus, for the case of single antenna relays, it will take twice the time to transmit as compared to the time that the continuous link would take if available for the two-relay case, and thrice the time for three and four-relay cases and so forth. Thus, the modulation used is M_A-QAM, where $M_A = 4^{\frac{L}{2}+1}$ if the

number of relays is even and $M_A = 4^{\frac{L+3}{2}}$ otherwise. When $N_R = 2$, the modulation used is given according to $M_A = 4^L$. The squared minimum distance for this algorithm is then given by

$$d^2_{\min_{\text{RA-DAC}}} = \frac{\alpha^2_{M_A-\text{QAM}}}{2} \sum_{i=0}^{L-1} g_{N_R,i,k} \ . \tag{C.7}$$

The corresponding gain in dBs obtained with the PRA algorithm in comparison with the equivalent DCA code is given by

$$G_L = 10\log\left(\frac{\frac{1}{\sum_{i=0}^{L-1} 4^i}\left(\sum_{i=1}^{L-1} 4^i \rho_{mi} + 1\right)}{\frac{\alpha^2_{M_A-\text{QAM}}}{2}\left(\sum_{i=1}^{L-1} \rho_{mi} + 1\right)} \right). \tag{C.8}$$

By replacing the modulation factor gain we obtain the following

$$G_L = \begin{cases} 10\log\left(\dfrac{\frac{1}{\sum_{i=0}^{L-1} 4^i}\left(\sum_{i=1}^{L-1} 4^i \rho_{mi} + 1\right)}{\frac{3\left(\frac{L}{2}+1\right)}{2\left(4^{\frac{L}{2}+1}-1\right)}\left(\sum_{i=1}^{L-1} \rho_{mi} + 1\right)} \right), & L \text{ is even} \wedge N_R = 1 \\ 10\log\left(\dfrac{\frac{1}{\sum_{i=0}^{L-1} 4^i}\left(\sum_{i=1}^{L-1} 4^i \rho_{mi} + 1\right)}{\frac{3\left(\frac{L+3}{2}\right)}{2\left(4^{\frac{L+3}{2}}-1\right)}\left(\sum_{i=1}^{L-1} \rho_{mi} + 1\right)} \right), & L \text{ is odd} \wedge N_R = 1 \\ 10\log\left(\dfrac{\frac{1}{\sum_{i=0}^{L-1} 4^i}\left(\sum_{i=1}^{L-1} 4^i \rho_{mi} + 1\right)}{\frac{3L}{2\left(4^L-1\right)}\left(\sum_{i=1}^{L-1} \rho_{mi} + 1\right)} \right), & N_R = 2 \end{cases} . \tag{C.9}$$

After some simplifications we get the final expression for the gain obtained when using the precoded algorithm instead of a DCA one, for $L \in \mathbb{N} \setminus \{1\}$, in (5.56).

D. Simulations for Additional Scenarios for the Precoded RA Schemes

For the RA schemes assisted by two RNs, several scenarios were considered by varying the SNR of each link. The SNR variations were made by the addition or not of 10 dBs to each link. However, whatever the values used, we would reach the same conclusions. Some additional scenarios are thus presented in this annex with increments of 5 dB in SNR links, in order to confirm this and so that the corresponding results can be used as reference for future works. We show same results of the same schemes referred to in Section 5.6 for two more scenarios: scenario 2.4, where the link between RN_1 and UT has a SNR 5 dB higher than the other two links, and scenario 2.5, where the second-hop of both cooperative paths has 5 dB more than the direct link (Table D.1). For the cooperative systems with three RNs, two more scenarios are also considered, according to Table D.2. Scenario 3.5 is when one of the cooperative links has a SNR 5 dB higher than the others, and scenario 3.6 is when all cooperative links have 5 dB more of transmission quality than the DP in the second-hop.

Performances of the PRA and reference systems are presented next, similarly to Sub-section 5.6.3. The results when the cooperative systems are assisted by two single-antenna relays are in Figure D-1 and Figure D-2. For the case when the two relays are equipped with two antennas, system performances are shown in Figure D-3 and Figure D-4, for scenarios 2.4 and 2.5, respectively. The performances for RA with three relays in the additional scenarios 3.5 and 3.6 are represented correspondingly in Figure D-5 and Figure D-6.

TABLE D.1: ADDITIONAL PROPAGATION SCENARIOS CONSIDERED IN MONTE CARLO SIMULATIONS FOR L=2.

	SNR_d	SNR_{c1}	SNR_{c2}
Scenario 2.4	SNR_d	SNR_d +5 dB	SNR_d
Scenario 2.5	SNR_d	SNR_d +5 dB	SNR_d +5 dB

TABLE D.2: ADDITIONAL PROPAGATION SCENARIOS CONSIDERED IN MONTE CARLO SIMULATIONS FOR L=3.

	SNR_d	SNR_{c1}	SNR_{c2}	SNR_{c3}
Scenario 3.5	SNR_d	SNR_d +5 dB	SNR_d	SNR_d
Scenario 3.6	SNR_d	SNR_d +5 dB	SNR_d +5 dB	SNR_d +5 dB

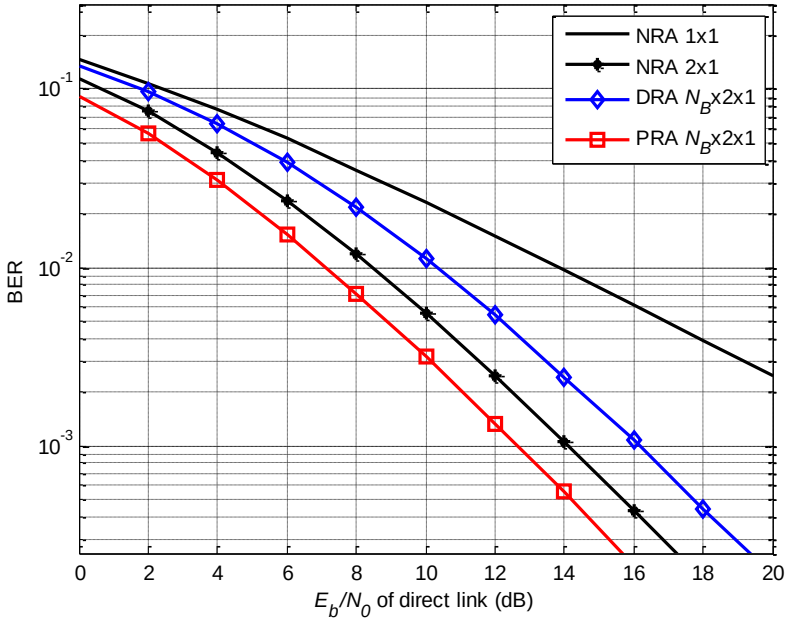

Figure D-1: BER of RA 2RN N_B×1×1 and reference systems for scenario 2.4.

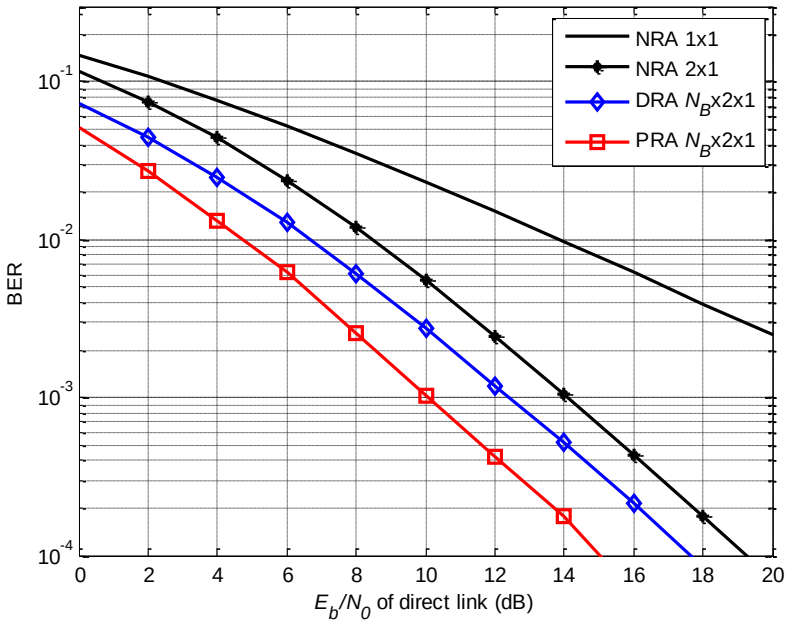

Figure D-2: BER of RA 2RN N_B ×1×1 and reference systems for scenario 2.5.

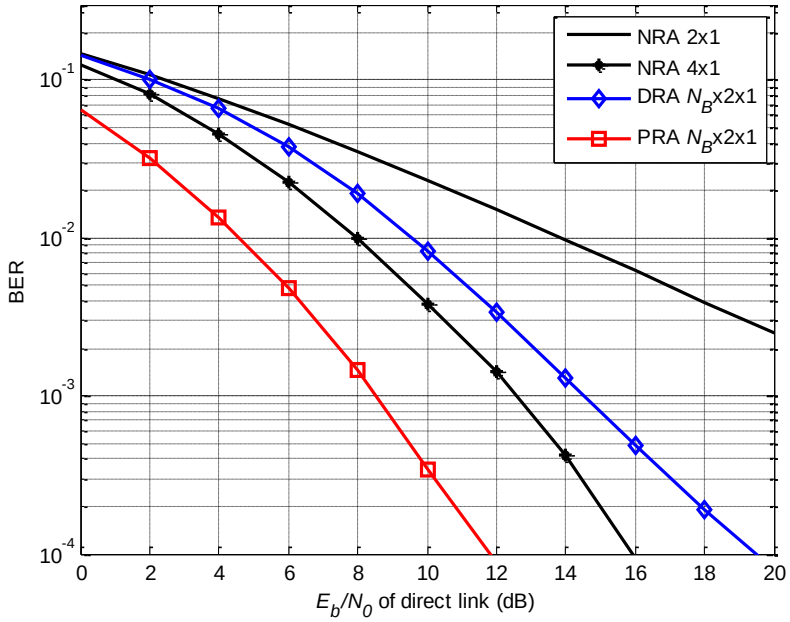

Figure D-3: BER of RA 2RN N_B×2×1 and reference systems for scenario 2.4.

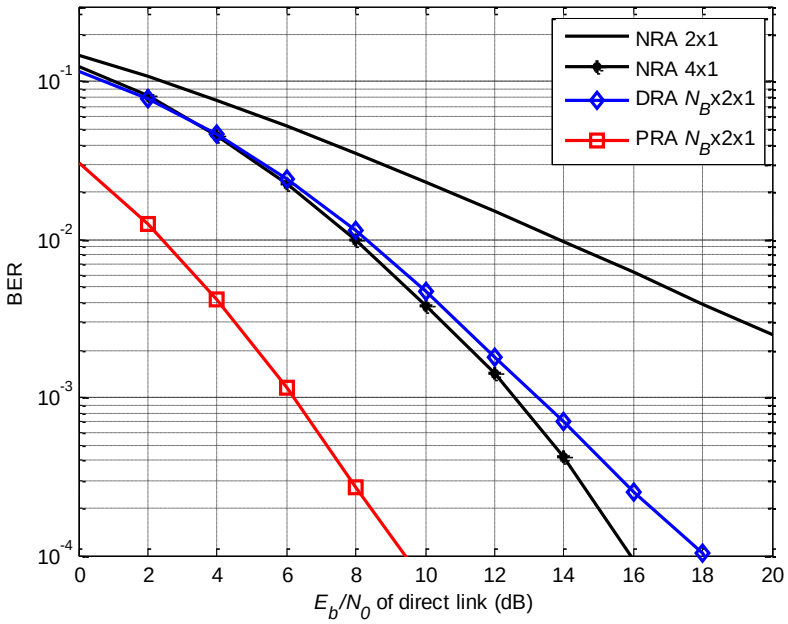

Figure D-4: BER of RA 2RN N_B×2×1 and reference systems for scenario 2.5.

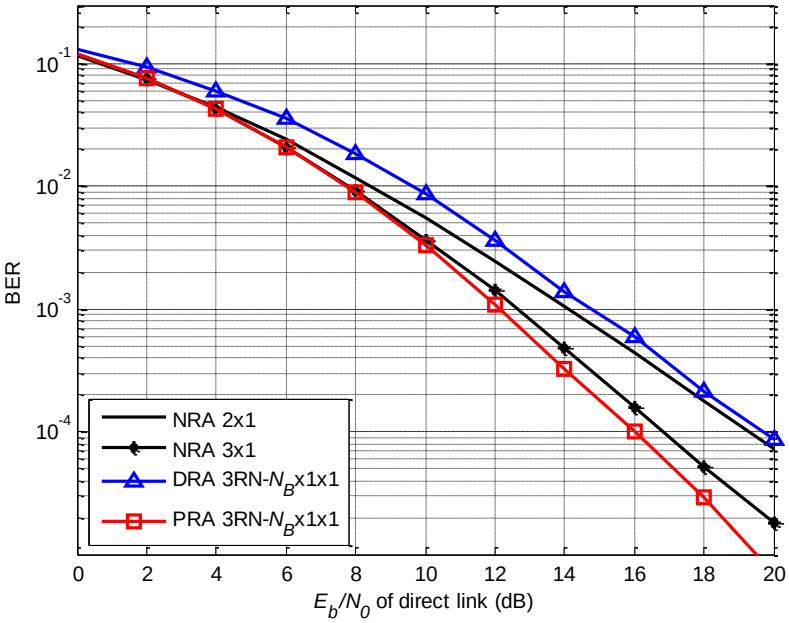

Figure D-5: BER of RA 3RN N_B×1×1 and reference systems for scenario 3.5.

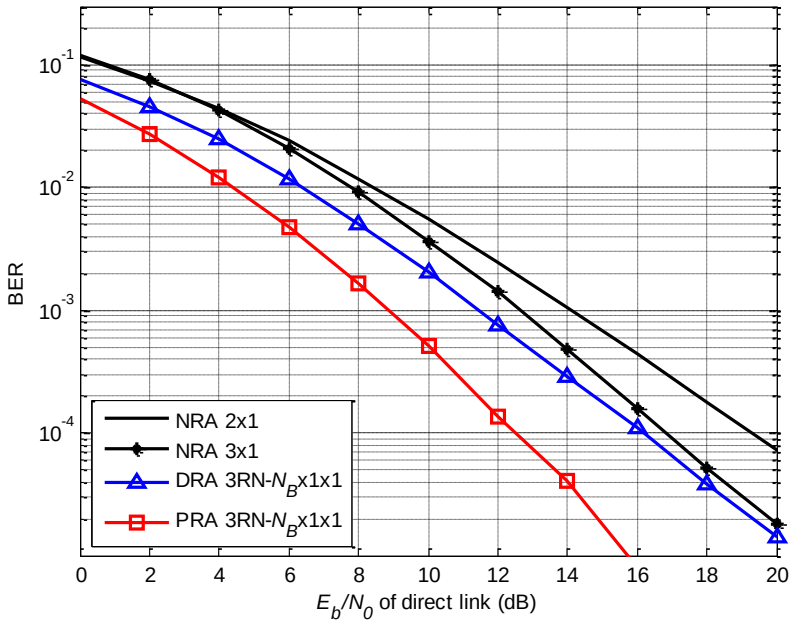

Figure D-6: BER of RA 3RN N_B×1×1 and reference systems for scenario 3.6.

E. Codes for the Precoding Algorithm for Two RNs

The precoded algorithm proposed for RA schemes, in Chapter 5, uses a code to transform L QPSK symbols into a single precoded symbol. This symbol is equivalent to have a symbol modulated by a 4^L -QAM modulation. Let us consider the case of two relay nodes, i.e., L=2, which is presented in Sections 5.3 and 5.4. In the proposed algorithm the precoded symbols are given by (5.1) or by

$$s_k = \mu\left((-1)^{x_k(1)} + j(-1)^{x_k(2)} + \frac{1}{2}\left((-1)^{x_{k+1}(1)} + j(-1)^{x_{k+1}(2)} \right) \right), \tag{E.1}$$

where s_k is the k^{th} soft-value of precoded symbols; $x_k(i)$, with i=1,2 is the correspondent i^{th} bit of the hard-value of the original symbol k; and μ is the normalization factor to ensure that the average energy over all symbols is one, which is given by $2/\sqrt{10}$. This code is named used precoding code (UPC) and its 16-QAM constellation mapping scheme is shown in Figure E-1. However this code has different Hamming weights between adjacent symbols, as can be observed in Figure E-2, which raises the hypothesis that a mapping scheme with a Gray code could be a better option.

Thus we consider the code based on a 16-QAM Gray mapping scheme, since in this case the Hamming distance between adjacent symbols is always one. This code is referred to as Gray precoding code (GPC) and the precoded symbols are given by (E.2). The constellation mapping

scheme is represented in Figure E-3. Nevertheless this code has a higher minimum distance than the UPC, confirmed for several particular cases of channel realizations.

$$s_k = \mu\left((-1)^{x_k(1)} + j(-1)^{x_k(2)} + \frac{1}{2}\left((-1)^{x_k(1)+x_{k+1}(1)} + j(-1)^{x_k(2)+x_{k+1}(2)} \right) \right) \tag{E.2}$$

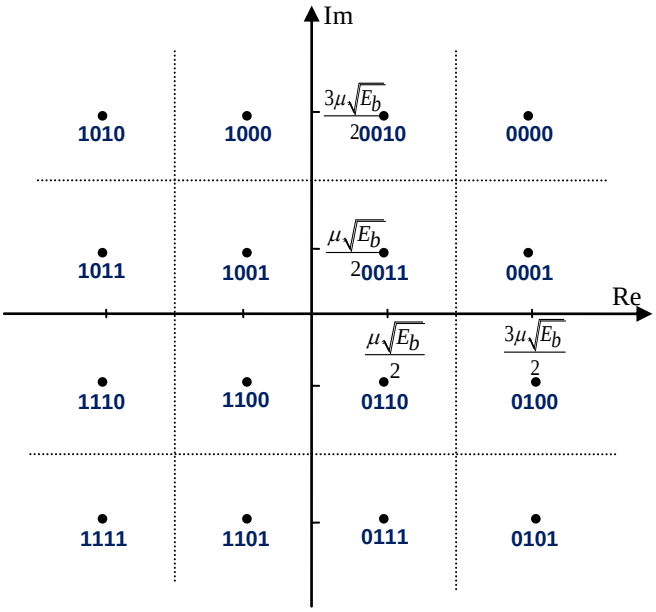

Figure E-1: Constellation mapping scheme for the UPC.

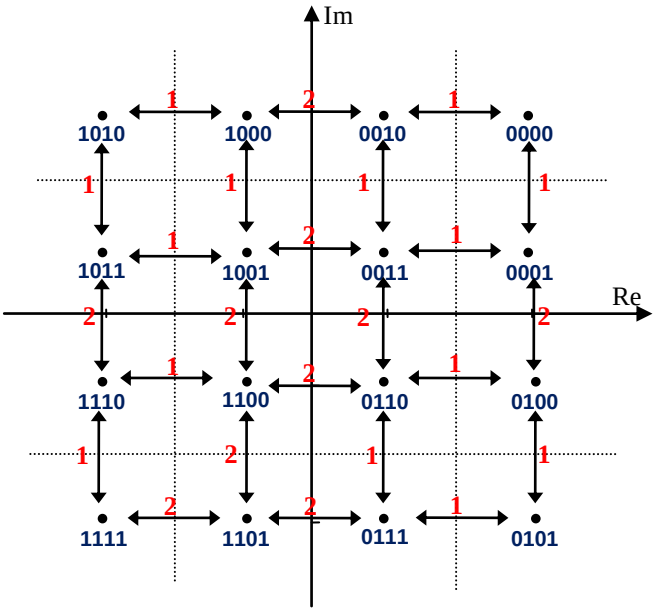

Figure E-2: Hamming distances for adjacent symbols for the UPC.

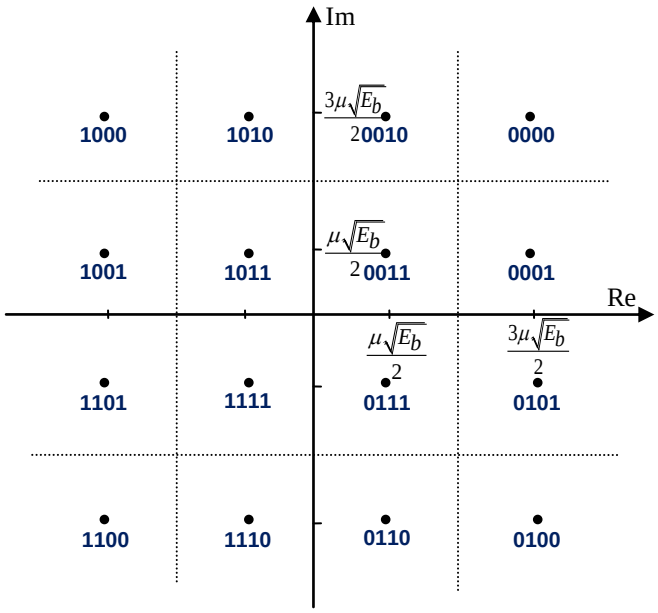

Figure E-3: Constellation mapping scheme for the GPC.